RADC-TR-80-52
Final Technical Report
March 1980

LEVEL II

⑫

ADAPTIVE TECHNIQUES FOR LARGE SPACE APERTURES

Martin Marietta Corporation

R. J. Richardson   Alan Fenn
John Coyner   Al Brook

DTIC
ELECTE
MAY 27 1980
C

ADA084631

ROME AIR DEVELOPMENT CENTER
Air Force Systems Command
Griffiss Air Force Base, New York 13441

80 5 27 006

This report has been reviewed by the RADC Public Affairs Office (PA) and is releasable to the National Technical Information Service (NTIS). At NTIS it will be releasable to the general public, including foreign nations.

RADC-TR-80-52 has been reviewed and is approved for publication.

APPROVED: *Robert F. Ogrodnik*

ROBERT F. OGRODNIK
Project Engineer

APPROVED: *Frank J. Rehm*

FRANK J. REHM
Technical Director
Surveillance Division

FOR THE COMMANDER: *John P. Huss*

JOHN P. HUSS
Acting Chief, Plans Office

If your address has changed or if you wish to be removed from the RADC mailing list, or if the addressee is no longer employed by your organization, please notify RADC (OCTM), Griffiss AFB NY 13441. This will assist us in maintaining a current mailing list.

Do not return this copy. Retain or destroy.

REPORT DOCUMENTATION PAGE

READ INSTRUCTIONS
BEFORE COMPLETING FORM

1. REPORT NUMBER	2. GOVT ACCESSION NO.	3. RECIPIENT'S CATALOG NUMBER
RADC-TR-80-52	AD-A084631	

4. TITLE (and Subtitle)

ADAPTIVE TECHNIQUES FOR LARGE SPACE APERTURES.

5. TYPE OF REPORT & PERIOD COVERED
Final Technical Report.
6 Nov 78 — 5 Nov 79

6. PERFORMING ORG. REPORT NUMBER
N/A

7. AUTHOR(s)
R. J. Richardson   Alan Fenn
John Coyner   Al Brook

8. CONTRACT OR GRANT NUMBER(s)
F30602-79-C-0017

9. PERFORMING ORGANIZATION NAME AND ADDRESS
Martin Marietta Corporation
P.O. Box 179
Denver CO 80201

10. PROGRAM ELEMENT, PROJECT, TASK AREA & WORK UNIT NUMBERS
62702F
45061401

11. CONTROLLING OFFICE NAME AND ADDRESS
Rome Air Development Center (OCTM)
Griffiss AFB NY 13441

12. REPORT DATE
March 1980

13. NUMBER OF PAGES
328

14. MONITORING AGENCY NAME & ADDRESS(if different from Controlling Office)
Same

15. SECURITY CLASS. (of this report)
UNCLASSIFIED

15a. DECLASSIFICATION/DOWNGRADING SCHEDULE
N/A

16. DISTRIBUTION STATEMENT (of this Report)

Approved for public release; distribution unlimited.

17. DISTRIBUTION STATEMENT (of the abstract entered in Block 20, if different from Report)

Same

18. SUPPLEMENTARY NOTES

RADC Project Engineer: Robert F. Ogrodnik (OCTM)

19. KEY WORDS (Continue on reverse side if necessary and identify by block number)

Radar Antennas   Large Space Structures
Unfurlable Antennas   Spacecraft
Antenna Arrays
Radiometers

20. ABSTRACT (Continue on reverse side if necessary and identify by block number)
Two missions which utilize large space apertures were considered on the program.
These were the space-based radar mission (SBR) and the space-based millimeter-
wave radiometer mission (MWR). The greater part of the effort was spent on the
radar mission. The intent of the program was to investigate reflector-based
alternates to the space-fed phased array system that is the current baseline
for the space-based radar program. The three major tasks on the program were
Task 1, Concept Development/Assessment; Task 2, Performance Analysis, Selected
Approach; and Task 3, Specific Mission Designs.   (Cont'd)

DD FORM 1473 EDITION OF 1 NOV 65 IS OBSOLETE
1 JAN 73

Item 20 (Cont'd)

The adaptive techniques of interest were those that might be required to com-
pensate for surface irregularities in the large, space-deployable reflectors
that would be required for these missions. This and other system requirements
were considered in selecting an antenna system for each mission.

The selected design for the SBR uses a 70 meter primary reflector with an
f/D of 1. The smaller field reflector is 28 meters in diameter and the planar
phased array feed is also 28 meters in diameter. The total number of active
modules is reduced by a factor of 4.3 from that used in the lens-array concept.
The orbit altitude was selected as 5000 n.mi. The FOV for agile beam scanning
is 20° x 11°, which is not sufficient for full-earth coverage. An attitude con-
trol concept was selected which uses gravity-gradient stabilization and rotation
about the gravity-gradient axis to provide full-earth coverage using a combina-
tion of electronic and mechanical steering. The system was packaged for launch
in a single shuttle, including the propulsion stage required to reach the oper-
ational orbit. Deployment is fully automatic and is done in the shuttle orbit
under the control of the orbiter crew. It is then boosted to its operational
orbit using a low-thrust liquid stage.

A similar design was made for a synchronous-orbit version of the SBR. It
uses a primary reflector 300m. in diameter. It requires four shuttle flights to
reach synchronous orbit using electric propulsion for orbit transfer or 6 shuttle
flights if chemical propulsion is used. Deployment of the major components is
done in shuttle orbit, but the components must be assembled by rendezvous at the
operational orbit. This is a much more difficult mission than the lower-orbit
SBR.

A brief look was also given to a reflectarray as another possible alternate
to the baseline lens-array SBR system. Its main advantage over the baseline
lens-array system is that a much shorter focal length can be used. This gives
a lighter and stiffer structure. The reflectarray was sized at 91 m. with an
f/D of 0.5 for the 5000 n.mi. orbit. It uses passive (phase shift only) reflect-
array modules. It can be packaged in a single shuttle vehicle.

A 400 n.mi orbit was selected for the MWR mission. This was selected as the
minimum altitude giving an acceptable level of atmospheric drag. It is gravity-
gradient stabilized and nadir-pointing, operating in a pushbroom mode. Operat-
ing frequency was selected at the 95 GHz atmospheric window. The FOV is quite
wide, 10,000 beamwidths. The pushbroom swath width on the ground is 125 n.mi.
Sensitivity is sufficient to detect a military tank in most weather conditions
except heavy rain. The resolution based on the individual beamwidths is 74 ft.
but a data processing technique based on using monopulse sum and difference
patterns can be used to improve this by a factor of 10 or more.

The structural concept selected for all of these designs is the deployable
box truss.

PREFACE

This technical report covers work done on Contract No. F30602-79-C-0017, "Adaptive Techniques for Large Space Apertures". The period of performance was 6 November 1978 to 5 November 1979. The sponsor was Rome Air Development Center, Griffis AFB, N.Y. The principal contributors to the program were R. J. Richardson, Program Manager and RF system design; John Coyner, structural design; Alan Fenn, antenna performance analysis; and Al Brook, attitude control system design. The RADC technical monitor was Robert Ogrodnik, whose direction and guidance are hereby acknowledged.

TABLE OF CONTENTS

TABLE OF CONTENTS (Continued)

v

TABLE OF CONTENTS (Continued)

vi

LIST OF FIGURES

LIST OF FIGURES (Continued)

LIST OF FIGURES (Continued)

LIST OF FIGURES (Continued)

LIST OF FIGURES (Continued)

LIST OF TABLES

LIST OF TABLES

EVALUATION

This study addressed design concepts of sensors employing large space apertures with operation at RF and millimeter (MMW) frequencies. Design analysis considered minimal launch vehicle requirements, automated deployment and maximum shape/stability behavior during mission operations (such as attitude control generated disturbances). Weight minimization and sidelobe criteria drove antenna form considerations (f/D ratio, etc). Potential aperture growth mission requirements (greater than 50 meter diameter) drive overall physical volume considerations as well as structural layout, the latter selected in a manner which eases deployment.

Study results have specified preferred design parameters and have given anticipated performance predictions for RF and MMW sensors. These designs are rated as feasible using near term technologies in space type structures and materials.

This technical assessment on aperture sizing will be utilized for Space Based Radar (R1C) and Advance Cruise Missile Surveillance (R2E) efforts.

ROBERT F. OGRODNIK
Project Engineer

1. INTRODUCTION

This report covers the work done on contract No. F30602-79-C-0017, "Adaptive Techniques for Large Space Apertures". The contract covered the period 6 Nov. 1978 - 5 Nov. 1979. The three major tasks on the program were Task 1, Concept Development/Assessment; Task 2, Performance Analysis, Selected Approach; and Task 3, Specific Mission Designs. Much of the work done on Task 1, particularly in the structural concepts tradeoff, had been done by us on an earlier contract sponsored by SAMSO, No. F04701-77-C-0180, "On-Orbit Assembly Concept Study".

Techniques for the deployment in space of very large structures, currently being developed, allow the consideration of a number of space missions utilizing very large aperture antennas. Two surviellance missions of particular interest to the Air Force are the Space-Based Radar (SBR) and the Millimeter Wave Radiometer (MWR). Both of these missions were considered on the program. The principal technical problems associated with these applications are:

o   The development of an appropriate structural concept capable of efficient packaging for launch, reliable deployment in space, and the achievement of adequate precision for use as an antenna.

o   Accurate and stable attitude and figure control of these large flexible bodies to maintain the required pointing accuracy as well as the RF performance of the antenna with acceptable damping periods following any maneuver.

o   An RF antenna system design that will give the desired flexibility, field of view (FOV), resistance to ECM, and beam agility to perform the desired mission.

The adaptive techniques of interest were those that might be required to compensate for surface irregularities in the large, space-deployable reflectors that would be required for these missions. This and other system requirements were considered in selecting an antenna system for each mission.

A number of antenna concepts were traded off against the requirements of the two missions and a concept was selected for each mission. The current program baseline concept for the SBR is a space-fed lens-array using a very large number of active transceiver modules to form the array. The principal weakness of this design is the high cost risk associated with the modules. Our selected approach gives a marked reduction in the required number of modules while still providing the flexibility to do the radar mission. The selected approach uses a large primary reflector 70 meters in diameter to achieve the necessary gain. A smaller field reflector and a phased array feed are used to provide the agility, FOV, and ECCM capability to do the radar mission.

A brief look was also given to a reflectarray as another possible alternate to the baseline lens-array SBR system. Its main advantage over the baseline lens-array system is that a much shorter focal length can be used. This

1

gives a lighter and stiffer structure.

The concept selected for the MWR mission is a reflective Schmidt tele-scope with diameter of 100 meters and a length of 300 meters. The reflecting surfaces are made up of metallized honeycomb panels. A linear array of feeds is used. This concept was selected for its wide FOV and relative simplicity.

A design effort was carried out for each mission. The structural concept selected in each case was the deployable box truss. RF performance was analyzed by computation. The structure was sized, weights were estimated and a packaging design for a shuttle launch was made. This included a sizing of the propulsion required to place the vehicle in its operational orbit. A first-cut design was also made for the attitude control and figure control systems.

Work done on the 3 program tasks is presented in chapters 2 through 4. Chapters 5 and 6 present our conclusions and recommendations.

2. TASK 1, CONCEPT DEVELOPMENT/ASSESSMENT

2.1 <u>RF Concept Tradeoff</u>. The two missions being considered have dis-
tinct requirements for their antenna systems. The radar mission needs a
fairly wide field-of-view (FOV), on the order of 50 beamwidths or more. As
a radar, it needs a single, highly agile beam and the capability to transmit
high pulsed power as well as to operate as a receiver. Very low sidelobes
and adaptive nulling capability are required. The bandwidth requirement is
on the order of 200 MHz and the frequency of operation is in the 1-2 GHz
region.

The radiometer mission requires a very wide FOV, 1000 beamwidths or more,
and needs a large number of simultaneous contiguous beams to form a push-
broom. It is a receive-only system with very wide bandwidth (5 to 10 GHz)
and high frequency (90 to 100 GHz) capability. These distinct requirements
lead to the selection of a distinct antenna type for each mission. The con-
siderations that entered into the tradeoffs for the two missions are sum-
marized below.

2.1.1 RF Concepts, Space-Based Radar. Only two generic concepts fit
this mission easily. These are (1), a full-aperture phased array, and (2),
a reflector-based system that allows the use of some kind of electronically
agile feed system for beam steering.

2.1.1.1 Phased Arrays. The baseline system being carried forward on
the Space-Based Radar program is a space-fed lens-array using dipole ele-
ments front and back, with an active transceiver/phase shifter module at
each element. Element spacing is not much larger than $1/2$ λ, giving a very
wide FOV. The only reasonable array alternative to this system is a space-
fed reflectarray. The reflectarray could use either active or passive
(phase shift only) modules as could the lens-array.

The principal advantage of the lens-array is that it is relatively for-
giving for large distortions of the array surface, up to several wavelengths
in magnitude, while the reflectarry must meet the surface distortion re-
quirements of a conventional reflector, i.e., around $\lambda/20$ or better. How-
ever, if advanced composite design techniques are used with a box truss
structure, this advantage disappears, at least for aperture sizes up to
around 500 ft. diameter, since the requisite reflector tolerances can be
held by the structure. A big disadvantage of the lens/array is that it re-
quires a very large f/D to give reasonable bandwidth performance because of
feed-to-array path length differences across the aperture. f/D = 2.5 has
been used in some designs. This requires a large high-gain feed and a very
long feed support tower which adds weight, expense, and deployment uncer-
tainties. More important, it causes the main structural vibration modes to
be extremely low frequency, less than 0.01 Hz for a typical design. This
has major adverse consequences for attitude control and system damping time.
The reflectarry solves this path-length problem by deploying the array on a
parabolic surface and feeding it from the focus. This allows the use of a
relatively short f/D on the order of 0.5, giving a much stiffer and more
compact structure.

We did not spend much time studying this concept since it was not the one selected for in-depth study. However, it does appear to offer some advantages over the baseline concept. A possible configuration is sketched in Figure 2.1-1. It is a passive reflectarray on a parabolic surface 300 ft. in diameter. This diameter gives sufficient additional directivity (2.3 dB) relative to the baseline 230 ft. system to make up for the passive module losses. $f/D = 0.5$ has been selected. A quadripod feed support is used for stiffness and reduced blockage. The feed system is an 8 x 8 Butler matrix, used for time delay compensation and adaptive nulling (similar to the Rotman lens used in the lens-array baseline). This feed array would have a square aperture around 6 ft. across, and would be composed of 64 small (0.8λ), contiguous horns. The spacecraft payload is mounted behind the feed. Each of these feed horns would be driven by a high-power (around 50 watts average) transceiver module to generate the required radiated power since the array modules are passive (phase shift only). A brief investigation of the shuttle packaging of this configuration is given in section 3.2. It was found that the vehicle could be packaged and delivered to a 5000 n.mi orbit using a single shuttle flight.

2.1.1.2 Reflector-Based Concepts. The principal disadvantage of any full-aperture phased array approach to the space-based radar mission is the extremely large number of element modules required. These may be quite expensive and with shielding, could be quite heavy. The virtue of any reflector-based system is that it achieves its large primary aperture and resulting high gain using a relatively simple reflector. The beam steering agility may be achieved in a number of ways, but it will generaly be much smaller and simpler than the full-aperture phased array. The penalty for this simplification is generally some loss in the wide FOV given by the full-aperture array.

There are two classes of beam steering systems for reflectors. One class utilizes lateral translation of a single feed or switching between feeds in a cluster to achieve lateral translation. The second class uses a small phased array feed and does beam steering by phase control of the array. This second class is preferable for a radar application because it avoids the problems associated with the switching of high-powered signals. The system selected by us is in this second class.

The system selected by us for detailed analysis is a two-reflector design consisting of a large primary reflector, a smaller field reflector, and a phased array feed that is about the same size as the field reflector. Its performance is analyzed in Chapter 3.1. It has the advantage that surface distortions of the primary reflector can be diagnosed by observing the fields at the phased array feed, a potential advantage for adaptive surface control of the primary reflector. Other, more complex, systems were considered briefly. One of these would replace the field reflector with a reflectarray. This gives a somewhat larger FOV, but it did not appear to be worth the added complexity for a large space-deployable system. The selected system is the simplest one that gives phased array steering for a large reflector.

4
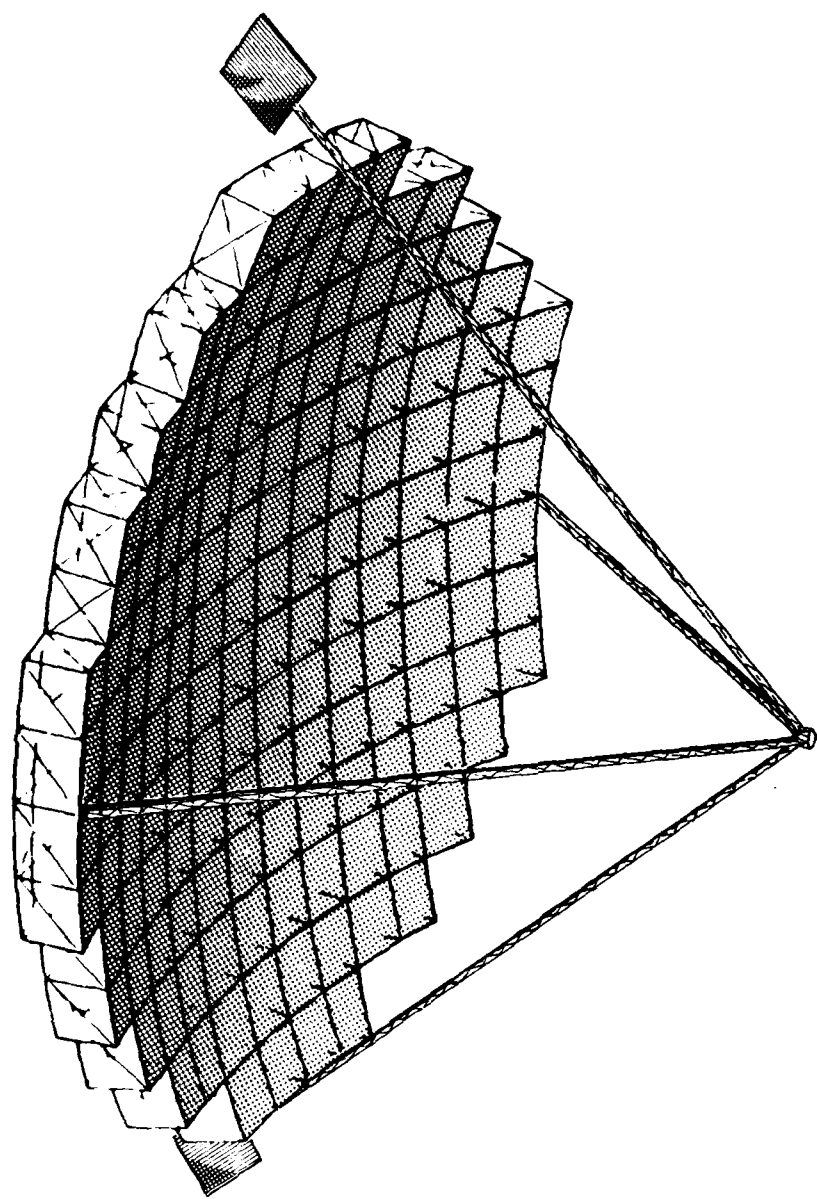
Figure 2.1-1 REFLECTARRAY SYSTEM

2.1.2 RF Concepts, Millimeter Wave Radiometer. A number of candidate antenna types were considered for the radiometer mission. The Schwartzschild system did not provide an adequate FOV. The torus antenna studied by Draper and others has a good FOV, but requires an extremely complex feed system to compensate for aberrations. There are a number of 3 and 4 reflector systems, analogues of optical telescopes, that would give the desired performance, but they are mechanically complex to deploy and are physically large relative to their effective aperture. Some of these disadvantages also apply to the selected system, a reflective Schmidt telescope. However, it only uses 2 reflectors, and would be simpler to deploy than the 3 and 4-reflector systems, so it was selected. The resulting design is described in Chapter 4.3. It gives a very wide FOV with nearly diffraction-limited performance and it uses only elementary feeds, so it appears to be an optimum system for the mission.

2.2   Structural Concept Tradeoff.

2.2.1   Introduction. A structural concept tradeoff study was performed
to determine the most promising candidate structure for meeting the require-
ments of the RF concepts described in Section 2.1. Each structural concept
was evaluated with respect to its ability to meet the aperture size require-
ments, packaging volume, mass of aperture, deployment and/or erection require-
ments, surface precision, and ability to be integrated into the desired RF
configuration (i.e. the two reflector radar). Listed below are the structural
concepts that were considered:

1)	Umbrella Radial Rib Double Mesh Antenna	Harris
2)	Wrap Radial Rib Antenna	Lockheed
3)	Erectable Radial Rib Antenna	General Dynamics
4)	Curved Astromost Radial Rib Antenna	Harris
5)	Radial Column Rib Antenna	Harris
6)	Articulated Radial Rib Antenna	Harris
7)	Maypole Antenna	Lockheed
8)	a – Hoop/Column Antenna	Harris
	b – Hoop/Column Radar	Grumman
9)	Polyconic Antenna	Lockheed
10)	Tetrahedral Truss Antenna	General Dynamics
11)	Box Truss Antenna	Martin Marietta
12)	Solid Panel Deployable Antenna	TRW
13)	High Frequency Radial Rib Antenna	Lockheed
14)	Expandable Module Astro Cell Antenna	Astro Research
15)	a – Hex Panel/Truss Antenna	Caltech
	b – Hex Panel/Truss Antenna	JPL
	c – Hex Panel/Truss Antenna	Draper Labs
16)	Rectangular Panel/Deployable Truss Antenna	Martin Marietta
17)	Electrostatic Membrane/Deployable Truss Antenna	General Research
18)	Thin-Film Controllable Antenna	MIT

In general, the candidate structural concepts fall into two operational
frequency regimes. Concepts 1 through 11 utilize a mesh type reflector sur-
face which is satisfactory to 20 GHz. Concepts 12 through 18 utilize either
rigid metalized panels or a metalized membrane which will operate at fre-
quencies greater than 20 GHz.

Also the candidate structural concepts fall into three generic structur-
al configurations; 1-Radial Rib, 2-Truss and 3-Hoop/Column. The radial rib
concepts have the advantage of minimal required structure to support the re-
flective surface and relatively simple deployment, but have the limitations
of low deployed stiffness, difficulty of integration into a multiple reflect-
or system, and inability to support solid panels for high frequency operat-
ion. The truss type concepts have the advantage of high deployed stiffness,
ease of integration into a multiple reflector system, and ability to support
solid panels for high frequency operationa, but have the disadvantage of
large numbers of structural elements and more complicated deployment. The
hoop/column or maypole concepts have the advantage of lowest weight and most
efficient packaging, but have the limitations of low deployed reflective sur-
face frequency, difficulty of forming a curved reflective surface, complicat-

ed deployment, difficulty of integration into a multiple reflector system, and inability to support solid panels for high frequency operation.

Based on the qualitative advantages and disadvantages of the three generic structural configurations, the truss type structure is the most promising candidate for the reflectarray, the two-reflector system, and the millimeter wave radiometer (Schmidt reflector).

2.2.2 Concept Description. The following paragraphs briefly describe each of the concepts that were evaluated.

Umbrella Radial Rib Double Mesh Antenna

Harris Corporation has developed the radial-rib concept for reflector antennas to the point of flight hardware models 16.7 ft in diameter (Figures 2.2-1-2-3) and larger. These models were used to demonstrate mechanical and electrical performance and to verify the analytical models used for design and prediction of performance. The demonstration of this technology clearly qualifies this design concept for flight application of antennas up to 18.3 m (60 ft) in diameter for operation up to K-band. This design capability takes advantage of the latest developments in structural composite materials and analytical tools for detail design and performance prediction. This basic design is currently planned for application on the tracking and data relay spacecraft, which will use two 5-m-diameter antennas on each satellite. The primary limitation of this design is the 80 ft diameter limitation based on packaging in the orbiter.

The basic structure of the antenna includes the ribs, feed support cone, hub, and deployment mechanism, while the RF reflective surface is formed by a dual surface configuration.

The parabolic reflector consists of tubular ribs which support and help shape the metallic mesh. The selection of the number of ribs is based on a tradeoff study considering weight, surface tolerance, and deployed dynamic performance. The dual-surface technique uses two surfaces, which are separated by the rib thickness and connected to one another by a large number of tensioned ties. The second surface, attached to the back of the ribs and tied to the front mesh by a large number of tensioned wires, is used as a drawing surface for contouring the front reflector mesh. By properly tensioning these tie wires, the reflector surface can be contoured to a good approximation to a parabolic shape. This design eliminates surface tolerance dependency on the number of ribs because the second mesh provides support for the RF reflective mesh. This design approach provides the flexibility to meet a wide range of structural and surface tolerance requirements with low weight.

The mechanical deployment system (MDS) provides a controlled deployment of the reflector from the stowed to the fully deployed position. This controlled deployment eliminates impact loading of the rib structures. The MDS is located inside the lower section of the feed support cone assembly and consists of a disk-shaped carriage, mounted to the moving section of a recirculating ball nut on a ball screw shaft. Connected between the carriage and the ribs are links that transmit the required force and motion to deploy the in-
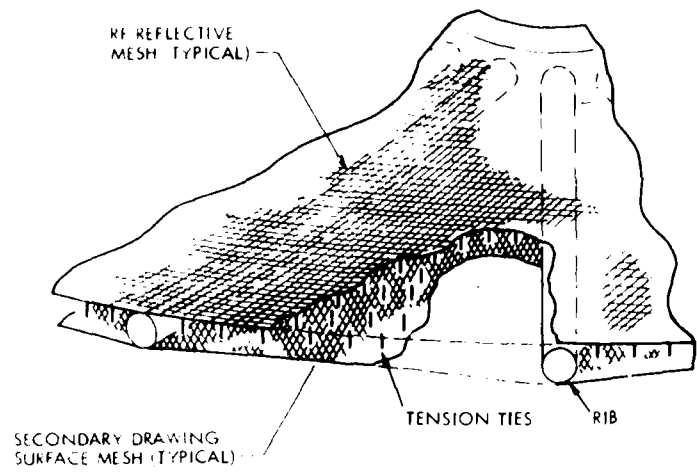
Figure 2.2-1   Harris Corporation Dual-Mesh Configuration
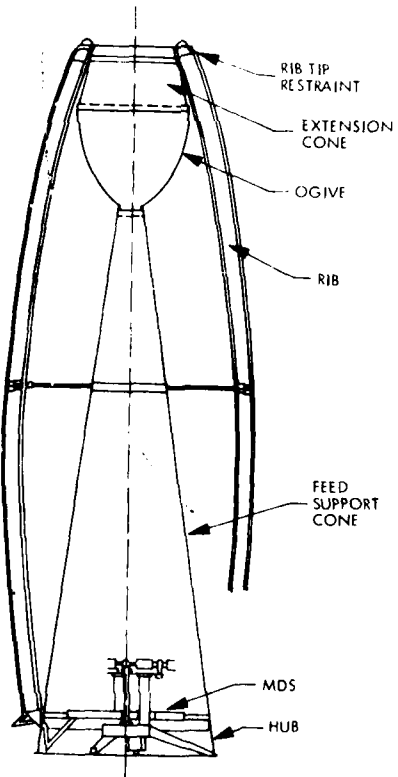
Figure 2.2-2   Feed Support Structure of Harris Corporation
Radial-Rib Antenna

9
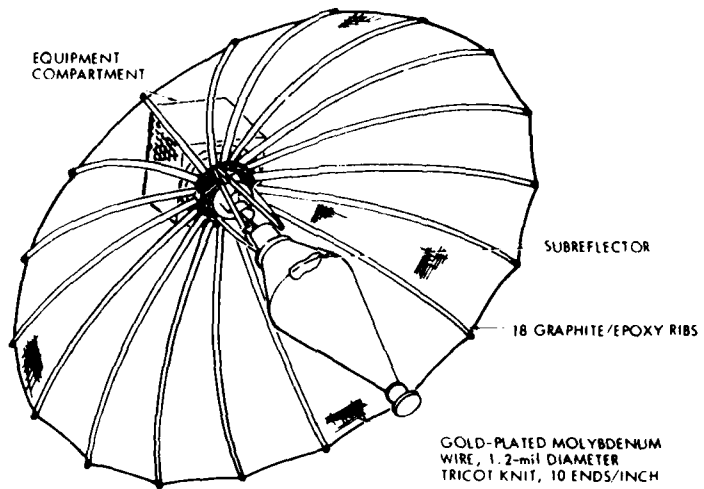
Figure 2.2-3   Design Elements of Harris Radial-Rib Antenna
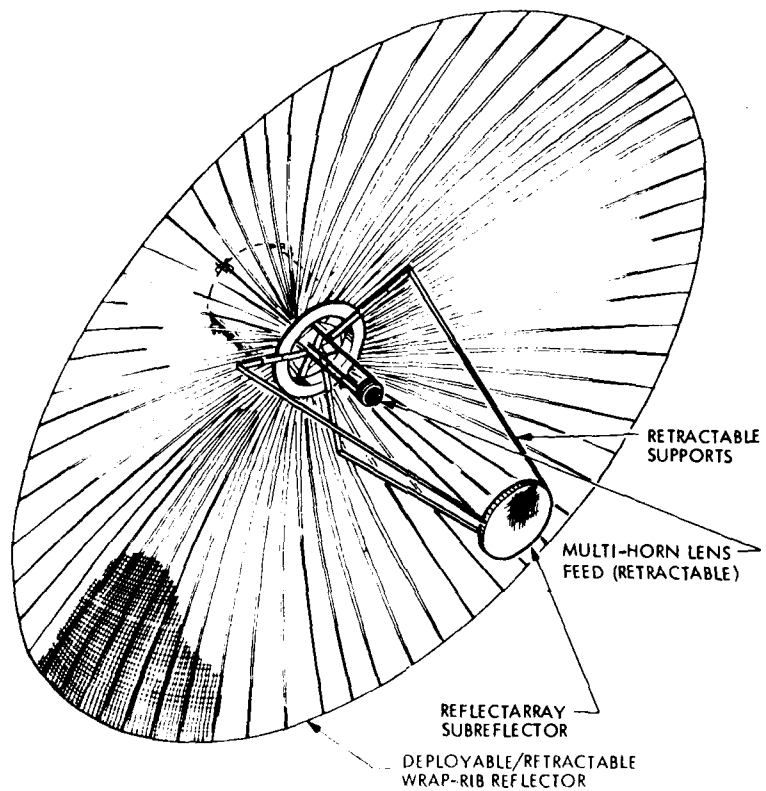
Figure 2.2-4   Typical Lockheed Wrap-Rib Antenna: Deployed
                Configuration

dividual ribs. Rotation of the ball screw moves the carriage and attached
links, which in turn produces the simultaneous rotation of each rib about
its bearing. Latching in the deployed condition is accomplished by driving
the ball-nut carrier and linkages through an over center condition (relative
to the pivot arms).

Wrap Radial Rib Antenna

Lockheed has developed the wrap-rib antenna to the point of numerous
flight applications for many different size antennas. The best known appli-
cation is probably on the ATS-6 spacecraft, which uses a 9.1-m (30-ft) para-
bolic, wrap-rib reflector antenna operating up to and above 8 GHz. The ATS-6
antenna, made with aluminum ribs, and conventional thermal blankets, repre-
sents a technology about 10 years old. Recent developments using this con-
cept have resulted in a manufacturing capability for fabricating wrap ribs
from structural composite materials with extremely low coefficients of thermal
expansion. New materials and processes for manufacturing mesh have been de-
veloped recently, and the analytical capability for the detail design of the
structure has been recently improved. These developments have made it possi-
ble to design, build, and predict antenna performance for wrap-rib structures
up to several hundred meters in diameter and perhaps larger for operation up
to, and possibly above, X-band. The primary limitation of this design is
the low deployed dynamic/frequency of the larger diameter wrap rib designs.

The wrap-rib antenna consists of a hollow, doughnut-shaped hub to which
a series of radial ribs, formed to the shape of a parabola, are attached. A
lightweight reflective mesh is stretched between these ribs to form the para-
boloidal reflecting surface. The feed system is usually located at the prime
focus of the paraboloid by one or more deployable support booms. A sketch
of the deployed wrap-rib antenna is shown in Figure 2.2-4. To furl the re-
flector, the ribs are wrapped around the hollow hub with the mesh folded bet-
ween them. (Figure 2.2-5).

The parabolic surface is formed by a flexible, lightweight reflective
mesh supported along each of the radial parabolic ribs. The number of ribs
or mesh panels used is dependent upon the desired rms surface accuracy, which
in turn determines the gain of the antenna excluding the gain loss due to
blockage by the feed support structure.

· The hollow, doughnut-shaped support hub has mounting pads to interface
the antenna system with a spacecraft or the Shuttle. It provides the support
points for each radial rib and stowage area for the radial ribs and the re-
flective mesh. The hub supports the "in space" deployment and refurl mecha-
nism as well as an "in space" surface-contour evaluation and adjustment
system, if such a system is used.

The flexible ribs are wrapped around a power-driven rotating spool that
constrains the stored energy of the wrapped ribs and deploys the reflector
surface at a controlled rate. The furling mechanism uses a sliding guide to
"wipe" the ribs in a rotating manner back into their stowed configuration.
The stowed configuration may be as small as one-fortieth of the deployed
diameter of very large antennas. The stowed configuration also lends itself

11
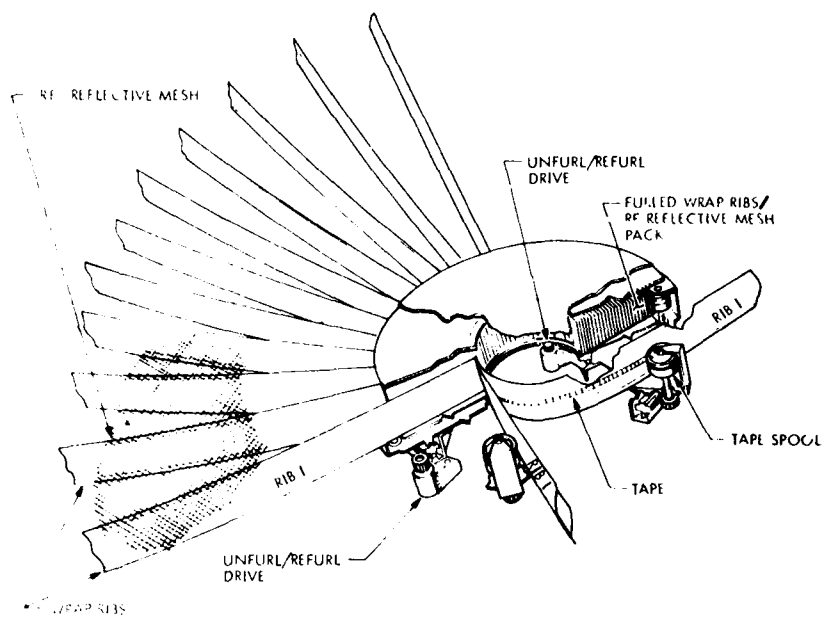
Figure 2.2-5   Lockheed Wrap-Rib Antenna: Furling Mechanism

12

to high load-carrying capabiltiy.

The feed or feed array used with this concept is dependent upon the reflector size and intended use. It may be a single horn illuminating the total surface; a cluster of horns, each illuminating a portion of the reflector surface, but forming one coherent beam; or a cluster of feeds forming individual spot beams. The cluster of feeds also may be replaced by a phased array used as a feed for either single or multiple beams or to generate specially shaped or steerable beams.

Dependent upon reflector size, the deployable feed support structure could be a simple, powered, folding structural boom; a structurally formed boom that is elastically buckled for storage on powered spools; a modified scissors structural-type boom that is powered for extension and retraction; or some type of telescoping boom. The boom will use conventional thermal control or will be built from materials with low coefficients of thermal expansion to ensure precise positioning of the feeds under varying thermal environments.

Erectable Radial Rib Antenna

General Dynamics Convair Division has performed a design study of an On Orbit Assembly (OOA) spacecraft. The study investigated and defined the new technology required to place large, low-density structures on orbit. The technology was applied to the conceptual design of an orbital assembly flight article. Deployment of the DoD/STSOOA Spacecraft module in low earth orbit (LEO) is illustrated in Figure 2.2-6, which depicts the radial arms, lens array, feedmast, and upper stage hub assembly. The separately deployed feedmast assembly is mated to the module at geosynchronous earth orbit (GEO). Figure 2.2-6 shows a typical section of the deployable radial arm. The radial arm and feedmast basic structural elements are tubular graphite-epoxy. Over-center lock hinges and thin metal "carpenter tape" hinges accommodate compact stowage in the Space Transportation System (STS) Orbiter cargo bay. The primary limitation of this concept is the difficulty of attaching the reflector surface and holding the required precision for a reflector application.

Curved Astromast Radial Rib Concept

This Harris design consists of a central hub with multiple Astromast cannisters attached radially around it (see Figure 2.2-7). The feed is also attached to an Astromast located in the center of the hub.

Astromasts are articulating lattice structures that are folded into a small volume when stowed and which extend fully when deployed. Deployment takes place by the individual sections of each Astromast rib being forced out of its respective cannister. Once fully deployed, the ribs form the desired parabolic shape. The reflective mesh is attached and shaped by the same secondary drawing surface technique used for the articulated rib concept.

The stowed size of this concept is very compact and easily compatible

13
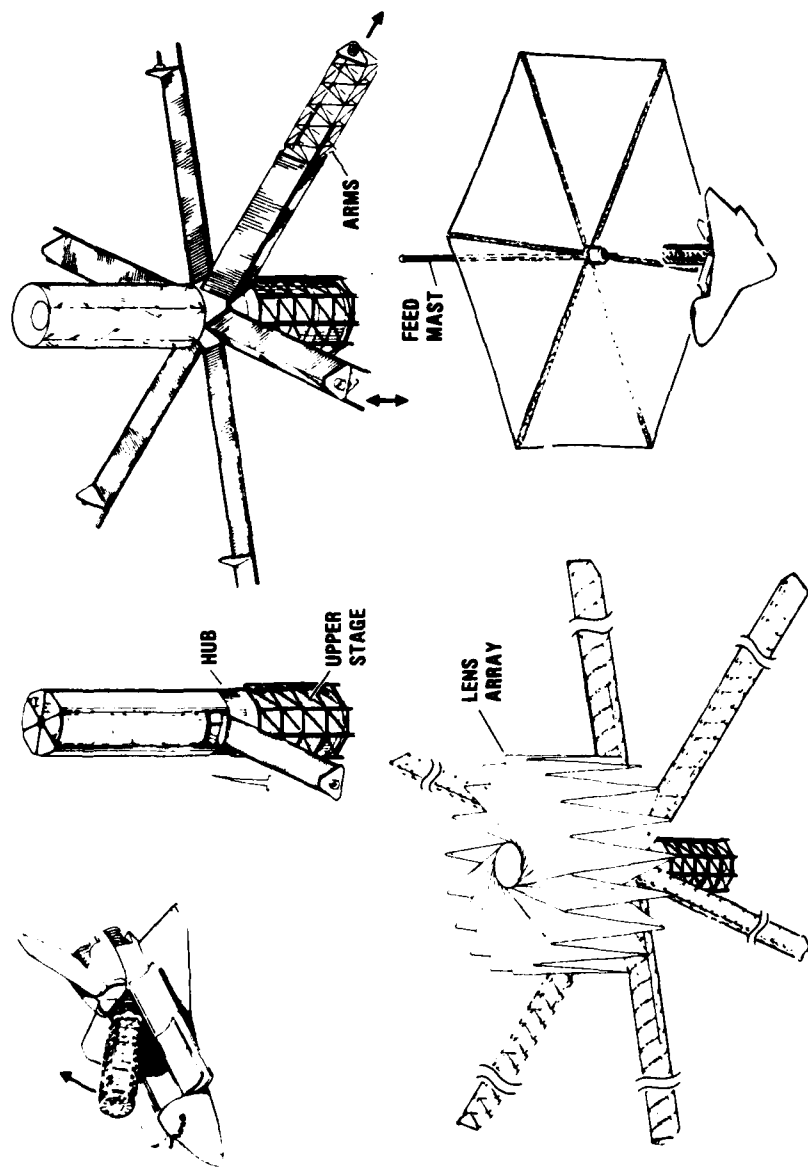
Figure 2.2-6 General Dynamics Radial Rib Concept

14

DIELECTRIC FEED SUPPORT

FEED SUPPORT ASTROMAST

CIRCUMFERENTIAL RIM

TIES

ASTROMAST CANISTER

HUB

REFLECTIVE MESH

RIB

REAR SURFACE
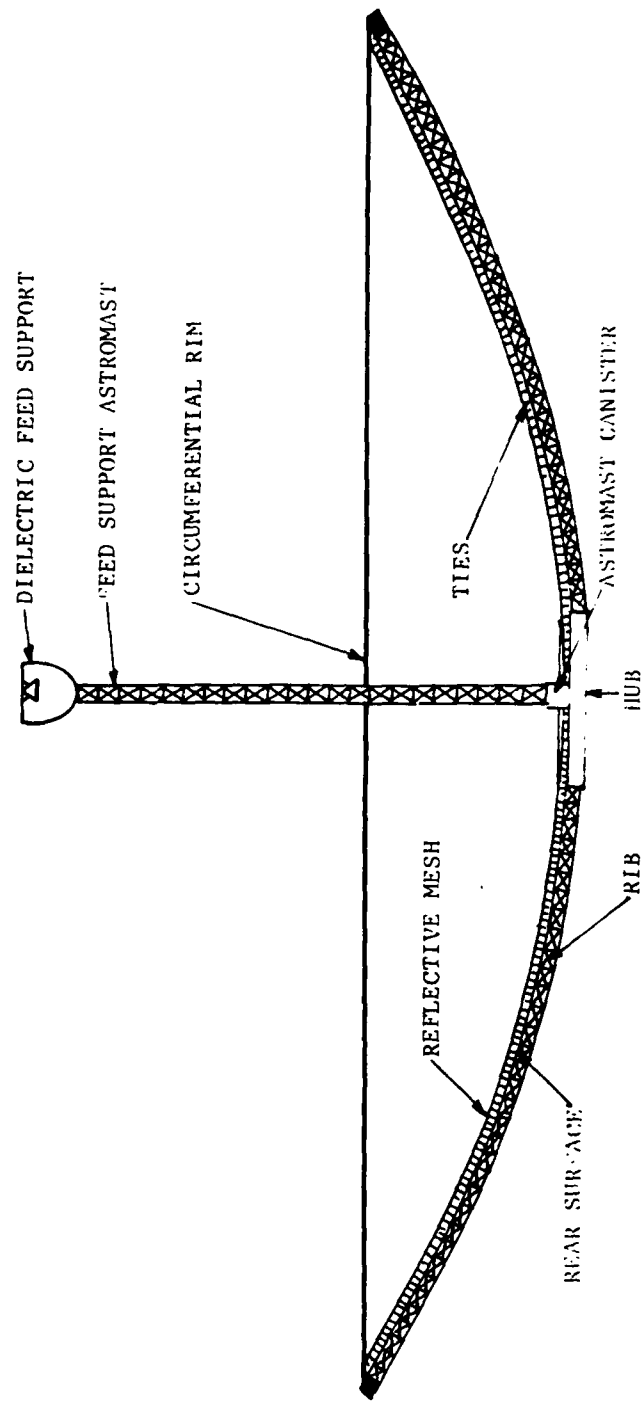
Figure 2.2-7   Harris Curved Astromast Radial Rib Concept

15

with the shuttle's storage bay. There are, however, serious drawbacks to this concept. The actual attachment of the mesh to the ribs would involve an extremely complex mechanism.

When stowed, the entire astromast is contained within its cannister. The mesh cannot be drawn into this cannister, so it must detach from the ribs as they are being stowed, and reattached upon subsequent deployments. The costs associated with the development of a curved astromast are very high and the additional cost of developing a mechanism capable of attaching and detaching the mesh makes the total cost prohibitive.

Radial Column Rib Antenna

The Harris Radial Column concept shown in Figure 2.2-8 employs straight extendable booms which would be either Astromasts or some other type of telescoping members. The reflective mesh is not attached along these ribs, but rather to large standoffs at the rib tips. The mesh shaping technique involves the use of a secondary drawing surface similar to the one described for the Hoop/Column concept. The mesh is supported at its periphery by a series of intercostals which in turn are attached to the tips of the standoffs. Thus, when the ribs stow, there is no mesh interference problem.

The radial ribs are column loaded due to the mesh and secondary drawing surface loads being reacted by stringers called column preload ties. These ties are attached to the standoffs at their lower end such that no net moment results at the tip of the rib. The inboard end of the rib is attached to the hub by a pin joint which has no moment carrying capability.

The primary limitation is the complicated deployment and its potential application near the 100m size and larger diameters appears limited.

Articulated Radial Rib Antenna

This concept (shown in Figure 2.2-9) is a logical extension of Harris ESD's current radial rib design, but has the flexibility to accommodate larger diameters and retain the same packaging efficiency. It consists of a center mast which supports the feed and to which rigid radial ribs are attached by pivots at the base. Because of the antenna diameters under consideration and the constraint of the limited stowed volume available, it is necessary to put an articulation at the midspan of each rib. The ribs approximate a parabolic contour and have adjustable standoffs to which the reflective mesh is attached. The surface is shaped between the ribs by the secondary drawing surface technique. The concept is attractive from experience standpoint, but there are serious packaging size limitations. The shortest stowed length with a single articulation in the ribs is one quarter of the antenna diameter. For a 100 m diameter antenna, this length would become prohibitive. Another articulation for each rib is possible, but the added mechanical complexity and probable mesh handling problems negated the potential advantages.

16
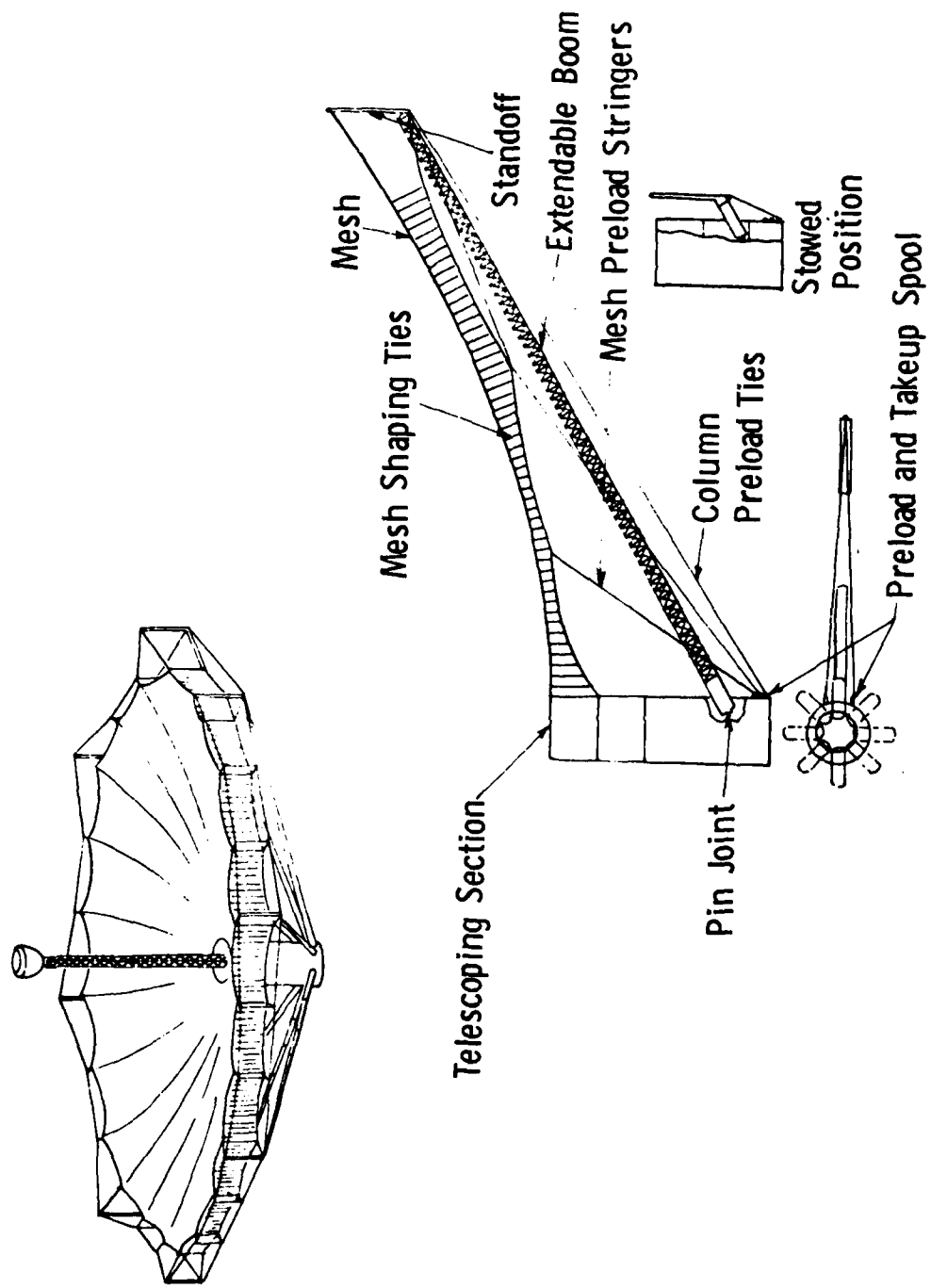
Figure 2.2-8   Harris Radial Column Concept

17
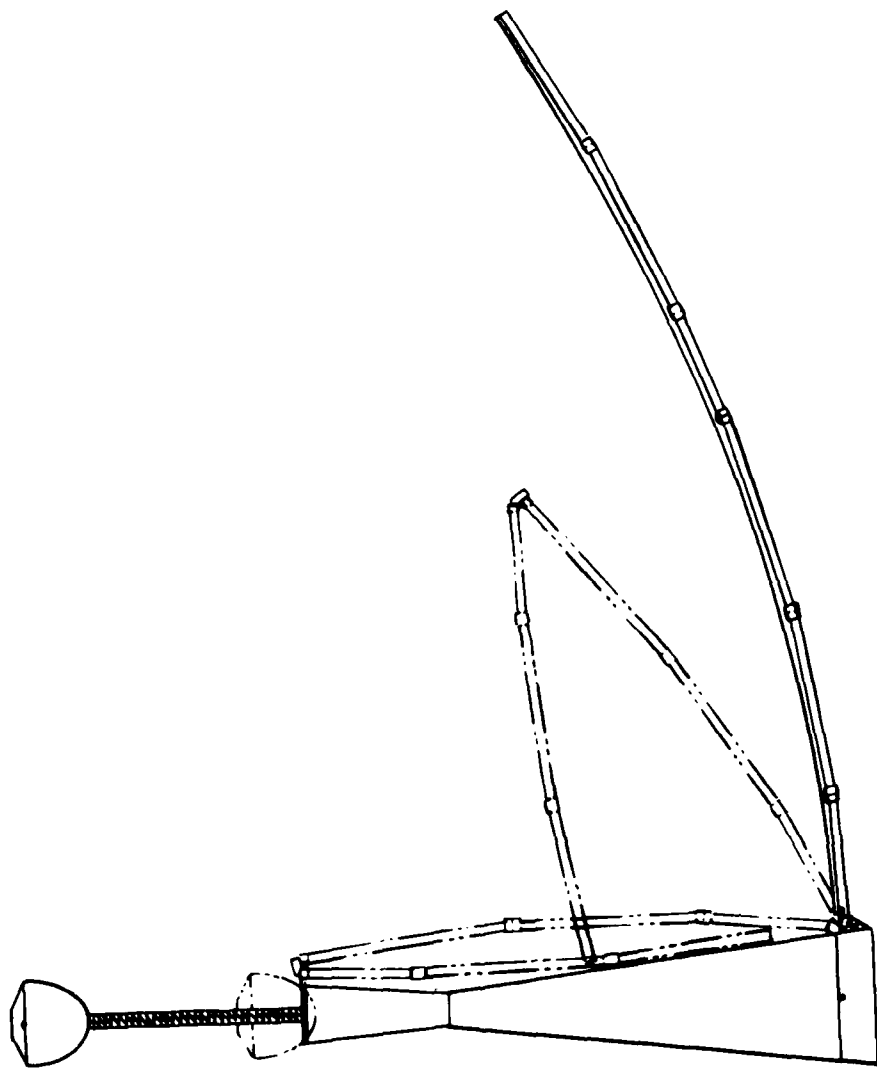
Figure 2.2-9   Harris Articulated Radial Rib Concept

Maypole Antenna

LMSC developed the maypole concept primarily for self-deployable reflector antennas from 100 m in diameter to 1000 m in diameter (Figure 2.2-10). The intended frequency for the smaller sizes is 8.5 GHz, which decreases to 1.0 GHz for the larger sizes. LMSC developed the concept to the point of a preliminary design for the estimation of parameters such as surface accuracy, thermal distortion, mechanical packaging efficiency, weight, cost, and basic dynamic characteristics. The primary limitation is the complicated deployment and poor surface accuracy.

The deployed maypole antenna resembles a "maypole" or a bicycle wheel. It consists of a long central column and hub, a rigid outer rim, and a system of tension cables (spokes) originating from the rim and terminating at both ends of the column. These tensioned spokes locate the rim with respect to the column and stabilize the basic structure. A reflective, paraboloidal mesh cup is suspended at the center of the wheel to form the reflector. The mesh is attached to the perimeter of the rim and the hub. The parabolic contouring of the RF reflective mesh is made possible by a series of mesh ribs that are attached to the reflector surface along radial seams. The mesh ribs are tapered, with respect to their attachment to the reflective surface, and terminate into a single cable that is attached to the lower portion of the central column. The proper tension in the mesh rib cable and tension field in the RF mesh result in a parabolic contour of the radial lines of intersection of the two mesh systems. Collectively, these lines of contour approximate a parabolic surface. An increase in the number of ribs improves the surface quality.

The structural design is based on the capability of the outer rim member and the column to withstand the compression loads resulting from the tension loads in the spokes. Very large reflectors use very low tension loads in the spoke ties. These loads are held at a stable low value by "load maintainer" mechanisms in series with each spoke. The "sufficiently rigid" outer rim and the center column become feasible because of the low load values in the spokes.

In addition to providing for gravity gradient stabilization of the antenna system against solar pressure, the central column can be used to carry spacecraft control modules, depending on the magnitude of the mass moment-of-inertia ratios. The maypole concept, for very large antennas, is expected to become feasible when near-zero thermal-coefficient-of-expansion materials become available for the mesh, the structural rim, the central column, and the tension tie spokes. Active surface evaluation and control will be required for antennas of this concept when operating in the gigaHertz frequency range.

Initial investigation has shown that a 300-m-diameter antenna based on this concept, which operates in the frequency range of 1 to 2 GHz, can be stowed within the cargo volume and weight limits of one Space Shuttle flight.

DEPLOYED
STRUCTURAL
RING

TENSION
CABLE

MESH
RIB

CATENARY
CABLE

MESH
PARABOLIC
SURFACE

TELESCOPING STRUCTURE
CENTER COLUMN
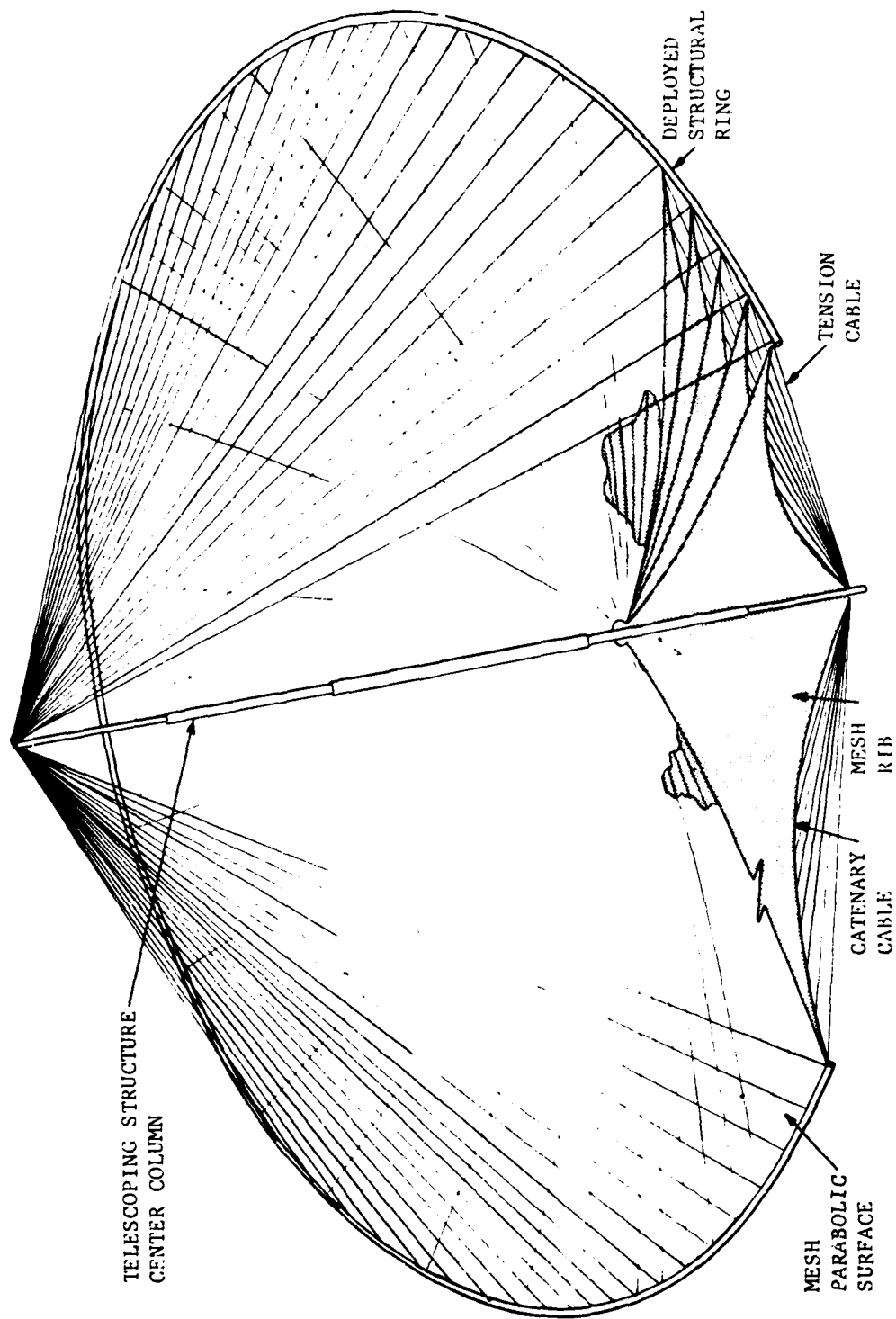
Figure 2.2-10   Lockheed Maypole Parabolic Reflector

20

Hoop/Column Reflector

The Harris Corporation hoop and column reflector antenna concept for self-erectable structures is intended for designs up to 100 m in diameter (Rigure 2.2-11). This concept has been developed to the point of a preliminary design for sizes up to 45.7 m (150 ft) in diameter and a 1.8-m-diameter conceptual demonstration model. The 1.8-m mechanical model was used to verify the basic conceptual design in addition to leading to solutions of the kinematic problems associated with deployment. The preliminary design has been complemented with the development of analytical techniques for prediction of antenna performance for larger size structures. The primary limitation of this design is the complicated deployment and surface control requirements. The fundamental elements of the support structure include the hoop; upper, lower, and center control stringers; and the telescoping mast. The reflector consists of the mesh, mesh shaping ties, secondary drawing surface, and the mesh tensioning stringers. The basic antenna configuration is a type of "maypole," with a unique technique for contouring the RF reflective mesh.

The hoop's function is to provide a rigid, accurately located structure, to which the reflective surface attaches. It is comprised of 40 rigid sections which articulate at hinges joining adjacent segments. These segments consist of two tubular, graphite fiber members parallel to each other and attached to a long hinge member at each end. These long hinges allow the separation between the tubular members of the hoop segment required by the geometry of the mesh-secondary drawing surface. Torsion springs located in each hinge supply the total energy required to deploy the hoop.

The central column or mast is deployable and contains the microwave components and control mechanisms. It consists of tubular graphite/epoxy shell members that nest inside each other when stowed. Aside from housing various components, the mast provides attachment locations for the reflective surface and the stringers.

Five sets of stringers are used on the hoop/column concept. Three of these sets are used for hoop deployment and its control; the other two sets are used for mesh shaping. The hoop-control stringers are located at the upper end, the center, and the lower end of the extendible mast; they extend radially outward to their attachment positions at the hinges of the hoop. The upper and lower control stringers accurately position the hoop throughout its deployment. The center control stringers are used for rate control during deployment and for moving the hoop joints toward the mast, against their spring forces, during the automated stowing sequence. The remaining two sets of stringers (mesh tensioning stringers) are located just above the lower control stringers and are used to shape the reflective surface into the proper contour. All of these stringers are made of stranded quartz cords for high stiffness and thermal stability.

The reflective surface is produced by properly shaping a knitted mesh fabric. The mesh is made of 1.2-mil-diameter, gold-plated molybdenum wire. The mechanism that permits shaping of the mesh consists of numerous radial quartz stringers to which the mesh is directly attached (mesh surface

21
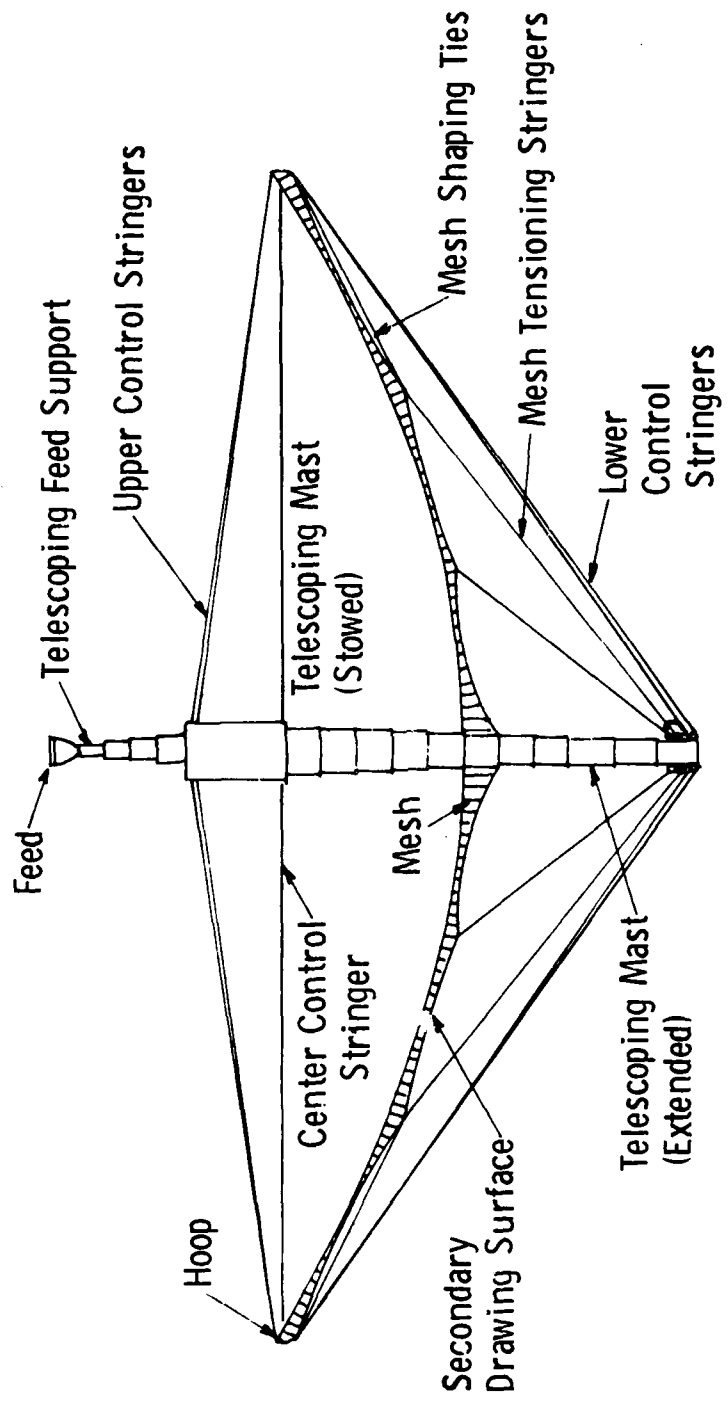
Figure 2.2-11   Harris Hoop/Column Concept

stringers) along with a similar set of stringers (secondary drawing surface stringers) positioned beneath them. Short ties (mesh shaping ties) made of fine Invar wire connect the RF mesh surface stringers to the secondary drawing surface stringers as shown (see Figure 2.2-12). When the RF mesh tensioning stringers are tensioned, they in turn tension both the secondary drawing surface stringers and the mesh shaping ties to produce an essentially uniform pressure distribution on the mesh. This pressure distribution allows shaping of the mesh to a good approximation of a parabolic curvature. This configuration for a single gore element is shown in Figure 2.2-12. The surface accuracy is affected by the number and spacing of the mesh shaping ties. The greater the number of ties, the greater the surface accuracy.

Two groups of drive mechanisms are used in the hoop and column concept. One group, used to extend the mast, consists of one basic set of mechanisms for each section of the telescoping mast. The second group of drive mechanisms is used to adjust the control stringers and consists of motor-driven spools to which the stringers are attached. There are five sets of spools, one for each group of stringers. The spools are used to retract and discharge the stringers during the deployment and stowing sequence and are positioned around the mast in the locations described for the stringer attachments. A torque motor drives each set of spools independently, as required by the specific position and velocity of the hoop joint being controlled. The deployment sequence is shown in Figure 2.2-13.

Hoop/Column Radar

The Grumman space-fed phased-array concept for self-deployable antennas is intended for designs up to several hundred meters in diameter for operation at L-band or S-band (Figure 2.2-14). Grumman developed this concept to the point of a preliminary design for a 60-m-diameter antenna and a 1.3-m (4-ft)-diameter mechanical model. The mechanical model was used to demonstrate and evaluate the basic mechanical conceptual design. Detailed design of a 300-m antenna was used in a NASTRAN finite element analysis, static and dynamic, to determine the tolerance-holding properties of the design. It was determined that tolerances can be held well under one one-hundredth of a wavelength at L-band. The primary limitation is the complicated deployment and the low frequency of the deployed membrane.

The Grumman antenna concept is a planar-type array whose basic support structure is a "wire-wheel" type configuration. This concept development was centered around the design of 61-m-diameter and 300-m-diameter space-fed, phased-array antennas for operation at L-band.

The basic elements of the support structure include the drum, rim assembly, fore and back stays, and telescoping mast. The phased array itself is composed of 32- to 72-gore panel assemblies and their tensioning devices (Figure 2.2.-15). The compression rim assembly is located and supported about the drum by the spring-loaded radial stays that extend from the rim to reels located on the drum assembly. This basic configuration is the "wire-wheel." The antenna drum for the 61-m antenna is 7.1 m long and 1.47 m in diameter, and is fabricated principally of aluminum alloy in frame-reinforced, thin-skin cylindrical configuration. Two support rings, external to and

23

HOOP

MESH SURFACE
STRINGERS
(QUARTZ)

RF REFLECTIVE
SURFACE

SECONDARY DRAWING
SURFACE STRINGERS
(QUARTZ)

MESH SHAPING TIES
(INVAR)
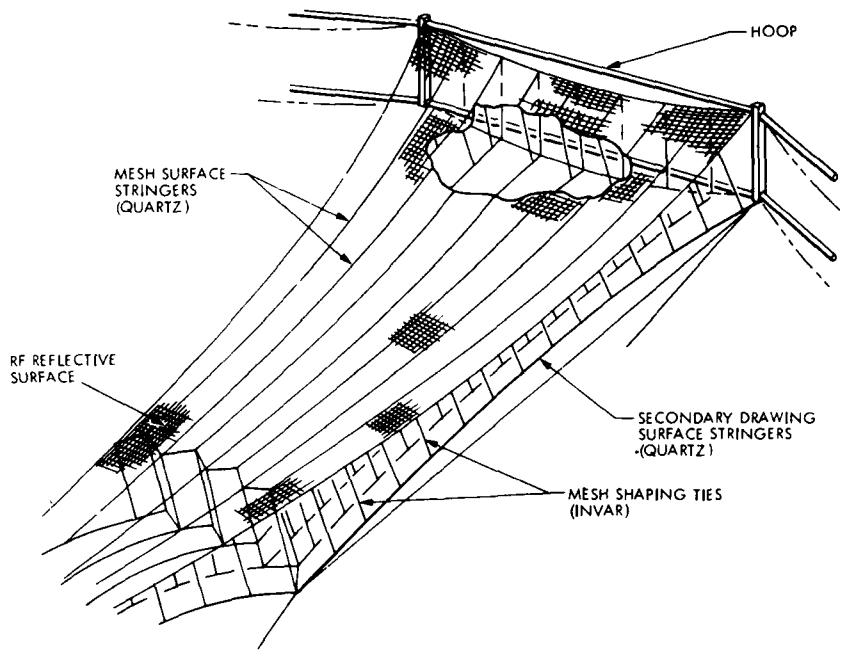
Figure 2.2-12   Mesh Shaping Configuration of Harris
Corporation Hoop and Column Antenna

24
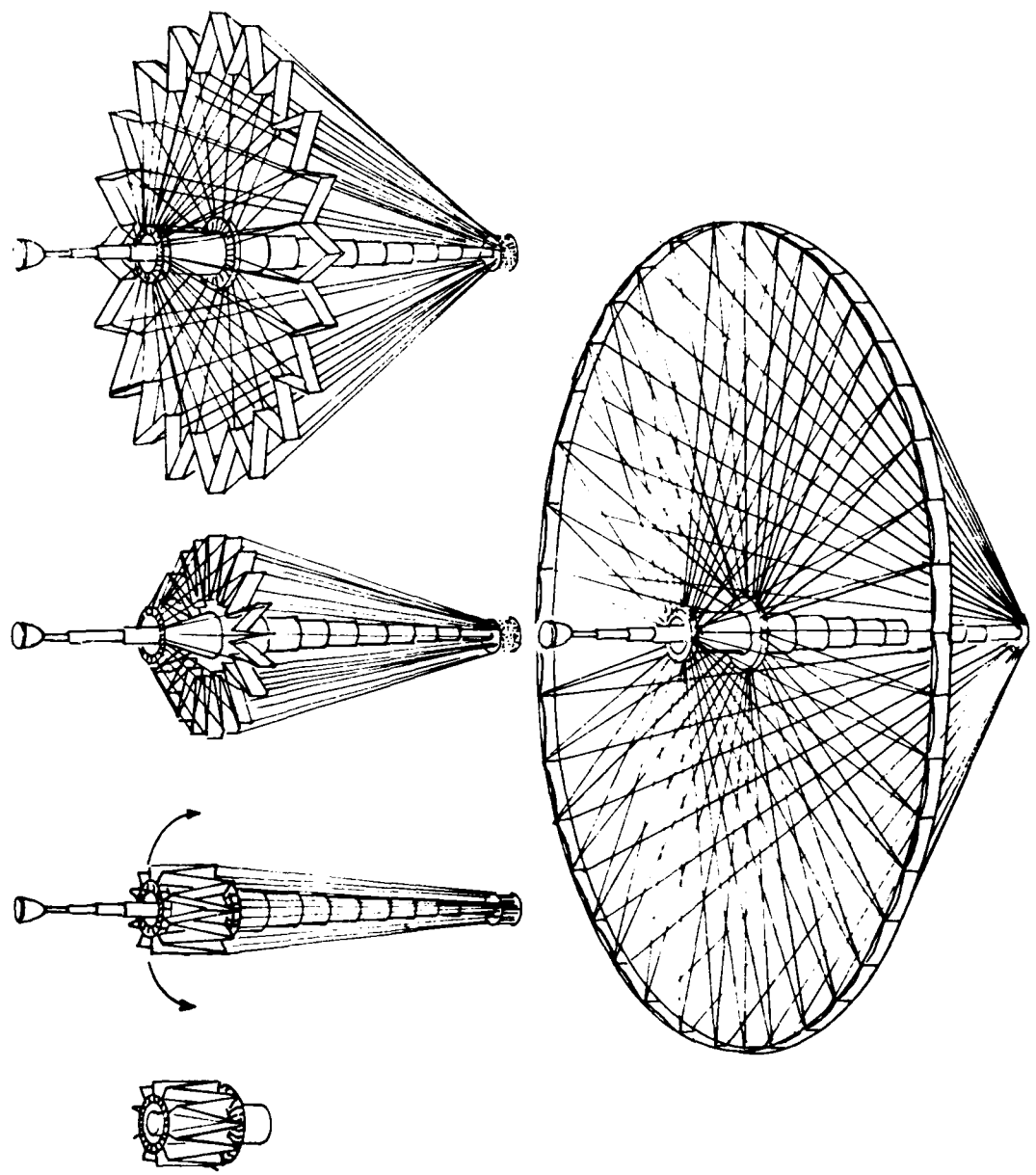
Figure 2.2-13   Harris Hoop/Column Deployment Sequence

25
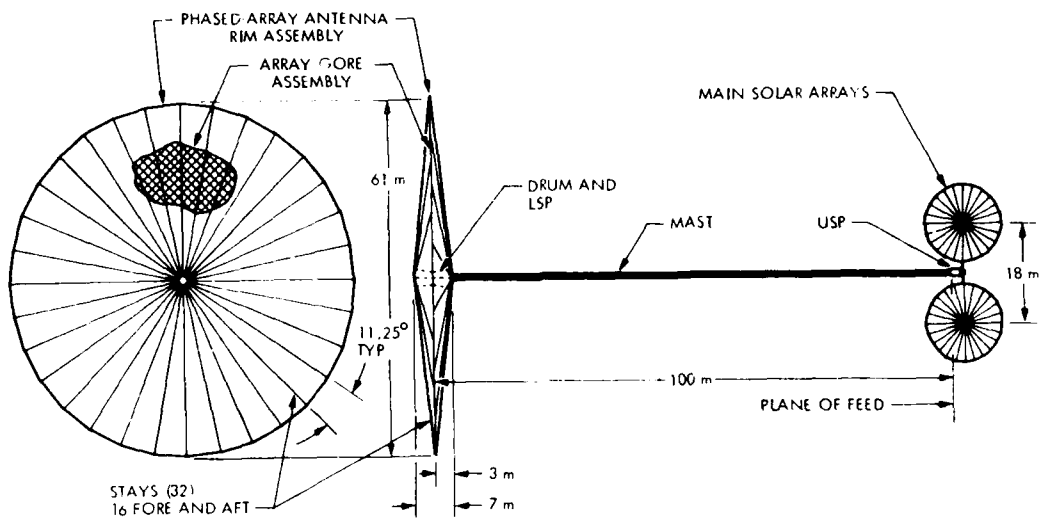
Figure 2.2-14   Basic Structural Elements of Grumman Phased-Array Concept
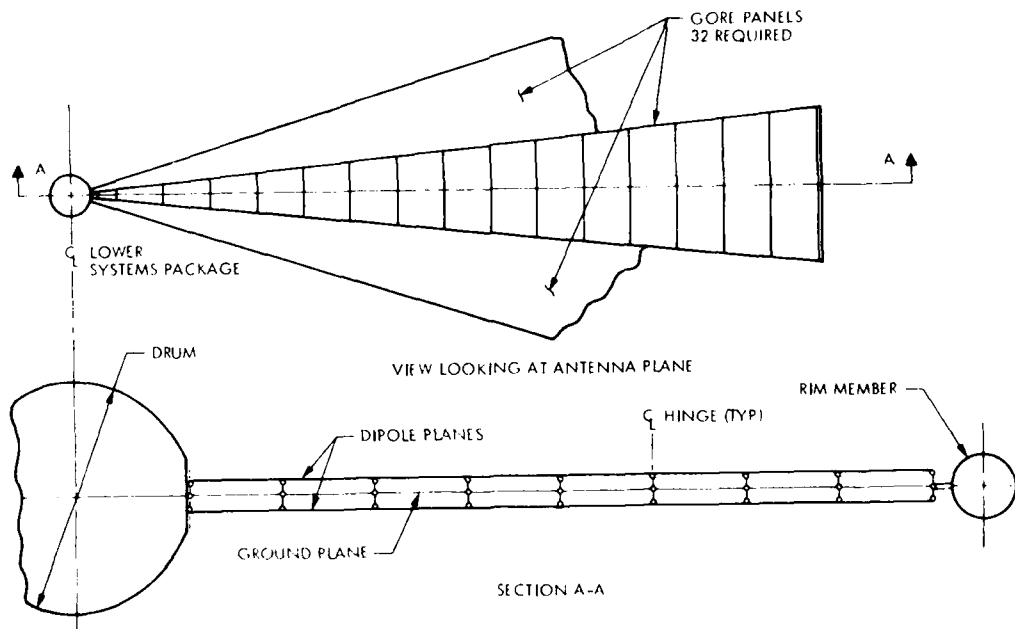
Figure 2.2-15   Grumman Phased-Array Planar Configuration

26

supported by the drum, and a multiplicity of antenna gore edge/batten support studs transfer the deployable hardware launch loads to the primary structure. The compression rim assembly is composed of 32 thin-wall graphite/epoxy tubes, 5.96 m long and 1.08 mm in diameter. The radial stays are graphite/ epoxy strips, 0.003 by 2.5 cm (1 in.). The gore panel assemblies are tensioned between the rim and the drum so that they form a plane. Operation of the antenna at L-band requires a rim assembly radial tolerance of the radiating elements of less than 0.8 cm (0.3 in.) and axially less than 4.6 cm (1.8 in.).

A 91.4-m Astromast locates and supports the antenna feed system and power source which consists of two deployable 14.2-m-diameter solar arrays that are based on the same depolyable antenna concept. The Astromast canister is located within the drum structure.

Polyconic Antenna

The parabolic surface of the polyconic reflector developed by LMSC is formed by a series of circular conical segments of lightweight reflective mesh as shown in Figure 2.2-16. These conical segments are positioned by mesh ribs and a series of radial booms mounted to a central hub. The radial structural booms and polyconic reflective mesh surfaces are folded in a vertical direction like an umbrella. The length of booms will determine the necessity of intermediate folds of each boom.

The parabolic surface is formed by a lightweight reflective mesh held in place by circular mesh ribs which are anchored to radial stiff booms. The desired surface accuracy is obtained by the use of many circular conic secttions joined, one to the other, in the circumferential direction. Each junction of one conic segment to the next is held by circular mesh ribs, the top edge of which forms the circular conic junction desired. The bottom edge is terminated in a catenary member which can be adjusted in length to produce desired reflective surface accuracy. The higher the surface accuracy desired, the larger the number of conical sections required. Like the wrapped rib reflector, the polyconic reflector must be designed to be sufficiently rigid to permit slewing without excessive weight or oscillation decay time.

The hub construction must provide support for the boom deploy and retract mechanism. It must provide the structural base for the hinged booms, it must provide the structural base for the feed mounting central boom and it must provide mounting positions for the automated "in space" surface contour evaluation and adjustment system.

Each radial boom is deployed from a vertical position. If the reflector surface is very large, each boom must be folded onto itself some number of times in order to fit the folded booms into the Space Shuttle cargo bay length. Screw jack controlled leverage will deploy the booms with articulation extension of the booms.

The feed is similar to that described for wrapped rib concept.

27

CATENARY
CIRCUMFERENTIAL
MESH RIBS

BOOM FOLDING
AND TILT SYSTEM

CIRCULAR
CONIC MESH SEGMENTS

CATENARY MESH
RIBS SUPPORT BOOM
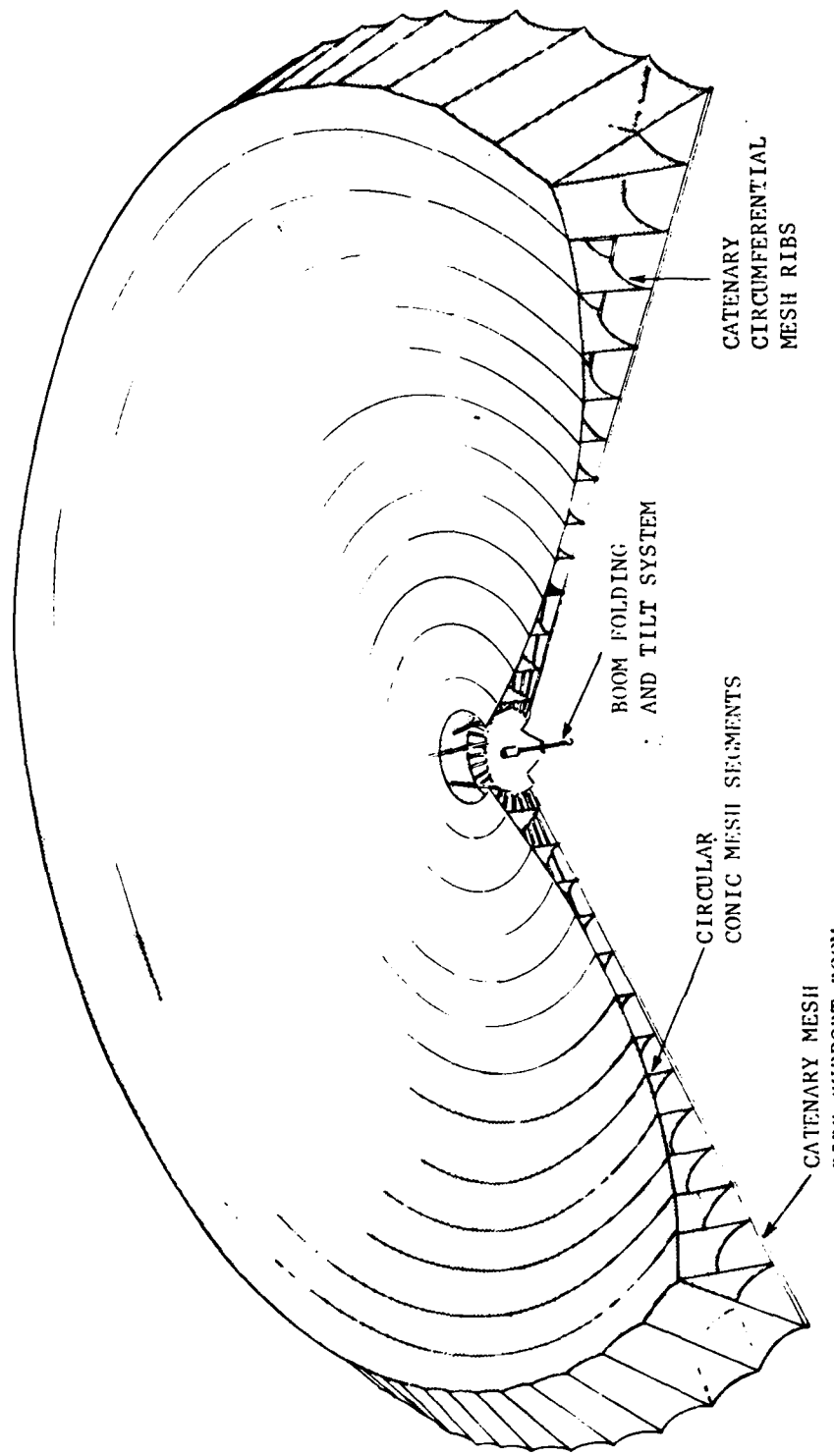
Figure 2.2-16   Lockheed Polyconic Reflector Concept

28

Since the radial booms that support the reflective surface do not wrap around the hub, as in the wrapped rib reflector, but fold into a vertical stowed position, the stowed configuration is limited only by the length of the cargo compartment. Dependent upon antenna diameter, some or all of the feed support boom may be of a fixed construction. The necessary extension beyond the approximate 60 foot fixed boom may be of similar construction to that described for the wrapped rib antenna.

The primary limitation of this concept is the complicated structure configuration and the deployment sequence.

Tetrahedral Truss Antenna

General Dynamics Corporation has developed the parabolic erectable-truss antenna (PETA) concept to the point of a hardware demonstration of a 5.2-m (18-ft)-diameter model (Figure 2.2-17). This model and other smaller models successfully demonstrated the antenna's self-deployment characteristics, provided verification of the mathematical models, and provided measured mechanical and RF performance information. This concept has been under development for more than 10 years; however, the latest version is based on using structural composite materials with low coefficients of thermal expansion. This concept has been developed to the point of flight readiness for antennas up to 15.2 m in diameter and larger. This concept has excellent characteristics to meet the mission requirements.

The PETA concept is a basic building block used in numerous combinations to achieve the desired shape and size of antenna structure. The basic element is a deployable tetrahedral truss that is hinged by spider links at each corner. Each tetrahedron forms one truss bay, which can vary in number from 4 to 10 or more, across the major diameter of the reflector structure. This configuration is the basis of the support structure for the RF reflective mesh and feed support structure. Components of the reflector structure have the same basic configuration design, regardless of the number of bays. Therefore, as the number of bays increases, for a given diameter, the number of mesh support points increases and the reflector surface improves. The selection of the number of bays, for a given antenna size and application, is a function of cost, reliability, weight, and surface tolerance. For example, the minimum weight for the larger size antennas, for a given material, is 6 or 8 bay versions. For this configuration, the basic reflector structure shape is hexagonal rather than circular, so the equivalent reflector diameter is about 10% less than the maximum point-to-point width.

Deployment of the basic tetrahedron is made possible by hinging of the struts at their centers with carpenter tape. This type of hinge provides for zero slop while maintaining with sufficient strain energy to accomplish deployment and an excellent mechanical lock-up in the deployed configuration. Deployment of the composite structure, which consists of a series of tetrahedrons, is essentially equivalent to that of a single bay.

Various materials including aluminum, titanium, and graphite/epoxy have been evaluated for application to the basic truss design. The choice of materials strongly influences the weight, cost, thermal distortion and

29

PACKAGED

PARTIAL DEPLOYMENT

FULLY DEPLOYED

HINGE

SPIDER

DIAGONAL

56.97 (60-FT. EQUIV.)

6 BAYS

10 BAYS

4 BAYS

8 BAYS

FEED MODULE

FEED SUPPORT (EXPANDABLE TRUSS)

24 FT.

15-FT. (FOLDED)
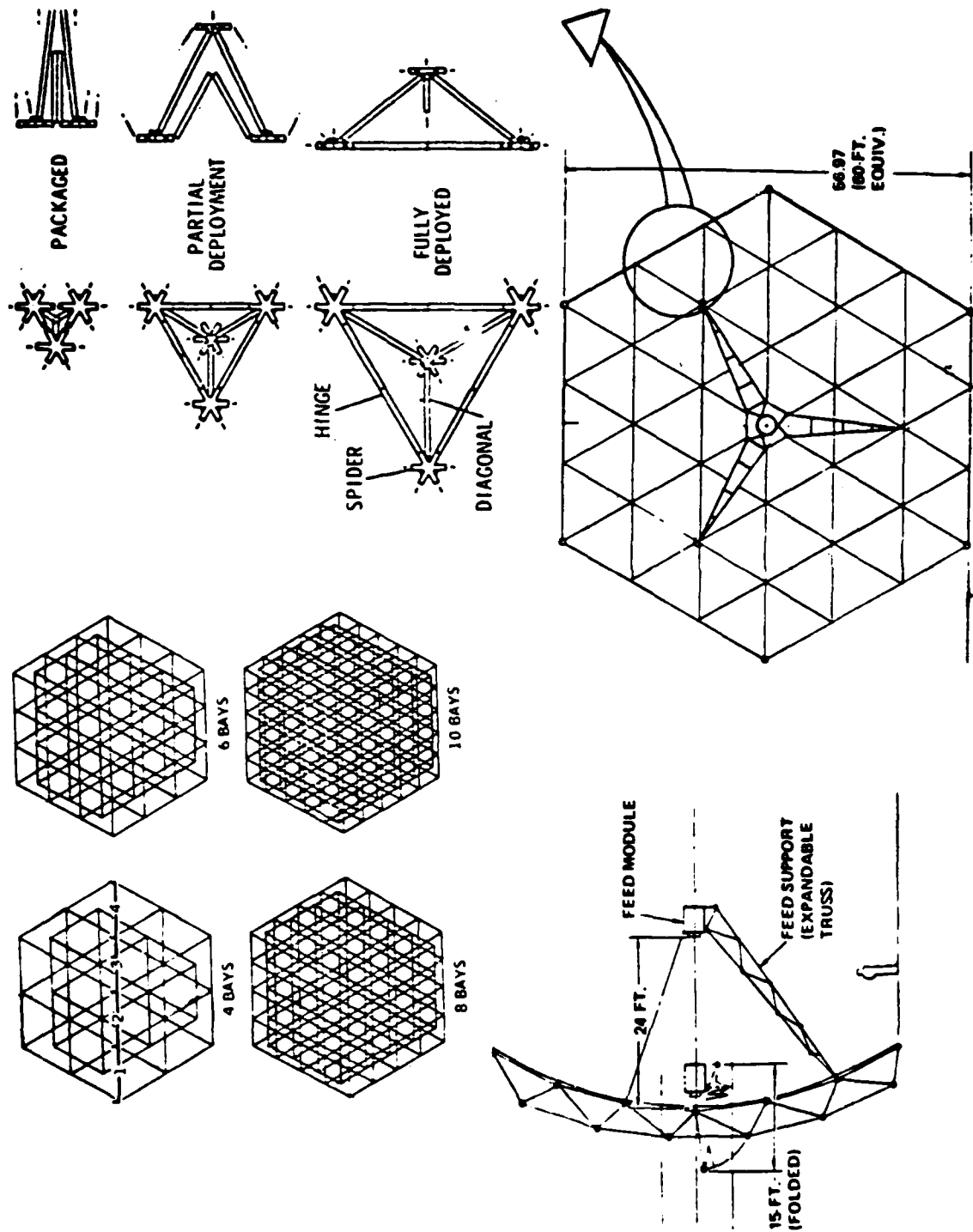
Figure 2.2-17   General Dynamics Expandable Truss

30

mechanical packaging efficiency of the antenna. Aluminum tubes provide the lowest cost material, but result in relatively high weight and thermal distortion. Perforated-wall aluminum tubes reduce thermal distortion and weight at some increase in cost. Perforated-wall titanium tubes produce low thermal distortions with weight slightly in excess of perforated aluminum tubes. Graphite/epoxy tubes produce a very lightweight truss with almost twice the packaging ratio of the perforated aluminum version, because of the smaller tube diameters that can be used with this material.

The RF reflective mesh is supported across each bay by a series of tension ties and a webbing attachment system that interfaces the tension ties with the mesh. The tension ties are attached to standoffs at each spider and span each bay with a simple grid pattern. The webbing system in turn is attached to the tension ties at a number of points to provide a finer grid pattern to which the mesh is attached. The resulting configuration of the mesh is eight flat surface elements, within each bay, that collectively approximate a parabolic surface. For example, in an 8-bay antenna there would be 64 adjustable flat sections across any single diameter of the antenna. However, for antenna high-frequency applications, 13 mesh-to-webbing ties are used along the edge of each bay.

Box Truss Antenna

Under contract to the United States Air Force's Space and Missile Systems Organization, Martin Marietta Aerospace has evolved a deployable box truss, large space structure concept that utilizes the shuttle Orbiter in an extremely efficient manner. Figure 2.2-18 shows the steps in the low earth orbit operations for this concept. An antenna module and an orbital transfer stage are carried to orbit in the cargo bay. The stowed module and its upper stage are being rotated up and out of the cargo bay on an aft-mounted hinge. After the initial steps are taken while attached to the orbiter, the module and stage are detached from the shuttle, after which the bulk of the deployment operation takes place. After the module is fully deployed and checked out, the upper state transfers it to an operational orbit.

The concept is applicable to a wide variety of large aperture sensor systems or platforms. Utilizing state-of-the-art technology in graphite/epoxy structural members combined with the natural efficiency and stability of a deep truss, the concept will provide a combination of high passive precision and low weight. This concept has excellent potential for meeting the mission requirements.

Figure 2.2-19 illustrates the basic concept's operating principle. Vertical members connect the front and back surfaces of the truss and carry support posts upon which the antenna surface is mounted. Surface tubes, hinged in the middle, connect each vertical member to each of its neighbors. Each truss square, composed of surface tubes and vertical members, is stabilized by diagonal tension tapes. For stowage, each surface tube folds about its mid-link hinge and the diagonal tapes form a coil between the stowed mid-link hinges.

Structural deployment is accomplished in low earth orbit (LEO) near the

31
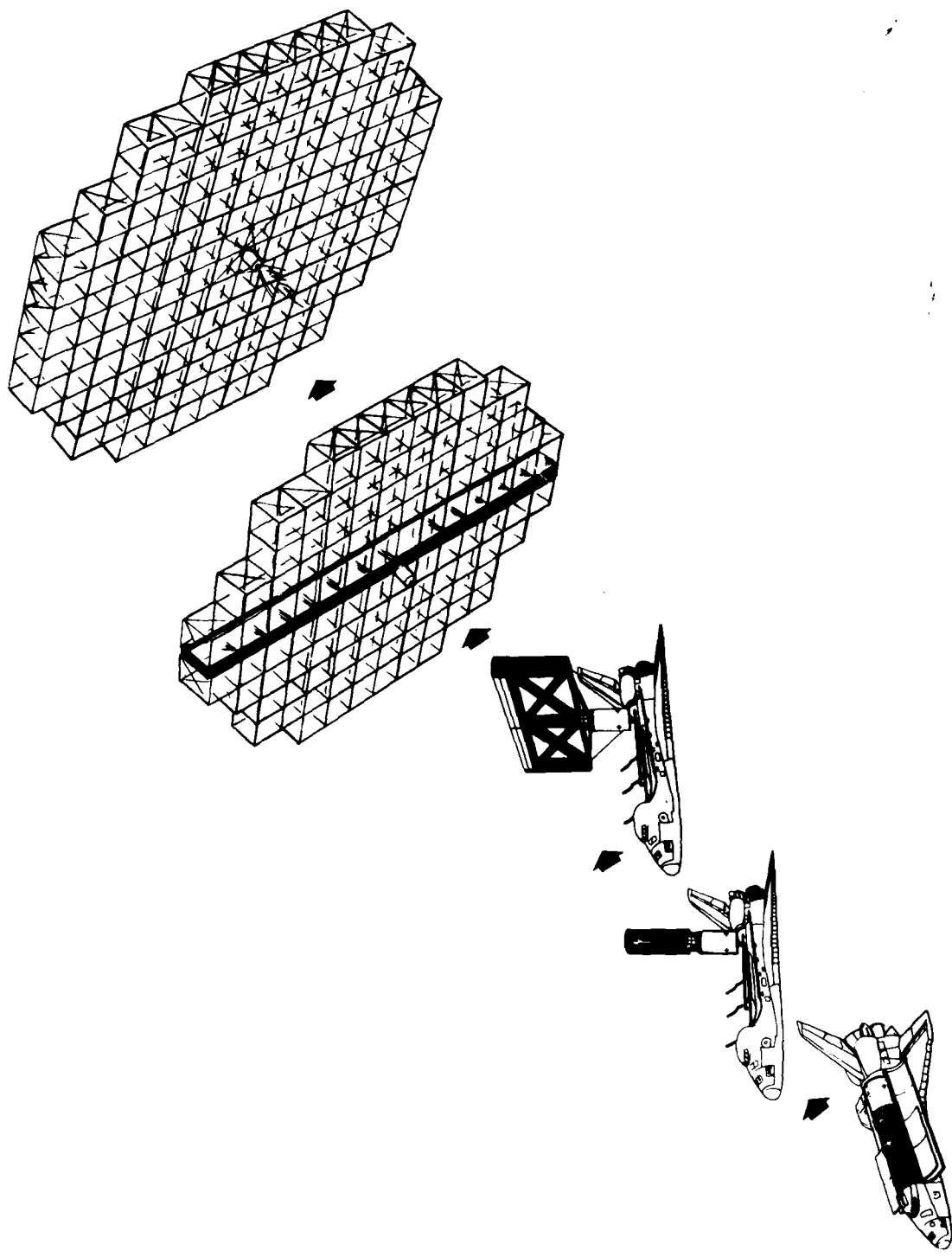
Figure 2.2-18   Box Truss Deployment Scenario

32

Mesh Support Posts

Cube

Truss

Frame

Surface Tube

Vertical Member

Diagonal Tape

Stowage

Midlink Hinge

End Fitting
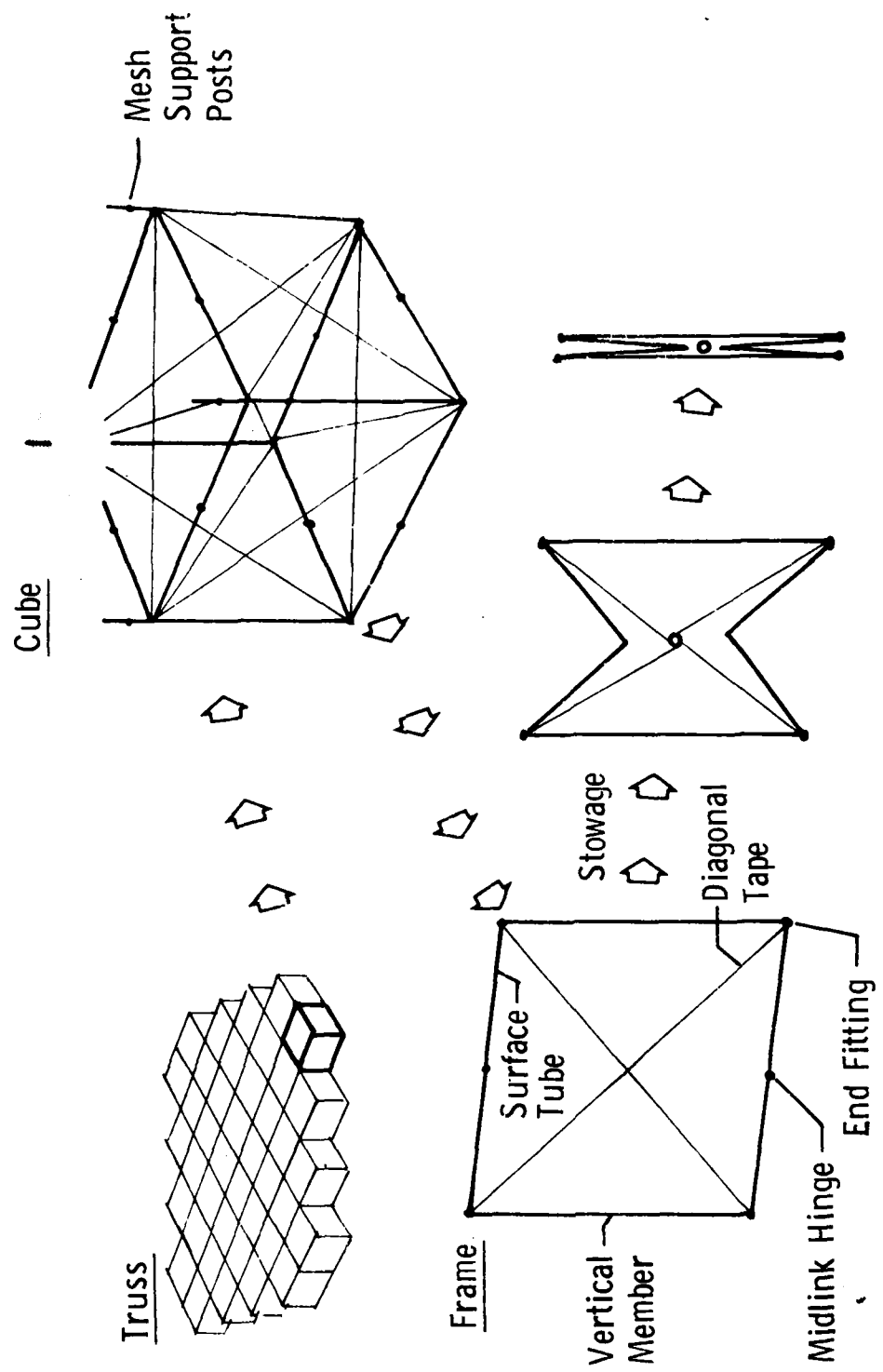
Figure 2.2-19   Martin Marietta Deployable Box Truss

33

orbiter in a sequence of controlled steps. Figures 2.2-20 and 2.2-21 give an example of this sequence for a truss that is composed of 24 cubes forming six rows and six columns. In the example, the cube faces forming the innermost row on each side of the centerline are deployed first. Following verification that this step has been completed successfully (a procedure followed between all steps), the outermost rows are deployed. Symmetrical pairs are always deployed simultaneously to balance reaction forces. This preserves the deploying structure's attitude and center of gravity position. The row deployment step involving the middle rows on each side results in full deployment in the row direction. Figure 2.2-21 illustrates the three column deployment steps, in this case working from the outside to the center, in a sequence that completes truss deployment.

Prototype designs for all structural members and mechanisms have been defined. Electrically controlled, redundant, deployment release latches connect each vertical member's end fitting to the neighboring stowed verticals' end fittings. These latches provide the desired controlled release sequence. Redundant coil springs in the mid-link hinges drive the deploying structure. As each surface tube swings out to its deployed condition, a spring-loaded latch in the mid-link hinge locks the tube straight and provides the impulse necessary to tension the diagonal tapes and array surface.

Deployment dynamics anlayses have been made for typical cube faces throughout the deploying truss. Since boundary conditions vary from cube face to cube face, e.g., the outboard mass being accelerated by a given cube face's springs varies, the spring torque profiles are tailored to their locations in the truss. The springs are sized by three requirements: (1) with all springs operating at ten percent over nominal (energy input), the surface tubes are not overstressed; (2) with one spring out of each pair of redundant springs failed, enough energy is still available to deploy each cube face and tension its diagonal tapes and array surface; and (3) with nominal spring performance, all cube faces in a given row or column will deploy at the same rate. Typically, a row or column requires approximately 45 seconds to deploy.

Various types of antenna surfaces have been considered for large aperture spaceborne antennas. These range from simple R.F. reflective meshes to multi-layer phased arrays that include power distribution and subarray electronic modules. The concept for array surface stowage on the deployable box truss involves double-accordion pleating. One set of pleats is parallel to the truss column direction and the second set, at ninety degrees to the first, parallels the rows. As shown in Figure 2.2-22, the small row pleats unfold as the rows are deployed, leaving the larger column pleats still folded. The latter then unfold sequentially as the column deployment steps take place.

This array folding concept, with its orthogonal fold lines, accommodates mesh surfaces easily and, more importantly, allows the surface to contain regularly-spaced, non-foldable objects such as subarray electronic modules. In the case of the planar phased array surface, these modules are located on 30-inch centers throughout the surface. The column fold lines on 60-inch centers and the row fold lines on 6-inch centers are located to avoid all of the modules.

34

Stowed

Attached to Orbiter
After Separation

Row Deployment
Complete
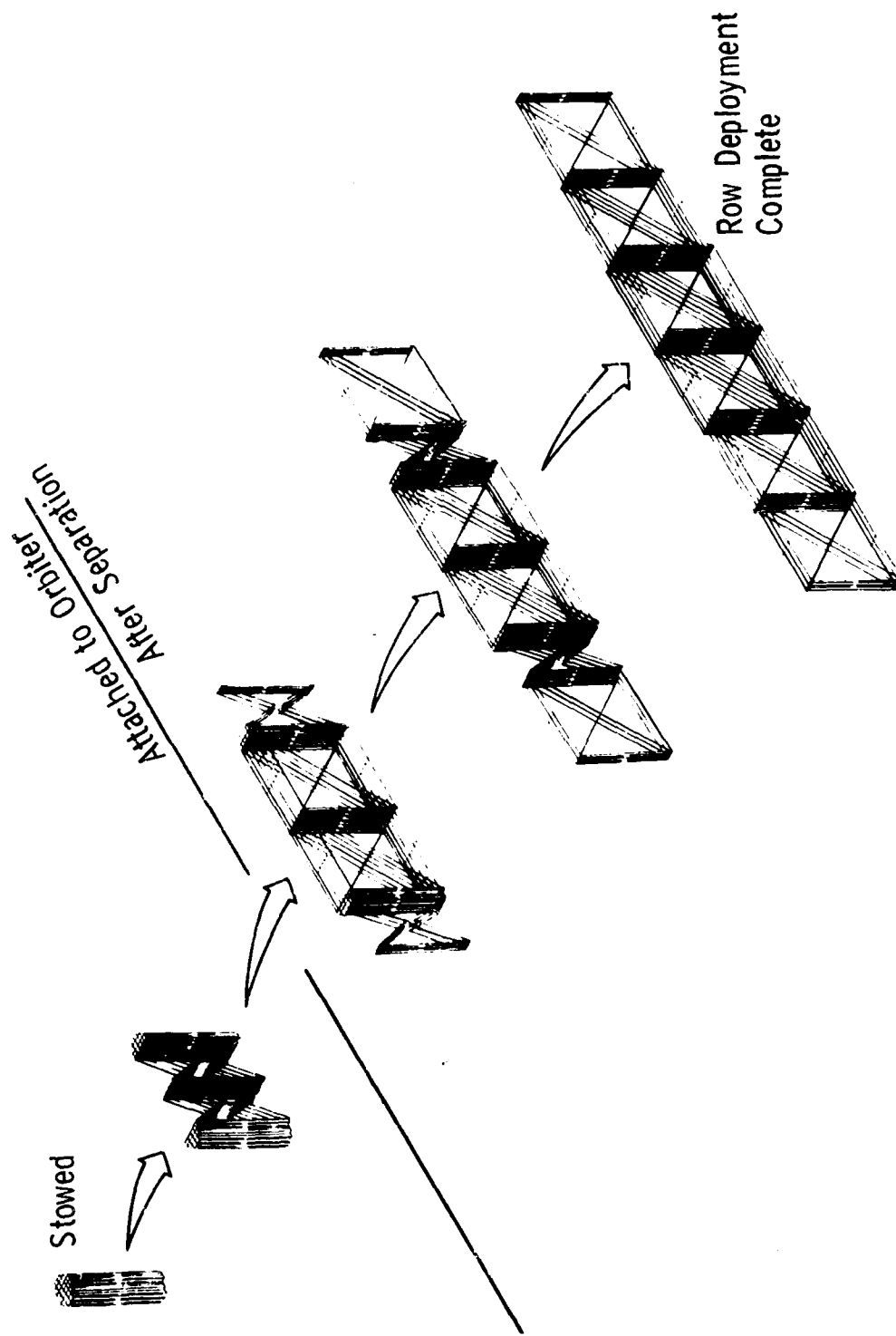
Figure 2.2-20   Box Truss Step By Step Row Deployment

35

Second Columns

First Columns

Fully Deployed Truss

Third Columns
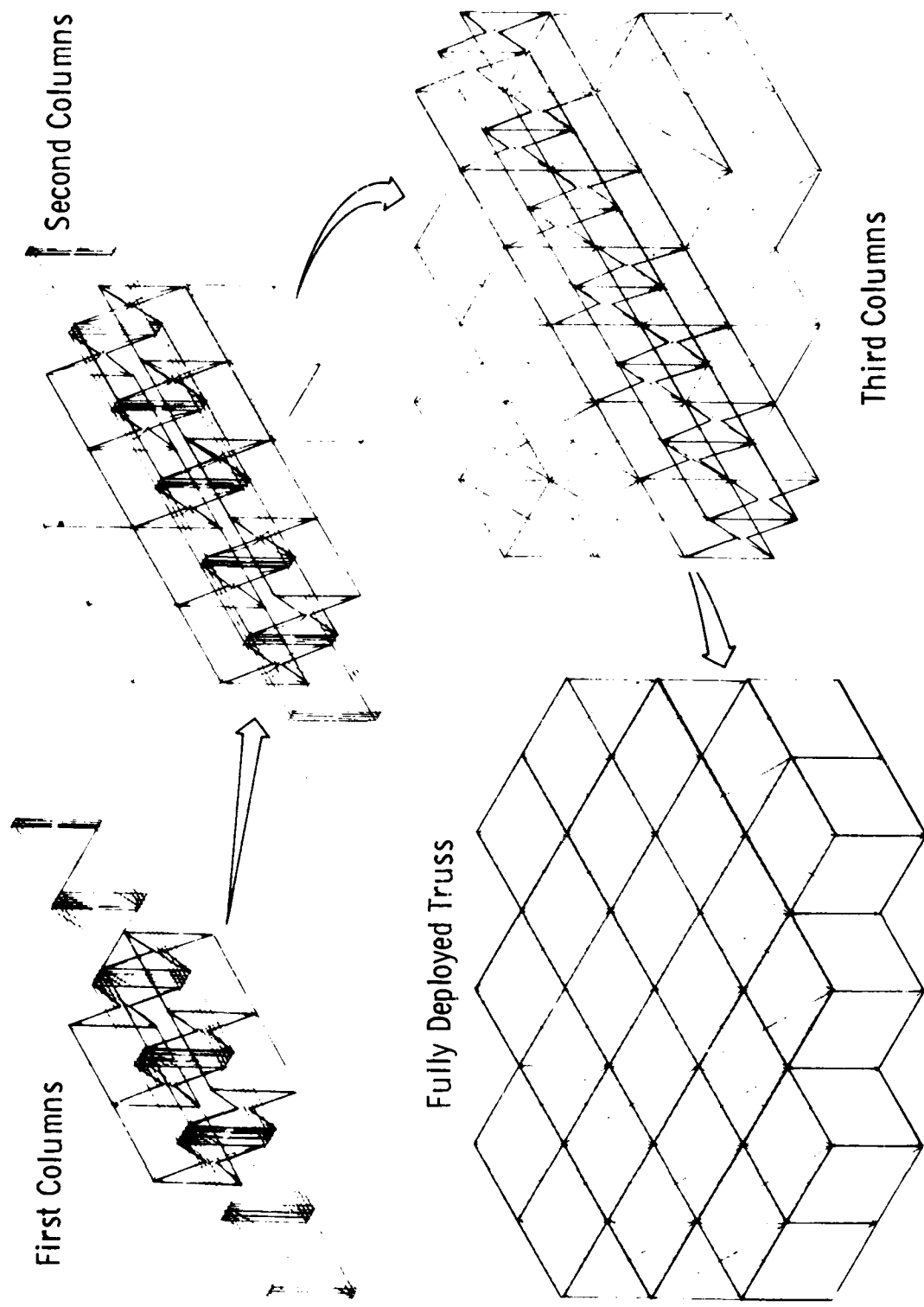
Figure 2.2-21   Box Truss Step By Step Column Deployment

Solid Deployable Reflector

TRW demonstrated concept feasibility with a 2.1-m (7-ft) mechanical model and developed the preliminary design for a 7.3-m (24-ft)-diameter, precision-deployable antenna reflector capable of operation at frequencies up to 60 GHz (Figure 2.2-23) and above. The antenna design provides RF efficiency of 70%, with a beam pointing error less than 0.04 deg. The estimated 72.5-kg (160-lb) weight for this design includes the subreflector, support structure, and communication beam autotrack feed package. The deployed natural frequency is estimated at 5 Hz. The mechanical design features graphite/epoxy composite hinged-panel construction. The design is capable of withstanding conventional or Shuttle launch loads. The primary limitation of this concept is that the maximum allowable diameter is 50 ft for a Shuttle package launch.

This deployable antenna concept provides a large, lightweight, precision contour parabolic reflector. The concept was developed for a shaped Casse-grain antenna application with a single high-efficiency data beam/multimode autotrack system. The design is applicable to multibeam configurations. Greater than 70% efficiency can be attained at 60 GHz with a beam pointing error of less than 0.04 deg. The reflector is constructed of graphite/epoxy facesheets and aluminum core sandwich to provide an extremely light-weight reflector. The reflector weight is 67.6 kg (149 lb) for a 7.3-m-diameter design, including thermal paint and the stowage release mechanism. The subreflector/support struts weight 1.3 kg (2.8 lb). The feed system weights 2.95 kg (6.5 lb). The total estimated weight is about 72.5 kg without contingency.

The center section is a one-piece honeycomb sandwich construction. The folding panels are rigid honeycomb sandwich. The main panels hinge from a support ring under the center section. The two intermediate panels lie bet-ween, and are connected to, the main panels and to each other with two or more hinges. The hinges have adjustable stops to locate the panels accurate-ly in the deployed configuration. Springs are used in the hinges to drive the panels to the deployed position. Adjacent inboard hinges of the main panels are interconnected with a compound universal coupling to ensure syn-chronization of all panels during deployment. The deployment rate is con-trolled by either a damping device or a geared motor. The furled reflector is restrained by a pin puller, which is ordnance released, and supported on one of the tiedown fittings. The tiedown fittings extend beyond the edge of the intermediate panels and are connected at a common joint on the re-flector axis.

A 4.9-m-diameter reflector was chosen for a "paper" study consisting of a preliminary design, structural analysis, thermal distortion analysis, and a weight estimate. The 1.3-cm (1/2-in.)-thick sandwich construction for the reflector utilized three-ply graphite/epoxy face-sheets 0.2229 mm (0.009 in.) thick, and an aluminum core with a 0.6-cm (1/4-in.) cell size and density of 25.6 kg/m (1.6 lb/ft). The support ring under the fixed cen-ter section was a rectangular tube cross-section 5.1 cm x 7.6 cm x 0.76 cm (2 in. x 3 in. x 0.030 in.) thick. The hinges interconnecting the panels were made of aluminum. The main panel inboard hinges that attach to the

Row Deployment

Double Accordion-Pleated Surface

Column Deployment
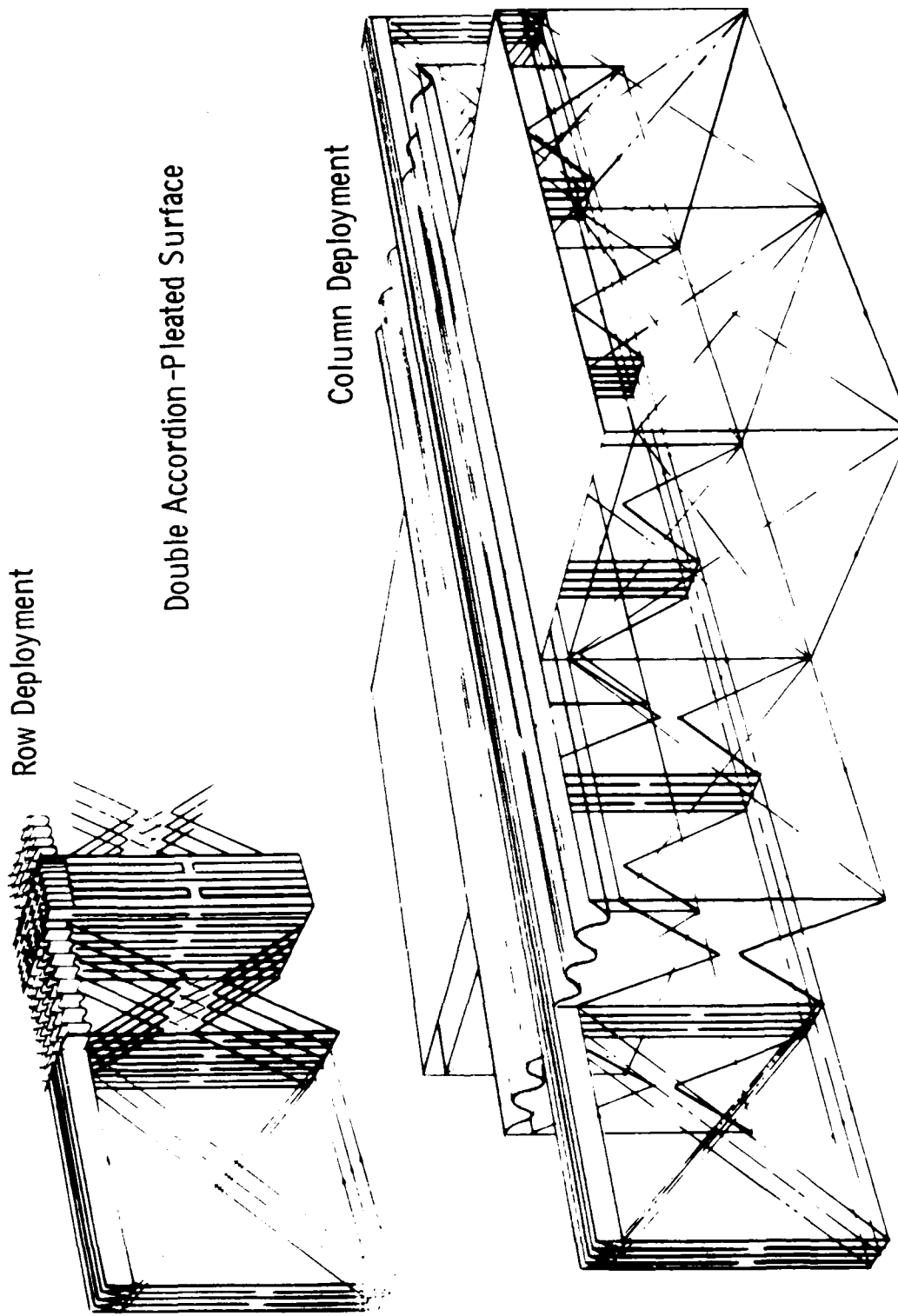
Figure 2.2-22   Box Truss Antenna Surface Stowage/Deployment

38
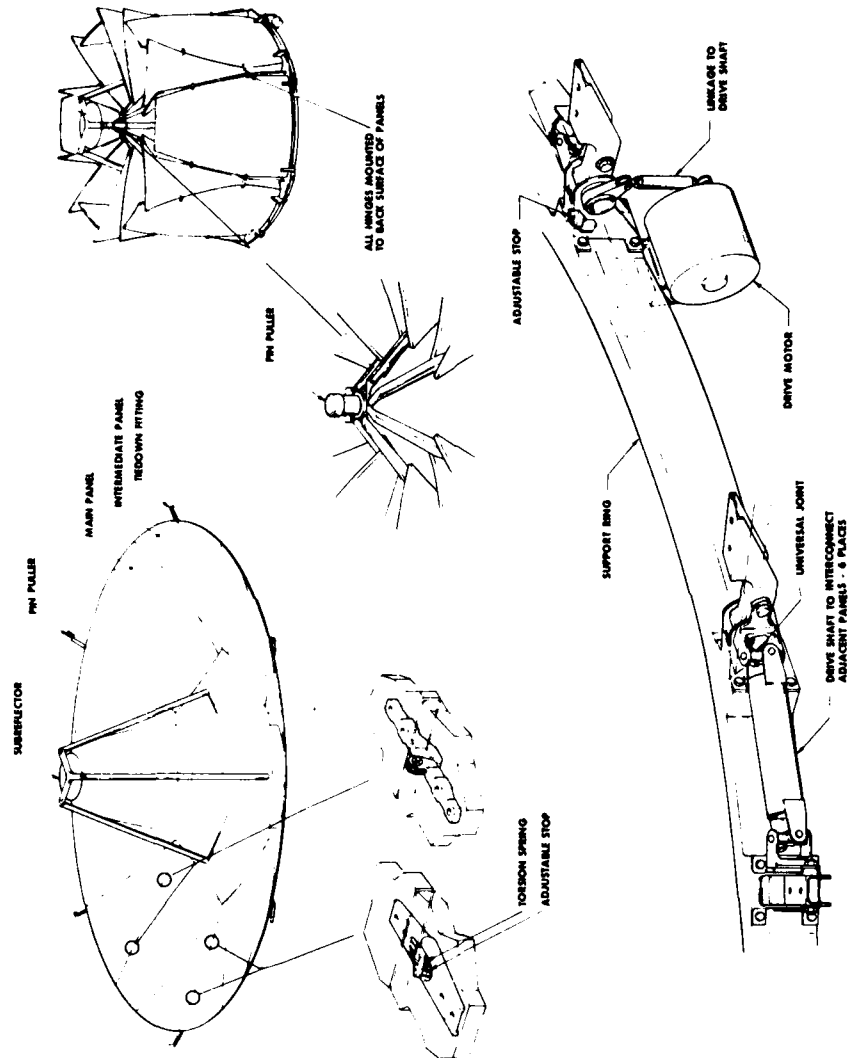
Figure 2.2-23   TRW Solid Deployable Reflector

39

support ring were made of graphite/epoxy composite. Because of weight considerations, no thermal control shroud or insulation was used to reduce temperature gradients. However, thermal insulation could have been used on the back of each panel. Load factors of 12 g lateral and 10 g axial relative to the reflector axis were assumed for the structural analysis.

High Frequency Radial Rib Antenna

LMSC recently developed a concept for a high-efficiency, large-aperture, millimeter-wavelength parabolic reflector antenna. With this concept, an antenna up to 18.3 m (60 ft) in diameter for operation up to 60 GHz can be accommodated by one Shuttle payload (Figure 2.2-24). This concept, which is based on the application of the very latest composite materials technology, is currently being developed into a preliminary design. The primary limitation is the diameter limitation of 60 ft.

The basic structure for this concept consists of a series of radial ribs that fold about their base, which is attached to the antenna hub structure. The RF reflective surface is formed by a series of individual concentric rings that are individually supported by the radial ribs. This series of thin, conical rings, whose edges are accurately aligned with adjacent rings, approximates the desired parabolic shape. The rings themselves are made from very thin strips of graphite/epoxy, 0.25 mm (0.010 in.) thick. The thin rings are similar to carpenter tape in that they can be elastically folded for the stowed configuration and then deployed into a predetermined circular shape made possible by the physical properties of the rings. Each ring is attached to each rib for its support, but not to the adjacent rings. The width and number of rings used determine the surface accuracy.

Deployment is accomplished with an electromechanical mechanism for rotation of the ribs and deployment of the feed support structure. The Space Shuttle payload compartment is expected to accommodate an antenna of this concept up to 18.3 m in diameter.

Expandable Module Astro Cell Antenna

Astro Research Corporation and NASA Langley have developed a modular approach to assembly of large precision reflectors. (See Figure 2.2-25). The individual modules are packaged for launch, so as to utilize the volume of the Shuttle properly, and then expand in orbit.

This concept can be used to construct large platform-truss areas for supporting "payload panels" which may be accurate reflectors, waveguide arrays or solar-power panels. The module's shape and stowed configuration are selected to utilize the Shuttle payload volume efficiently. Note that the "payload" is preattached to the structure at three points which could include means for adjusting the panel position. The assembled surface can be made curved by appropriate precut lengths of the module's structural members.

The structure consists of the upper and lower triangular frames and the diagonals. The curved "longerons" are not part of the primary structure; they are prebuckled and therefore supply the forces necessary to pretension
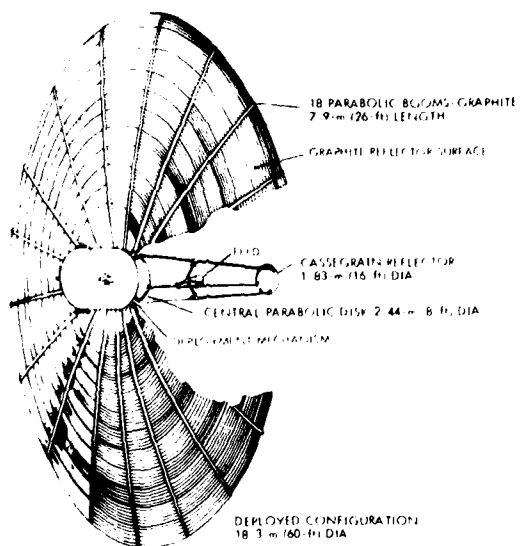
Figure 2.2-24   LMSC High-Frequency Radial-Rib Antenna
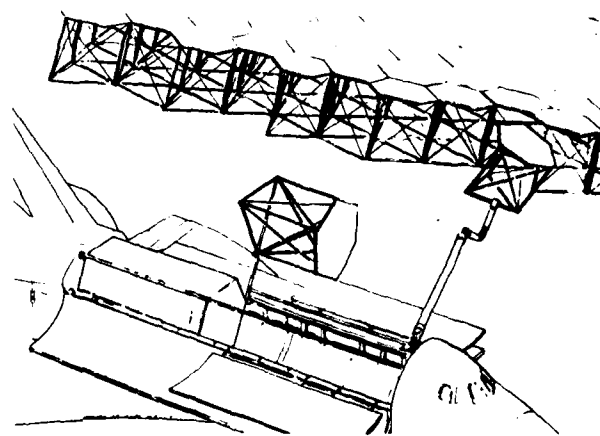
Figure 2.2-25   Astro Research Expandable Module Assembly
                 Approach

the diagonals. The module is capable of carrying compression with full stiffness. The design of the hinges and other attachments has been carefully throught out so as to achieve maximum compactness. The depth of the packaged module is just the sum of the triangular-frame thicknesses. The deployment motion is quite similar to that of one bay of an Astromast lattice column.

The joints between modules must provide a good structural tie. They must also provide for electrical connections. One attractive concept for meeting these requirements is the probe-and-drogue. The probe-and-drogue arrangement facilitates engagement, and a torqued fastener on the end of the probe precompresses the joint to cement the marriage. Full modularity is enhanced by providing the universal triangular transition piece in which the variations in electrical circuitry can be accommodated.

Hex Panel/Truss Antenna

There are a wide variety of millimeter-wave antennas that utilize rigid honeycomb panels that are assembled to a deployable or erectable tetrahedral truss structure. Three concepts are shown in Figures 2.2-26, 2.2-27 and 2.2-28. These concepts differ from the expandable module Astrocell in that the structure is deployed or erected and then the honeycomb panels are attached to the structure.

Rectangular Panel/Deployable Truss Antenna

Martin Marietta has developed an approach to deploying and assembling a large millimeter wave reflector system. The concept shown in Figure 2.2-29 utilizes an automatically deployable box truss structural platform. The panels which are assembled to the truss after truss deployment are graphite epoxy honeycomb and are rectangular. The rectangular shape was selected to maximize the packaging efficiency in the Orbiter while providing the largest panel segments. The box truss structure is configured with a matching rectangular configuration. This allows each panel to attach to the vertical corners of a box.

Panel adjustment provisions are provided at the three vertical members where the panels are attached to the structure. These adjustment mechanisms allow panel location adjustment to eliminate the effects of thermal deflection of the support structure.

Electrostatic Membrane/Deployable Truss Antenna

The Electrostatically Controlled Membrane Mirror (ECMM) developed by General Research is revolutionary approach to achieving large, very light reflectors for radar, radio astronomy, radiometry, and optical devices. (See Figure 2.2-30). The ECMM is a thin, electrically conducting membrane that is accurately tensioned and positioned by electrostatic (Coulomb) forces. The reflector's shape (figure) is maintained by varying the electrical potential between the membrane and segmented electrodes behind it, using closed-loop control. An important component of this adaptive structure is the figure sensor, which monitors the surface quality to furnish error
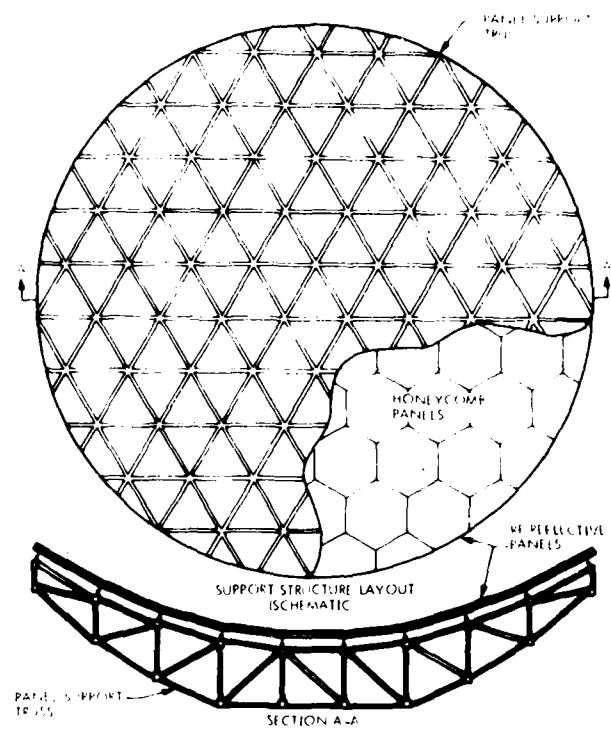
Figure 2.2-26   Caltech Configuration of 10-m Millimeter-
                 Wave Antenna
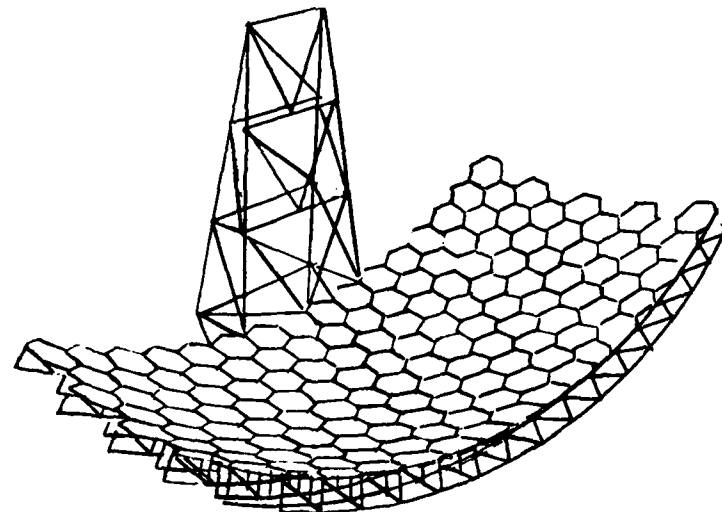
Figure 2.2-27   Rigid Panel Millimeter Wave Radiometer
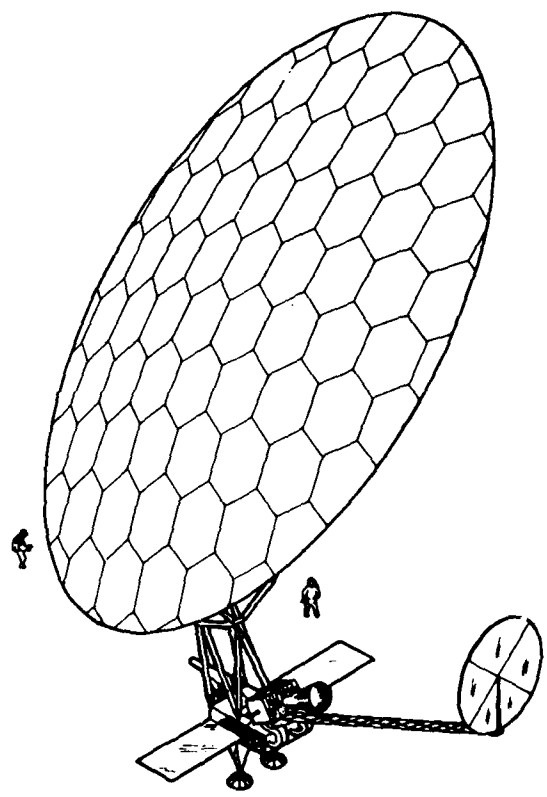
Figure 2.2-28   A 28 Meter Deployable Truss With Hexagonal Panels
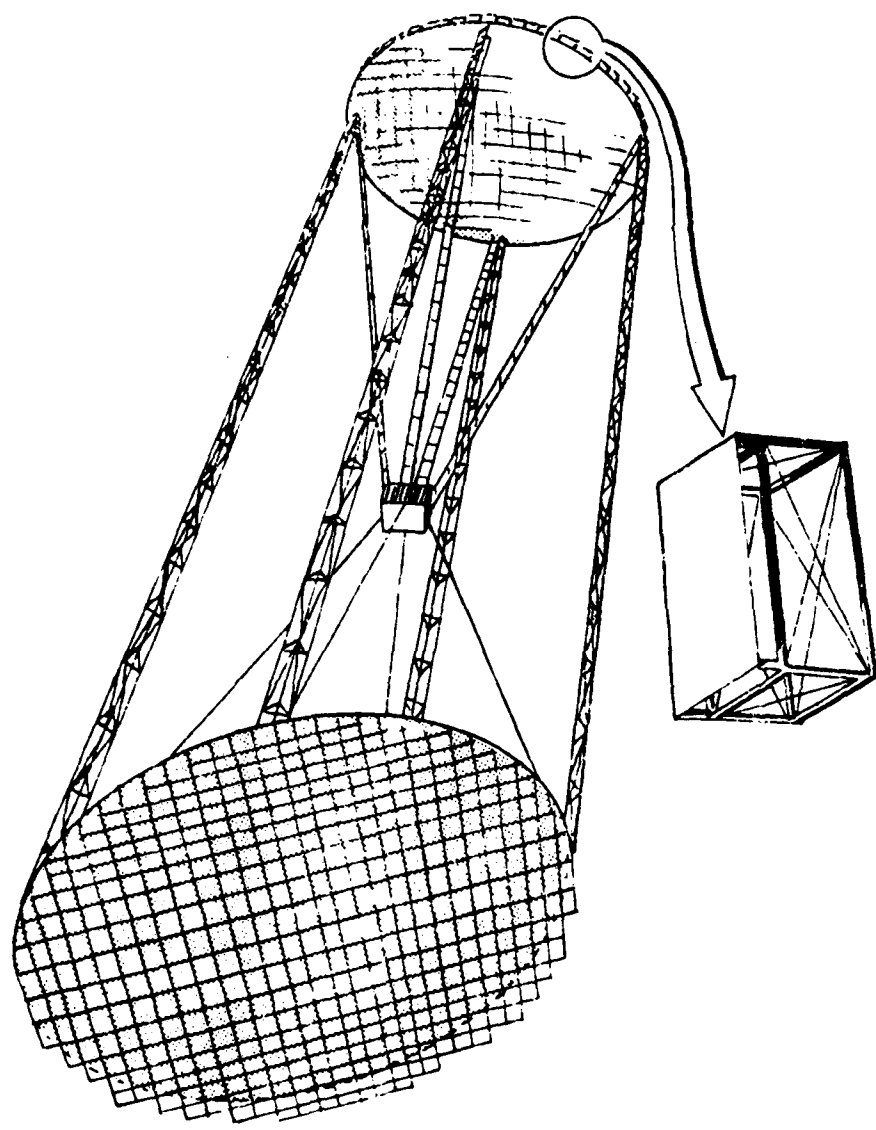
Figure 2.2-29   Martin Marietta Radiometer Concept Using Box Truss
And Solid Panels

45

signals to the control loop.

Analytical and experimental efforts in the last several years indicate the possibility of employing the ECMM for high-surface-precision reflectors in both ground and space applications. In both situations, design goals are to achieve a ratio of aperture diameter to RMS surface waviness of 10^5 to 10^9. Achieving such precision in light structures is difficult if not impossible without some form of active control. With active control-positioning the membrane to a required figure automatically--surface precision may be achieved despite the presence of various disturbances. In effect, great improvements in surface accuracy over passive reflectors are expected because optical-electrical circuitry can provide long-term positional stability of the membrane.

The ECMM, is essentially a charge capacitor with the deformable reflector as one of its electrodes. When a voltage is applied between the unstressed membrane and the back electrodes, the electrostatic attractive force draws the membrane inward. An electrical network is used to generate the required high field strength between the supported back electrodes and the deformable membrane electrode. The pressurized membrane deforms to a doubly curved surface, unlike "draped-mesh" reflectors, which are made up of flat or singly-curved sections. A membrane acted upon by a pressure loading naturally forms a concave surface of the sort required for most antenna reflectors. The fixed back control electrode is segmented into electrically isolated elements, each supplied with a different control voltage and thus exerting a different field strength and pressure on the membrane. Like pneumatic pressure applied to a deformed balloon, the electrostatic force is always normal to the (conducting) membrane; but unlike pneumatic pressure, the electrostatic loading can be rapidly changed and can be different at different points on the membrane, thus forming different reflector geometries.

Thin Film Controllable Antenna

Massachusetts Institute of Technology is currently developing a new and unique antenna concept that seeks to approach the ultimate limit for RF performance (Figure 2.2-31). Antenna beam widths of several arc seconds are sought for mesh or 2- to 10-μ-thick film that is configured to the approximate reflector shape by its basic support structure, and then distended electrostatically into a high-precision surface. This concept has been evaluated analytically for antennas from 20 m to 1000 m in diameter. The construction of a 1-m-diameter conceptual mechanical model that is currently in process at MIT will be used to demonstrate and evaluate this concept. The development of this concept is based upon obtaining high-precision RF reflecting surfaces by using a distributed control system and very lightweight and flexible reflector surface materials whose excellent packaging efficiency is expected to accommodate construction of large antennas.

The antenna configuration consists of a basic reflector support structure, which could be either deployable or erectable; a precision RF reflective surface; and a secondary surface that is located "behind" and almost parallel to the primary surface. The secondary or "command" surface is supported and contoured to the approximate desired reflector shape by the basic support

46
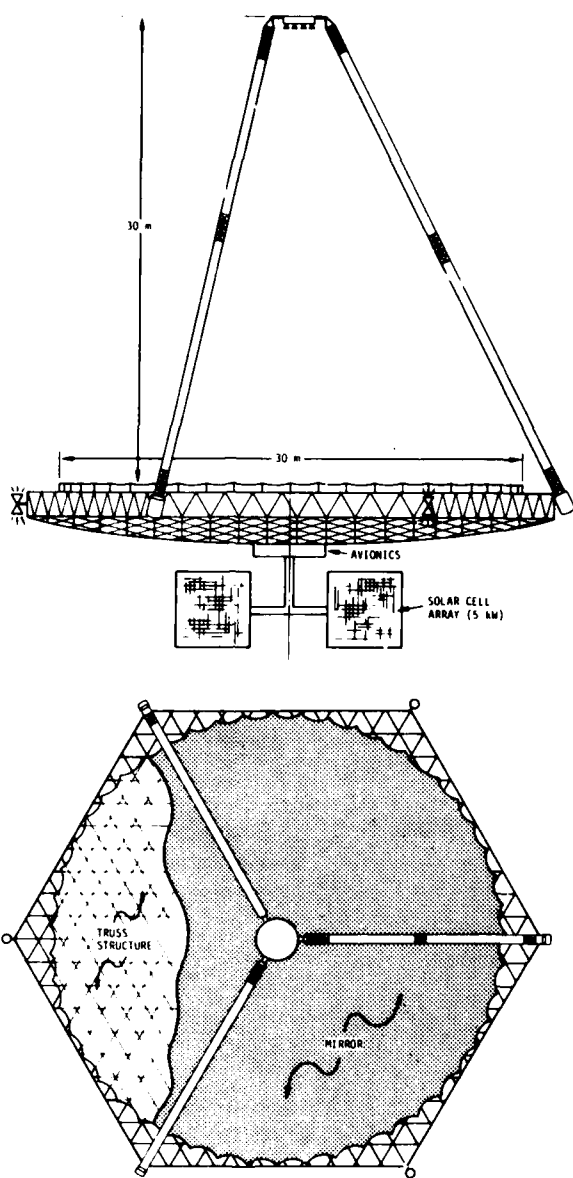
Figure 2.2-30   General Research 30 Meter Electrostatic Controlled
                  Radiometer

47
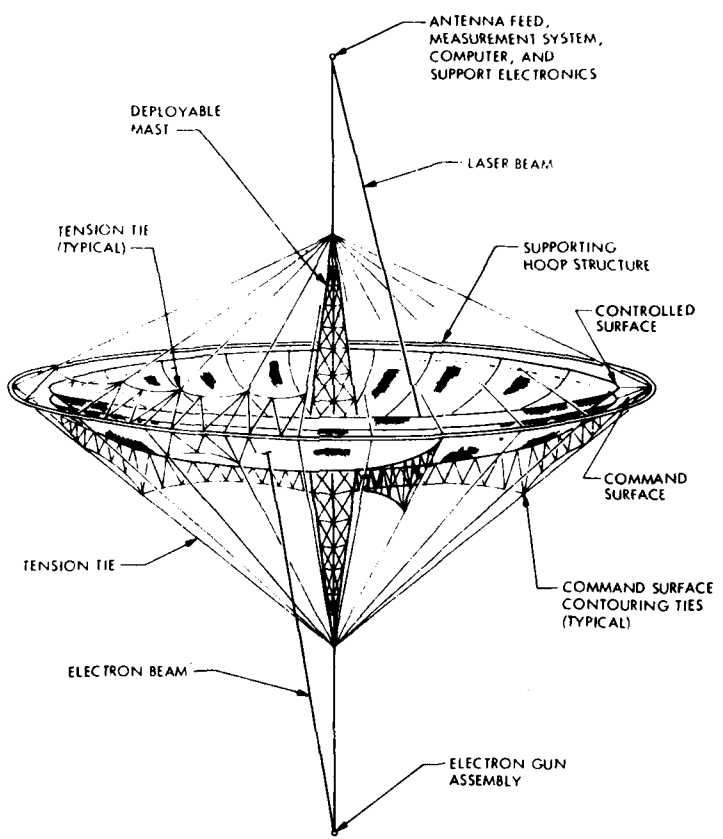
Figure 2.2-31   MIT Controlled Thin-Film Antenna Concept

structure. The shape of the extremely flexible RF reflective surface is produced by 10^4 to 10^6 discrete electrostatic forces acting between the "controlled" surface and the "command" surface. These forces are made possible by 10^4 to 10^6 electrically insulated elements, which are located on the command surface and controlled by a single electron gun with the capability of changing the electric charge on each element. The magnitude of the electric charge is a few thousand volts. The control system for the electron gun is based on the output of a surface sensing system utilizing a rapidly scanning laser that continuously measures the quality of the RF surface. For flight applications below geostationary Earth orbits, the electrons from the gun may be deflected significantly by the terrestrial magnetic field, so other approaches to charge control might have to be used, especially for larger antennas.

This type of thin-film or mesh support structure is expected to be between 5 and 50 g/m^2. If the mechanical packaging efficiency of the support structure is high, then it is conceivable that an antenna of 1 km could be accommodated by one Space Shuttle payload. For an antenna of this size, analyses have shown that the controlled surface and the command surface should be separated by several meters, and the command surface must be within a few meters, peak to peak, of the desired reflector shape. Various configurations of deployable support structures have been investigated for application to the distributed control reflector technique. The basic "maypole" - type deployable antenna support structure seems to be the most promising.

2.2.3   Concept Comparison. An evaluation of the identified candidate structures was performed to determine the concept that meets the operational requirements, has manageable risk, could be launched in equal to or fewer launch vehicles, and was more adaptable to modularization and integration into a multiple reflector system.

Three mission configurations were identified for concept comparison; two reflector radar mission, reflectarray mission, and schmidt reflector mission. Table 2.2-1 presents the results of the comparison for the two reflector mission and the reflectarray mission. The box truss was selected for the two reflector mission primarily because of its efficient packaging and ease of integration into a two reflector system. The box truss was also selected for the reflectarray mission because of its packaging efficiency, low weight, and surface precision.

The schmidt reflector comparision (shown in Table 2.2-2) presents a different set of critical parameters. With respect to packaging and assembly operations the electrostatic membrane is the best. However the ability to achieve an operational S/C in the early 1990's is questionable. The Astrocell concept or the rectangular panel/deployable box truss approaches use technology that can be projected to a 1990 flight, but the systems are not as efficient from a weight or packaging standpoint and are more complicated with respect to orbital operations.

49

Table 2.2-1   Two Reflector and Reflectarry Concept Comparison

	Size Limitation	Mass	Packaging Efficiency	Orbital Operations	Surface Precision	Structural Stiffness	2-Reflector Integration	TOTAL
Umbrella Radial Rib	0	3	1	5	4	3	2	18
Wrap Radial Rib	4	4	4	5	3	3	2	25
Erectable Radial Rib	4	3	3	3	3	3	2	21
Curved Astromast Radial Rib	3	3	3	3	2	2	2	18
Radial Column Rib	3	3	3	3	3	3	2	20
Articulated Radial Rib	2	3	2	3	3	3	2	18
Maypole	5	5	5	2	2	1	1	21
Hoop/Column	5	5	5	2	2	1	1	21
Polyconic	4	3	4	1	2	1	1	16
Tetrahedral Truss	4	4	4	4	5	5	4	30
Box Truss	4	4	4	5	5	5	5	32

NOTE: Grading is 0 to 5 where 5 is maximum with respect to the missions.

50

Table 2.2-2   Schmidt Reflector Concept Compariosn

	Size Limitations	Mass	Packaging Efficiency	Orbital Operations	Surface Precision	Structural Stiffness	2 Reflector Integration	TOTAL
Solid Panel Deployable	0	3	2	5	5	4	1	20
High Frequency Radial Rib	3	4	3	5	4	1	1	21
Expandable Astro Cell	4	4	3	2	5	3	4	25
Hex-Panel & Truss	4	4	3	2	5	4	4	26
Rectangular Panel and Box Truss	5	4	4	3	5	5	4	30
Electrostatic Membrane/Truss	5	5	5	5	5	3	3	31
Thin Film Controllable	5	5	5	5	5	1	2	28

NOTE: Grading is 0 to 5 where 5 is maximum with respect
to the mission.

2.2.4   Surface Figure Control Actuators.   Large antennas in space, that operate at relatively high frequencies, require precision surface control and this in turn requires precision support from the attached space structure. The relationship between surface precision and antennas diameter for the box truss structure is given in Figure 2.2-32. For a 1000 foot diameter reflector, the RMS error is 0.7". Assuming that a 20:1 ratio of RMS error to wavelength λ is required, then the maximum operating frequency for this 1000 ft. dia. reflector is around 0.8 GHz. It is apparent that active surface control systems will be required for higher frequency large space antennas. This type of control may be used to change the relative dimensions between the reflector and supporting structure or to actually deflect the supporting structure by changing the lengths of selected structural members. Linear actuators are the most suitable for achieving compact integration with the load carrying structure and for achieving the precision adjustments desired. Two classes of linear actuators have been considered; one for fine adjustment and one for coarse adjustment. For initial design of these actuators the coarse adjustment stroke is set as 2.0 inches total range with incremental adjustments of 0.010 inch; the fine adjustment stroke is 0.050 inch total range with incremental adjustments of 0.002 inch.

Figure 2.2-33 shows a box truss deployable structure suitable for supporting either a flat array or a curved reflector. Adjustment techniques for truss structures are two; 1) the mesh position or standoff height relative to the supporting structure is varied or 2) structural member lengths are varied to induce compensating distortions into the total structure.

Adjusting the mesh position offers the advantage of decoupling one adjustment from another at the many points of attachment; one point may be adjusted while the others remain unchanged and unaffected.

For very large antennas (>2000 ft.dia) actuator strokes of greater than 2.0 inches will be required although the incremental requirement will remain unchanged at $\pm$ 0.010 inch.

The technique of producing array surface curvature change by changing the length of truss members on the opposite side of the box structure requires only very small stroke actuators. Changing the length of all members on one side can result in a 100:1 amplification in the peripheral displacement, therefore the total stroke required for one actuator need only be a small part of the total desired displacement.

The actuators depicted in Figures   2.2-34 & 35   are shown as part of tubular structural arrays. These basic mechanisms could be adapted to lines, tapes, and other shape members. All torques are reacted internally and the outward manifestation is a simple change in length.

The driving motor is shown in each case as a gear motor. These require a separate input to stop whenever they have moved a required distance. As an alternative, stepper motors may be employed; steps as small as $1\frac{1}{2}°$ rotation, may be obtained and when this fineness of control is coupled with threaded and/or mechanical reductions, very small increments of displacement are possible with very good control.
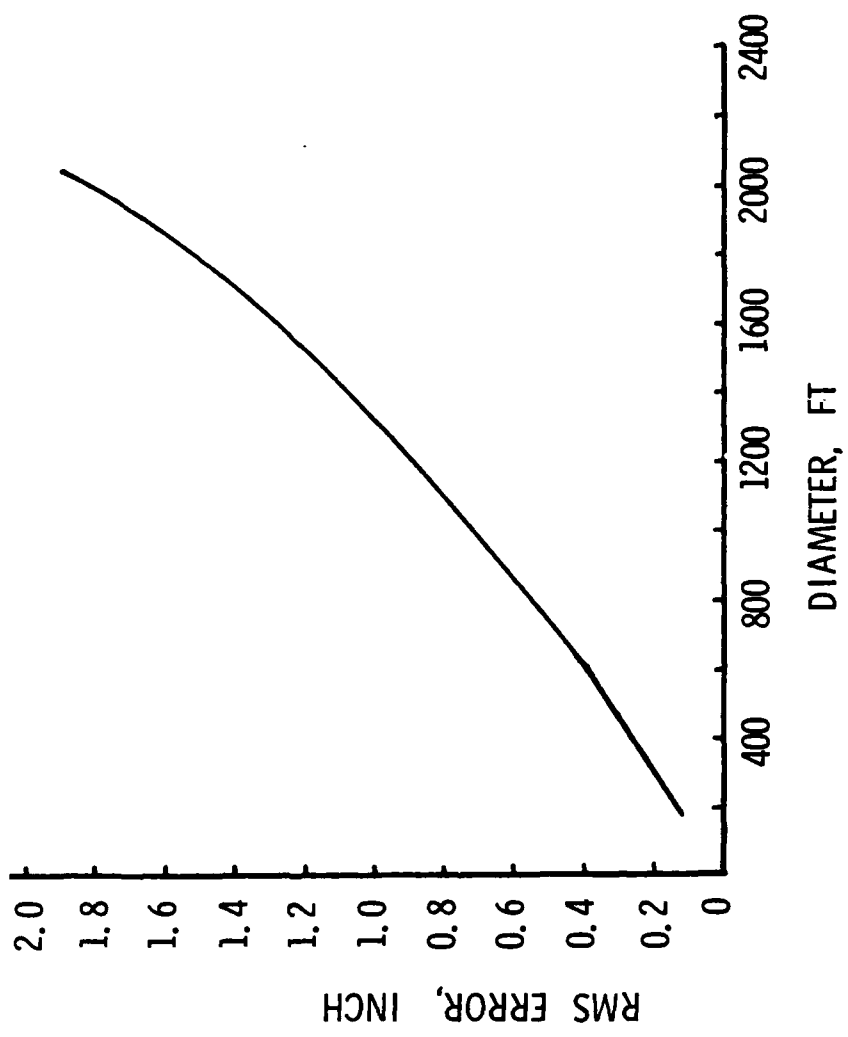
Figure 2.2-32   Surface Precision For Passive Box Truss Structure

53

Optical
Retro-Reflector

Surface
Location
Linear
Actuator

Box Truss Shape
Linear Actuator
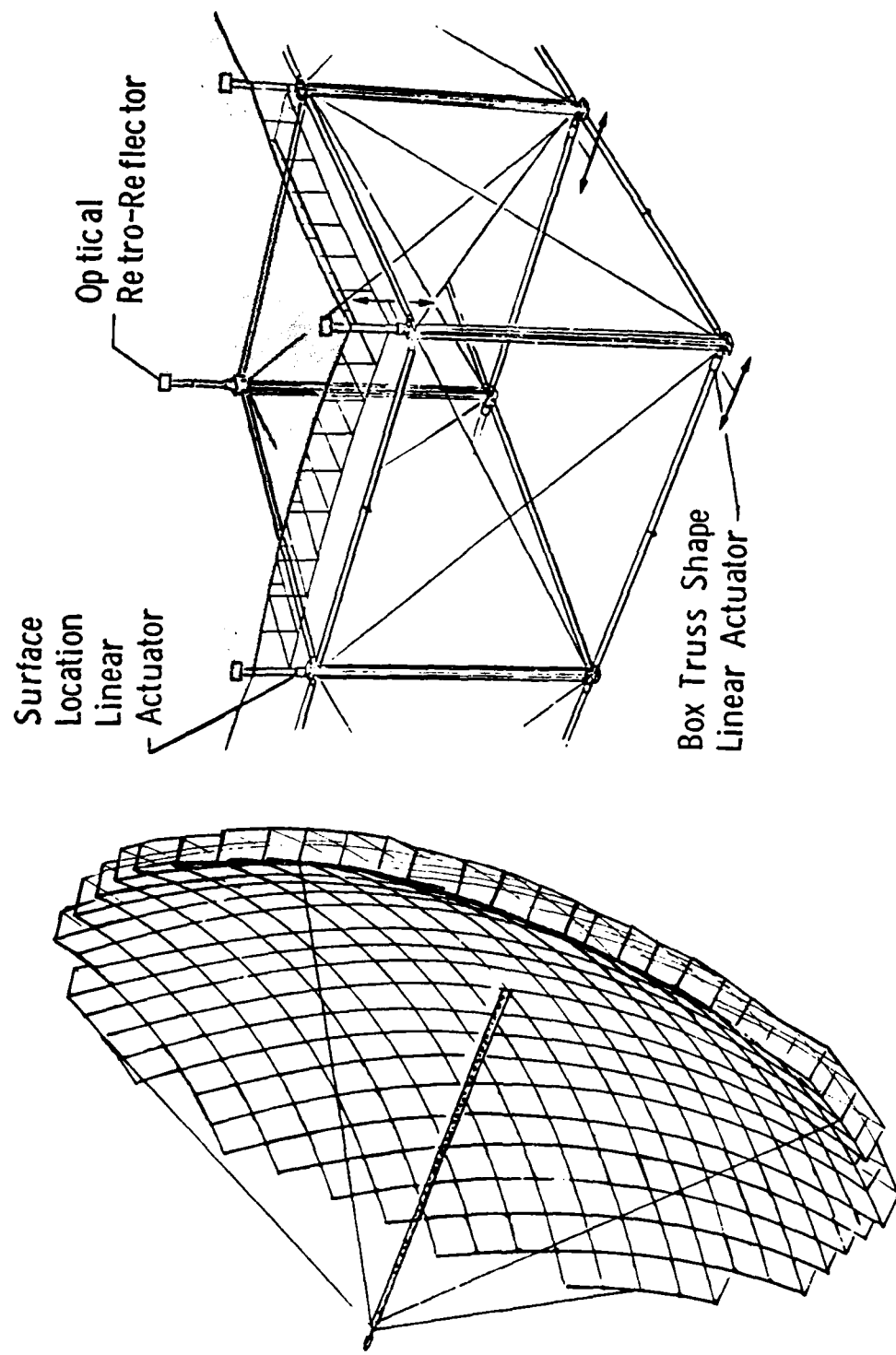
Figure 2.2-33   Truss Adjustment Provisions

54
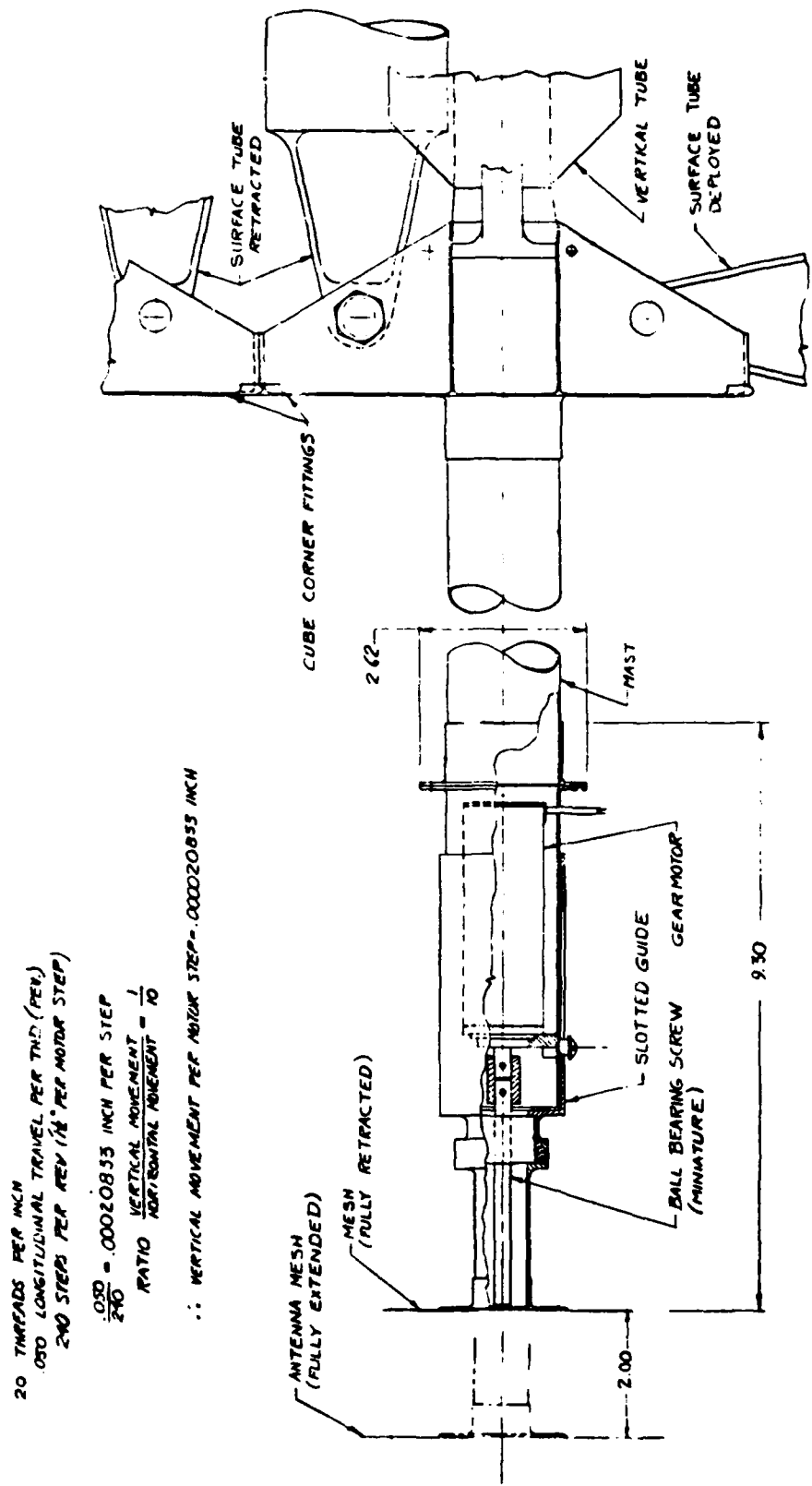
Figure 2.2-34   Long Stroke 0.010 Inch Incremental Actuator

55
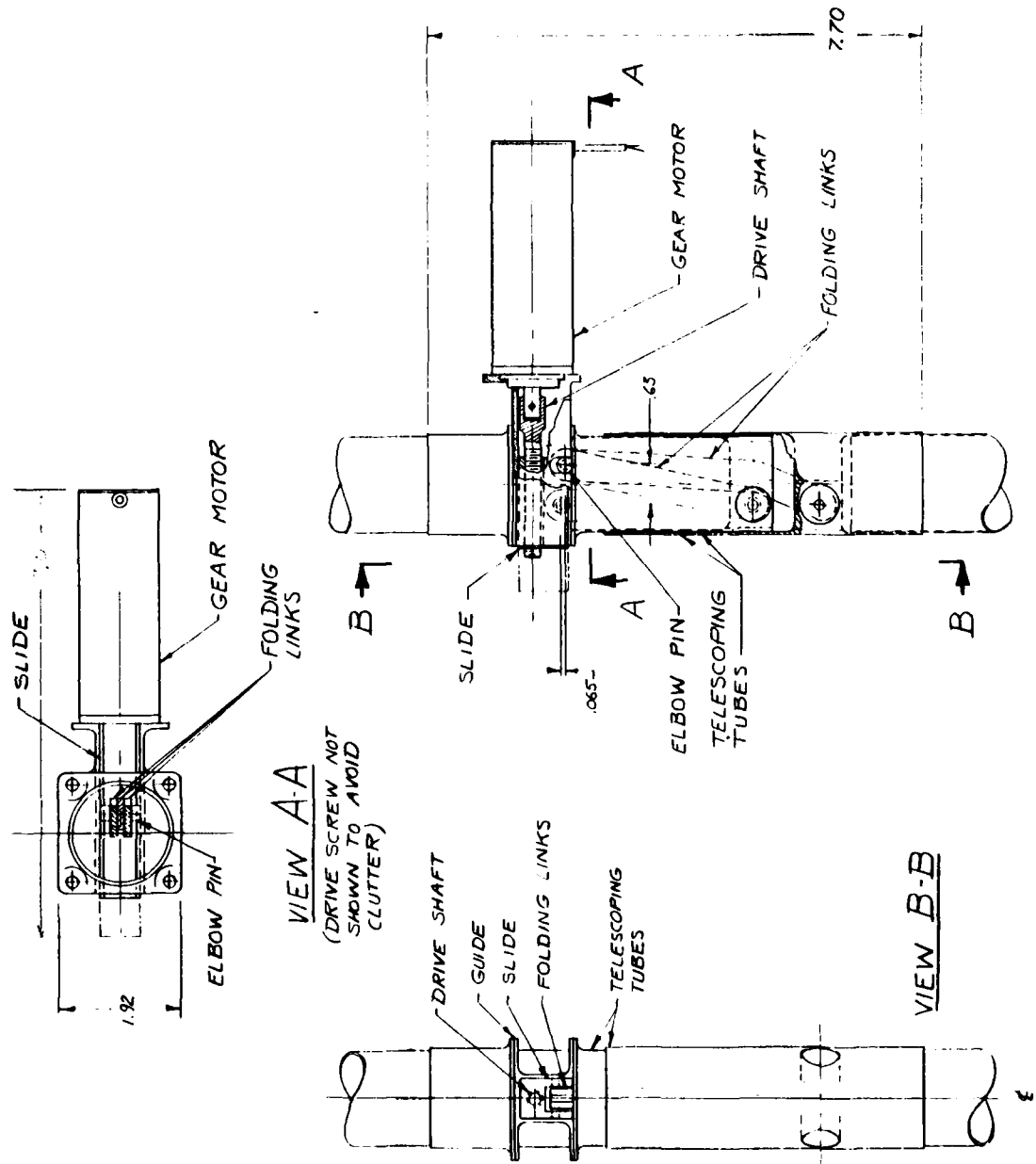
Figure 2.2-35   Short Stroke - 0.0002 Inch Increment Actuator

56

The actuator with the 2.0 in. stroke employs a ball screw device for extending or retracting the head piece. The two parts of the barrel which move relative to one another are telescoping and relative rotation is prevented by a removable bushing working through a slot in the opposing barrel. The screw shaft is coupled directly to the motor and the reduction available is first that of the screw pitch and secondly in the control of the motor. If a stepper motor is used very fine control can be achieved.

Warner Electric Brake miniature ball bearing screws are obtainable in 3/16 inch dia with a 20 thread per inch pitch. This gives 0.05 advance or change in length per revolution of the screw. If a stepper motor with $1\frac{1}{2}^{\circ}$ steps is used then each step is:

0.05 in/rev - 240 steps per revolution = .000208 inch/step

This far exceeds the stated requirement. Fifteen deg steps would be more appropriate and yield:

0.05 inch/rev - 24 steps/rev = .00208 inch/step

A ball bearing screw was chosen for this direct drive application for a number of reasons. The mechanical efficiency is higher than that of a conventional thread; rolling friction vs sliding friction. The motion of the screw is as smooth as the motor permits and very small accurate increments of movement can be obtained with rolling contact which minimize starting friction and eliminates the tendency to stop-start and stutter when a slow smooth linear motion is desired. The high efficiency achieved through rolling contact also permits preloading one ball nut against another to virtually eliminate backlash or end play. The useful wear life is much greater than that of a conventional screw. The ball bearing screw wear life is determined by metal fatigue rather than the ordinary wear characteristic of sliding threads. And finally, ball bearing screw systems are able to return consistently to predetermined locations without the use of positive stops.

The actuator with 0.065 stroke is shown in Figure 2.2-3 with both a gear motor and conventional screw thread drive. A stepper motor with ball bearing drive is preferrable for the reasons just enumerated above.

This small range actuator utilizes the relationship of the "over center machanism" or that of a pushrod just before reaching 'top dead center'. The rotation of the links through a significant angle produces a relatively small displacement along the axis established by lining up all three pins in the rotating links (stroke axis). An added feature is that the force inducing the rotation is amplified considerably along the stroke axis. The motion to be applied to the structure incorporating this linear actuator comes about by rocking the folding links back and forth with a slide which grips the elbow pin and is driven by the motor and screw. The incremental motion possible with this arrangement gives exceedingly fine control.

57

The ratio of slide motion normal to the displacement motion is:

$$\frac{.63}{.065} = 9.69:1$$

Assuming a 20 thread per inch pitch for the screw and 15° steps for the stepper motor:

$$\frac{.05 \text{ inch/rev}}{24 \text{ steps/rev}} \times \frac{1}{9.69} = .000214 \text{ inch stroke/step}$$

If finer increments were desired, a $1\frac{1}{2}^{\circ}$ step motor could be used which cuts the increment by a factor of ten, yielding .0000214 inch stroke/step. This degree of control should move than suffice for any microwave or millimeter wave antenna application.

2.3 Surface Figure Measurement.

2.3.1 Summary

2.3.1.1 Objective. Large space antennas will require monitoring and control of their surfaces to achieve desired performances. It is the objective of this task to identify and develop the necessary technology base leading to that goal. The fundamental metrological problem involves three parts: (1) the establishment of a master coordinate system against which a distributed set of elements in space can be related; (2) development of the ability to measure accurately the coordinates of those elements within the coordinate systems; and (3) implementation of techniques to drive those elements to desired coordinate positions in order to achieve specified antenna performance. In the material that follows, most of the effort has addressed the second of these three parts.

2.3.1.2 Position Measurement Requirements. Position measurement requirements involve not only RMS accuracy, but also several other critical physical and operational criteria. Some important requirements are listed below. For the two missions treated in this study, the parameters listed represent limiting requirements, derived from the millimeter wave radiometer mission.

Included with surface measurements are related requirements for pointing and stabilization. This is in recognition of the fact that an operational control system must integrate the functions of surface control, attitude control, slewing and pointing to be optimum and effective. The problems of each are not mutually exclusive.

Table 2.3-1   Position Measurement Requirements

Measurement	Requirement	Typical Value
Surface	RMS Accuracy	$\lambda/20$ (150μm @ 100 GHz)
	Panel Element Size	15 x 15 ft (Shuttle Compatible)
	Number Control Points	900 (100m Dia)
	Control Response Time	Minutes
Pointing And Stabilization	Accuracy	0.2 Beamwidths (~1 arcsec)
	Slew and Settling Time	1 Hr.

2.3.1.3   System Level Characteristics. In addition to specific surface control requirements, there are a number of system level requirements that should be incorporated. These are listed below and represent design goals. Multiple, precision sensors refer to the need to integrate surface control with slewing and pointing functions. Because of potentially large amounts of raw measurement data, decentralized processing would relieve the data processing burden of a central data system. Real-time outputs in the timeframe of minutes are required to maintain control of very large structure thermal bending modes. Immunity to natural backgrounds, such as the sun, earth, moon, etc, would be an essential operational feature. Other features leading to simplicity of operation and potential cost savings are

also listed.

Table 2.3-2   System Level Characteristics

● Multiple, precision sensors (Celestial, Inertial, Surface)

● Decentralized control (Dedicated Microprocessors)

● Real-time measurement outputs (Minutes)

● Background Immunity (Sun Glints, Earthshine, etc)

● Sensor outputs compatible with on-board processing

● Modular system elements (Simple, Rugged, Inexpensive)

● Maximum reliance on existing technology base

2.3.1.4   Selected Approaches for Precision Surface Control. On the
basis of large space structure surface accuracy requirements, the most likely
measurement approaches will utilize one or more of the techniques listed in
Table 2.3-2. In a general sense, they range from the least to the most
stringent control capability, or, alternatively, from the smallest to the
largest structures. Nothing will be said about passive control, which refers
to the small, low-frequency antennas.

Pulsed LIDAR techniques with retroreflector targets are a technology well
in hand, exhibiting ranging accuracies down to the millimeter regime. Multi-
ple target coverage is also well demonstrated by current laser radar systems
that scan in angle via internal beam steering. Subsequent discussions will
concentrate on the remaining two items on the list, namely, staring angle
sensors and the synthetic wavelength interferometer (SWI) concept.

Table 2.3-3   Selected Approaches For Precision Surface Control

● Passive

● Pulsed LIDAR with Retroreflectors

● Staring Angle Sensors with LEDs

● Synthetic Wavelength Interferometer (SWI) with Retroreflectors

● Hybrid (Combination) Systems of the above

2.3.1.5   Operating Regimes for Active Surface Control. In Figure 2.3-1
operating regimes for active surface control are plotted as functions of
both frequency and diameter. The millimeter wave radiometer missions has
such stringent control requirements that the synthetic wavelength inter-
ferometer (SWI) is the only possible control technique.

60
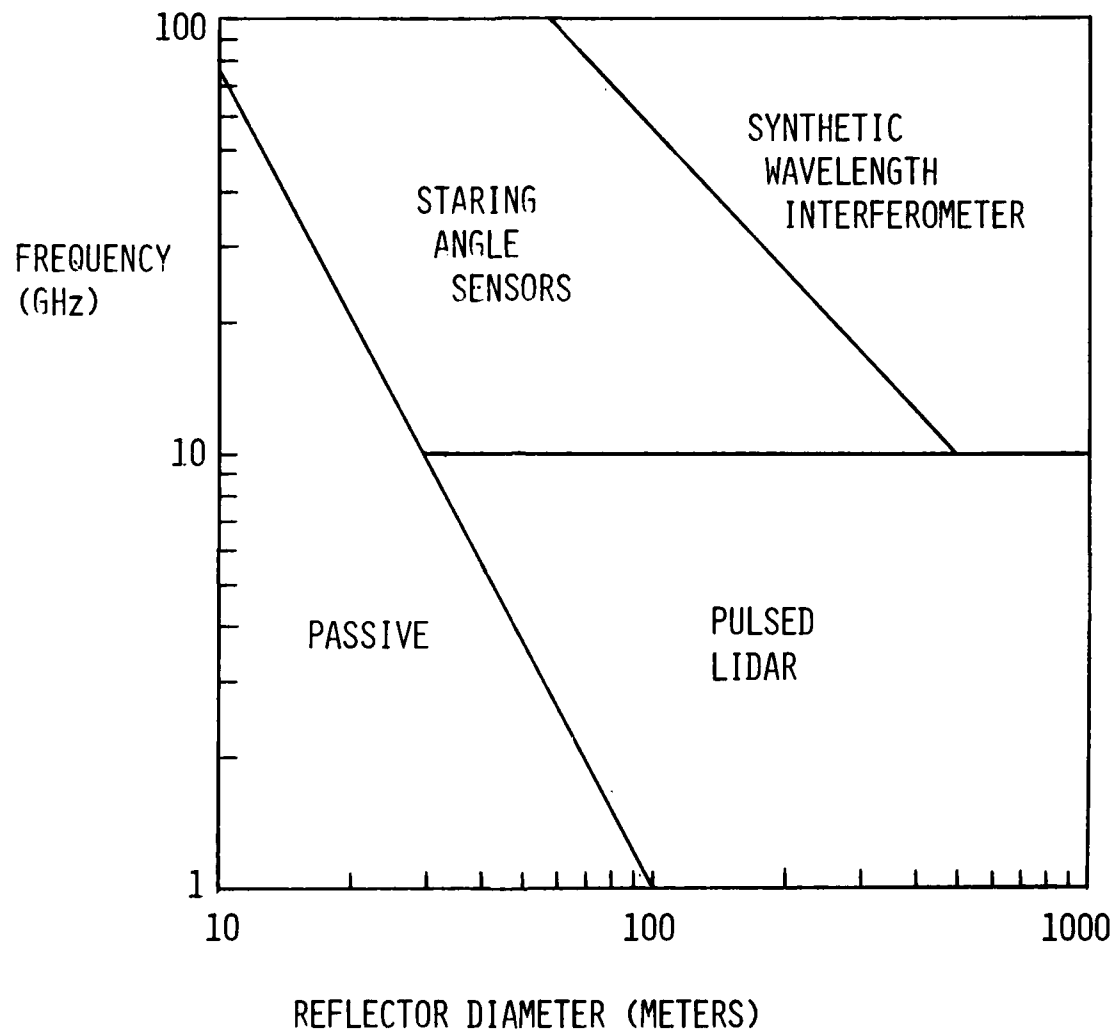
Figure 2.3-1   Operating Regimes, Surface Figure Sensing

61

2.3.1.6   Surface Figure Measurement - Conclusions. From the analyses
of this task it has become clear that several viable options for surface
figure measurement and control are possible. The technology associated with
these options is available now; it is current state of the art. Specific
sensor concepts, like the synthetic wavelength interferometer, are already
in the laboratory breadboard or prototype stage, and do not exhibit any ser-
ious limitations. The problems associated with control of surface figure,
vehicle attitude and pointing cannot be separated. A single, overall control
system must integrate these functions. Finally, while no serious limitations
have been found in the concepts for surface figure control, it is important
in the near future to evaluate one or more of them in detail for a specific
antenna or structural design, putting together the dynamics of the structure
and its environment, the physical implementation of the surface measurements,
processing algorithms, and control actuators in a complete simulation of the
problem.

2.3.2.   Detailed Discussion

2.3.2.1   Potential Surface Measurement Approaches. Table 2.3-4 sum-
marizes potential approaches to the problem of surface measurement, demon-
strated or proposed. Attitude sensors by themselves do not provide measure-
ments of deflections. Holography and photogrammetry are not real-time. Of
those remaining, some exhibit more accuracy, while others are more complex.
As will be shown presently, the specific requirements of a system often
dictate the most desirable surface measurement approach.

Table 2.3-4   Potential Surface Measurement Approaches

Approach	Comments
Attitude Sensors	Do not measure deflections.
Mirror-Prism Configurations Polarization Techniques	
Holography	Record on film (not real-time).
Photogrammetry	Record on film (not real-time).
Angle Sensors	
Servoed Beam Steering	Complex.

Image Tube
  CCD Array
  Lateral Effect Silicon Photo-
  diode
	"Staring" Angle Sensors

LIDAR (Optical Radar)	Ranging to mm accuracy.
Synthetic Wavelength Interfer- ometer	Potential sub-millimeter ranging.

62

Lateral Effect Silicon Photodiode (LESP) - Pictured in Figure 2.3-2 are two versions of the lateral effect silicon photodiode (LESP), the critical detecting element of a staring angle sensor. The word "staring" is used for emphasis, because the sensor is fixed, observing a fixed target. Scanning angle sensors, observing many different targets, are judged to be too complex at the present time. The primary reason for this is that the measurement to be made is a differential angular <u>displacement</u>. Staring sensors observe this directly, while scanning sensors must take a difference between two encoded angles (usually large). Control of angle errors imposes penalties in complex servo control of sensor pointing.

The LESP provides a position readout of the image of a target (a light emitting diode, or LED) by the ratio of current difference out either end of the detector to total photocurrent. This can be obtained in either one or two dimensions, as shown. Existing detectors have demonstrated one part in 10^4 motion sensing ability, or about one micrometer shift of the image in the sensor focal plane.

Other detector options for the sensor include the image tube and two-dimensional CCD arrays. Both could provide 1 in 10^4 sensing accuracy; however, the image tube is relatively complex and can suffer difficult-to-control metrical distortions. The CCD array would have to be fabricated into a 500 x 500 array to be useful, which taxes the current state-of-the-art.

All angle sensors must contend with a common problem when measuring small displacements at great distances. This dilemma is explored more fully below.

Angle Sensing Dilemma - The problem for angle sensors arises under measurement conditions outlined below in Table 2.3-6, which correspond to very large antennas operating at high frequencies ($\lambda/20$ criterion very small). The penality occurs in requiring long focal length optics to match the object (target) displacement to the image motion, for the ratio of image to object shift is equal to the ratio of image to object distance. Under the conditions given below, the image distance is 10 meters, leading to a focal length for the optics of 9.8 meters.

Because staring angle sensors and targets proliferate on a one-to-one basis, large structures under precision control cannot tolerate several hundred optical systems of this size. Angle sensors will find utility, therefore, only on structures of modest size and/or operating at lower frequencies for which much greater target displacements are acceptable.

Table 2.3-6   Angle Sensing Dilemma

Measurement Conditions

o   RMS target movement - $50\mu m$

o   Target distance - up to 500 m (or more)

o   Target image movement - $1\mu m$ (on LESP or CCD array)

63

SINGLE AXIS
PLANAR DIFFUSE SILICON
(UDT-PIN-3244)

DUAL AXIS
PLANAR DIFFUSE SILICON
(UDT-SC/10D)

I_1

I_2

5mm

10mm
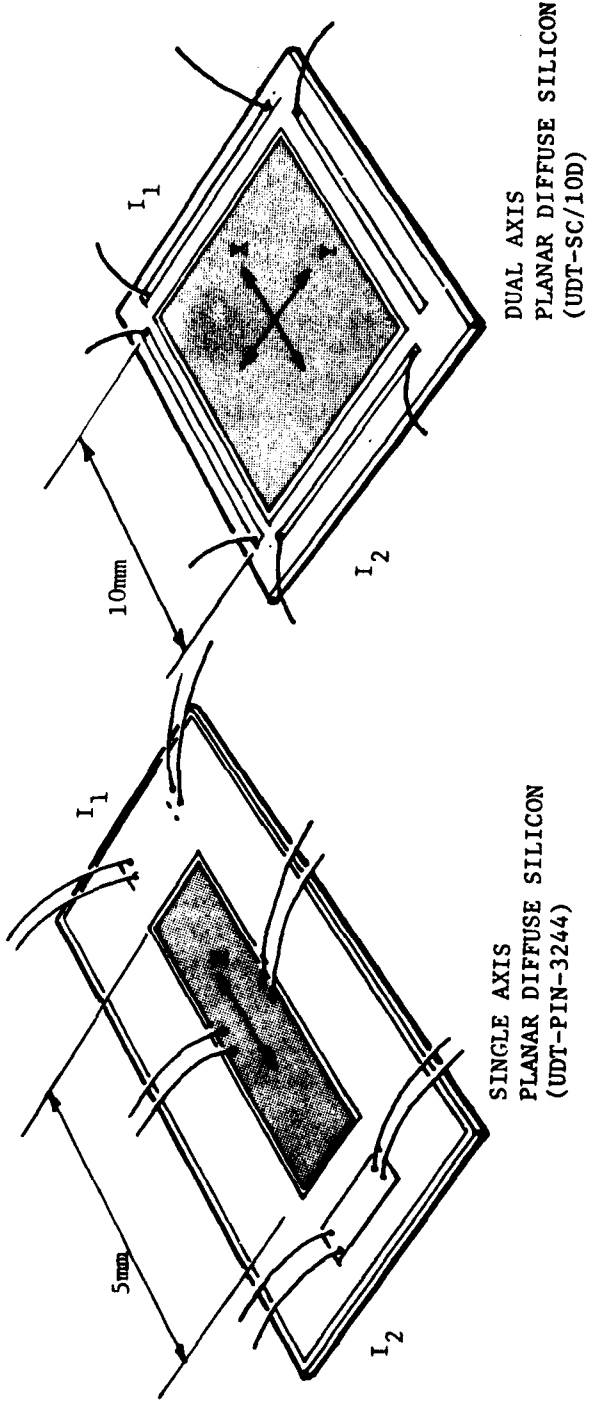
- $X = (I_1 - I_2)/(I_1 + I_2)$; Y-AXIS TREATED SEPARATELY, BUT SIMILARLY.
- PROVIDES 1 PART IN 10^4 MOTION SENSING (1 μm IN FOCAL PLANE).

Figure 2.3-2   Lateral Effect Silicon Photodiode (LESP)

64

Optics Penalty

$$\frac{X_i}{X_o} = \frac{S_i}{S_o} \quad \text{where} \quad X_i = 1\mu m = \text{image movement}$$

$X_o = 50\mu m = \text{object movement}$

$S_i = \text{image distance}$

$S_o = 500 \text{ m} = \text{object distance}$

$S_i = 10 \text{ m} \quad \text{Image Distance}$

$$\frac{1}{S_i} + \frac{1}{S_o} = \frac{1}{F} \quad (F = \text{focal length})$$

$F = 9.80 \text{ m Optics Focal Length}$

Conclusion

Angle sensing imposes requirement for unacceptably long focal length optics.

Synthetic Wavelength Interferometer (SWI) - Illustrated in Figure 2.3-3 is a device concept that will provide precision position (range) measurements, even over large distances. It has been dubbed the Synthetic Wavelength Interferometer (SWI), and simultaneously combines coarse ranging via phase modulation of a laser beam with precision location of target position via a heterodyned Michelson interferometer.

The technology of Michelson interferometers and heterodyne detection is well in hand. Laboratory breadboard models of the SWI incorporating RF phase modulation have been built and tested, and show near theoretical performance.

SWI Measurement Characteristics - The sensor utilizes all techniques (Michelson interferometry, heterodyne interferometry, phase modulation) simultaneously. Coarse range is provided by one or more frequencies of RF phase modulation, the "fringe" distance of the coarsest being comparable with the total distance to the target (retro-reflector). Refinement of the range is provided by the heterodyned interferometry, which interpolates the final, fractional fringe measurement of the RF phase modulated signal to a finer level of precision. Final position determination is provided by the Michelson interferometry, which performs the same function on the fringe measurement of the heterodyne technique. Each levle of fringes measurement provides a count of the total integral number of fringes present in the next finer level.

The critical requirement for the concept to work is that the phase (fringe) measurement at each level must be accurate enough so that there is no ambiguity in the total fringe count of the next finer level. This leads to a phase measurement accuracy requirement of the form:

65

- CONVENTIONAL INTERFEROMETER SENSES CHANGES IN PATH DIFFERENCE
  BETWEEN REFERENCE (SENSOR) AND WORKING (TARGET) MIRROS.

- HETERODYNE FORM PRESERVES ALL AMPLITUDE AND PHASE RELATIONSHIPS,
  BUT AT AN INTERMEDIATE FREQUENCY (IF) OR OPTICAL DIFFERENCE
  FREQUENCY, WHERE

$$\lambda_{eff} = \lambda_1 \lambda_2 / (\lambda_2 - \lambda_1)$$

- MULTIPLE IFS ARE GENERATED BY BEATS BETWEEN MULTIPLE LINES IN
  THE LASER OUTPUT

- PHASE MODULATION OF LASER OUTPUT GENERATES EQUIVALENT "SYNTHETIC"
  WAVELENGTH, ORDERS OR MAGNITUDE LONGER THAN ABOVE WAVELENGTHS.

- IN ALL THE ABOVE, PHASE ANGLE IS GIVEN BY

$$\emptyset = 4\pi R / \lambda$$

- A MEASUREMENT OF $\emptyset$ IS FUNCTIONALLY EQUIVALENT TO A DETERMINATION
  OF RANGE R.
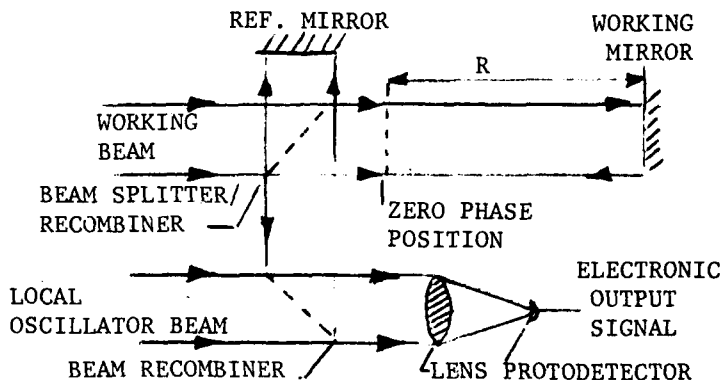
HETERODYNE FORM OF MICHELSON INTERFEROMETER TRANSFORMING
FROM OPTICAL TO ELECTRICAL DOMAIN WHILE PRESERVING WAVE
AMPLITUDE AND PHASE RELATIONSHIPS.

Figure 2.3-3   SYNTHETIC WAVELENGTH INTERFEROMETER (SWI)

66

$$\Delta\emptyset_i < 2\pi \ \frac{\lambda_i + 1}{\lambda_i}$$

where $\lambda_i + 1$ is the effective wavelength of the $(i + 1)$st level.

SWI Operating Range Potential - In Table 2.3-7 is given an example of the potential operating range (and precision) of a SWI. For the example, a CO_2 laser with several lines in the 10.6μm range region is used. The lines are:

R (16) at 10.28μm

P (18) at 10.57μm

P (20) at 10.59μm

Heterodyned, optical difference frequencies used are given by:

$$\lambda_{eff} = \lambda_1\lambda_2/(\lambda_2 - \lambda_1)$$

Examples used are:

R (16) - P (18); λ_{eff} = 374.7μm

P (18) - P (20); λ_{eff} = 5.6 mm

Finally, RF phase modulation at 10,000, 100 and 1 MHz provides coarse range information. Shown in the table are the unambiguous range increments over which the various techniques apply. For each technique, the range increment is limited on the long side by one full fringe in total path difference (twice the range change), and on the short side by an arbitrary criterion of 1/100th of a fringe. Note that as one moves upward through the levels, each one overlaps the next finer level, thus enabling an unambiguous total fringe count in that level to be established.

The important question to be answered is, however: Are the phase measurement accuracies in each level sufficient to ensure no loss in fringe count at handoff, according to the criterion developed earlier? Table 2.3-8 examines this question for our example sensor.

Table 2.3-7   SWI Operating Range Potential

Operating Mode	Example	Unambiguous Range Interval (Meters)
Fine	CO_2 laser at 10.6 μm	5×10^{-6} to 5×10^{-8}

Table 2.3-7 SWI Operating Range Potential (Continued)

Operating Mode	Example	Unambiguous Range Interval (Meters)
Intermediate (Optical Difference Frequency)	CO_2 Heterodyning R (16) - P (18) lines $\lambda_{eff} = 374.7\mu m$	2×10^{-4} to 2×10^{-6}
	CO_2 Heterodyning P (18) - P (20 lines $\lambda_{eff} = 5.6$ mm	3×10^{-3} to 3×10^{-5}
	10,000 MHz modulation	1.5×10^{-2} to 1.5×10^{-4}
Coarse (Phase Modulation)	100 MHz modulation	1.5 to 1.5×10^{-2}
	1 MHz modulation	1.5×10^{2} to 1.5
	Lower Frequency Mod.	Up to 10^{3} to 10^{4}

SWI Phase Measurement Accuracies (Example) - Tabulated below are the required phase measurement accuracies within each measurement level to ensure an unambiguous fringe count in the next finer level. Note that handoffs from 1 MHz modulation to 100 MHz modulation and from 100 MHz modulation to 10,000 MHz modulation requires a phase measurement accuracy of 3.6 degrees, which is about at the limit according to our criterion of 1/100th fringe. The other steps in the process appear to be easily achieveable.

Table 2.3-8 SWI Phase Measurement Accuracies (Example)

$$\Delta\emptyset_i \quad 2\pi \frac{\lambda_{i+1}}{\lambda_i}$$

Level	λ_i	$\Delta\emptyset_i$(degrees)	Comments
1 MHz Mod	300 m	3.6	Marginal Phase Accuracy
100 MHz Mod	3 m	3.6	Marginal Phase Accuracy
10,000 MHz Mod	30 mm	67.2	Achievable
P (18) - P (20) Beat	5.6 mm	22.1	Achievable
R (16) - P (18) Beat	374.7μm	11.1	Achievable
CO_2 Direct Interference	10.6μm	?	Established by Required Position Determination Accuracy

68

2.3.2.2   Operational Regimes for Active Surface Control.   In Figure
2.3-1 are plotted approximate regimes of frequency and aperture size wherein
specific active surface control sensing techniques are applicable.   Boundar-
ies between regimes are "soft" in that different criteria of performance can
affect their locations.

At the small aperture end is the region within which active control of
antenna surfaces is not required.   The boundary to this region is determined
by the predicted capabilities of the box truss structure.

Below about 10 GHz, and for larger antenna diameters, pulsed LIDAR rang-
ing can be used to measure the locations of retroreflector targets distri-
buted over the antenna surface.   The upper frequency limit is established
both by the inherent range accuracy limitation of current LIDAR systems
($\sim$1 mm), and by the criterion for target displacement measurement accuracy.
For full aperture illumination at a given frequency, the criterion adopted
was a measurement accuracy of one-twentieth of a wave-length.   The vertical
scale on the right of Figure 2.3-1 identifies $\lambda/20$ for each frequency.

At intermediate aperture diameters, but higher operating frequencies,
staring angle sensors observing LED targets can provide the required $\lambda/20$
measurement precision, in combination with (relatively) crude LIDAR range
measurements to establish scale.   Uncertainties in scale enter into the
equations only as second order effects, and need not have comparable pre-
cision to the angle measurements.   The frequency-aperture boundary for angle
sensors was established by the physical size of required optics, focal
lengths no greater than 30 cm being the limiting factor.

For the largest apertures and highest operating frequencies, the con-
trol technique selected is the synthetic wavelength interferometer operating
on retroreflector targets.

Two points are clear from the figure.   First, use of the pulsed LIDAR
technique, with its well-known technology and potential beam scanning capa-
bility, appears to be marginal. It should be pointed out, however, that op-
erations at lower frequencies than 10 GHz could be controlled with this
technique.   Second, the millimeter wave radiometer mission falls squarely in
the high-frequency, large diameter region requiring the synthetic wavelength
interferometer control technique.   This mission represents a most challeng-
ing problem, not only in terms of the complexity of the control problem
itself, but also in terms of possible numbers of sensors, control point
actuators, and potential weight and power of the control sub-system.

2.3.2.3   Typical Control Sequence for Parabolidal Antenna.   This sub-
section illustrates how a large, parabolidal antenna might be controlled
under operational conditions in space, and parenthetically, how the control
functions for vehicle attitude, pointing, and surface figure are inter-
related.   At the initiation of a measurement cycle, targets located at sur-
fact control points, antena feed, and vehicle inertial navigation base are
sampled by the surface figure monitoring sensors.   It is irrelevant what
these sensors are for this discussion; they may be any of those discussed
in earlier subsections.   Depending upon the dynamical idiosyncrosies of the

69

antenna structure, observations may have to be made from up to three separate locations to fully describe the displacements of the control points with respect to a single reference point.

These measurement data are then processed to determine the best fit to a desired paraboloidal surface, the location of the surface focal point, and, using reference data from the vehicle inertial navigation base, the directtion in space of the surface's pointing axis. Initially, the actual pointing direction of the antenna is compared with the desired pointing direction to determine whether an attitude correction is required. In general, minor pointing errors can be corrected by repositioning the antenna feed. Only if the pointing error exceeds some threshold would the correction be affected by a vehicle maneuver. In such a case, disturbances would be introduced into the structure, abrogating all previous measurements. Thus, the measurement cycle would have to be repeated.

If no attitude correction is required, the system would examine the actual position of the feed with respect to the required focus/fine pointing position. Should a correction be required, the feed would be commanded into the required position. This would require a 3 DOF actuated platform for the feed mount. At this time it is not certain that such a movement would affect the antenna surface figure, thus demanding that the measurements be recycled. In full generality, however, this would be the case.

The final step, once beam direction and antenna feed positioning has been accomplished, would involve determination of the antenna surface target residuals with respect to the best fit parabolidal surface. If the residuals result in an RMS surface degradation in excess of specifications, control poirt actuators would be commanded to correct the surface back within specifications. The measurements would then be recycled to verify all elements to be within tolerances.

If no corrections are required, the control system may or may not be placed in a standby mode until the next cycle time. The exact duration of this "cycle" time is not specified, but would be dependent upon the dynamical and thermal characteristics of the particular antenna structure in the space environment. The entire process may be quasi-continuous, with no "rest" periods available to the control system at all. Alternatively, the system may be adaptive, adjusting its cycle times to conform to "learned" conditions.

It is clear that the problems associated with attitude control, vehicle pointing, and surface figure control are highly interrelated, and must be treated as an integrated whole. Basic data for the solution of these control problems come from the inertial reference sensors (navigation base) and from the surface figure control sensors. Finally, a natural sequence of events, or operational hierarchy seems to suggest itself for successful implementation of the control of large structures in space.

2.4 Attitude Control

2.4.1 Purpose of The Attitude Control System. The purpose of an attitude control system is to stabilize and point the antenna. In order to accomplish this the attitude control system must sense attitude, generate error signals, generate corrective commands and provide actuation. The generalized control schematic is shown in Figure 2.4-1. In the case of large orbiting antennas the scope of the attitude control system is broad, encompassing the following functions:

Attitude Sensing and Positional Navigation (Autonomous Navigation) - In the general case of orbiting antennas it is necessary, or desirable, to relate the location of the target on, or near earth, to the location of the antenna itself, and further to know the location of the antenna in a convenient coordinate reference frame. An inertial coordinate system is usually chosen, whose origin in the center of the earth. Antenna and target locations can be easily expressed in this system and related readily to latitude and longitude; and also the information sensed by inertial reference systems and stellar update systems is essentially in this coordinate system.

To ascertain the location of the antenna and its pointing direction inertial reference units and/or optical sensors viewing a fixed star, earth limb, solar aspect, or lunar limb are usually mounted on the antenna. Landmark sensors are also available and will provide attitude information, and in some cases positional data.

Overcoming Disturbing Torques and Forces - Disturbing torques and forces arise due to aerodynamic effects, solar pressure, gravity gradient and a host of lesser causes. Typical environmental torques are shown in Figure 2.4-2 as a function of altitude. Other disturbing effects also exist due to earth shadowing, season changes, solar activity producing solar winds, earth oblateness and earth reflectance of solar energy, on-board machinery, magnetic effects, outgassing and venting.

In addition to torques, aerodynamic and solar pressure produce forces which tend to alter the orbits and can cause severe stationkeeping problems. Disturbances will be discussed in detail below.

Flexible Body Stability - The analysis used to design the control system must consider the antenna and its appendages as a flexible body. Analysis to date has indicated bending modes of significance exist from below .1 Hz to above 5 Hz including mast modes and mesh modes and that significant cross coupling among axes is present which adversely affects stability.

An analysis of flexible body stability and control is beyond the scope of this program but must be a vital part of any point design.

Slewing - Any mission having a frequent retargeting requirement could require relatively high slewing rates. This imposes a burden on the attitude control system to provide the torques required, required settling time, limit the modal excitation and fine point. These requirements are not generally consistent implying compromises which are dependent on the

71
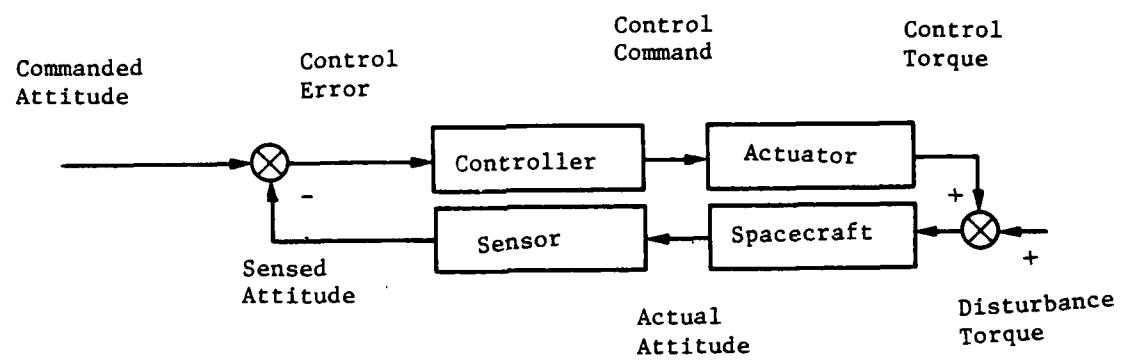
Figure 2.4-1   GENERALIZED CONTROL SCHEMATIC

72
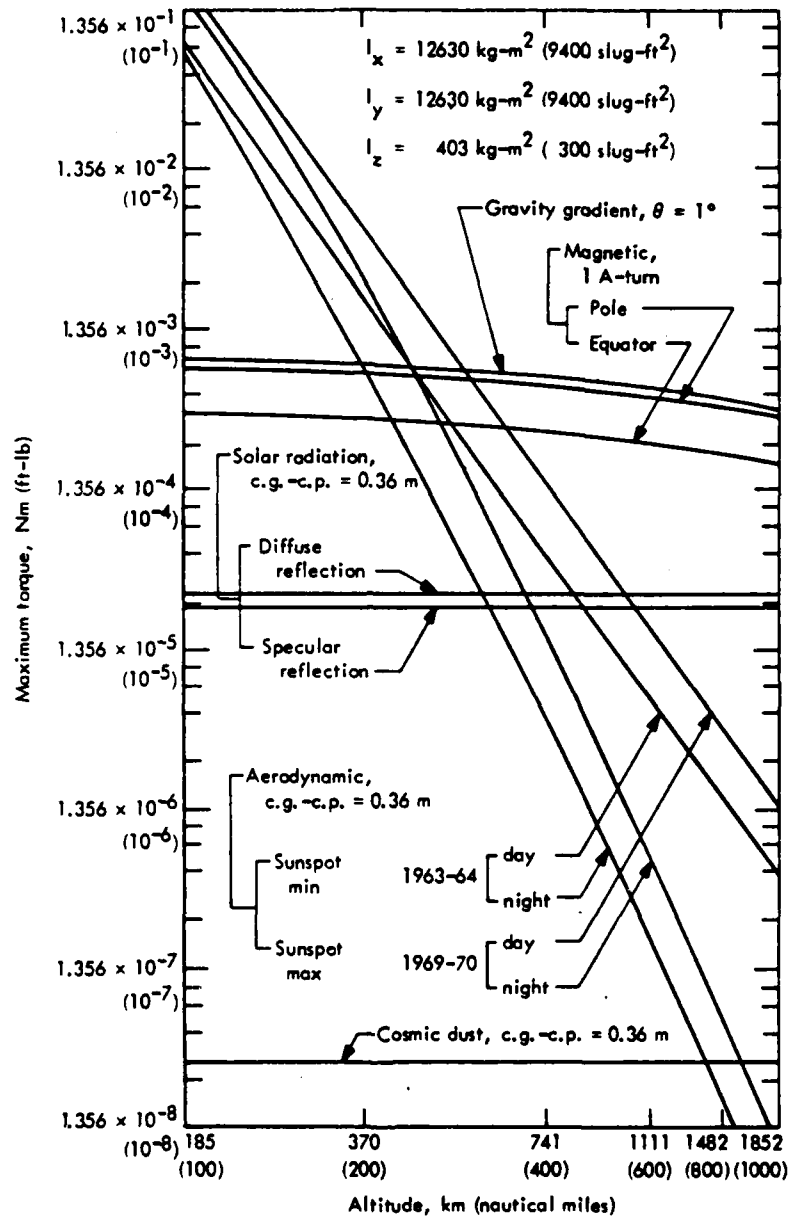
Figure 2.4-2   Relative Magnitudes of the Environmental Torques
on an Earth Satellite

73

particular type of structure and the detailed mission response times and accuracies.

Fine Pointing - Certain missions impose fine pointing requirements on the order of an arc sec or less. This requirement implies that the antennas have highly precise knowledge of its own attitude in inertial space and of its own position as well as possessing the ability to sense attitudes-to-target precisely and to control its attitude with fine precision.

Controllers - To accomplish the pointing and slewing of the antenna, and to overcome the disturbing torques requires that devices be incorporated into the antenna which are capable of producing forces and torques. All these devices involve momentum interaction; either momentum exchange between the antenna and the universe by reaction jets, or momentum transfer within the antenna using large rotating wheels whose speed or direction of rotation can be varied. Usually, combinations of reaction jets and momentum wheels are employed.

2.4.2 The Elements of Attitude Control. The elements of attitude control which are unique to large space structures and particularly to antennas of the missions of interest are their pointing requirements and the sizeable environmental disturbances they experience. Therefore, the discussion below will be devoted to the critical function of these element, namely, sensing of attitude and position, the disturbing forces and torques and the controllers which must overcome these disturbances while at the same time providing the fine pointing required.

2.4.2.1 Attitude Determination. The pointing accuracy requirements of the antennas along with the desired life of the spacecraft place stringent requirements on the design of the system. Other features such as sensor characteristics (does the sensor provide scanning? Do electronics require shielding? etc.) and the type of control system used also help to define the architecture of the overall system.

Attitude Determination sensors can be characterized in one of two ways. Either the sensor is part of a real-time reference system where attitude information can be obtained directly at any time, or the sensor takes periodic measurements. The first type of sensor is generally an Inertial Reference Unit (IRU), and the second usually consists of a sensor which measures a line of sight to some observable. The most common observables are the stars, planetary limbs, the sun, radars or other electromagnetic emitters.

Automation of the attitude determination system requires onboard processing capabilities. Variation of the mission requirements and configuration place certain demands on the architecture, speed, and processing capabilities of the onboard computer. If the computer is too slow, the system will be data bound, and if the processing capabilities are not adequate to solve the problem, the system will be processor bound. All of these factors must be understood and weighed in order to incorporate automation into the satellite system.

Attitude determination involves solving for the angular offsets between

74

a coordinate system fixed within the body of the spacecraft and a reference coordinate system established by the mission requirements. The primary reference systems used to determine attitude are described below:

Inertial Reference Frame - The inertial coordinate system most commonly used has its origin fixed at the earth's center. The X axis is oriented along the 1950 epoch vernal equinox; the Z axis lies along the symmetrical earth rotation axis (North Pole); and the Y axis forms a right-hand triplet. This system is usually chosen when a star tracker or other star detection device is used because star catalogs have been established in these coordinates.

Earth Reference Frame - The earth reference frame, like the inertial reference frame, has its origin fixed at the earth's center. The X axis of this frame has its direction fixed along the zero longitudinal plane; the Z axis points through the North Pole as in the inertial reference frame; and the Y axis completes the ortho-normal coordinate system. This coordinate system is sometimes used for missions utilizing gravity gradient and other earth sensitive attitude sensors. It is also an important reference frame for geographic correlation because data can eventually be related to the latitude and longitude from which it came. A transformation matrix converts the coordinates of a point in the earth reference frame to coordinates in the inertial reference frame.

Local Vertical Frame - The local vertical reference frame is centered within the spacecraft. The X axis is oriented along a vector pointing from the earth's center to the spacecraft; the Z axis is located normal to the flight path pointing in the direction of the angular momentum vector; the Y axis completes the right handed system. For a circular orbit the Y axis is in the direction of the velocity vector.

Body Fixed Frame - This coordinate system is centered in the spacecraft and represents the structure of the vehicle. Attitude is determined by resolving two or more vectors in one of the reference coordinate systems relative to the body frame. A transformation of this data is then made to derive pitch, yaw, and roll errors.

Attitude Sensors - Attitude determination systems exist in a variety of configurations of different sensors (Figure 2.4-3). Most of the advanced systems incorporate some sort of Inertial Reference Unit (IRU) and a reference update system. This combination is advantageous because it minimizes the shortcomings of an IRU and a reference update unit. The IRU is used to maintain a reading of the spacecraft attitude. However, due to the properties of gyroscopes, this reading will drift from the actual value. At some limit of attitude uncertainty, the reference unit will then update the gyro by providing a precise input of the attitude. Attitude undertainty will be a function similar to that shown in Figure 2.4-4.

The two basic types of Inertial Reference Units are the gimballed platform and the strapped down gyro system. A comparison between these two generic systems was performed under an internal research task based on the system concept, sensor impact, software impact, and calibration impact (K. Yong, et at., 1978). A summary of this tradeoff is provided in Table
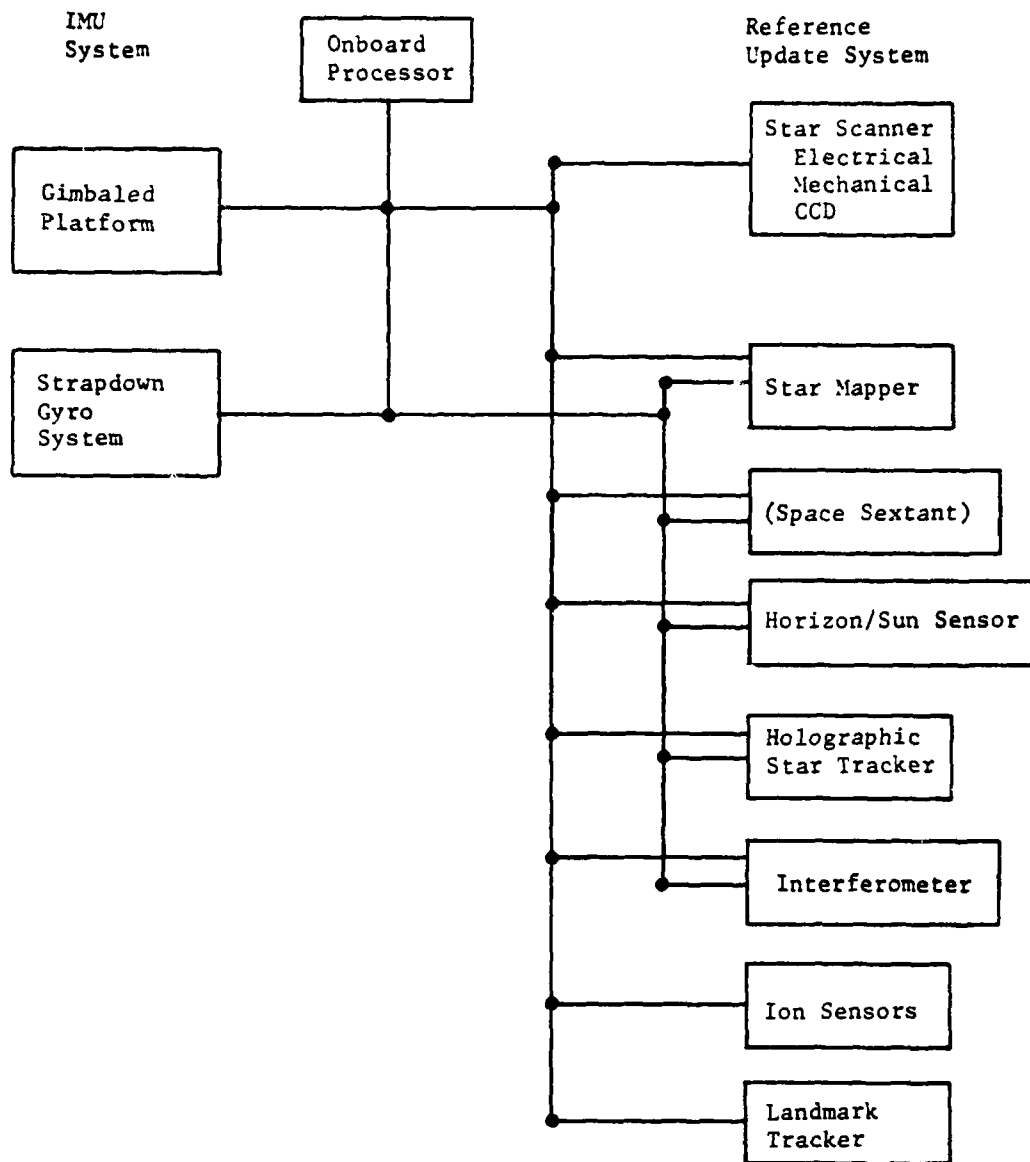
Figure 2.4-3   ALTERNATE ATTITUDE DETERMINATION SENSOR
CONFIGURATIONS

76
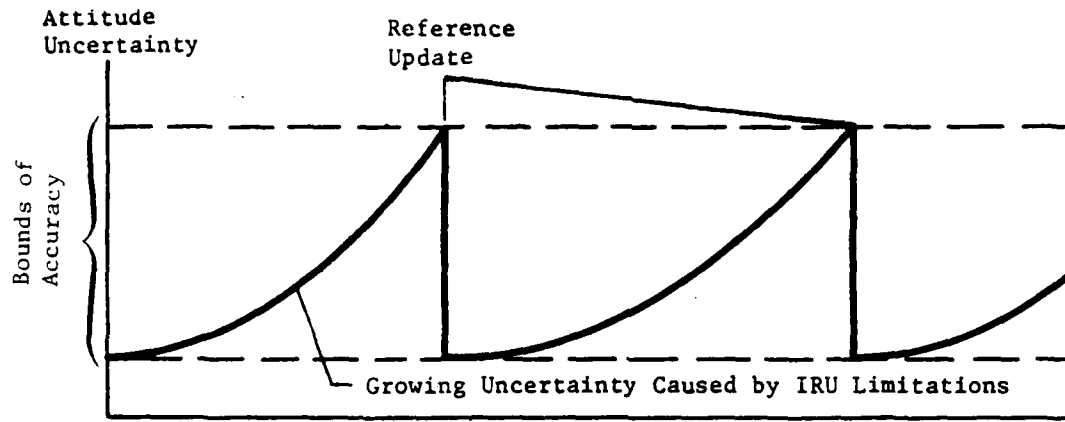
Figure 2.4-4   Attitude Uncertainty As A Function Of Time

2.4-1. It was generally concluded that gimballed platforms are superior for
short duration missions due to the limited software and calibration require-
ment. However, for long term missions where reliability and accuracy become
the major driving forces, gimballed systems should not be considered. The
advantages of using a strapdown system over the gimballed platform in a long
life mission are listed below:

1. Eliminates all errors associated with platform stabilization. This
     increases the long-term reliability.

2. The gimballed platform has the limitation of working within a defined
     range for each gimbal. The strapdown system, being free from
     gimbal lock, allows all attitude motion.

3. Due to the absence of mechanical platform gimbals, the strapdown
     system is smaller in size, lighter in weight, more rugged in
     mechanical structure and consumes less power.

Strapdown inertial reference systems were studied extensively under NASA
contract OADS (NAS4-23428). The initial study concluded that two degree of
freedom (TDF) gyro systems may be considered above single degree of freedom
(SDF) gyros. The advantages of using a TDF gyro package are as follows:

1. Provides higher reliability for the same number of gyros used.

2. Less effect of sensor accuracy.

3. Provision for more redundant measurements for better data reduction.

	Concept	Sensor Impact	Software Impact	Calibration Impact
Gimbaled IMU	Inner Platform remains inertially fixed. Resolver/encoder outputs measure space vehicle attitude (Euler angles) directly.	Gyros are operating a benign environment that is ideal for maximum performance. Drift rates of less than 0.01°/h are obtainable.	Minimal compared to strapdown system.	IMU calibration is minimal compared to strapdown system.
Strapdown	Gyro outputs are intergrated to estimate spacecraft attitude.	Very demanding in areas of scale factor stability, linearity and asymmetry coning motion, alignment vibration, noise and bandwidth.	Very demanding in computational requirements such as truncation, quantization, roundoff and bandwidth. Sensitive to spacecraft motion.	Requires calibration of gyro scale factor, drift, alignment.

Table 2.4-1   Strapdown/Gimballed IMU Comparison

Steller Sensors - Steller sensors measure a Line of Sight (LOS) angle to a star whose position is known. Each star sighting yields two components of attitude information which is used to update a current estimate. There have been several approaches to solving the star sighting problem, and the sensors which have evolved can be separated into four classes:

1.   Gimballed star trackers;

2.   Electronically scanned star trackers;

3.   Star mappers; and

4.   CCD star trackers.

Gimballed Star Tracker - The gimballed star tracker searches for and acquires known stars using a mechanical gimbal action. The sensor has a relatively small instantaneous field of view (FOV) (1° x 1°) with the gimbal motion providing a much larger effective FOV. Pointing control is usually provided through the use of a null seeker electronics package which causes the gimbals to move so that the star remains centered within the instantaneous FOV. Gimballed star trackers, such as those used on the Appolo Telescope Mount have achieved accuracies of 30 arc seconds. Other gimballed star

trackers have accuracies ranging from 1 to 60 arc sec. This type of sensor, however, has several serious disadvantages:

1. Gimbal apparatus reduces long term reliability.

2. Possible to track either the wrong star or particles such as paint chips.

3. Errors in determining star position with respect to null, and gimbal angle readout errors effect the overall accuracy.

4. Increased size and weight due to gimbal mount.

Electronic Star Tracker - This type of star tracker is an electro-optical device which electronically scans a small instantaneous FOV over a larger effective FOV in order to acquire stars brighter than some fixed threshold. The scanning pattern is usually produced by an image disector tube and associated electronics. During acquisition the scanning pattern is a raster type until a star is detected. At this point, the raster scan is normally halted and the star is tracked using a much smaller scan pattern until the star leaves the effective FOV.

The electronic star tracker has no moving parts so it is usually lighter, smaller in size, and has a longer life time reliability than the gimballed star tracker. In addition, it generally has a higher sensitivity, greater signal to noise ratio, and is relatively more rugged mechanically than the gimballed type tracker. However, it too has disadvantages as discussed below:

1. Subject to errors from stray electronics, magnetic field variation, and temperature variations.

2. Because of the finite acquisition time, a maximum attitude rate limit is imposed to ensure quality output data.

3. Narrow field of view might limit the mission applicability.

Star Mappers - The star mapper generally has a slit type aperture which utilizes the spacecraft rotation to provide a scanning motion for the sensor during steller acquisition. The FOV of the sensor is thus scanned over the celestial sphere. It is limited to use on spinning satellites.

CCD Star Trackers - The CCD Star Tracker uses a charged-couple imaging array as a detector in place of an image dissector. The detector is a buried-channel line-transfer, charge-coupled device (CCD), with vertical and horizontal picture elements. A typical detector contains 488 vertical by 380 horizontal picture elements within an active image area of 8.8 mm by 11.4 mm. The detector is cooled to an operating temperature below 0°C.

The detector array is read out with high speed microprogrammable logic. At those places in the field of view where star energy is detected, the operation is slowed to allow analog to digital conversion of the signal

charge of each picture element, or "pixel" in the region. A micro-processor is employed to compute the location of the centroid of the star images to an accuracy of about 1/10 of the inter-pixel distance and to provide sequencing and control functions. The CCD unit possesses some distinct advantages over other types of star sensors. Those are: the ability to track multiple stars simultaneously, no sensitivity to magnetic fields, and improved accuracy. At the present time TRW, BBRC, and Honeywell are evaluating the performance of CCDs in the laboratory using experimental breadboard models. The preliminary characteristics of both the BBRC and TRW CCD units are presented in Table 2.4-2.

Horizon Sensors – The combination of a two-axis digital sun sensor and a horizon scanning sensor has often been applied to the problem of attitude determination. The two-axis digital sun sensor will provide the two-axis attitude information and, with the aid of a horizon sensor, can provide three-axis attitude information. It is generally a low cost, reliable sensor system with less software support required. However, because of the low resolution of the sensors and the lack of definition of the targets they sense, the sun/horizon sensor combinations are used only where relatively coarse attitude information is required.

Sun Sensors – Sun sensors can be divided into analog and digital types. However, analog sensors have several disadvantages and will not be treated here. The major component of digital sun sensors consists of a mask which encodes sun angles as digital numbers. Light passing through a slit on the front surface of a fused-silica reticle forms an illuminated image of the slit on the binary-code pattern which is on the rear surface. The image's position is dependent upon the angle of incidence.

Behind each column of the code pattern is a silicon photodetector. If the light falls on a clear portion of the pattern in a particular column, the photocell behind is illuminated producing an output "one"; if it falls on the opaque segment, the photocell is not illuminated and the output is "zero". The outputs of the cells are amplified, stored, and processed as required to furnish suitable output to telemetry or other data processors.

The gray code most commonly used for encoding quantitizes the field of view into 128 increments. Therefore, the accuracy obtainable is dependent on the front end optics and the width of the reticle. The accuracies which have been obtained are on the order of .1°.

Space Sextant – The space sextant approach to attitude determination utilizes the angle between several stars and two reference points located on the base of the sextant. The sextant consists of two Cassegrain telescopes, an angle measurement head, gimbals that provide three angular degrees of freedom for the telescopes, and a reference platform consisting of a planar mirror, porro prism assembly, and a gyro package (Figure 2.4-5). The space sextant was primarily designed for autonomous navigation, but the addition of the reference package allows attitude determination as well.

Attitude is determined by first making included angle measurements between two or more stars and a reference mirror fixed at the base of the

80

trackers have accuracies ranging from 1 to 60 arc sec. This type of sensor, however, has several serious disadvantages:

1. Gimbal apparatus reduces long term reliability.

2. Possible to track either the wrong star or particles such as paint chips.

3. Errors in determining star position with respect to null, and gimbal angle readout errors effect the overall accuracy.

4. Increased size and weight due to gimbal mount.

Electronic Star Tracker - This type of star tracker is an electro-optical device which electronically scans a small instantaneous FOV over a larger effective FOV in order to acquire stars brighter than some fixed threshold. The scanning pattern is usually produced by an image disector tube and associated electronics. During acquisition the scanning pattern is a raster type until a star is detected. At this point, the raster scan is normally halted and the star is tracked using a much smaller scan pattern until the star leaves the effective FOV.

The electronic star tracker has no moving parts so it is usually lighter, smaller in size, and has a longer life time reliability than the gimballed star tracker. In addition, it generally has a higher sensitivity, greater signal to noise ratio, and is relatively more rugged mechanically than the gimballed type tracker. However, it too has disadvantages as discussed below:

1. Subject to errors from stray electronics, magnetic field variation, and temperature variations.

2. Because of the finite acquisition time, a maximum attitude rate limit is imposed to ensure quality output data.

3. Narrow field of view might limit the mission applicability.

Star Mappers - The star mapper generally has a slit type aperture which utilizes the spacecraft rotation to provide a scanning motion for the sensor during steller acquisition. The FOV of the sensor is thus scanned over the celestial sphere. It is limited to use on spinning satellites.

CCD Star Trackers - The CCD Star Tracker uses a charged-couple imaging array as a detector in place of an image dissector. The detector is a buried-channel line-transfer, charge-coupled device (CCD), with vertical and horizontal picture elements. A typical detector contains 488 vertical by 380 horizontal picture elements within an active image area of 8.8 mm by 11.4 mm. The detector is cooled to an operating temperature below 0°C.

The detector array is read out with high speed microprogrammable logic. At those places in the field of view where star energy is detected, the operation is slowed to allow analog to digital conversion of the signal

79

Table 2.4-2   Preliminary Characteristics of CCD Star Tracker

Characteristic	Units	TRW	BBRC
Accuracy (1 sigma)			
Vertical	arc-s	2.4	
Horizontal	arc-s	4.1	
Total	arc-s	4.75	5.0
Physical			
Weight	lb	7	7
Volume	in.	6 x 6 x 12	
Power	W	9.5 at 28 Vdc	26 at 28 Vdc
Development			
Status		Breadboard in Test	Breadboard in Test
Field of View			
Total	deg	6.0 x 8.53	7.1 x 9.2
Instantaneous	arc-min	0.81 x 1.35	
Optical System			
Focal Length	mm	76.0	70.0
f/No.		0.87	
Transmission		0.75	
Detector			
Type		Fairchild CCD	
Number of Elements		488 x 380	488 x 380
Image Area	mm	8.8 x 11.4	8.8 x 11.4
Configuration		Front Illuminated, Interline Transfer	Front Illuminated, Interline Transfer
Electronics			
Intergration Time (for +6 M Star)	s	0.100 Max	0.100 Max
Read Rate (for +6 M Star)	s	0.100	0.100
Star Position Output			
Vertical	Digital	12-bit Serial	
Horizontal	Digital	12-bit Serial	
Star Magnitude	Digital	12-bit Serial	
Update Interval	s	0.100 Max	0.100 Max
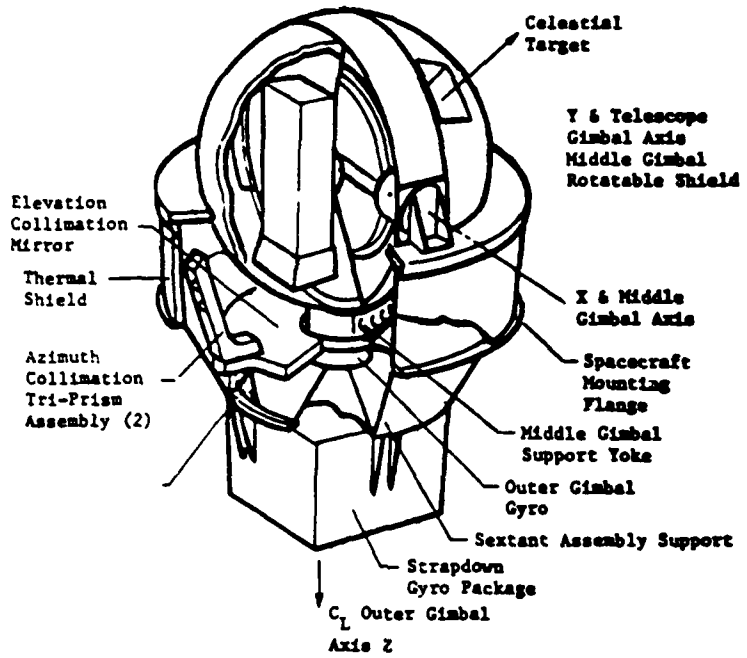
Sextant Collimation Off Mirror - Elevation Measurement
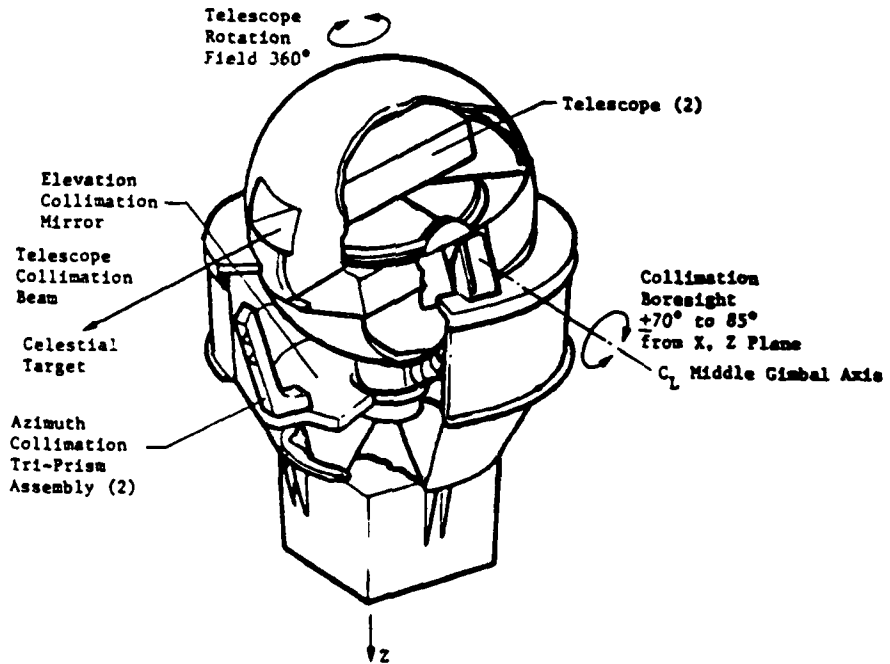
Sextant Collimation Off Porro Prisms - Azimuth Measurement

Figure 2.4-5 Attitude Determination with Space Sextant

82

sextant. A light source within the telescopes allows it to autocollimate off the mirror, thus providing a reference for one of the telescopes. The included angle relative to the reference mirror fixes the attitude in one direction with respect to inertial space. The other attitude directions are fixed by making included angle measurements between one or more stars and a porro prism assembly mounted on the reference mirror in such a way that the prism is elevated above the plane of the mirror. The two measurements are then processed to yield precise attitude information.

This attitude information is then used by an on-board filter to update the gyro uncertainty. Using this configuraiton, the three axis attitude uncertainty can be kept below 1/2 arc sec. The system characteristics are shown in Table 2.4-3.

Instantaneous FOV	Accuracy, 3-Axis	Size, in.	Weight, lb	Power, W	Life, yr
6 arc-min	0.5 arc-s	21.3x20x21.3	60	30	5

Table 2.4-3   Space Sextant Characteristics

Landmark Trackers - Landmark trackers utilize sightings of known earth features to yield attitude information. There are many types of earth features ranging from radar emitters to natural features such as lakes, and the methods used to detect these features differ as greatly. However, all the concepts rely on obtaining the Line of Sight (LOS) angles to some point on the earth whose position is accurately known and stored onboard.

The accuracy which is theoretically obtainable can be as good as 1 arc sec. for some types of Landmark trackers. However, Landmark trackers are not as well suited for attitude determination as other systems relying on sightings of celestial objects. The qualities which led to this conclusion are listed below.

Crosscoupling Between Attitude and Position - There is a severe crosscoupling between the position of the satellite and its attitude when LOS measurements are being made (Figure 2.4-6). A downtrack error can easily be mistaken as an error in pitch. There are proposed methods of obtaining several sightings within the field of view and using this information to derive both position and attitude. However, such a system would be nowhere near real time, and the onboard memory requirements would be tremendous.

Algorithms Too Involved - The algorithms to derive attitude from a Landmark sighting, assuming that position is known, are much more involved than those required by a star tracker or horizon/sun sensor combination. Because of the virtually infinite distance to stars, their coordinates can be stored in an inertial reference frame, and attitude can be derived directly from several sightings. Likewise, horizon/sun sensor systems directly derive the local vertical whereas landmark trackers do not.

Development Required - The technology required to implement a Landmark tracker attitude reference system has not evolved to the degree that star

83
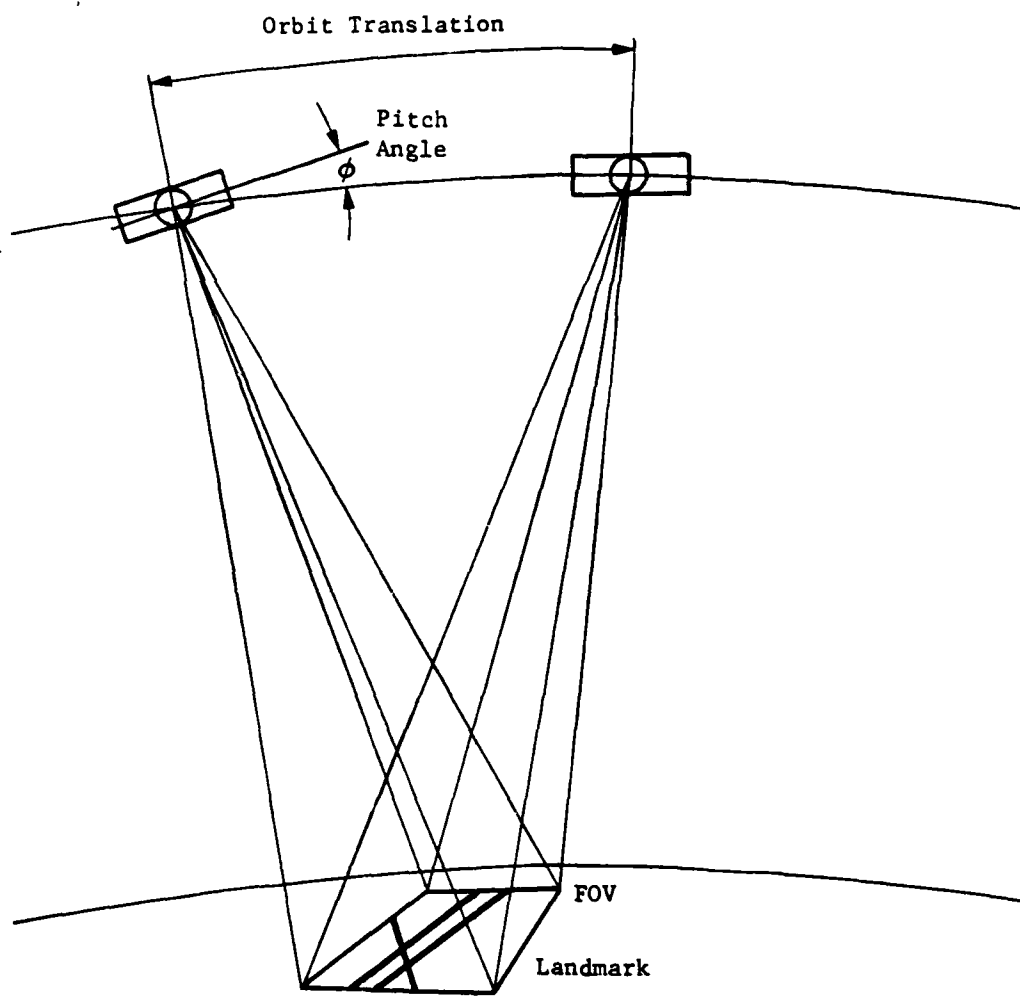
Figure 2.4-6   Position/Attitude Crosscoupling of the Landmark Tracker

trackers has. Most of the development in these trackers has been directed at solving the autonomous navigation problem, not attitude determination.

Landmark trackers are much better suited for navigation updates than for attitude updates, and so they should possibly be dismissed from this application.

RF Interferometers - Interferometers can be used to derive attitude information by measuring a line of sight angle between the spacecraft axis, defined by an antenna array, and an RF emitter whose position is accurately know. The angle is measured by detecting the phase difference of an RF signal arriving at two pairs of receiving antennas. A very large antenna with a monopulse feed can be used in lieu of an interferometer. This may be useful for missions that require a large antenna.

Complete attitude information can be obtained by knowing the position of at least two transmitters, and the angle of arrival of their signals. There have been two investigations for using an interferometer as an attitude determination sensor. The first, designated as the Interferometric Landmark Tracker (ILT), utilizes ground based radar emitter whose positions can be accurately stored onboard. These emitters include airport radar systems and perhaps tracking stations. Although the ILT differs from optical Landmark trackers in several ways such as the speed involved in measuring the LOS angles, and the memory required to store each landmark, the system is still limited by the crosscoupling errors.

The second approach to using an interferometer is in the conceptual stage only, but the method involved is promising. The Global Positioning System (GPS) is designed to be a navigation aid. However, through the use of an interferometer placed onboard the user spacecraft, attitude information can be derived as well.

Unique determination of three axis attitude information involves measuring relative to the spacecraft axis, two linearly independent vectors to GPS satellites using two independent interferometers. The accuracy obtainable from such a system is between $.02^{\circ}$ and $.6^{\circ}$.

Summary - The attitude sensing requirements of all missions of interest for this program can be met. The basic system envisioned in each case is an IRU, backed up by a horizon sensor-sun sensor set for coarse attitude update or a stellar sensor or Space Sextant for fine statellite update when necessary. The use of landmark is, of course, mission dependent.

2.4.2.2 Position Knowledge (Autonomous Navigation). Autonomous navigation systems can be separated into three groups--position-sensitive angular measurements to celestial objects, Earth-based target reference measurements, and range measurements to known beacons. In systems utilizing angular measurements to celestial objects, the satellite determines the local vertical to the Earth's surface and then measures the angles to three separate known stars. From these measurements, position and attitude information can be derived.

Systems using Earth-based target reference measurements to determine position and attitude depend on Ground Control Points (GCP) or landmarks which can be identified from space. GCPs have many forms--pinpoint light sources, EM emitters, linear features, or specified areas on the ground. Although different systems detect different forms of GCPs, the parameter measured is always the angle to the center of a feature whose coordinates are known. From these measurements and measurements taken from an attitude determination system, complete position and attitude information can be obtained.

Systems relying on known beacons determine range to three or more known points and triangulate to solve for position. Range is determined by acquiring some sort of navigation signal transmitted by the beacons. The signal contains information about the position of the transmitter and time of signal origination. The receiver then solves for the propagation time by knowing the time of signal reception; then assuming a constant propagation velocity, the range is calculated. Several systems are separated in Table 2.4-4 into one of these categories. Table 2.4-5 briefly summarizes the operation for seven autonomous navigation systems, representing the above categories.

It has been estimated that by 1980 the performance of a spaceborne computer will match that of a CDC 6600, operating at just over 10 mega instructions per second (NASA, A forecast of Space Technology 1980-2000, January 1976). With the increased capability of onboard processors, it will be beneficial (in terms of cost and effectiveness) to automate many of the mission activities which currently require extensive ground processing. Automation will not only minimize the amount of ground support equipment and post-flight analysis required to operate a satellite (a major cost factor), but the end-to-end process of data handling could be cut to the point where analysis of the data could be performed on a near real-time basis.

In summarizing autonomous navigation systems, it is necessary to consider the type of mission being flown, the required lifetimes, and accuracies necessary.

Two of the major limitations of earth observation missions are the stationkeeping of the vehicle and the registration of the data being received. It would be most beneficial if an autonomous navigation system could perform both of these functions. The registration of image data can be performed in one of two ways; either a very precise navigation system or a landmark tracker can be used. A satellite in a sun synchronous orbit of 912 km (567 nm) using the SS-ANARS system (highest overall accuracy) whose accuracies are quoted as being 244 meters (800 feet) for position and 1 arc sec for attitude, would have an uncertainty in ground position, as seen by the sensor, of approximately 250 meters (820 feet) assuming no pointing errors for the sensor, (Figure 2.4-7). This uncertainty value may not be acceptable for some feature identification or mapping functions; therefore, a landmark tracker should be used to minimize the ground position error to within acceptable limits (perhaps 30 meters (100 feet)).

86

Position sensitive angular measurements to celestial objects

     LES 8/9   Sun – Local vertical
     SS–ANARS   Moon – Star
     AGN   Planet – Star

Earth-based target reference measurements

    Natural landmark identification

    1) area correlator
    2) linear feature detection

Artificial landmark identification

    1) Systems using optical emitters (lasers, search lamps)
    2) ILT using microwave emitters (radars)

Range Measurements to known beacons

    GPS   Earth orbital beacons

Table 2.4-4   Autonomous Satellite System Concepts
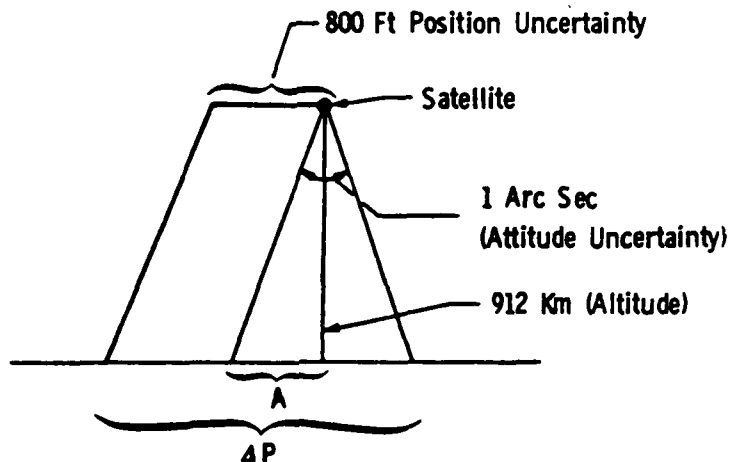
$$\Delta P = 800 \text{ Ft} \times \frac{1 \text{ Meter}}{3.28 \text{ Ft}} + 912000 \tan (1 \text{ arc sec}) = 250 \text{ Meters}$$

Figure 2.4-7   Ground Position Uncertainty

87

Table 2.4-5 Summary of Antonomous Navigation Systems, Part 1

System	Agency/Contractor	Application
Autonomous Guidance and Navigation Mark IIIA Mark IIIB	NASA Hq, OAST RTOP 506-19-25 and 5(6-19-21 Contractor: JPL, Pasadena, CA Manager: Alan R. Klump JPL, Ext 679! or 6769(lab)	Designed for interplanetary use on non-lander vehicles 1. Flyby missions 2. Satellite and asteroid exploration
Lincoln Experimental Satellite	DOD - Air Force Contractor: MIT Lincoln Labs Contact: Dr. S. Srivastava Lincoln Labs, Ext 5878	Satellites in synchronous orbit 1. Change of orbit is possible
Global Positioning System	DOD NASA-OADS Contractor: Receiver: APL and Magnavox OADS: Martin Marietta (onboard attitude determination system) APL: Fric Hoffman and R. E. Willison Martin Marietta: John Wilson	Applicable to Earth orbiting satellites below the GPS orbit (10,900 nautical miles)
Space Sextant SS-ANARS	DOD - Air Force Contractor: Martin Marietta, Denver Division Manager: Dale Mikelson	Designed for Earth orbiting satellites 1. Independent of orbit 2. Easily modified to include interplanetary vehicles or planetary orbiters
Known Landmark Detection (area correlator)	Internal IR&D at Martin Marietta Project number: D-53D Principal Investigator: Lloyd Gilbert (303)-973-3369	Designed for Earth orbital satellites) 1. Accuracy improves for low Earth orbits *Conceived as a final processor for SS-ANARS or GPS to achieve high accuracy position determination
Known Landmark Tracker (detection of linear, features) with a star tracker for attitude reference	Internal IR&D at Honeywell Aerospace Principal Investigator: Peter Kau (813)-531-4611, Ext 3365	Low Earth orbiting satellites
Artificial Landmark Tracker	Agency: Goddard Space Flight Center Contractor: Charles Stark Draper Laboratories Manager: Bob White 258-1297 Contact: Robert Var 258-1560	Low Earth orbiting satellites

Table 2.4-5   Part 2

Status	Level of Autonomy

Sensor development in breadboard stage
Preliminary software design completed
Dedicated costs: approximately 8 man-years
Mark IIIA system to be flown on Jupiter Orbiter
  with Probe (JOP) 1982
Mark IIIB system in development for post-JOP
  missions
Active contacts: RTOP 506-19-25 and 506-19-21
	Mark IIIA
	  Contains - AGN sensor
	                  - measurement extraction
	                  - maneuver execution
	  Relies on Earth -
	    - optical orbit determination
	    - maneuver determination
	Mark IIIB
	  Complete autonomous navigation with
	    optional override from Earth
	Both phases contain extensive onboard
	  processing and ground support.

LES 8 and 9 launched in 1975; currently functioning Development costs: unavailable	Fully autonomous n single orbit Must obtain a command from Earth to change orbits.
Receiver/Processor unit 1. Development stage: breadboarded and tested OADS Onboard/Attitude Determination System Contract number NAS5-23428	Fully autonomous
Orbital demonstration scheduled for December 1980 Dedicated costs: $110,000 IR&D sources $9 million sales to USAF Active contract: F04701-77-C-0043	Fully autonomous

Studies of several correlation algorithms and
the initial design concept of the parallel
processor were conducted in the fall of 1977
 	
Current project: IR&D DSFD
  demonstration of orbit and attitude deter-
  mination in a simulated environment to be
  completed by Dec 1978
Dedicated costs: 1977 - $15,000
                          1978 - $40,000 IR&D sources
	Position determination shown to be
	  feasible with full autonomy
	Attitude determination, using known
	  landmarks, is being investigated
	If attitude determination is
	  unfeasible, a star tracker and
	  gyro can be used to obtain this
	  information

Sensor in breadboard stage undergoing testing
Several algorithms for linear feature identifi-
  cation are being investigated
Lab demonstration in 1975 using film for
  video input
Dedicated costs: $350K - 500K from '71 to present
	Fully autonomous

Advanced Earth Observation System Instrumentation study completed in 1975 No further contracts issued Goddard contracts Dedicated costs: $300K (est)	Relies on ground stations to process the raw data and uplink attitude and orbit corrections 1. Concept could be automated

Table 2.4-5   Part 3

Measured Parameters, Error Sources and Accuracy, 1 sigma	Physical Characteristics

Directions to satellites and planets
Intensity measurements of starts
Accuracies:
  Direction - 10µ rad fine targets
  Intensity - 20% accuracy for absolute magnitude
          5% for relative magnitudes
	Computer (using the FTSC)
	  Size: 1.3 cu ft
	  Weight: 50 lb
	  Power: 35 W
	Sensor
	  Size: no projections
	  Weight: 15 kg
	  Power: 20 W
	Subsystems: General purpose computer, CCD sensor, external memory for star catalog and ephemeris data, AD converter, ground systems, propulsion

Measured parameters
1. Time of sun transit (an Earth, satellite, sun angle of 90 and 270 deg)
2. Angles from the satellite to the two limbs of the Earth's disc
Accuracy: 0.02 deg in any orbit
	Physical characteristics - excluding IR sensor
	  Size: 6x6x8 in. sun transit sensor 4 cu in.
	  Weight: 6 lb
	  Power consumption: 6 W
	  Subsystems: Control, hardwired algorithms, IR sensor, sun transit sensor, Earth command, propulsion.

Measured parameters: the distance to each GPS satellite by using transition time of signals, doppler shift of signal.
Data obtained from GPS signal: time of signal origination, GPS ephemeris, ephemeris of all 24 GPS satellites, doppler shift of signal
Accuracy Time: 9 nanoseconds
      Position: 12 meters (spherical)
      Velocity: 0.0061 meters per second
Error sources: nonisotropic, inhomogeneous atmospheric effects gravity harmonics and drag
	Physical characteristics of receiver/processor assembly
	  Size: 16.4x12x8.4 cu in.
	  Weight: 38 lb
	  Power: dual channel - 40 W
	      single channel - 32 W
	      standby mode - 5 W
	requires external oscillator for timing signals
	Subsystems: Antenna/preamplifier, receiver/processor, dual oscillator, interface unit

Measured parameters included angles between
1. Stars and moon's limb
2. Stars and Earth's limb
3. Stars and a plane defined by the gyro package
Accuracy of angle measurement: 1 arc sec
  Position: 800 ft after 24 hours
  Attitude: RMS 3-axis error 1.0 arc-sec
Error sources: misalignment between prism faces, electronics offset, nonuniform bearing preloads, telescope axis misalignment
	Physical characteristics:
	  Size: 21.3x20x21.3 cu in. - sensor
	      7.0x9.0x13.0 cu in. - support electronics
	  Weight: 60 lb - sensor
	      25 lb - support electronics
	  Power: 30 W from three transformers
	  Life Expectancy: 5 years
	  Subsystems: Sensor (telescopes, drive motors, measurement wheel, etc), support electronics (Processor to control motors, keep lunar ephemeris data, etc)

Measured parameters include direction to the center of known landmark areas
Accuracy: ground position accuracy is good to one tenth of a picture element resolution (8 meters for the Landsat MSS sensor) under ideal conditions (limited noise)
Error sources: Cloud coverage, seasonal effects, pointing errors
	Physical characteristics:
	  Size: undetermined
	  Weight: 25 lb excluding the MSS sensor (est)
	  Power: 75 W (est)
	  Subsystems: Processing unit, image system (MSS), sync logic, G&C system, Chip library (external memory)

Measured parameters:
1. Direction to the center of linear features on the earth's surface
2. Direction to known stars
Accuracy: varies as R x ∆P x 1/3
  where R = altitude
          ∆P = pointing error
          1/3 = interpolation between pixels
Error Sources: Cloud coverage, pointing errors- minimal errors due to seasonal effects
	Physical characteristics:
	  Size: 2400 cu in.
	  Weight: 70 lb
	  Power: 100 W average
	  Subsystems - navigation sensors, processing unit, memory (landmark file), G&C system

Measured parameters: 1. ground position of certain artificial landmarks (such as search lights) 2. direction to certain known stars Accuracy: slightly better than one picture element (80 meters for Landsat) Error sources: misalignment of sensors, electronics bias, cloud coverage	Physical characteristics Onboard system not studied in contract

Table 2.4-5   Part 4

Computational Requirements	System Benefits

SAMSO's Fault Tolerant Spaceborne Computer (FTSC) is being considered
Program capacity: approximately 128,000 32-bit words
External memory: approximately 450,000 32-bit words
Speed: not critical
Reliability: 95% for five years
Architecture: multiprocessing (probable)
Interfaces: AGN sensor through a dedicated microprocessor science sensor
Power: approximately 35 W }
Weight: approximately 50 lb } FTSC projections
	1. Possible use of SAMSO's FTSC (lower development cost)
	2. Automatic switch to Earth control if autonomos system is found to be faulty
	3. Autonomous determination of target position and rotation rate
	  a. update knowledge of planetary ephemerides
	  b. accurately initialize a lander or orbiter

No general purpose processor onboard Hardwired algorithms with a low duty cycle 2 times a day Future systems could include a general purpose computer with a small memory requirement and low duty cycle	1. Retains ability to be repositioned in any orbit 2. Because of the small size and low duty cycle, the satellite is free to spend time on scientific endeavors 3. Fairly simple sensor configuration 4. Has flown already
Does not require external computations 1 Processor contained in receiver unit	1. No external computational requirements 2. High position accuracy 3. Real-time computation of position
Computer Configuration: Minicomputer Memory Required: Lunar ephemeris data 6K words (16-bit) Total memory 26.5K words Speed: Input/Output 50K bits/sec Interfaces: Roll and yaw gimbals, flight computer (FTSC)	1. System adaptable for interplanetary use 2. High accuracy for both position and attitude 3. Can be used with equal accuracy in any orbit 4. Flight test model to be used with FTSC 5. Position and attitude determination using the same unit

Computer Configuration: Six parallel microprocessors feeding into three parallel processors feeding into a final processor
Memory: Bubble memory 92K bytes
       RAM memory 45K bytes
Speed: 4 MHz
Time Required for Location for Best Fit: approximately 27 sec
	1. Automatic scene annotation
	2. Data reduction by eliminating unwanted scenes (such as ocean and cloud covered areas)
	3. Does not require extensive sensor technology
	  - could be used with MSS
	4. High position accuracy

Computer Configuration: Microprocessors
  Configuration: undetermined*
  Memory: 16K
 	
*Parallel processor being examined
	1. Minimal effects caused by seasonal variations of Earth's surface
	2. Automatic scene annotation
	3. Accuracy of position determination can be improved by using image enhancement techniques
	4. Near real-time determination of position

Computer Configuration
 	
  Onboard system not studied in contract
	1. Real-time determination of position/attitude
	2. No extensive sensor technology required
	  - could be used with a MSS
	3. Not studied for automation

91

Table 2.4-5   Part 5

System limitations	Sensor

: Extensive computational requirements	800x800 element CCD (probable)
	  FOV of each element approximately 50μ rad
	  Total FOV approximately 2.3 deg
	
	A dedicated microprocessor calculates the
	direction to a certain star or to the center
	of an extended object

1. Limited accuracy (instrumentation
   pointing limited;
   - corrects for low frequency perturba-
     tions in orbit
2. Accuracy deteriorates for low Earth
   orbits due to atmospheric effects
	IR sensor to scan Earth's disc
	Sun transition sensor to detect
	  a sun, satellite, Earth angle of 90 or 270 deg

No attitude determination in the GPS
receiver/processor unit
   - requires external attitude deter-
     mination such as a star tracker
	Antenna 200 deg receiving cone

Increased mechanization
   - angular measurement head
   - bearing problems
	Sensor. 8-element silicon detector; the four
	   outer elements provide coarse acquisition
	   (6 arc-min) and the inner array of sensor
	   elements provides fine tracking (1 arc-sec)

1. Not real-time computations
     - not necessarily critical
2. Cloud coverage limits accuracy
3. Seasonal changes limit accuracy
     - effect can be reduced by
       updating chip library
4. Heavy computational requirements
	Studies carried out using data tapes from
	Landsat's MSS

1. Cloud coverage limits accuracy
2. Only one component of position
   information is derived for each
   landmark sighting
	Sun Sensor
	
	Down Sensor: Array type, perhaps CCD or a
	   linear array

1. Requires special landmarks that must
   be maintained
2. Limited accuracy caused by pulse
   configuration of signal
     - limits scientific pointing
	Ground tracking sensor: Multi Spectral Scanner
	
	Star sensor: Standard Ball Company sensor
	   developed for NASA

92

Landmark trackers have the ability to determine the ground position of the sensor's FOV, but it is difficult to differentiate between errors in the position and attitude of the spacecraft. If the satellite were tilted along its pitch axis, the FOV of the sensor would be very similar to the FOV seen if the satellite were translated (maintaining its attitude) along its flight path. Using landmark techniques, it is difficult to determine the position of the satellite without knowing the attitude and vice versa. However, the landmark techniques are ideal for image registration since they determine the absolute ground position of the sensor's FOV.

Benefits and limitations of each approach to landmark identification are shown in Table 2.4-6. From this tradeoff, it is apparent that the area landmark registration approach is superior to other approaches. Although the technique requires significant computational support, processors are currently being developed which could handle the increase load. Also, using a single processor, the registration technique requires an excessive amount of time to provide a position update, however initial studies shows that this time could be drastically reduced by hardwiring the correlation algorithm. The technique of area registration not only provides inputs to a navigation system, but a general purpose image processor allows autonomous annotation of sensor data, inputs to a sensor pointing system, and deterministic data acquisition and transmission.

For our missions the GPS system and Space Sextant are the prime candidates. It is difficult to label one of these systems as being superior due to the difference in concept. GPS will realize a greater position accuracy, but does not have a capability for autonomous attitude determination. In addition, the ground support system is both costly and vulnerable. The space sextant provides both navigation and attitude information, but is limited by its size and weight. The use of either of these systems will depend upon a detailed mission analysis.

2.4.2.3 Disturbing Torques and Forces. The sources of disturbing torques are solar radiation, aerodynamics, gravity gradient, magnetic and internal disturbances.

Solar Radiation Torques and Forces. Solar radiation forces and torques are a function of the exposed surface area projections on a plane perpendicular to the solar vector and surface properties.

When the computations were applied to a large antenna with 300,000 sq ft area, a lever arm of 200 feet, in a synchronous equatorial orbit (characteristic of a possible radar mission), it was determined that the average torque over a 5 year lifetime was .74 ft lbs in pitch and roll. The peak torque was 1.17 ft lb. In addition to producing torque on the vehicle, in the above example, solar pressure produced translational motion away from the sun as shown in Figure 2.4-8. When stationkeeping is a requirement this effect is severe. In the above example 209 lbs of propellant with a specific impulse of 2800 seconds were required to maintain station for 5 years (587, 354 lbs sec of impulse).

93
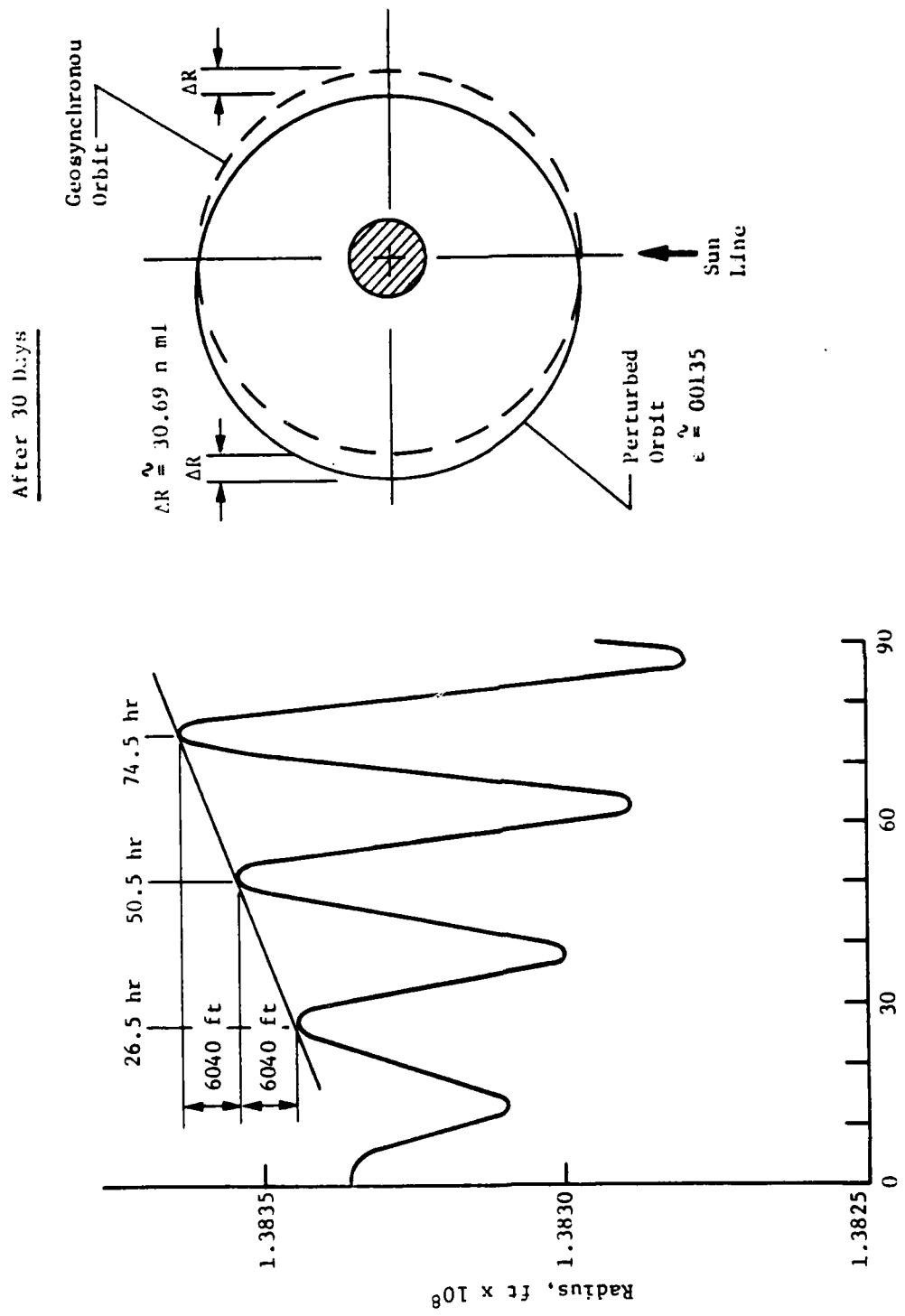
Figure 2.4-8 Solar Pressure Effects

Landmark Tracking Techniques	Benefits	Limitations
Artificial L/M Tracker (Accurately placed optical beacons)	Fast Relatively small computational support for one L/M sighting	Requires upkeep of ground based emitters Accuracy limited to pixel resolution Small percentage of clouds can obscure the emitter Study was conducted with the idea of using ground processing System cannot provide other functions
Interferometer L/M Tracker (RF emitters)	Fast Relatively small computational support for one L/M sighting	Requires upkeep of ground based emitters Limited accuracy Cannot provide other functions Requires sizeable antenna which is generally not a primary sensor
Linear Feature L/M Tracker	Fast No upkeep of Ground Systems	Severely affected by clouds Does not yield complete positions information for each sighting Cross-coupling between crosstrack and downtrack errors

Table 2.4-6   Tradeoff of Landmark Tracking Techniques

Aerodynamic Torques and Forces - A simplified expression used in computing the aerodynamic torque is:

$$L_a = P_a \ell_a A_a \sin\alpha$$

where:

L_a = torque due to aerodynamic pressure; foot-pounds

P_a = aerodynamic pressure; pounds/ft^2

ℓ_a = distance between center of mass and center of aerodynamic pressure; feet

A_a = surface area exposed to aerodynamic pressure feet^2

α = vehicle angle of attack; radians

Aerodynamic pressure as a function of orbit altitude is given in Figure 2.4-9.

The aerodynamic torque as a function of latitude, exposed area, and lever arm is plotted in Figure 2.4-10.

From Figures 2.4-9 and -10, it can be ascertained that aerodynamic torques will be significant for the low altitude Millimeter Wave Radiometer mission.

Atmospheric drag can impose significant forces and torques on large, low density vehicles in low earth orbit. For long-life, large, low density spacecraft remaining in LEO, the minimum acceptable operational altitude is 400 n.mi. On such a spacecraft, drag makeup thruster vectors should be aligned with the vehicle's center of pressure to minimize attitude disturbances.

The average value of atmospheric drag at discrete altitudes is given in Table 2.4-7. These values are for solid frontal area (area projection perpendicular to orbital velocity vector).

Altitude (n.mi)	Drag (lb/ft^2 Frontal Area)
100	1.3×10^{-3}
200	1.3×10^{-5}
300	6×10^{-7}
400	4×10^{-8}
500	7×10^{-9}

Table 2.4-7   Atmospheric Drag vs. Altitude
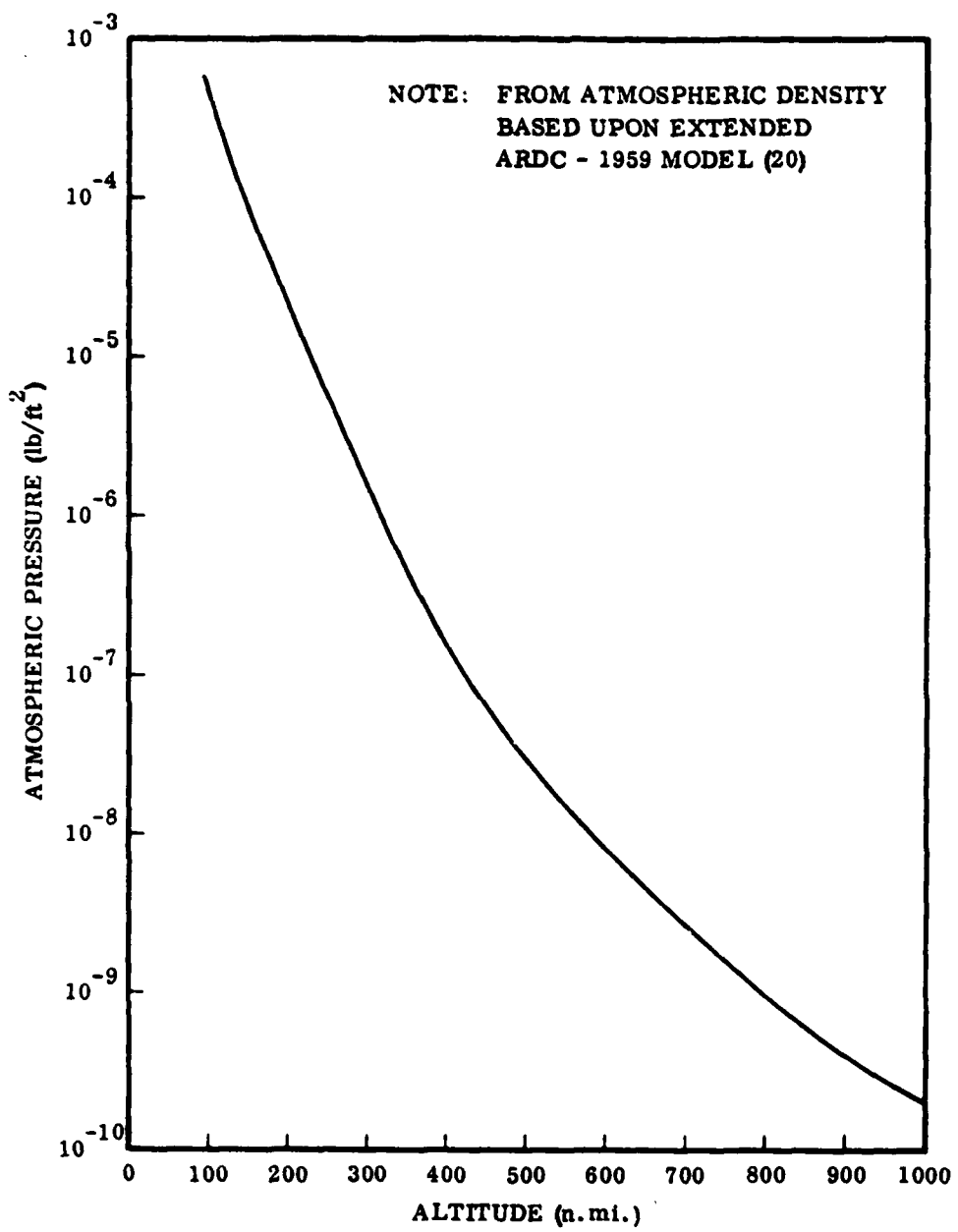
Figure 2.4-9   Atmospheric Pressure as a Function of Orbit Altitude
(Assuming Circular Orbits)

97
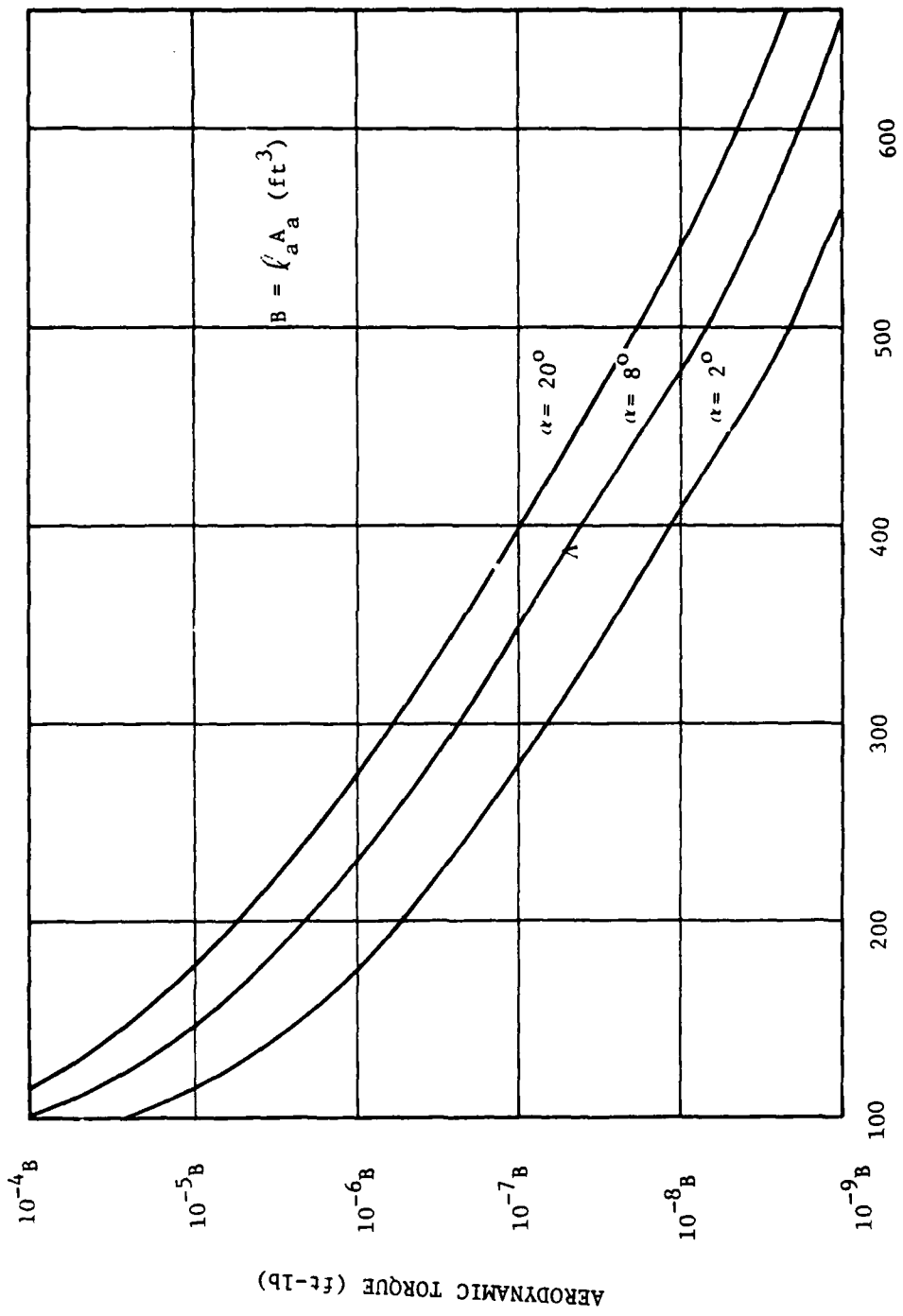
Figure 2.4-10 Aerodynamic Torque as a Function of Orbit Altitude

98

An example was analyzed with respect to atmospheric drag and its impact on propellant consumption and atmospheric drag. The example is shown in Figure 2.4-11

The example is a nadir-point parabolic dish that is in low earth orbit (LEO). Using its projected area and the drag values from Table 2.4-7 yields the drag values shown. Multiplying these drag values by the number of seconds in a five year mission gives the total impulse required for drag makeup during the mission. These impulses were converted to storable propellant (I_{sp} = 228) pounds and electric propulsion (EP) propellant pounds (and supporting power required) as shown. At 300 n.mi, 70,000 lb. of storable propellant would be required or, with EP, 6000 lb. of propellant and an average of 11,000 watts are required. These values are large although the EP approach is marginally acceptable if one neglects earth shadow cycling of the power supply.

At 400 n.mi, drag is down sufficiently that either storable propellant or EP can be used for drag makeup. Either could be resupplied during the mission and with resupply, the mission could be extended easily beyond five years. Therefore 400 n.mi appears to be an excellent choice for a minimum altitude, long-life, large, low density spacecraft.

1000' DIAMETER,
250' DEEP
PARABOLIC DISH

(STAYING IN LEO)

ORBITAL VELOCITY

PROPELLANT PER 5 YR FOR ORBIT MAINTENANCE		
LB @ I_{sp} = 228	LB @ I_{sp} = 3000 AND WATTS	
1.4×10^8 LBS	1.1×10^7 LBS	2×10^7 WATTS
1.4×10^6	1.1×10^5	2×10^5
7×10^4	6×10^3	11,000
4400	370	700
900	60	110

STORABLE PROPELLANT (I_{sp} = 228) REQUIRES ALTITUDE $\geq$ 300 n.mi AND PREFERABLY $\geq$ 400 n.mi

PLASMA OR LOW PROPULSION, POWERED BY SOLAR ARRAY, REQUIRES ALTITUDE $\geq$ 300 n.mi

Figure 2.4-11   Drag Make-Up Examples

99

Gravity Gradient Torque - The gravity gradient produces a torque about the center of mass of the structure. This torque is a function of the mass distribution and inertias of the structure. A good approximation can be calculated from

$$L_{cggx} = -L_{ggx} = -\frac{3}{R_o 3}(I_{zz} - I_{yy}) \sin 2\theta \cos^2\theta$$

$$L_{cggy} = -L_{ggy} = -\frac{3}{R_o 3}(I_{zz} - I_{xx}) \sin 2\theta \cos\phi$$

$$L_{cggz} = -L_{ggz} = -\frac{3}{R_o 3}(I_{xx} - I_{yy}) \sin 2\theta \sin\phi$$

where

$\mu = GMe$

G = universal gravitational constants

M_e = mass of earth

R_o = orbital radius from center of the earth

I_{xx}, I_{yy}, I_{zz} = principal axes inertias

θ = pitch angle

ϕ = roll angle.

A vehicle with substantially different moments of inertia along its principal axes will be significantly affected by gravity gradient torques. Calculations were run for a 170,000 lbm vehicle with

$$I_{xx} = I_{yy} = 267.E6 \ SF^2$$
$$I_{zz} = .63E6 \ SF^2$$

The vehicle was essentially a large antenna of 160,000 lbm with a 1500 foot mast with mass of 3000 lbm on the tip of the mast.

The torque about nadir was:

L = 16.7 ft-#/deg around nadir.

Gravity Gradient Torques are therefore an effect which must be taken into account when designing an antenna to slew or to fine point.

Magnetic and Eddy Current Torques - The magnetic torques on the vehicle are due to eddy current induced in the S/C, electrical currents in the S/C, and magnetic dipole from residual magnetism in "hard" magnetic materials and residual magnetism and induced magnetism in "soft" magnetic material in

the S/C. A hard magnetic material means a material in which the magnetic moment is essentially unchanged by small changes in the field around it. Conversely, the magnetic state of a "soft" material is predominatly determined by the ambient field.

The eddy current torques are due to induced eddy currents in the S/C and its interaction with the Earth's magnetic field. Since most of any large antenna would be made of graphite-epoxy tubes, guy wires, and hinge and latch mechanisms, which are conductive, there will be eddy current torques induced in the S/C. Modelling eddy current torques in this type of configuration is complex. Previously the eddy current torques have been modeled in a vehicle where the currents are induced into a cylindrical skin. The eddy current torques can be minimized by eliminating conducting loops or opening the loops by using non-conductive materials. The epoxy surrounding the graphite fibers in the composite tubes and guy wires will prevent the formation of conductive loops from the truss members.

The magnetic dipole moment is produced by residual magnetism in the "hard" and "soft" magnetic materials in the S/C and induced magnetism in the "soft" magnetic materials. There is an uncertainty in induced magnetism in "soft" magnetic materials. The residual magnetism in soft magnetic materials will change from the Earth-based measurement and cannot be predicted when the vehicle is in orbit. The dipole moment changes considerably from the prior-to-launch measurement. The difference between the prior-to-launch measurement and the on-orbit measurement is probably due to induced eddy currents and induced magnetism in soft magnetic materials. If the Earth's and the S/C magnetic field can be approximated by magnetic dipoles, the magnetic torques can be calculated by the following equation:

$$\overline{T} = \overline{M} \times \overline{B}$$

$\overline{M}$ = spacecraft magentic dipole ($A\text{-}m^2$)

$\overline{B}$ = Earth magnetic field (Tesla)

$\overline{T}$ = S/C torque (N-m)

A pessimistic estimate of the S/C dipole moment used for small spacecraft is 1000 pole-cm (1 $A\text{-}m^2$). Now, our missions vehicles are on the order of 100 times longer. A previous study made with a vehicle of this longer class assumed a dipole moment of 100 $A\text{-}m^2$. The torque produced by this dipole moment and the earth's magnetic field is negligible given that three orders of magnitude larger torques exist from other sources and will be compensated by the control system.

Torques due to High Current Flow in the S/C - The torque on the S/C due to current flow within the vehicle would tend to align the current along the Earth magnetic field. These torques can be eliminated by using a twisted pair or using ac current.

Other internal sources of forces and moments include thermal inputs and moving and deploying mechanical equipment within the spacecraft. The moving

101

mechanical equipment (e.g., masts, booms, gimbals, actuators, and wheels) primarily produce orientation disturbances.

Secondary spacecraft subsystems can product orbit perturbations as well as orientation disturbances. These secondary sources include outgassing and venting.

2.4.2.4 Controllers.

Types of Controllers - The means to generate control torques can be classified into three broad categories. All involve momentum interaction: momentum exchange between the spacecraft and the universe by reaction jets, between the spacecraft and moving parts in the vehicle (momentum exchange devices), and finally, interaction with the environmental field.

Jets of conventional type are particularly appropriate for stopping initial tumbling, execution of large-angle maneuvers, and for compensating for large disturbance torques. They have the disadvantage of eventually running out of fuel, limiting the lifetime of the spacecraft. This can be alleviated somewhat by using them in a constant thrust, pulsed mode, and permitting the spacecraft attitude to drift within given dead bands (limit cycle operation). This limits the pointing accuracy. Even when a secondary control system is used to point an antenna segment accurately on a separate, hinged compartment the sudden onset of angular acceleration due to the pulse firing is a substantial disturbance to the secondary control, which is of no little significance when high pointing requirements are needed. On the other hand, electrical propulsion systems are, in principle, suitable for long life operation if the electric energy is available. Their main disadvantage is the low thrust limitation, requiring another actuating system for maneuvering and for coping with large disturbance torques.

Momentum exchange devices are capable of long term operation and high accuracy when properly designed. Also, they are capable of delivering large torques. However, they have a limited angular momentum absorption capability; they saturate.

To avoid the saturation condition (which results in at least partial loss of control), a secondary means to generate torque is required. (Desaturation or momentum management system).

Torques generated by interaction with the ambient fields are due to four main sources: the magnetic field of the earth at lower altitudes and up to an altitude of about 10 earth radii; the atmosphere; and the radiation field from the sun.

The magnetic method is based on sending currents through three orthogonal coils attached to the vehicle or through a single coil double-hinged on the spacecraft. The current in any coil produces a magnetic moment which tends to align itself with the local magnetic field vector, thereby producing a torque on the vehicle. This method has certain drawbacks, such as the effect on vehicle instrumentation of the fields generated within the vehicle. Also, at any instant, torque can be produced only along components normal to the

102

local magnetic field vector. Practical limitation in the power supply and the coil size makes the generation of large torques unfeasible.

Aerodynamic forces, in principle, can be used to provide control torques about orientations which deviate slightly from a velocity vector oriented attidue. Satellite lifetime considerations will limit the areas of the aerodynamic panels used and hence also the torque magnitudes.

Selection of Momentum Exchange Controllers - For long lifetime space missions, it would be desirable to forego the use of active controllers since these devices impose penalties in terms of reliability and the weight of the propellant (required to provide primary control or to desaturate momentum exchange devices). Passive conprol is possible in systems where accurate pointing is not a requirement and which do not require slewing. Gravity gradient in antennas with long masts by itself will produce simple harmonic motion about the local vertical. The oscillation however is undamped and some method such as the reaction booms, simple active controllers or any of several spring mass systems metnioned in the literature must be incorporated to damp out the oscillation.

For our missions, with their pointing accuracies and slewing requirements, we will be forced to use some form of active control, at least for those portions of the mission when data are being taken. Due to the size of the antennas and the associated disturbing torques and forces, the use of momentum exchange devices, either reaction wheels or CMGs, backed up by reaction jets for momentum desaturation and stationkeeping is indicated.

Classification - The three basic elements, reaction wheel, single gimballed CMG, and double gimballed CMG are part of or assembled to a set of six functional units of which all configurations are composed:

1. Reaction wheel (RW)

2. Gimballed reaction wheel (GRW), single or double gimballed.

3. Single gimballed control moment gyro (SGCMG).

4. Scissoring single gimballed CMGs.

5. Double gimballed CMG (DGCMG).

6. Mechanically synchronized double gimballed CMGS.

All configurations built up from those six units may be ordered into the following ten groups:

1. Arrays of RWs.

2. Sets of RW arrays.

3. Arrays of gimballed RWs.

103

4. Sets of scissoring SGCMGs (V-pairs).

5. Arrays of SGCMGs.

6. Sets of SGCMG arrays.

7. Pair of DGCMGs.

8. Arrays of DGCMGs.

9. Sets of mechanically sychronized DGCMGs.

10. Hybird sets.

Examples – A large number of practical configurations have been proposed.
The most important ones will be discussed here in some detail in order to
facilitate a comparative evaluation.

Arrays of Reaction Wheels – At least three RWs are required to satisfy
control torque requirements.

N Skewed Reaction Wheels – Any number of RWs can be arranged to form
skewed arrays, but only 3, 4, 6, and 10 can be arranged completely symmetri-
cal. The advantages of using more than four lies in the larger degree of
redundancy, an enchanced possibility for energy exchange (to minimize power
requirements), and a more efficient momentum envelope. The disadvantages
mainly are increasingly complex control laws and an increase in total weight.

Six Reaction Wheels Arranged in Two Orthogonal Sets – These may be op-
erated either independently in two sets with one set serving as a backup
used only during peak control torque requirements or with all six operating
simultaneously using the energy interchange mode (or power transfer minimiza-
tion). Alternately, each pair of parallel RWs may be operated in an energy
interchange mode without cross feed to the other two pairs, resulting in a
simpler control law.

Three Single Gimballed RWs with Orthogonal Gimbal Axes – This is the
simplest configuration to combine two control systems into one unit; namely,
a fine pointing control using the gimbal rates as the control variables
while maintaining constant rotor speeds (CMG mode), and a coarse control for
large maneuvers using the rotor speeds as the control variables and locking
the gimbals (RW mode). The simultaneous use of all six control variables
requires a much more complex control law which may not be competitive with
other configurations.

Sets of Three Scissoring Single Gimballed CMGs – A scissoring pair of
single gimballed CMGs consists of two SGCMG with parallel gimbal axes ini-
tially oriented such that the moment a oppose each other and gimbals are
mechanically or electrically slaved to rotate by the same angles in opposite
directions (scissoring). The vector sum of the momentum vectors lies always
along one axis, the output axis. Three of these "V-pairs" of SGCMGs ortho-
gonally arranged make up a 3-axis control system. All axes are independent,

104

free of cross coupling. The required control law is extremely simple, featuring only a gain inversely proportional to the cosine of the gimbal angle about each axis. This simplicity of operation is the reason why this system is one of the earliest investigated. Since six CMGs are required to produce a modest momentum envelope of the shape of a cube, the overall system tends to be relatively heavy. Adequate redundancy is achievable with the heavy cost of providing a complex control law used only for failed CMG operation.

Array of Three Orthogonal Single Gimballed CMGs - This is the simplest SGCMG configuration possible. The momentum envelope is reasonable if one can live with the many singular relative attitudes of these SGCMGs (conditions which produce no torque component along one axis with finite gimbal rates) in connection with another type of control system (a reaction jet attitude control system for coarse control, for instance), fine pointing control can be maintained. A momentum envelope without any singularities inside exists with zero bias momentum. The corresponding control laws are reasonably simple. But, the lack of redundancy and the singularities mentioned above render this system impractical when used by itself.

Array of Four Skewed Single Gimballed CMGs - The gimbal axes are mounted tilted from one reference direction about equal angles in a symmetric fashion. When this angle corresponds to arc tan 2, the gimbal axes are parallel to the body diagonals of a cube. Various momentum storage envelopes can be accommodated by choice of the tilt angle. An elongated momentum ellipsoid can be inscribed in the momentum envelope of a skewed configuration with a large tilt or skew angle. An oblate ellipsoid fits in the envelope of the configuration with a small skew angle. These configurations are single redundant and are not free of singularities.

N Skewed Single Gimbal CMGs - Better redundancy and better momentum storage envelopes can be achieved if more than four SGCMGs are arranged in a skewed configuration. The complexity increases with the number of the CMGs. An improvement in the momentum envelope will be partially offset by the weight increase of the more numerous smaller CMGs. The weight optimal configuration for a given minimum spherical envelope is expected to consist of 4, 5, or 6 SGCMGs, depending on the design requirements. A previous study contains the results of a selection study for a large spacecraft application; naming the 4-CMG configuration the lightest in weight, and the 5-CMG configuration the best in overall performance.

Two Sets of Orthogonal Single Gimballed CMG Arrays - Three pairs of parallel SGCMGs are arranged with parallel pairs of gimbal axes orthogonal to each other. The configuration corresponds to the set of six scissoring SGCMGs with the synchronizing mechanism removed. The effect is to substantially increase the momentum storage capacity while requiring comparatively more complex control laws. The arrangement is triple redundant and suitable for a standby-mode operation; one set of three SGCMGs would be operating to maintain accurate pointing within a small momentum envelope, while the other set is inactive but also activated for large angle maneuvering.

105

Pair of Double Gimballed CMGs - This is the simplest DGCMG configuration. As with all DGCMG configurations, the gimbal actuators must carry the full CMG torques and are sensitive to forcing functions at the nutation frequency caused by inner and outer gimbal inertial cross coupling. The pair of DGCMGs has four degrees of freedom. One, the rotation of the CMG momenta about the momentum vector sum, does not produce any net torque and can be used to avoid gimbal stops. The condition where the spin vectors of the CMGs are antiparallel (zero momentum condition for equal CMG momenta) is singular in the sense that no control torque can be generated along the spin axis. The momentum envelope is sperical outside the gimbal stop wedges and slightly smaller within.

Array of Three Orthogonal Double Gimballed CMGs - The outer gimbals are mounted orthogonal to each other. This configuration has adequate redundancy. The loss of a complete CMG still allows 2-CMG operation reverting in configuration to the previous example. The major drawback, apart from the problems associated with DGCMGs, is the complexity of a satisfactory control law. This configuration was used on Skylab, and a great deal of literature on this configuration is available. The principal difficulty stems from problems involved in avoiding reaching the gimbal stops. When the total momentum magnitude is large enough (57% of saturation), then there are maneuvers where hitting the gimbal stops cannot be avoided without introducing other control torques or producing attitude errors.

A large number of hybrid configurations are possible. The scope of this work does not allow the discussion of all the reasonable possibilities. The simpler configurations combine a two axis CMG element like a DGCMG; a pair of two parallel SGCMGs, or a pair of synchronized two degree of freedom CMGs with a uniaxial device like a SGCMG or a scissoring pair of SGCMGs.

Characteristics of Certain Configurations - The weight of a reaction wheel system for three axis control consists of the weight of three momentum packages plus the weight of wiring and miscellaneous hardware. The power reuqired by the system is the motor power plus the dissipated power. Reaction wheel weight and power for a single axis are shown in Figures 2.4-12 and 2.4-13, respectively. Our larger antennas would fall in the upper portion of the curves.

The weight of a CMG system is obtained by adding the weight of the electronics to the weight of the control packages. However, the weight is not proportionate to CMG size. Typical weights of 3 CMG, 4 CMG and 6 CMG system versus angular momentum are shown in Figure 2.4-14; power requirements are shown in Figure 2.4-15.

Reliability of the systems drops as their complexity increases. A reliability comparison versus cost plot, Figure 2.4-16 (Vendor Supplies Data), indicates that high reliability, for 5 years, is significantly more cheaply obtainable with a 4 reaction wheel system than a 6 CMG system.

Reaction Jet System - In order to desaturate the momentum exchange devices and to provide the force necessary for stationkeeping or orbit maintenance (when required), systems of reaction jet must be used in con-

106
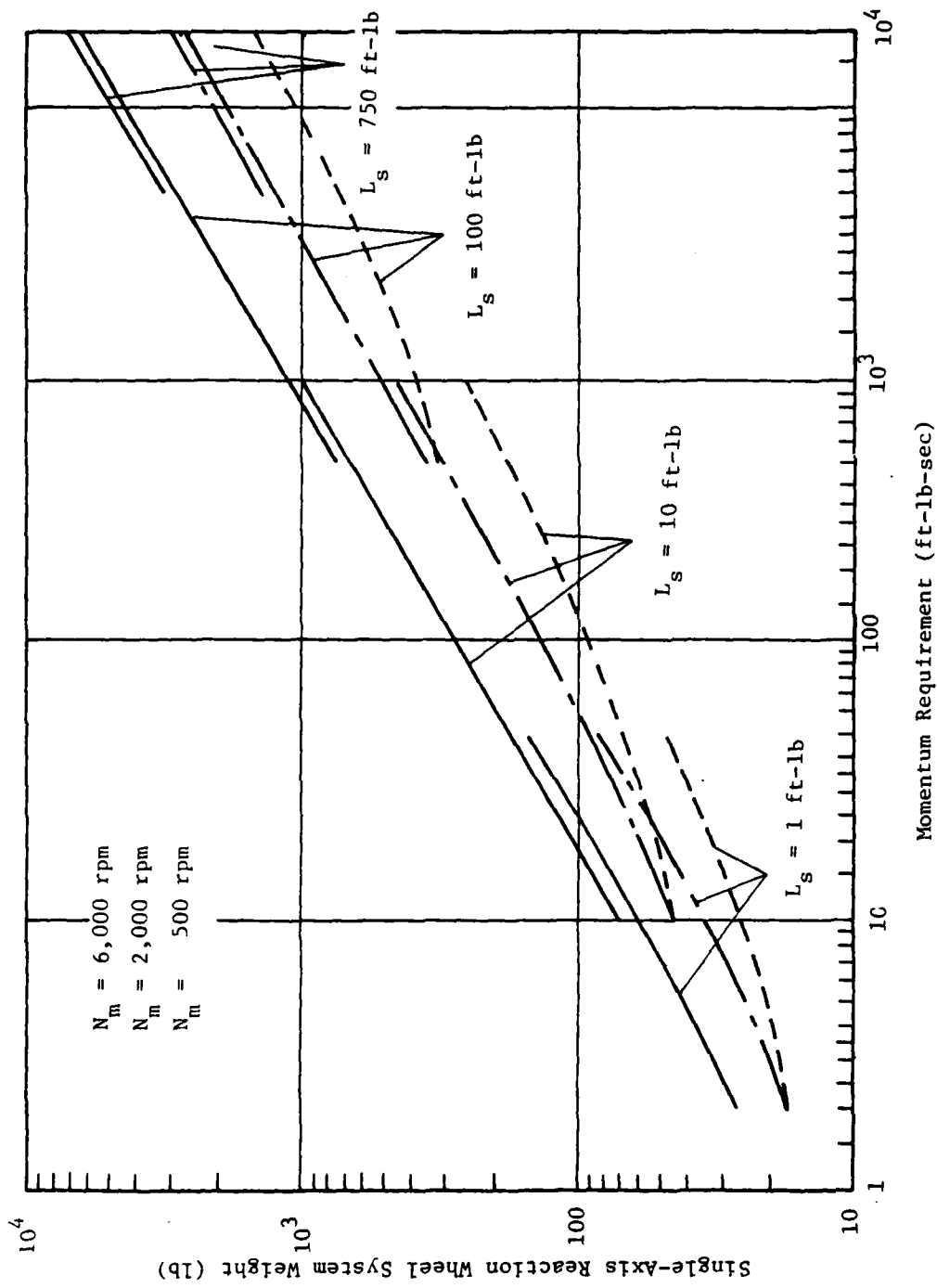
Figure 2.4-12 Reaction Wheel System Weight (Single Axis) as a Function of Momentum Capability
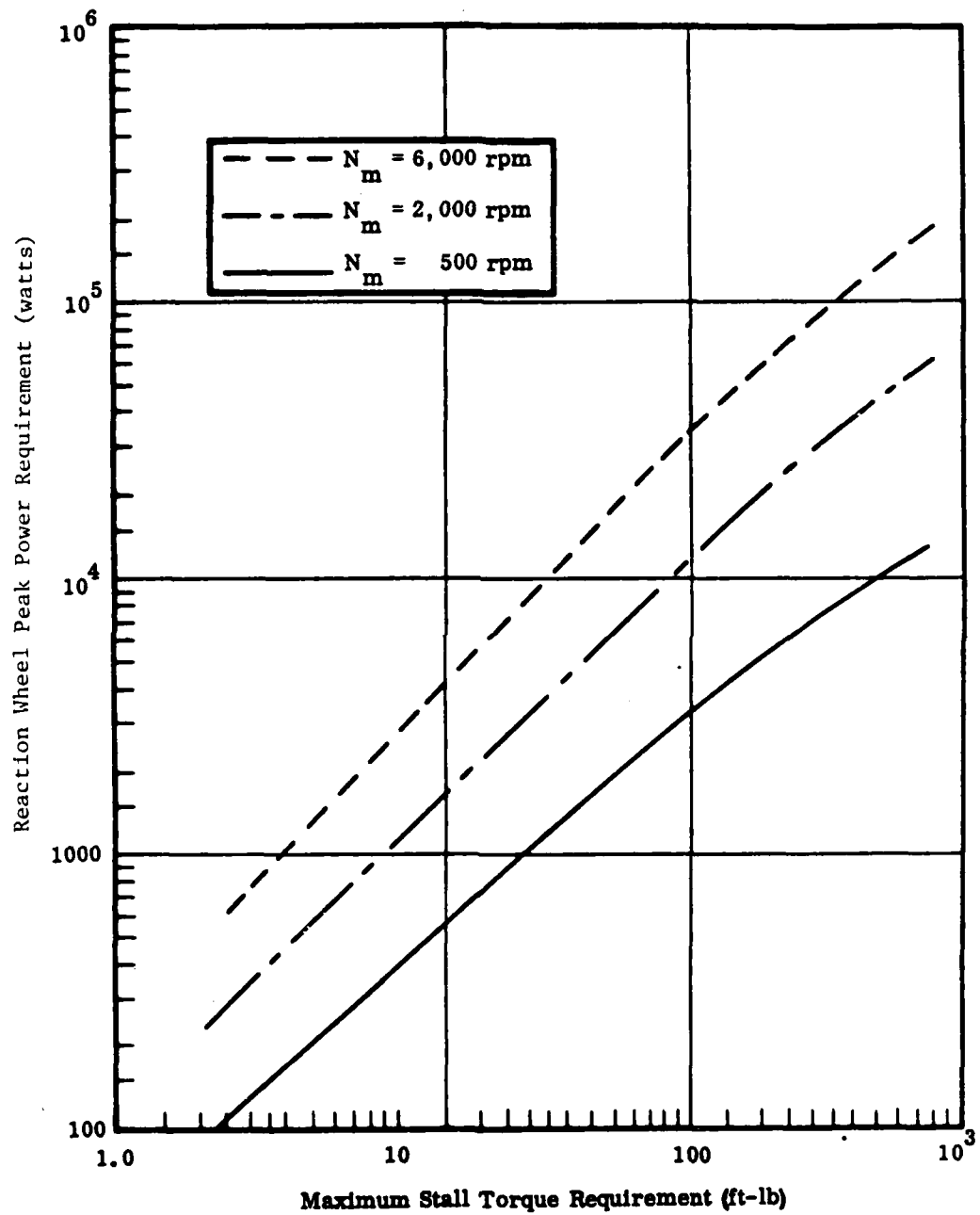
Figure 2.4-13 Reaction Wheel Peak Power Requirements (Single Axis) as a
Function of Momentum Capability

108
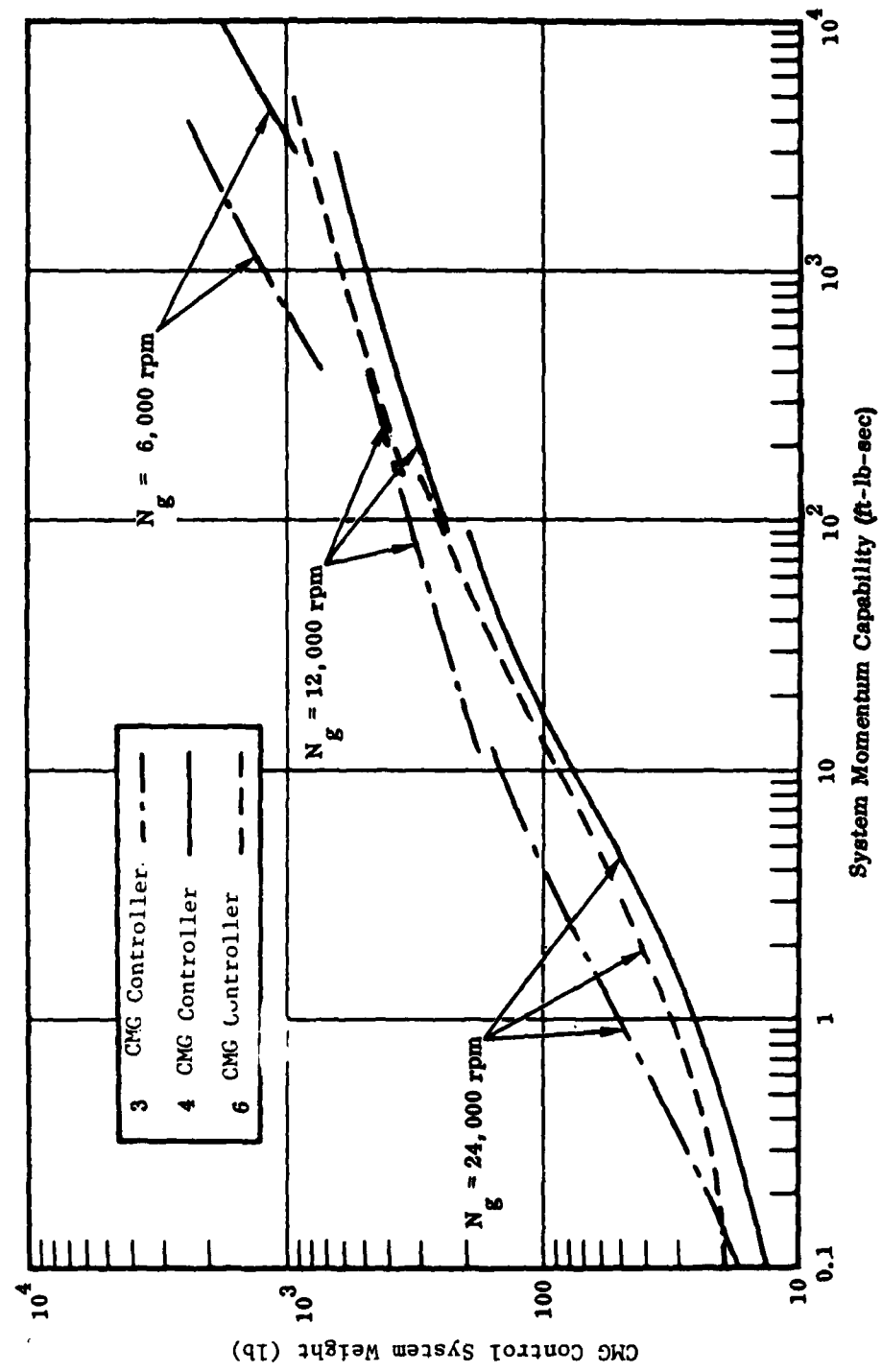
Figure 2.4-14 CMG Control System Weight as a Function of System Momentum Capability
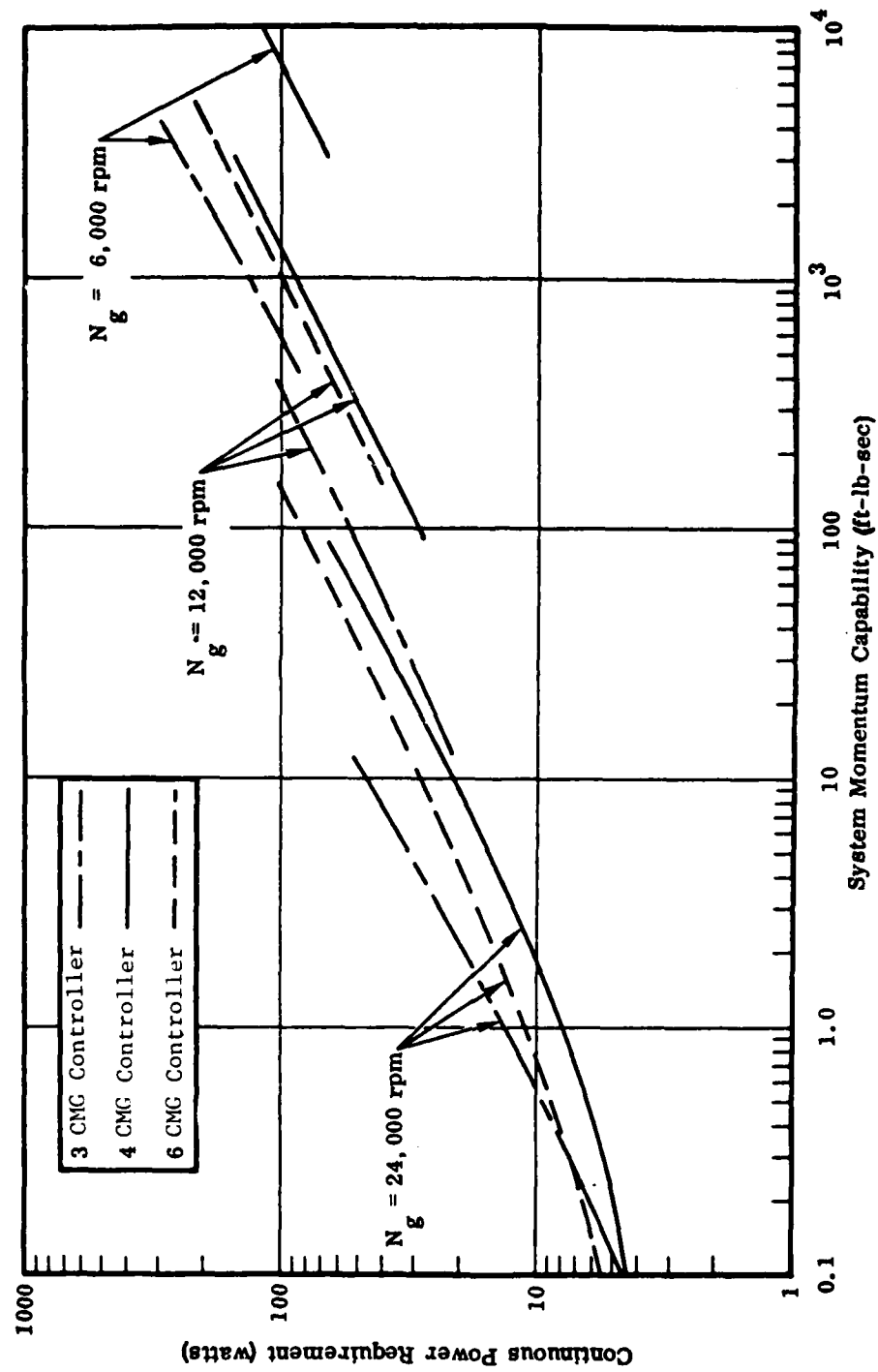
Figure 2.4-15 Continous CMG Power as a Function of System Momentum Capability
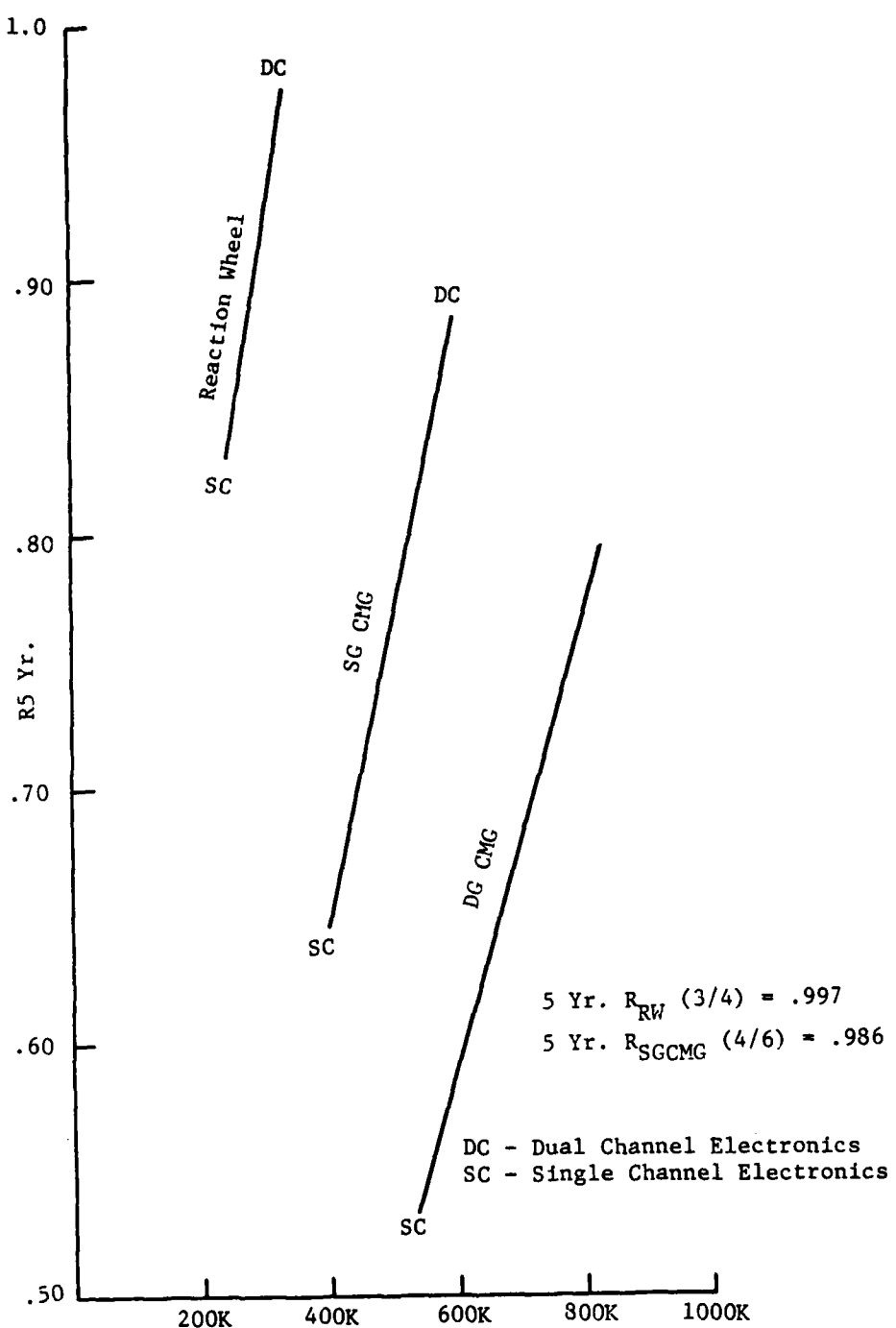
Figure 2.4-16   Reliability vs Cost

111

junction with the CMGs or reaction wheels.

Specified reaction control system designs are dependent upon the boost phase of flight as well as the useful on-orbit phase. A reaction control system designed for a recent SAMSO-sponsored design for a synchronous orbit radar antenna of 600 foot diameter employed a combination of a bipropellant system and a mercury ion system. The actual process of selecting a momentum exchange/reaction jet attitude control system is dependent upon a detailed mission analysis, control function analysis and the structural characteristics of the particular antenna. The process should begin as soon as the mission is understood as it, itself, impacts the design of the structure as well as performance of the antenna and packaging of the structure in the Orbiter's Cargo Bay.

2.4.3 Conclusions & Limitations. Attitude control can be achieved to satisfy the requirements of each of the missions.

- Subsystems exist to satisfy the attitude determination requirements sensing with respect to the fixed stars, lunar limb or landmarks.

- Subsystems exist to satisfy the requirement of certain missions to possess accurate knowledge of the location of the antennas in space and/or with respect to landmarks.

- Disturbing torques can be overcome by any of several types of controllers.

- Slew requirements can be met.

Disturbing forces exist which will drive the antenna off station or alter the orbit. To overcome this effect would require substantial propellant.

Extended operational orbital lifetimes (over about 5 years) will require either an improvement in the state of the art of controllers or an unusually high degree of redundancy with its associated penalties.

3. TASK 2, PERFORMANCE ANALYSIS, SELECTED APPROACH, RADAR SYSTEM

3.1 RF Performance Analysis

3.1.1 Introduction. Adaptive antennas have received considerable attention in recent years. [1,2] Emphasis has been placed on receiving systems which utilize the received energy from one or more sources in the field of view in conjunction with a feedback processing system to produce a prescribed radiation pattern. The two most common radiation patterns are a maximum gain pattern in the direction of the sources and a pattern with minimum in the direction of some of the sources (adaptive nulling) for anti-jamming applications. This class of systems requires little a-priori information on the location or characteristics of the source (other than the frequency range) to perform properly.

A second class of systems which can be referred to as feedforward systems, requires a-priori knowledge in order to provide a prescribed radiation pattern. This a-priori knowledge is usually in the form of stored information in a computer. For example, steering phases provided to a phased array to scan the beam where a one-to-one relationship exists between the steering phases and the beam pointing angle. The use of a-priori information allows the adaptivity to be obtained either by electrical or mechanical means, or a combination of both. A hybrid system, commonly used in phased arrays, utilizes feedforward phase control to point the main beam and then uses feedback loops to adaptively generate nulls in the sidelobe region.

Another class of adaptivity of particular interest to this program is adaptive figure control for very large space-deployable antennas. This can also be achieved by either electrical or mechanical means. It is a two-part problem. The first part is the sensing of the figure errors and the second part is the correction of these errors.

One very useful class of antenna systems for this application is a two-reflector system consisting of a large primary reflector, a smaller field reflector, and a phased array feed system that is substantially smaller than the primary reflector. The field reflector is designed such that the image surface of the primary reflector lies on the surface of the phased array feed. This sytem has the advantages of a phased array in electronic beam steering and adaptive nulling, but it has the increased directivity given by the much larger primary reflector. Further, the imaging property of the field reflector provides a method of determining the distortions on the main reflector from observations of the fields of the phased array feed. This system has been investigated under RADC sponsorship [3-8] on a number of study contracts.

[1] IEEE Trans. Antennas and Propagation, (Special Issue on Active and Adaptive Antennas), vol. AP-12, March 1964.

[2] IEEE Trans. Antennas and Propagation, (Special Issue on Adaptive Antennas), vol. AP-24, No. 5, September 1976.

[3] W.D. White, L. J. Kuskowski, and L. K. DeSize, "Final Report on Investigation of Multifeed Antennas and Wide-Angle Optics," Technical Report No. RADC-TR-61-12, December 1960, 250575.

We have continued this investigation in our program.

Of primary concern with respect to physically large reflector antennas is the effect of distortions in the reflector shape on the gain and the radiation patterns. A reflector that departs significantly from its nominal parabolic shape could direct much of the energy it collects to regions outside the feed cluster. This problem can be corrected by a mechanically adaptable reflector surface. If the distoritons are minor, a phased array located along the image surface of the primary reflector can be used to measure the distortions and also to compensate for them electrically. For larger distortions the phased array can relay information to the mechanical actuators to perform mechanical corrections on the primary reflector surface. An antenna having both electrical and mechanical adaptivity can always optimize its gain better than one having only electrical adaptivity. To detect distortions, individual elements in the phased array are monitored for phase and amplitude. This information is compared against stored data for an undistorted primary reflector to infer the mechanical corrections required in the reflector surface or electrical corrections needed by the phased array.

In this study adaptive techniques were applied to the analysis of a two-reflector phased-array fed antenna system. The primary reflector and the field reflector are both of parabolic shape and are confocal. The phased array follows a stepped-parabolic contour that represents the image surface of the primary reflector. The primary reflector is assumed to be made up of N equal arc length parabolic segments that can undergo displacements and rotations independent from one another. Each segment's orientation can be controlled by mechanical actuators placed behind the primary reflector. The mechanical model used is the deployable box truss discussed elsewhere in this report, with the box diameter typically 20-25 ft. Mechanical actuators for the adaptive surface control are placed at the corners of the boxes. The reflecting surface is supported at these points. The surface would be a continuous reflecting mesh for microwave frequencies. It could be composed of separate rigid panels for millimeter wave frequencies. In either case, the local distortions of the supporting truss will be small compared to the spacing between control points. Under these circumstances, the surface segments between control points can be modeled as a perfect parabola to good accuracy, with the distortions modeled as displacements and rotations of these segments.

The basic offset-fed antenna system is shown in Figure 3.1-1 . The offset-fed system is desirable for reducing blockage effects. The field re-

[4] C. J. Wilson, "Electronically Steerable Field Reflector Techniques", Technical Report No. RADC-TR-64-521 February 1965, 612903
[5] G. E. Skahill, L. K. DeSize, and C. J. Wilson, "Electronically Steerable Field Reflector Antenna Techniques," Technical Report No. RADC-TR-66-354, August 1966, 802459.
[6] D. A. Hildebrand, "Design and Evaluation of Two-Reflector Antenna Systems," Technical Report No. RADC-TR-66-582, November 1966, 644107.
[7] G. E. Skahill and Walter I. Satre, Jr., "Reflector Antenna Zoom Techniques", Technical Report No. RADC-TR-67-459, September 1967, 9/821090.
[8] T. E. Manwarren and A. Farrar, "Reflector Antenna Zoom Techniques", Technical Report No. RADC-TR-67-510, October 1967, 824237.
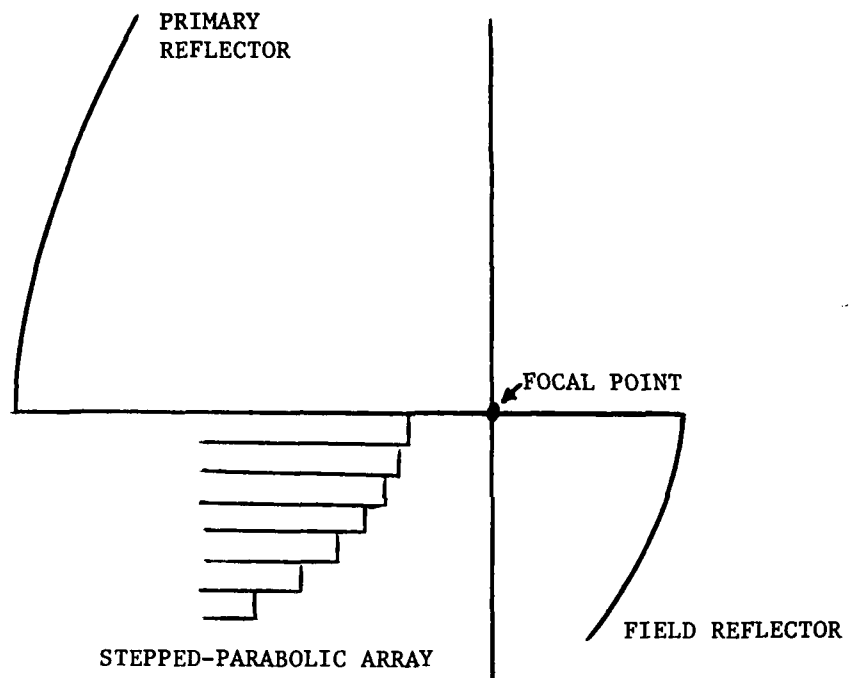
Figure 3.1-1   Two-reflector system with phased array feed.

115

flector and phased array are assumed to be small enough so that they can be built with materials to maintain a precision surface.

In Section 3.1.2 ray tracing is applied to the analysis of two-reflector phased array fed systems. The effect of primary reflector distortions is included in the analysis. The detailed derivations of important equations are given in Appendix A and B. In Section 3.1.3 the analysis is applied to the offset and symmetric planes of two-reflector systems. Beam scanning characteristics and adaptive nulling results are presented. It is demonstrated that phase compensation by the array improves the antenna gain significantly when a distortion is present.

3.1.2 Theory For Analyzing Two-Reflector Phased Array Fed Systems

3.1.2.1 Introduction. The objectives of this study of the two reflector phased array-fed system were to:

1. Determine whether distortions in the primary reflector can be detected and defined by the phased array.

2. Determine the effects of distortions on the far-field patterns and the ability of the array to improve performance by phase compensation.

3. Determine beam scanning losses and the effect of beam scanning on sidelobe levels.

4. Investigate adaptive nulling.

The usefullness of a two-reflector system in monitoring distortions is that the field reflector provides an image of the primary reflector surface. This is equivalent to using a Fourier-transform matrix network, e.g. the Butler matrix [9]. For beam scanning purposes the two reflector system is useful in reducing the number of phased array elements required. The number of phased array elements in a two-dimensional system is reduced proportionally by the square of the magnification M of the system, where

$$M = \frac{D_1}{D_2} \tag{3.1-1}$$

D_1 = Diameter of the primary reflector

D_2 = Diameter of the field reflector

This relation is shown for the two-reflector conformal parabolic system in Figure 3.1-2. The offset system is used in order to reduce blockage effects.

----

[9] A. W. Rudge and D.E.N. Davies, "Electronically controllable primary feed for profile-error compensation of large parabloic reflectors," Proc. IEE, vol. 117, No. 2, February 1970.

116

PRIMARY REFLECTOR

D_1

D_2

FIELD
REFLECTOR

$$M = \frac{D_1}{D_2}$$
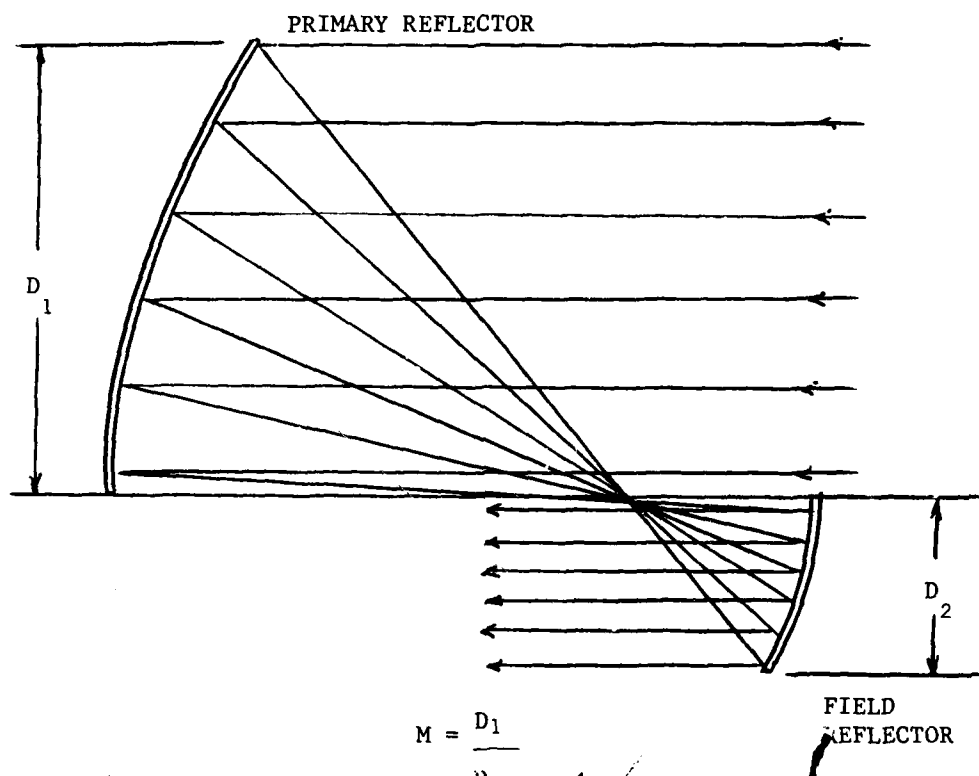
Figure 3.1-2   Two-reflector confocal system.

117

Part 3.1.2.2 of this section provides the theory for analyzing two reflector phased array fed systems. A simple ray tracing technique is used which is easily implemented on a computer.

3.1.2.2 Theory. In this section the theory used in analyzing the two reflector phased-array fed system (see Fig. 3.1-1) is discussed. Ray tracing is used to detect distortions in the primary reflector surface as well as to determine the proper phase distribution that is required on the phased array to achieve beam steering. The secondary far-field pattern due to some field distribution on the phased array is found by using Huygens point sources and superposition. The analysis is simplified by taking a planar cut of the antenna and restricting rays to this plane.

In order to detect distorted segments in the primary reflector, it is assumed that a cooperating source illuminates the primary reflector as a plane wave along boresight. This signal is received by elements of the array and the amplitude and phase is then compared against the undistorted case. The phased array surface is chosen to be the image of the primary reflector such that a one-to-one mapping exists between the two surfaces. This relation is shown qualitatively by shaded regions in Fig. 3.1-3 . Ideally, there should be many (ten to twenty) apertures per primary reflector segment in order to determine the precise orientation of each segment.

In the undistorted receiving case the incident plane wave is sampled on the primary reflector at equally spaced points in the x dimension such that at least five rays are received by each waveguide in the phased array. This is done to ensure convergence in the array field distribution. The total electric field received by any one of the matched waveguide-fed apertures is, by superposition, the sum of the electric field contributions of each ray that strikes the aperture. The signal at the element output is a weighted sum of each ray contribution. The weighting is dependent on the ray's angle-of-arrival and is fixed by the far-field pattern of the array element. A typical ray path is shown in Fig. 3.1-4 . The incident ray strikes the primary reflector at the point (x_1, z_1) whereby it is reflected to the subreflector at the point (x_2, z_2) and then to the phased array at the point (x_3, z_3). In appendices A and B two fourth order polynomial equations are derived which describe the ray path to the phased array surface (see Equations (A-34) and (B-13). The equations were found by enforcing the condition that the angle of incidence be equal to the angle of reflection at the surface of the primary and secondary reflectors. Equation (B-13) finds the incident point on the ideal parabolic image surface. This information is then used to determine which array element of the stepped parabolic surface receives this ray. The four roots in Equations (A-34) and (B-13) are solved for by the Newton-Raphson iterative technique. [10] A listing of the computer program that implements this technique is given in Appendix C.

For the incident wave shown in Fig. 3.1-4 the electric field at any point on the primary reflector is given by

----

[10] A. Ralston, A First Course In Numerical Analysis, McGraw-Hill Book Co., New York, 1965.
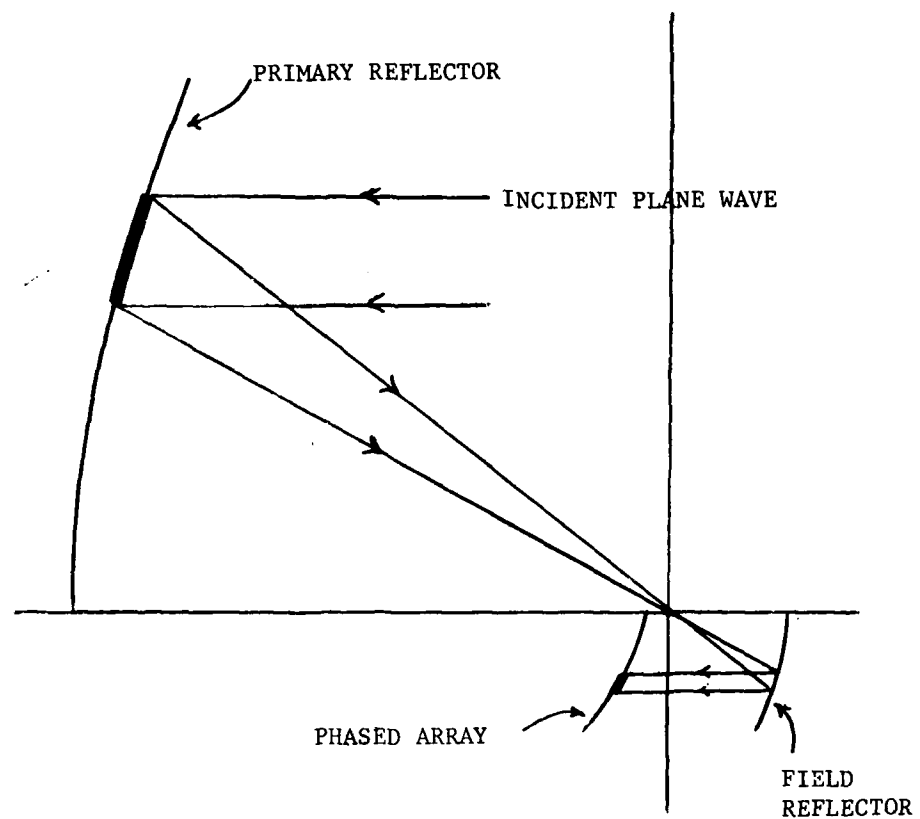
Figure 3.1-3   One-to-one mapping between primary
reflector and phased array.

119
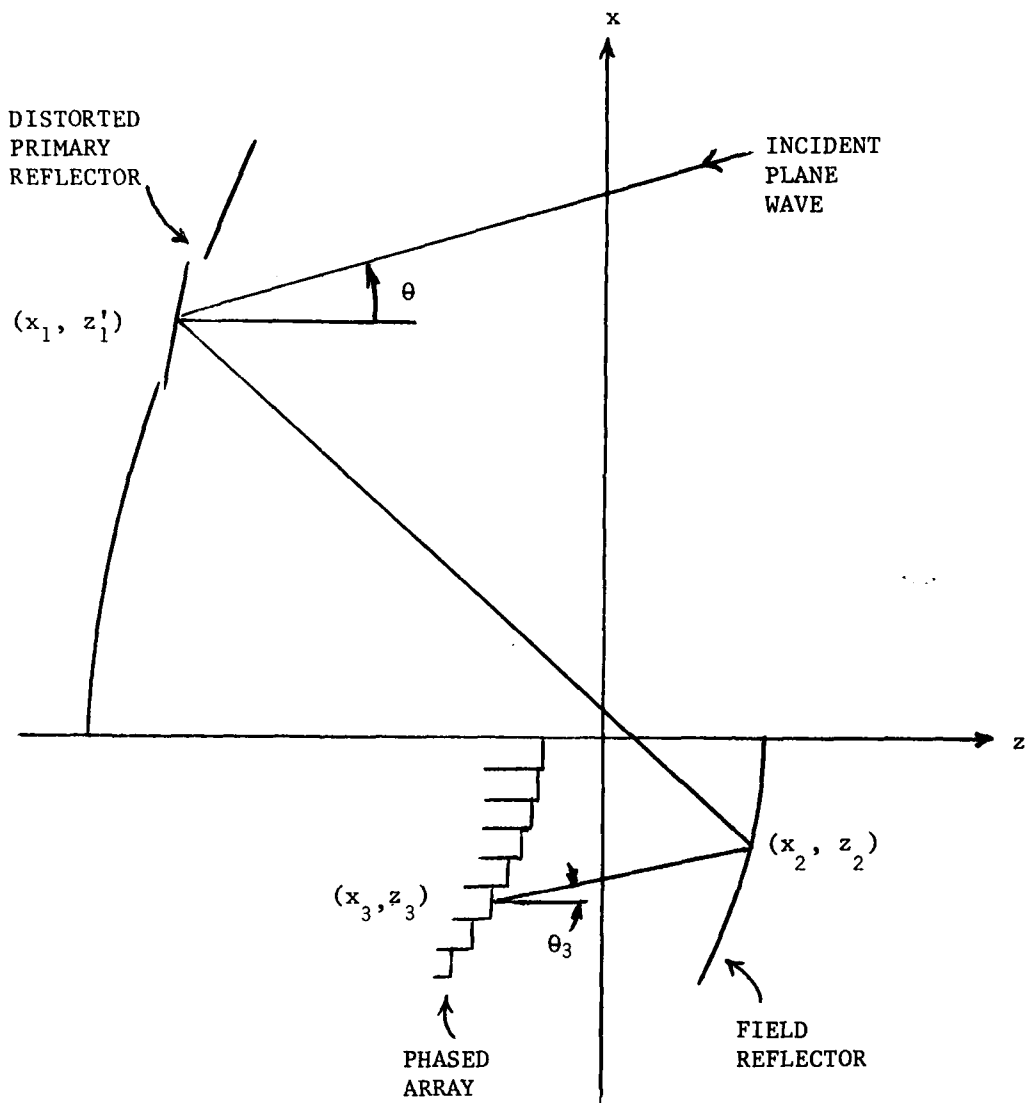
Figure 3.1-4   Two Reflector Confocal System with
Distorted Primary Reflector

120

$$\overline{E}^i = \hat{y}e^{j\beta(z_1'\cos\theta + x_1\sin\theta)} \tag{3.1-2}$$

where θ is the angle of incidence. Note that z_1' includes the effect of distortion (see Equation A-24). In terms of the path lengths ℓ_{21} and ℓ_{32} in Figure (3.1-4) the electric field received by the nth array element is

$$\overline{E}_n = \overline{E}^i \cdot e^{-j\beta(\ell_{21} + \ell_{32})} \cdot P(\theta_3) \tag{3.1-3}$$

where $P(\theta_3)$ is the pattern function of the array element and

θ_3 is the angle of incidence at the array element. In general, the element pattern is given by

$$P(\theta_3) = \cos^m\theta_3$$

where m is chosen according to the element aperture size.

Of interest is a "self-correcting" property of two-reflector confocal parabolic systems. By "self-correcting" is meant that for small distortions the one-to-one mapping between a region of the primary reflector and phased array surface is maintained. This property is demonstrated by two examples as follows: In case I consider two rays u and d as shown in Fig. 3.1-5 Ray u represents an incoming ray parallel to the antenna axis that is reflected by the undistorted primary at the point (x_1, z_1) and passes through the focal point. It then strikes the field reflector at the point (x_{2u}, z_{2u}). The slopes of the primary reflector and field reflector at the points (x_{1u}, z_{1u}) and (x_{2u}, z_{2u}) are denoted by m_{1u} and m_{2u}, respectively. Ray u then travels parallel to the axis until it reaches the array at the point (x_{3u}, z_{3u}). Ray d represents the same incoming ray but is reflected by a distorted segment. In this case the distoriton is a segment that is rotated counterclockwise. Ray d is incident on the primary reflector at the point (x_1, z_1'). The slope at this point, denoted by m_{1d}, is greater than m_{1u} so the reflected ray will strike the field reflector at the point (x_{2d}, z_{2d}) above the undistorted location (x_{2u}, z_{2u}). Since the slope at the point (x_{2d}, z_{2d}) denoted by m_{2d}, is greater than m_{2u} (which represents a counterclockwise rotation) the ray will be directed (compensated) down towards the point (x_{3u}, z_{3u}). The ray arrives at the array at the point (x_{3d}, z_{3d}) which will be close to but different than (x_{3u}, z_{3u}). Since the array is quantized, the two rays will generally arrive at the same aperture or occasionally the adjacent aperture. In case II the distortion now consists of a clockwise rotation of a segment. As shown in Fig. 3.1-6 the path of ray u (undistorted) is the same as in case I. Since the slope at the point where ray d (distorted) strikes the primary reflector is less than m_{1u} the ray will intersect the field reflector at the point (x_{2d}, z_{2d}) below the undistorted location (x_{2u}, z_{2u}). Since the slope at the point (x_{2d}, z_{2d}) is greater than m_{2u} (which represents a clockwise rotation) the ray will be directed (compensated) up towards the point (x_{3u}, z_{3u}). As in case I the ray will very often arrive in the same aperture or sometimes the adjacent aperture.
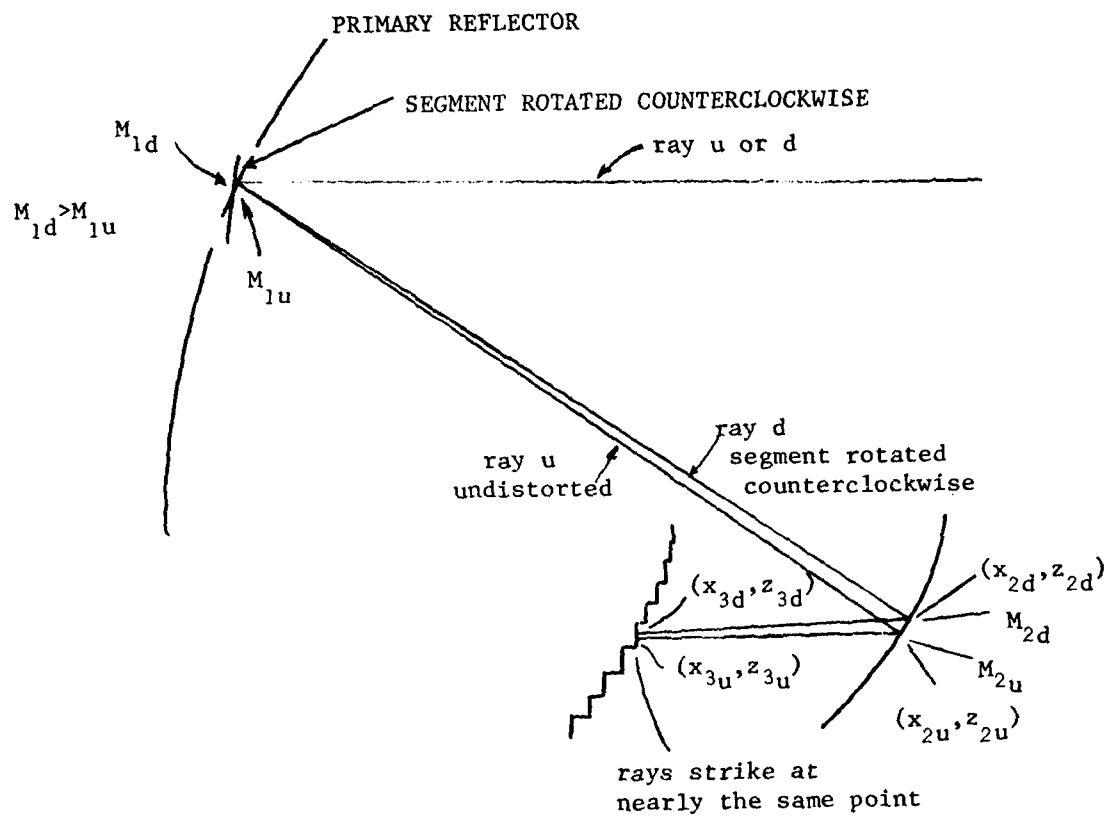
Figure 3.1-5   Ray path self correcting property of
                confocal parabloic system for a small
                distortion (counterclockwise rotation)

SEGMENT ROTATED CLOCKWISE

ray u

ray d

M_u

M_d

RAYS STRIKE AT
NEARLY THE SAME
POINT

$M_d < M_u$
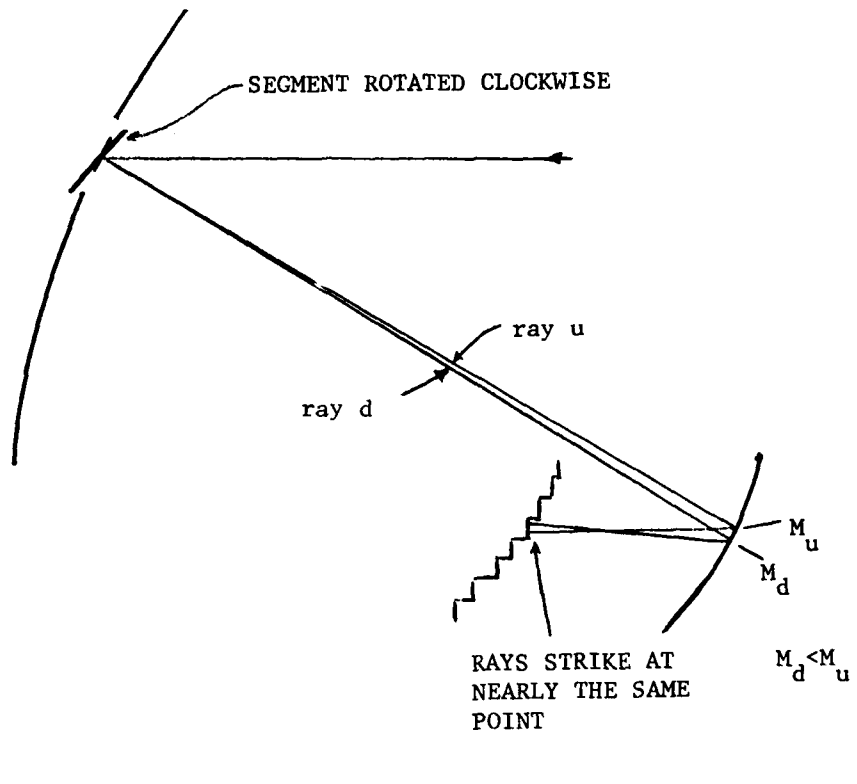
CASE II

Figure 3.1-6   RAY PATH SELF CORRECTING PROPERTY OF
CONFOCAL PARABOLIC SYSTEM FOR A SMALL
DISTORTION (CLOCKWISE ROTATION OF
SEGMENT)

123

Suppose now that the region occupied by, for example, ten apertures represents the mapping of the corresponding segment on the undistorted primary reflector. From the above two examples, the tube of rays which is incident upon a segment that has a small distortion will arrive at the same ten apertures. When every segment of the primary has some small distortion there will be very little overlap between tubes of rays received at the array. This means that for small distortions each group of array elements will provide phase and amplitude information only for its corresponding primary reflector segment.

Although the rays due to distortion strike at approximately the same location and with approximately the same amplitude as an undistorted ray, the phase will be significantly different. This is due to a change in path length equal to approximately twice the amount of distortion. Thus, if the phase received at the array due to the distorted primary are compared (by taking the difference) against the phases of the undistorted primary it should be clear what type of distortion is present (rotation and/or displacement).

Suppose that the phase and amplitude received by elements of the array have been determined for some incident wave on the primary reflector (distorted or undistorted). The far-field pattern due to this distribution can be found in the following manner: The phased array is replaced by Huygens point sources located at the center of each aperture whose field distribution is the conjugate of that which is received. Denote the location of point source n of the array by $(x_3, z_3)_n$ and let $(x_2, z_2)_m$ be an observation point on the field reflector, as shown in Fig. 3.1-7. Further, let θ_n be the angle measured from the normal to array element n and let ℓ_{23n} be the distance between points $(x_3, z_3)_n$ and $(x_2, z_2)_m$. If there are N number of array elements, the electric field at any point m on the field reflector is given by superposition as

$$E_m(x_2, z_2) = \sum_{n=1}^{N} E_n^* P(\theta_n) \frac{e^{-j\beta\ell_{23n}}}{\ell_{23n}} \qquad (3.1\text{-}4)$$

where $P(\theta_n)$ is the pattern function of the array element, E_n is given by equation (3.1-3) and *denotes conjugate. Similarly, with ℓ_{12m} representing the distance between a point on the field reflector and a point on the primary reflector, the field at any point on the primary is given by

$$E(x_1, z_1) = \sum_{m=1}^{M} E_m(x_2, z_2) \frac{e^{-j\beta\ell_{12m}}}{\ell_{12m}} \qquad (3.1\text{-}5)$$

where M is the number of sample points on the field reflector. Combining equations (3.1-4) and (3.1-5) and transforming to the aperture shown in Fig. 3.1-7 the aperture distribution is given by

$$E_a(x_1) = \sum_{m=1}^{M} \sum_{n=1}^{N} E_n^* P(\theta_n) \frac{e^{-j\beta(\ell_{12m} + \ell_{23n} + \ell_a)}}{\ell_{12m} + \ell_{23n}} \qquad (3.1\text{-}6)$$

124
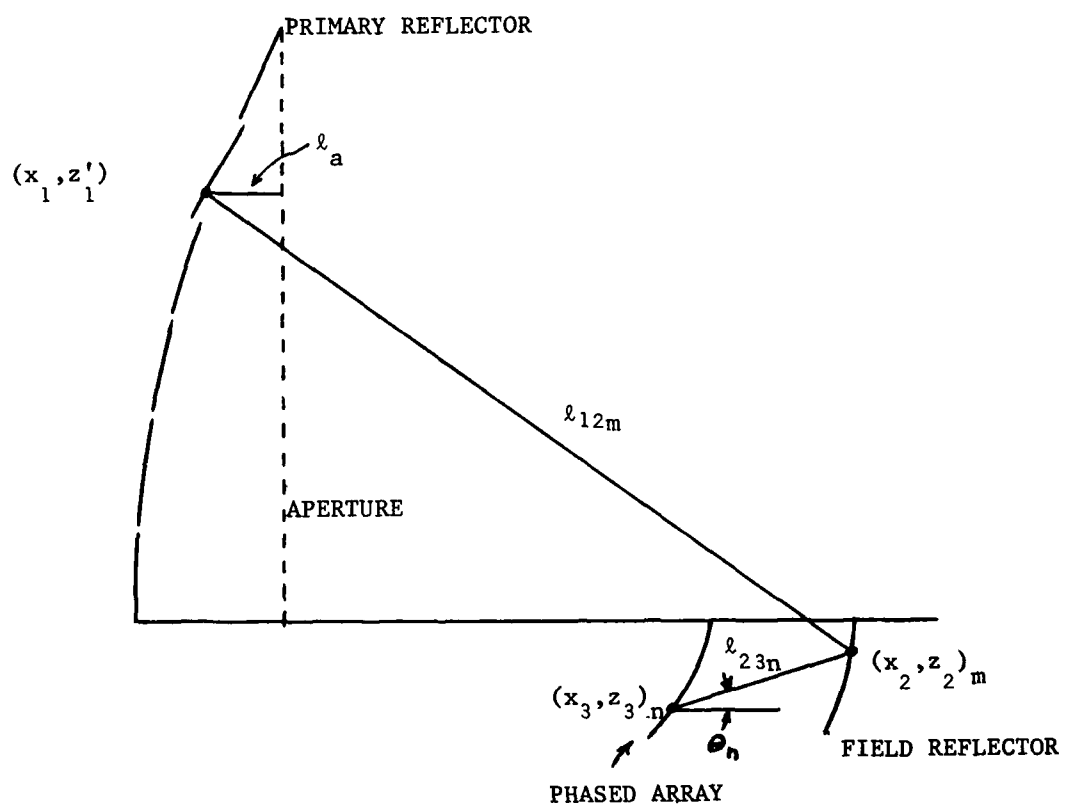
Figure 3.1-7   GEOMETRY FOR RAY TRACING ANALYSIS

where ℓ_a is the distance from the primary reflector surface to the aperture. Note that equation (3.1-5) includes the effects of reflector distortion if some is present.

The far-field pattern can now be expressed as

$$F(\theta) = \sum_{k=1}^{K} E_{ak} e^{j\beta x_k \sin\theta} \qquad (3.1-7)$$

where K is the number of sample points in the aperture,

θ is the observation angle measured from the antenna axis,

x_k is the sample point location, and

E_{ak} is determined from equation (3.1-6)

Equation (3.1-7) is simply the field radiated by a linear array of point sources. The aperture efficiency is defined by

$$\eta_{\theta_s} = \frac{\left| \sum_{k=o}^{K} E_{ak} e^{j\beta x_k \sin\theta_s} \right|^2}{K \sum_{k=o}^{K} |E_{ak}|^2} \qquad (3.1-8)$$

where θ_s is the beam scanning angle. The loss in gain is given by $10 \log_{10}\eta_{\theta_s}$, which includes the effects of spillover and distortion.

It is also possible to taper the illumination of the reflector for side-lobe control by an appropriate amplitude taper on the excitation of the array elements, E_n. η_{θ_s} also includes loss due to illumination tapering.

3.1.3 Two-Reflector Phased Array-Fed System Results

3.1.3.1 Introduction. A set of Fortran computer programs were written to analyze two-reflector confocal parabolic systems using the theory in Section 3.1.2. The set consists of five programs. There is one pair each for the offset and symmetric planes. Each pair consists of a program to compute the received array aperture distribution for some incident plane wave. The angle of incidence, θ, is a program input. The second program of each pair uses the conjugate of the received array aperture distribution (adjusted for amplitude tapering if desired) to compute the secondary far-field pattern and aperture illumination efficiency.

There are two separate pairs of programs because blockage and spillover computations are different in the offset and symmetric planes. A fifth program is used specifically for adaptive nulling pattern computation. These programs are listed in Appendix C.

3.1.3.2 Observation and Effects of Primary Reflector Distortions. The system shown in Fig. 3.1-8 was chosen as a representative case for determining the effects of primary surface distortions. It is assumed that the primary reflector is divided up into six equal arc length parabolic segments. Each segment, in general, can undergo displacement and rotation. The positions of the actuator control points for adaptive control of the shape

126
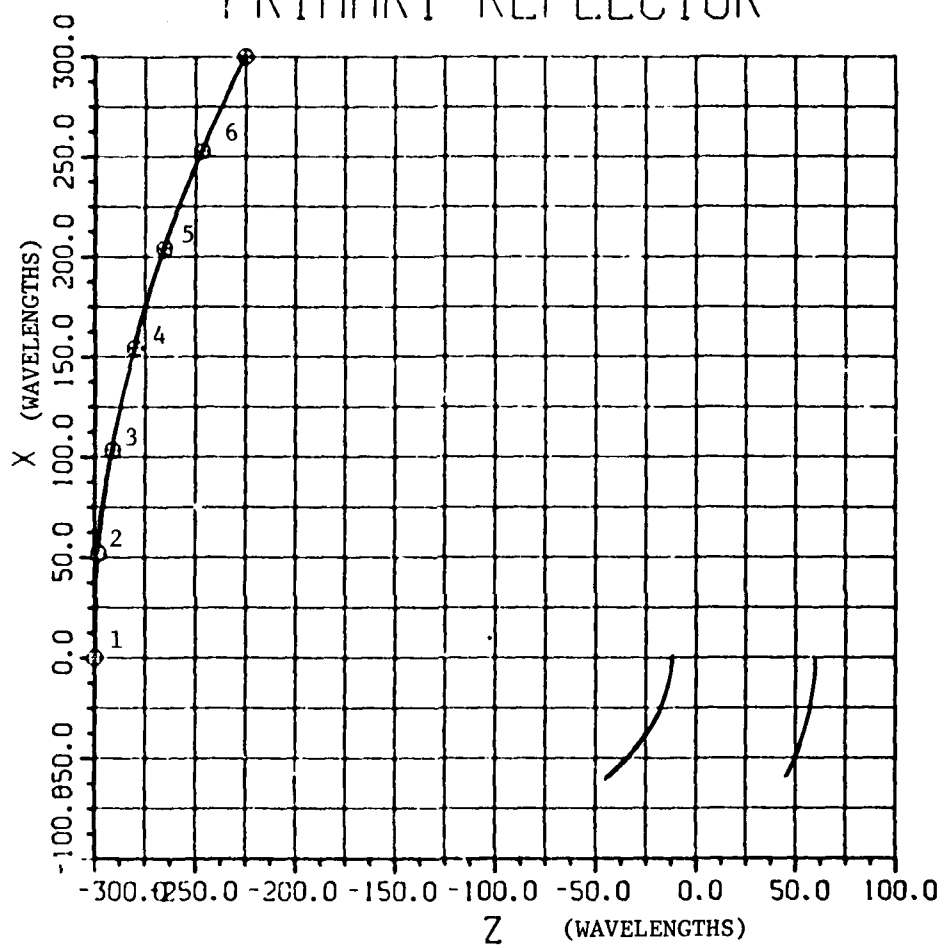
Figure 3.1-8   Two reflector phased array
                fed system.

127

of the primary reflector are indicated by circles. It is assumed that some cooperating source illuminates the primary reflector in order to monitor distortions by means of the received amplitude and phase at the phased array surface. The system is described by the following parameters.

$D_1 = 300\lambda$ (primary reflector diameter)
$D_2 = 60\lambda$ (secondary reflector diameter)
$D_3 = 60\lambda$ (phased array diameter)

$f_1 = 300\lambda$ primary focal distance
$f_2 = 60\lambda$ secondary focal distance
$f_3 = 27.27\lambda$ phased array focal distance
$d_a = 1\lambda$ phased array element diameter (=element spacing)

(note that f_3 is determined from f_1 and f_2 by equation (B-2)).

The array elements were assumed to be one-wavelength aperture horns, thus, there are sixty elements in one dimension of the array. The amount of distortion can be determined by taking the difference between the distorted and undistorted array aperture distributions. Segment number three ($105\lambda < x < 155\lambda$) of the primary reflector was chosen as a representative example. The corresponding region on the array is ($-21\lambda > x > -31\lambda$). An edge of this segment was then distorted by 0.1λ for four cases. The first case is for the top edge of segment tilted back 0.1λ (away from the field reflector). Very little can be determined from the amplitude difference in Fig. 3.1-9 because of the self-correcting property mentioned in Chapter II. The phase difference, however, describes very clearly what the position of segment number three is. Since 0.1λ corresponds to 36 electrical degrees, the expected phase delay at $x = -31$ on the array should be twice that or 72 degrees. The actual calculated value at $x = -31$ is shown to be -68 degrees in Fig. 3.1-9. The phase is then linear towards zero degrees at $x = -21$ corresponding to no distortion at the bottom edge of segment number three (as is the case). Similarly, Fig. 3.1-10 shows the expected phase difference for the top edge tilted forward (phase advanced). Figures 3.1-11 and 3.1-12 show the expected phase difference for the segment displaced back (phase delayed) and forward (phase advanced), respectively. Thus, it is clear that the orientation of a distorted segment can be determined from the received signal phase alone. To do this it is required to have a sufficient number of array elements per primary reflector segment. In the above examples ten were used.

Once a distortion has been detected it is possible to correct the surface by using mechanical actuators. For small distortions it is not necessary to do this because phase compensation by the array can be used. The effect of distortions on the far-field pattern and aperture illumination efficiency for the system shown in Fig. 3.1-8 are discussed next.

The secondary far-field pattern for an undistorted primary reflector is shown in Fig. 3.1-13. The aperture illumination considered is a uniform amplitude and phase distribution (boresight). The aperture illumination efficiency for this case is -0.36 dB. Now consider the case where segment number three is displaced back (phase delayed) 0.1λ which corresponds to Fig. 3.1-11. The secondary far-field pattern is shown in Fig. 3.1-14. The

AMPLITUDE DIFFERENCE

PHASE DIFFERENCE
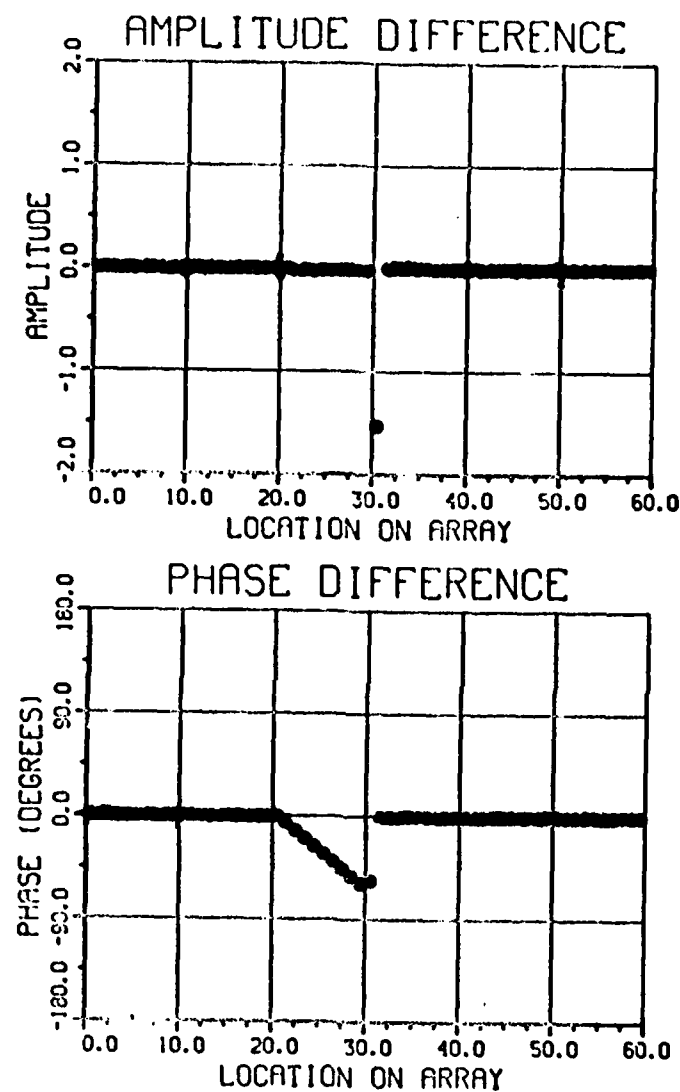
Figure 3.1-9   COMPARISON BETWEEN A DISTORTED (SEGMENT #3
                TOP EDGE TILTED BACK 0.1λ) AND UNDISTORTED
                PRIMARY REFLECTOR IN AMPLITUDE AND PHASE
                AT THE ARRAY.

129
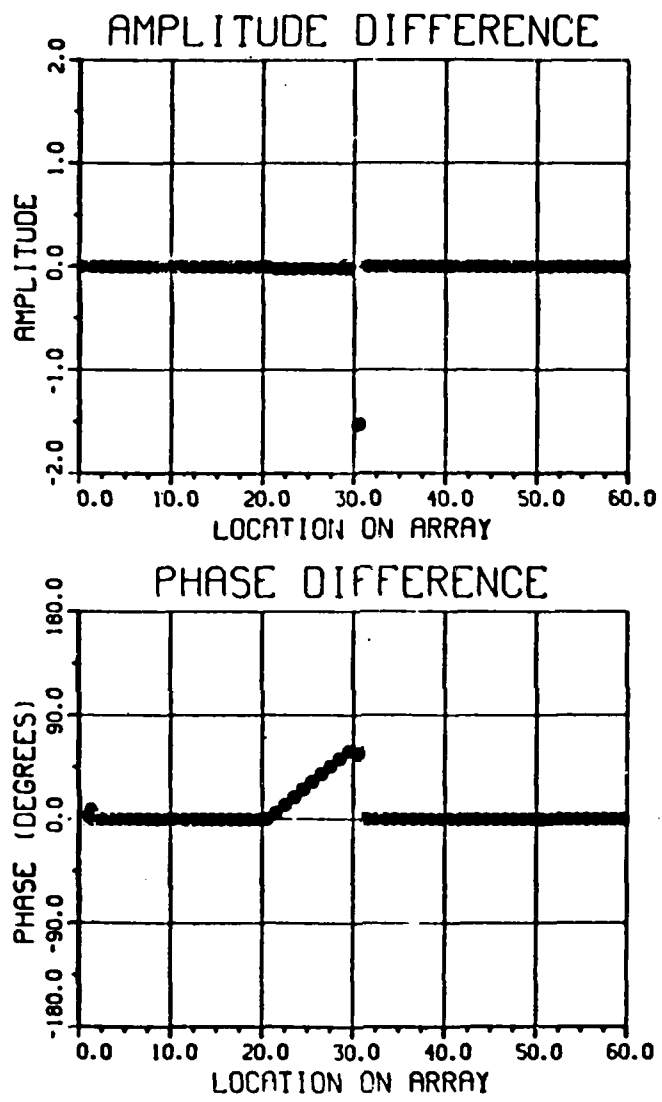
Figure 3.1-10   Comparison between a distorted (segment #3 top
                 edge tilted forward 0.1λ) and undistorted pri-
                 mary reflector in amplitude and phase at the array.

130
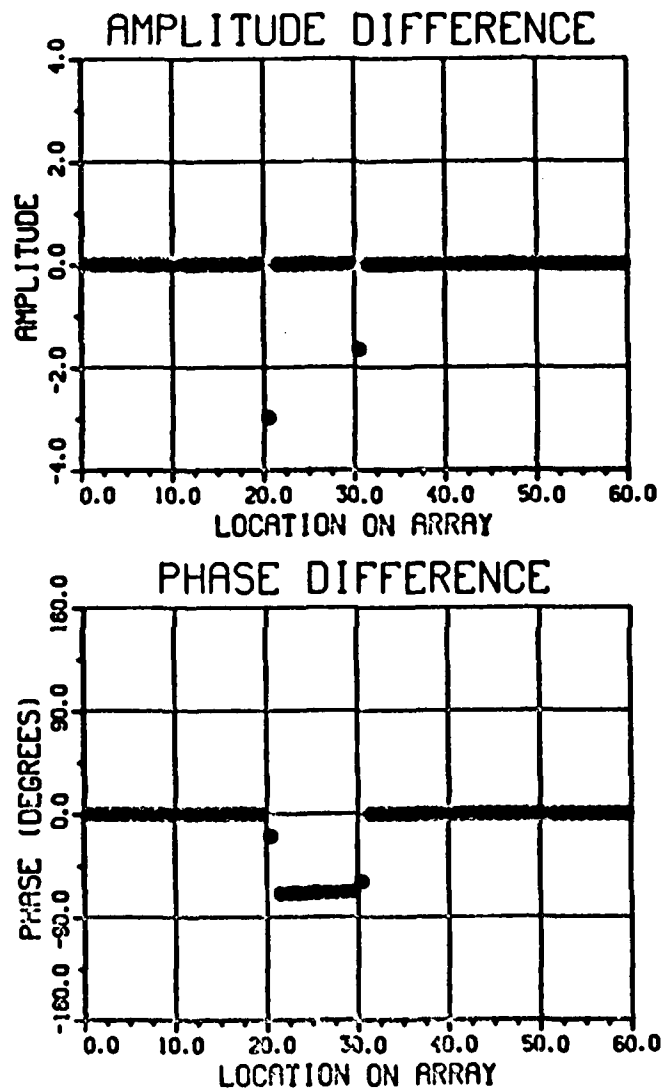
Figure 3.1-11   Comparison between a distorted (segment #3
                displaced back 0.1λ) and undistorted primary
                reflector in amplitude and phase at the array.

131

AMPLITUDE DIFFERENCE

PHASE DIFFERENCE
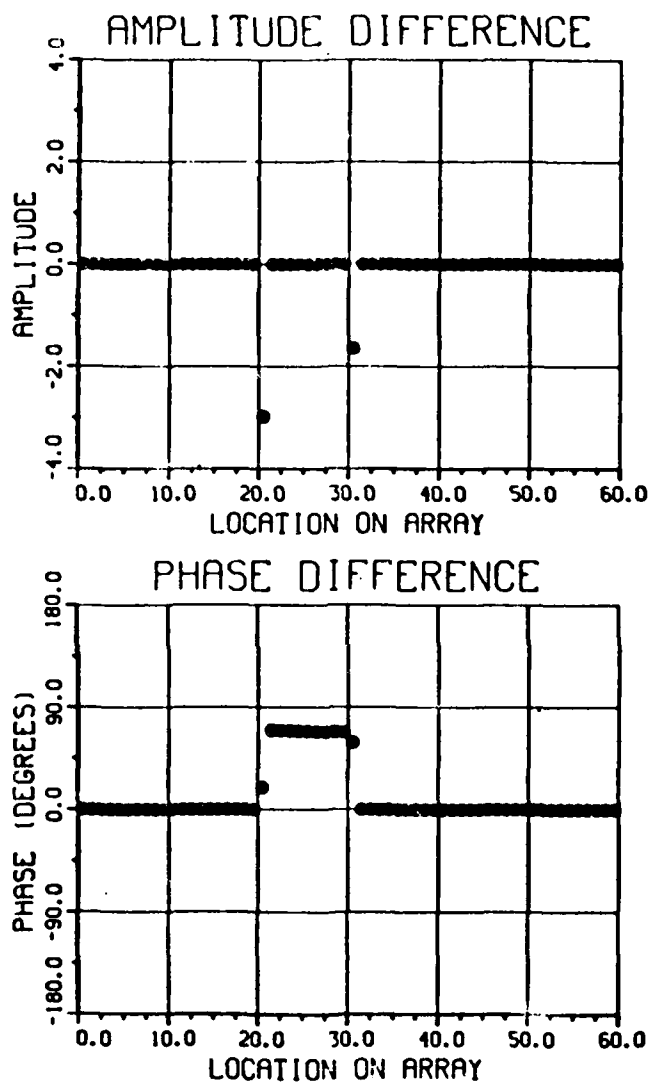
Figure 3.1-12   Comparison between a distorted (segment #3
                 displaced forward 0.1λ) and undistorted pri-
                 mary reflector in amplitude and phase at the
                 primary.

132
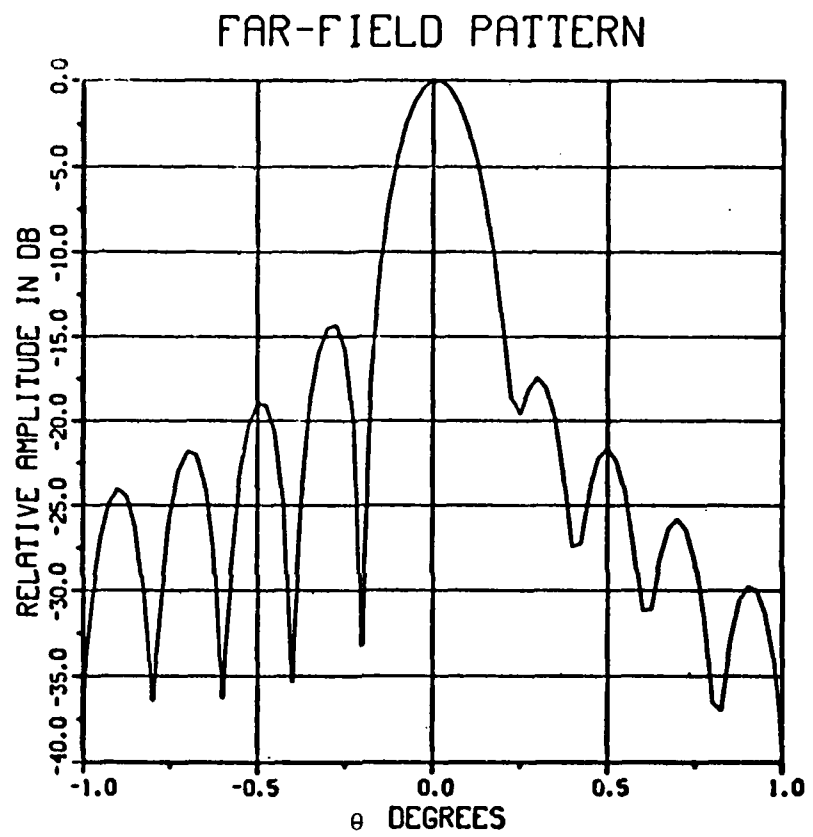
FAR-FIELD PATTERN

Figure 3.1-13   Far-field pattern for undistorted
primary reflector, boresight.

133
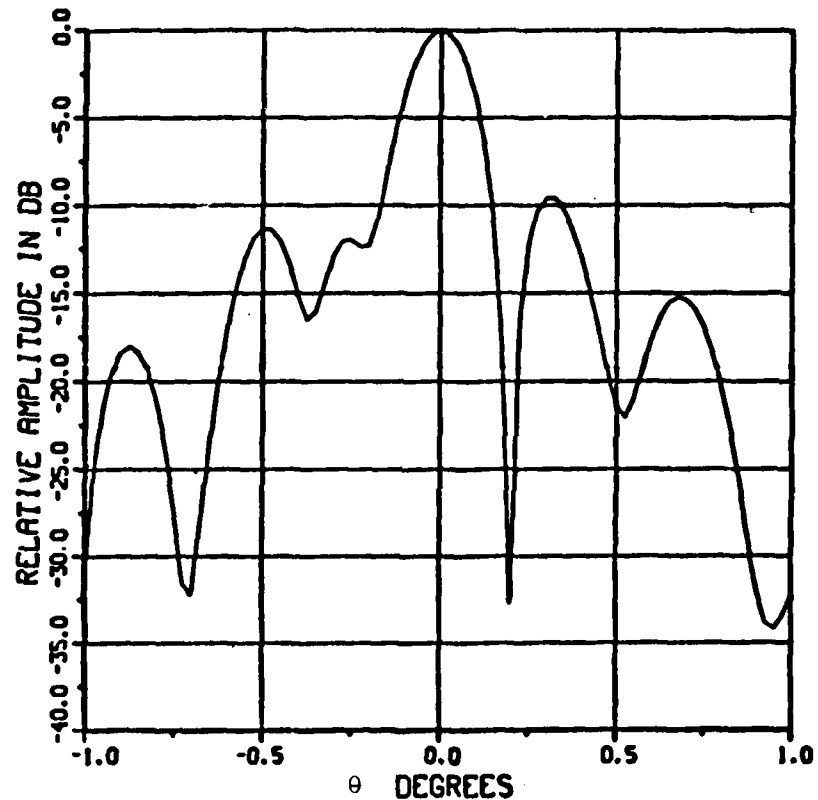
FAR-FIELD PATTERN

Figure 3.1-14   Far-field pattern for distorted-uncompensated
                 primary reflector (segment #3 displaced back
                 0.1λ)

134

main beam is seen to be unaffected but the sidelobe level has been raised by about 4dB. The aperture illumination efficiency has degraded to -1.07dB. In this case the array illumination is the original distribution received in the undistorted case. This distribution is then allowed to transmit in the presence of the distorted primary reflector. This case may be referred to as distorted-uncompensated. Figure 3.1-15 shows the far-field pattern obtained when the array provides phase compensation. The sidelobe level has now returned to within about 0.5dB of the undistorted case. The aperture illumination efficiency is now -0.43dB which is very close (within a tenth of a dB) to the undistorted case. In the next case consider segment number three to be displaced back (phase delayed) 0.25λ. The far-field pattern shown in Fig. 3.1-16 is significantly degraded. The sidelobe level is -2.5 dB as opposed to -14.5 dB in the undistorted case. The aperture illumination efficiency is -4.3dB which is nearly 4dB below the undistorted case. As shown in Figure 3.1-17 the sidelobe level can be improved to -12.5dB and the efficiency to -0.66dB by providing phase compensation by the array.

In the above two examples it is important to note that both sidelobe level and aperture illumination efficiency are significantly improved when array phase compensation is used to correct for distortions.

3.1.3.3 Beam Scanning Characteristics. A parametric study was performed on the symmetric two-reflector phased array fed system. The primary reflector had a fixed diameter $D_1 = 600\lambda$. The array elements used are one wavelength horns. The loss in gain as a function of beamwidths scanned from boresight was calculated for various magnifications, f/D ratios, oversized feed arrays, and oversized subreflectors. The effect of feed element aperture diameter and spacing was also investigated. Some representative examples are presented below.

Figure 3.1-18 shows the loss in gain for a system with f/D = 0.5 The aperture illumination used was uniform. The two curves shown are for a magnification of 5 and 10. It is clear that a lower magnification decreases the loss in gain with beam scanning. This is attributed primarily to a decrease in spillover losses. Figure 3.1-19 shows the loss in gain for $D_1 = 600\lambda$ and $D_2 = 120\lambda$ (M=5) with f/D = 0.5, 0.7, and 1.0. The cases where f/D = 0.5 and 0.7 are about a one dB improvement over f/D = 1.0. Figure 3.1-20 shows that the loss in gain can be reduced by increasing the size of the subreflector to reduce subreflector spillover. For this particular case where $D_1 = 600\lambda$ and f/D = 0.5 a twenty percent larger subreflector improves the gain by about one dB. In general, a larger subreflector will reduce the spillover losses. However, it was found that if the subreflector is too large, some unwanted effects occur which cause poor sidelobe performance. Some typical beam scanning far-field patterns are shown in Figures 3.1-22 to 3.1-26. This system has $D_1 = 600\lambda$, $D_2 = 120\lambda$, and f/D = 0.5. The array elements are one-wavelength horns. The pattern is good until thirty-six beamwidths when the sidelobes begin to degrade. In this case one beamwidth is equal to approximately 0.084 degrees (uniform distribution) with boresight as the reference.

All of the data presented so far assumed a uniform amplitude aperture distribution. One of the goals of this research was to achieve beam scanning

135
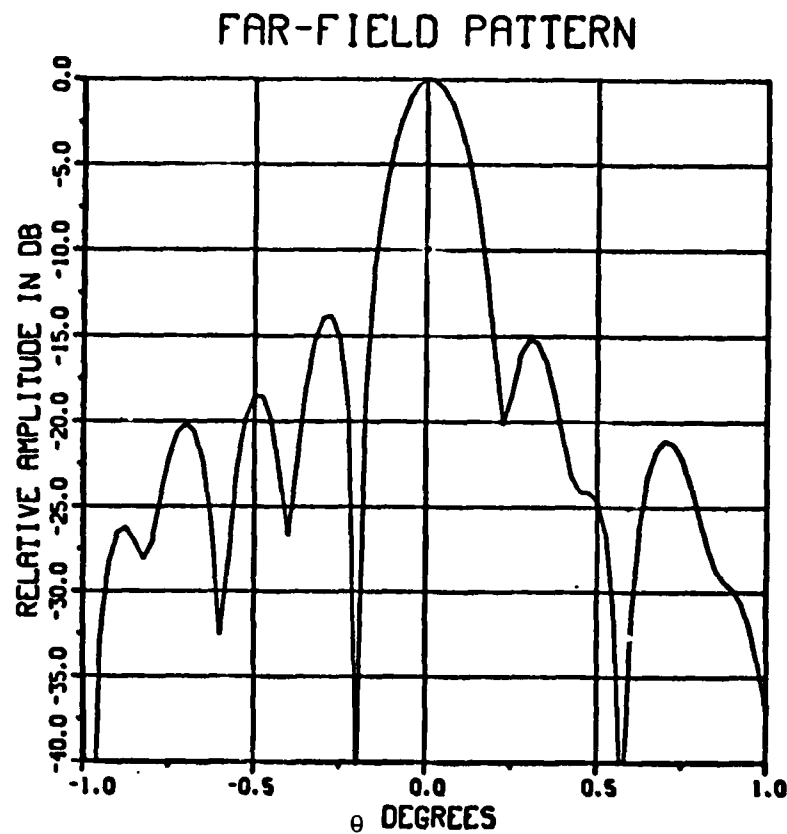
FAR-FIELD PATTERN

Figure 3.1-15   Far-Field pattern for distorted-compensated
                 primary reflector (segment #3 displaced back
                 0.1λ)

136
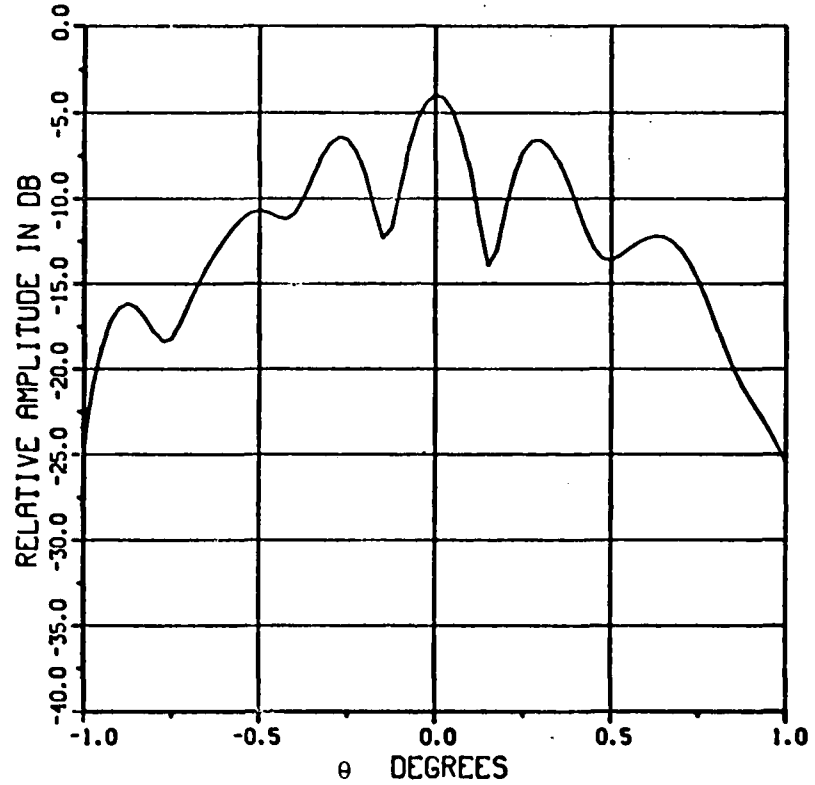
FAR-FIELD PATTERN

Figure 3.1-16   Far-field pattern for distorted-uncompensated
reflector (segment #3 displaced back 0.25λ),
boresight.

137
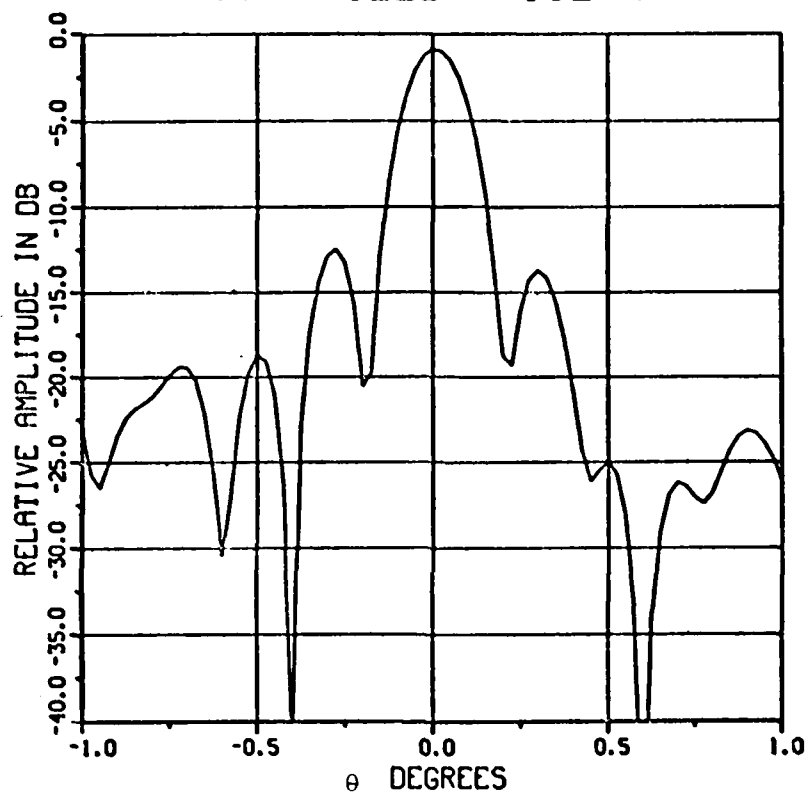
FAR-FIELD PATTERN

Figure 3.1-17   Far-field pattern for distorted primary
reflector (segment #3 displaced back 0.25λ)
with phase compensation at the array,
boresight.

138
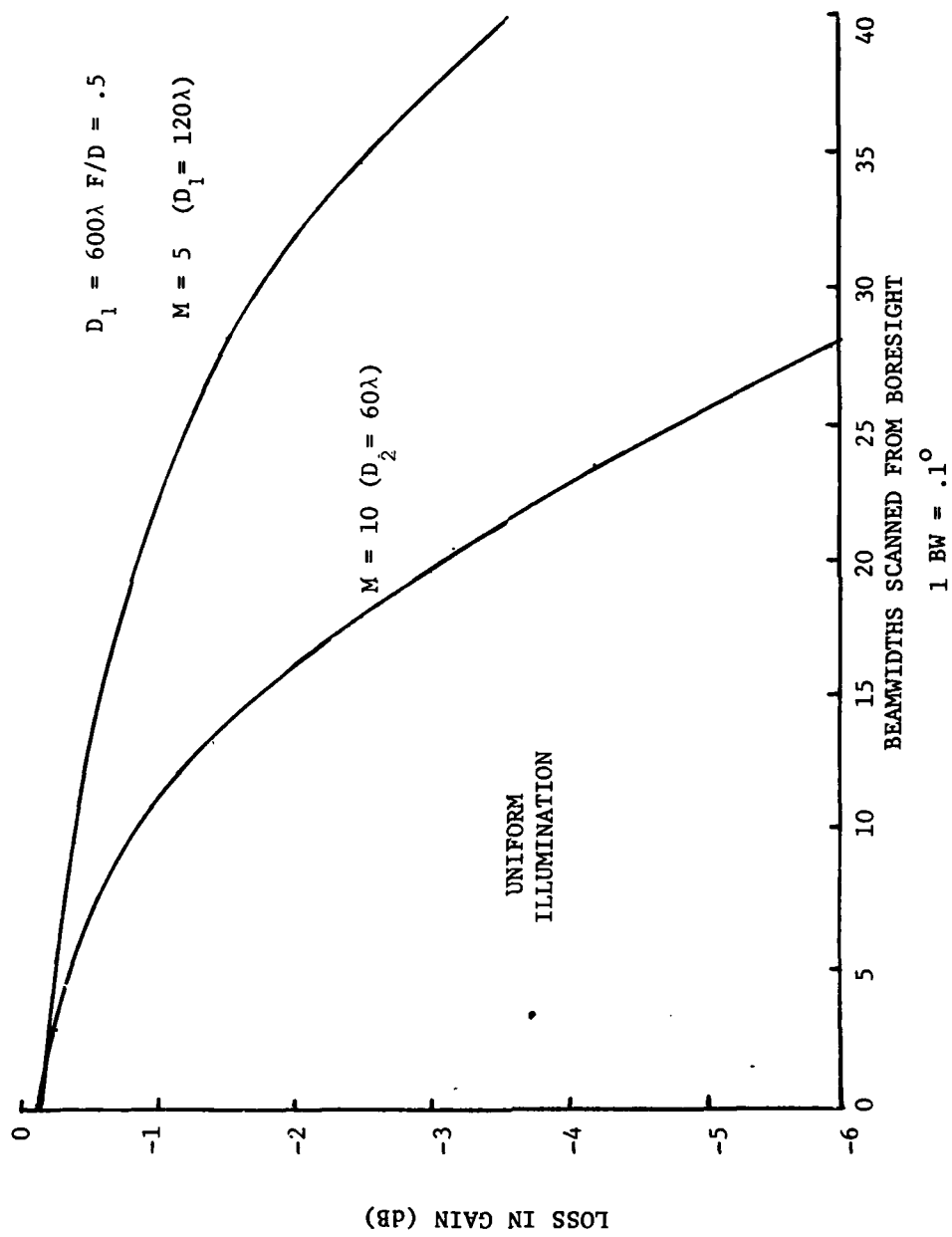
Figure 3.1-18   Beam scanning performance for two-reflector system
with magnifications of 5 and 10.

139
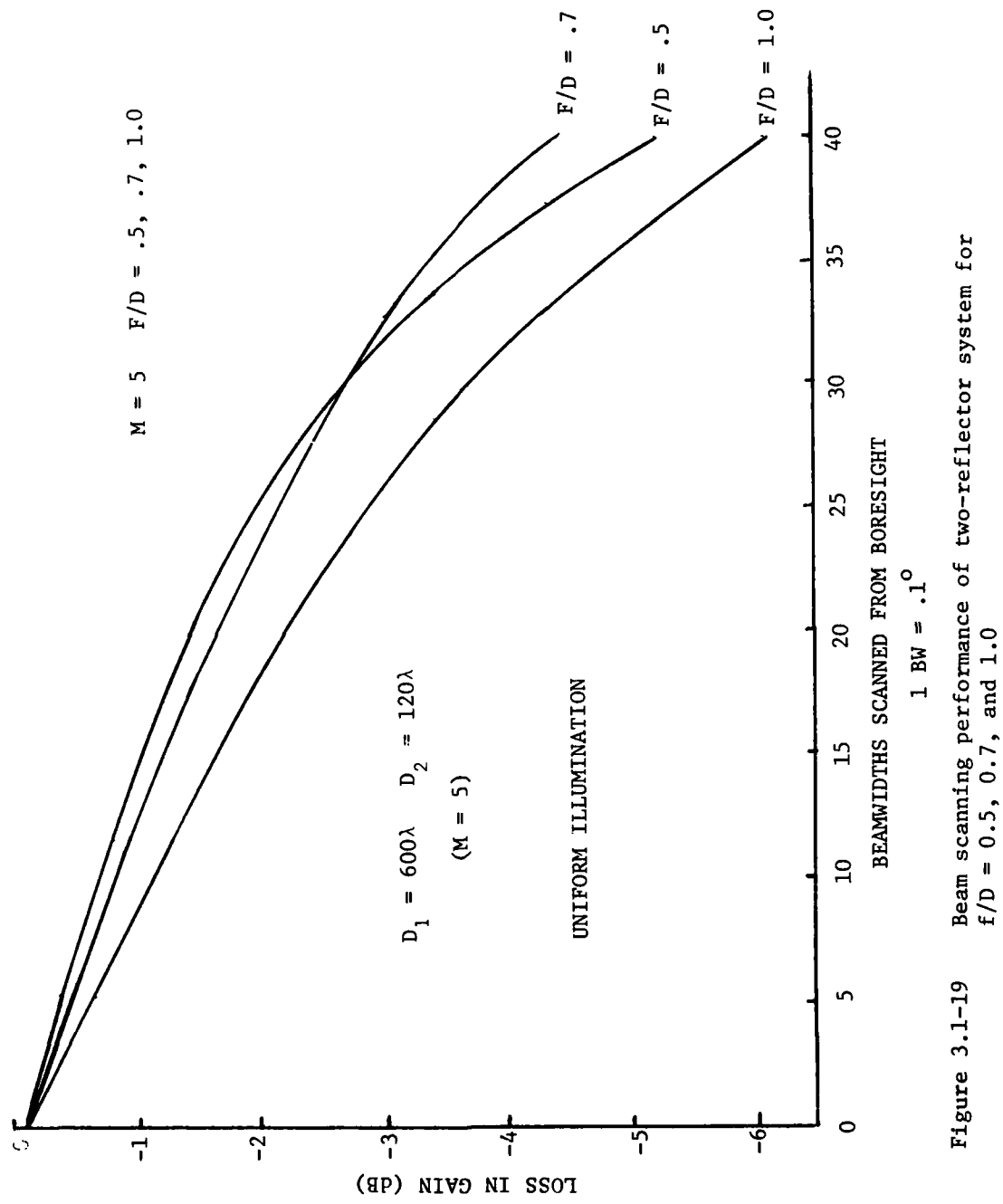
Figure 3.1-19   Beam scanning performance of two-reflector system for f/D = 0.5, 0.7, and 1.0

140
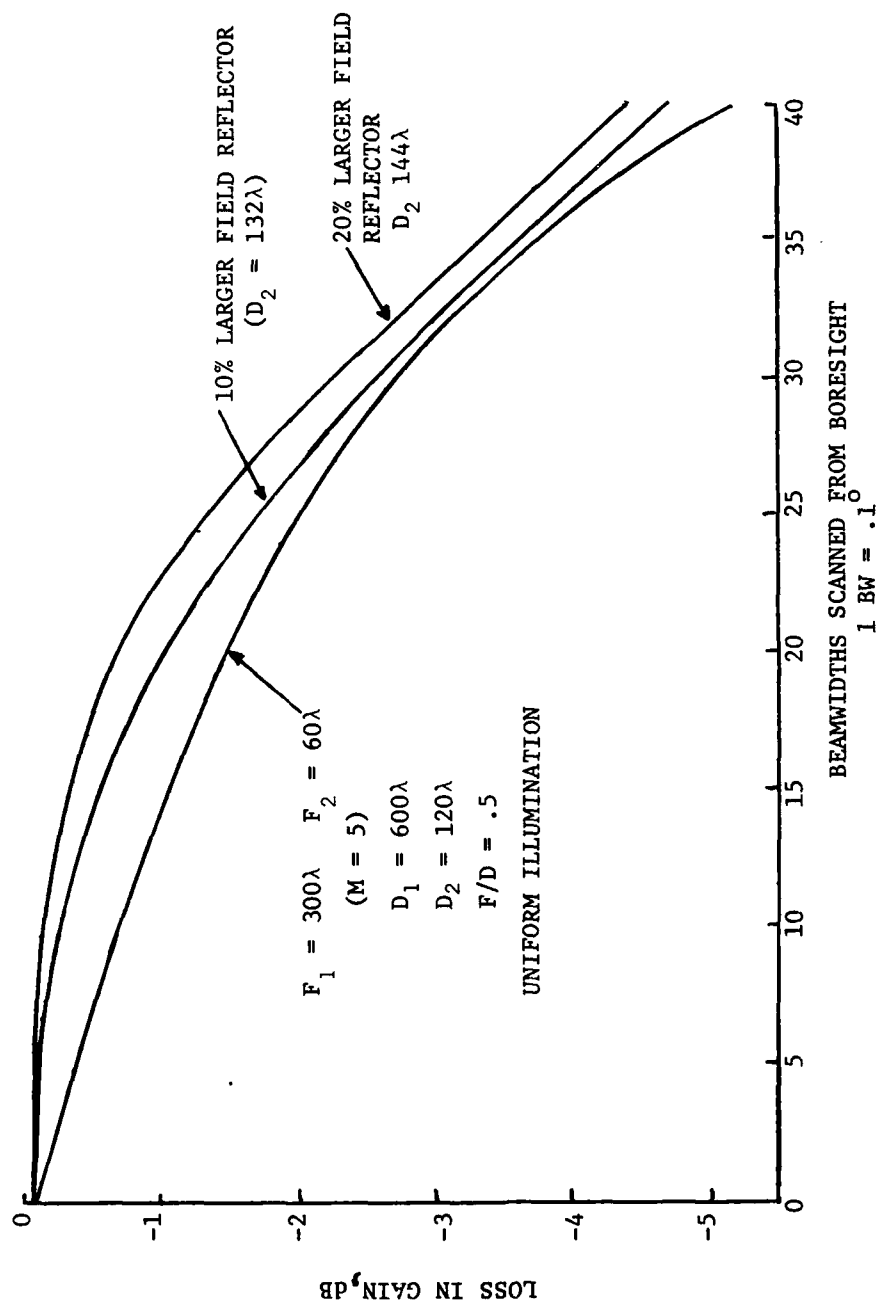
Figure 3.1-20   Beam scanning performance of two-reflector system for various oversized subreflectors.

141
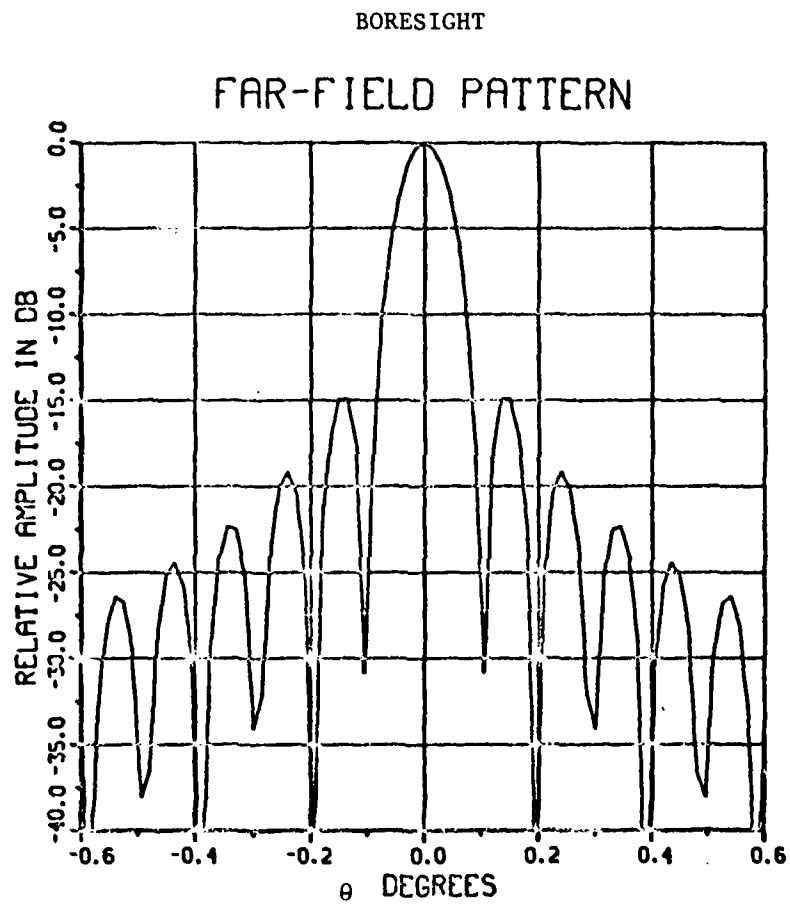
FAR-FIELD PATTERN

Figure 3.1-22   Far-field pattern of two-reflector
                system, boresight.

142

12 BEAMWIDTHS
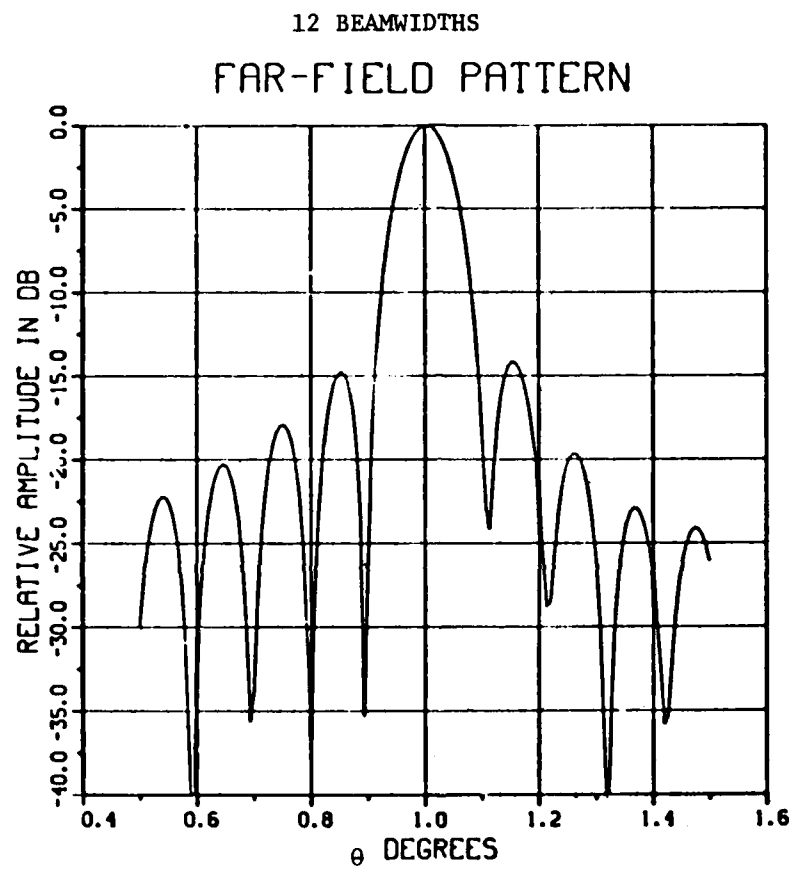
FAR-FIELD PATTERN

Figure 3.1-23   Far-field pattern of two-reflector
                 system, twelve-beamwidths off-axis.
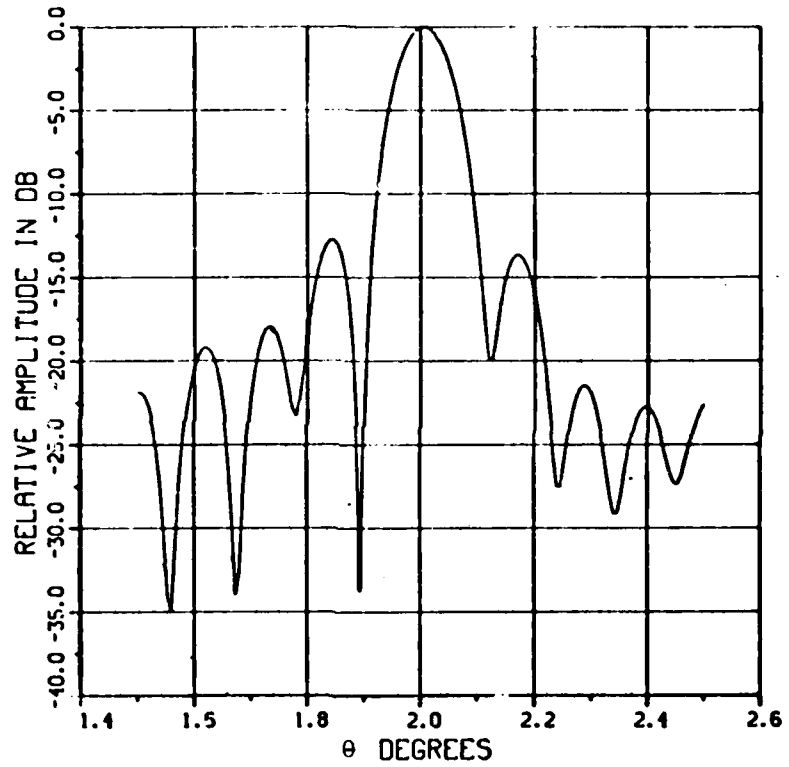
FAR-FIELD PATTERN

Figure 3.1-24   Far-field pattern of two-reflector
                 system, twenty-four beamwidths off-axis.

144
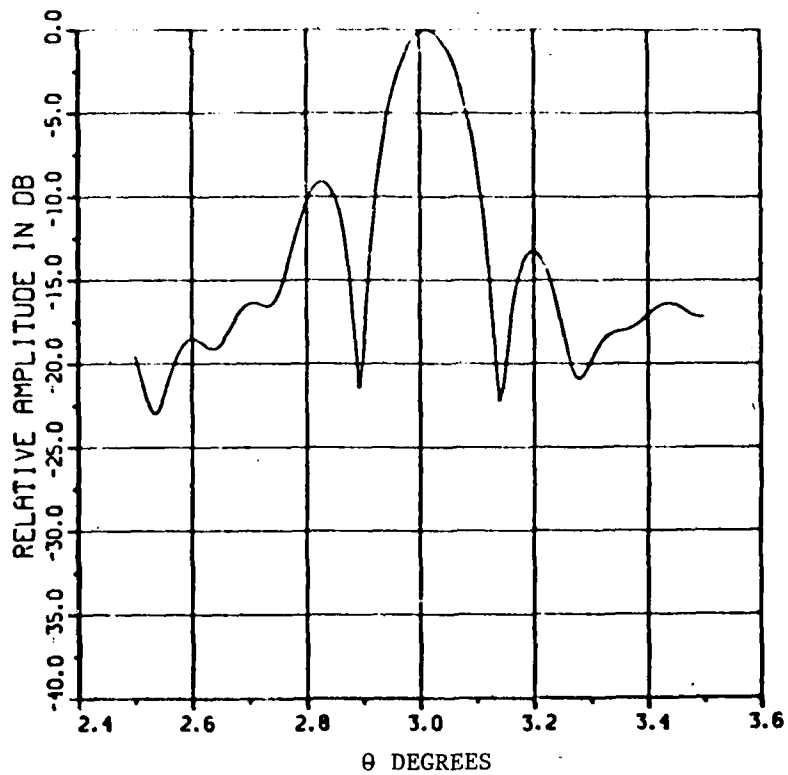
FAR-FIELD PATTERN

Figure 3.1-25   Far-field pattern of two-reflector
                 system, thirty-six beamwidths off axis.

145

48 BEAMWIDTHS

FAR-FIELD PATTERN
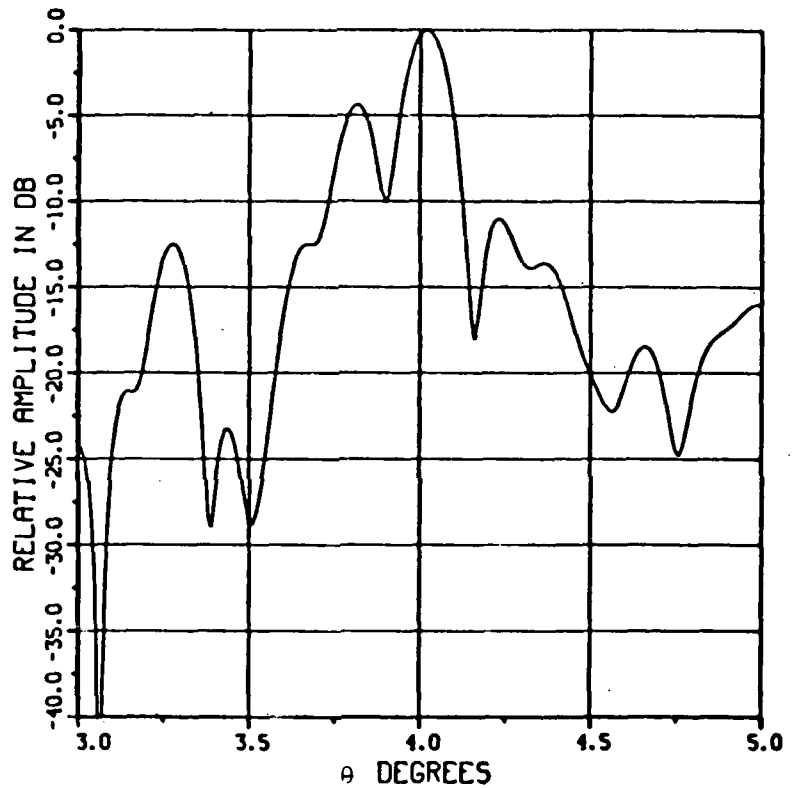
Figure 3.1-26   Far-field pattern of two-reflector
system, 48 beamwidths off-axis.

146

patterns with sidelobes that fall off very rapidly to about 60dB. The uniform
distribution is inadequate for this performance. In order to lower the side-
lobes a tapered distribution must be used. A distribution that will reduce
the sidelobes by about twenty dB (as compared to uniform) is the cosine-
squared distribution. [11] The effect of tapering the aperture distribution
is to widen the main beam and thus, reduce the antenna gain. As compared to
uniform illumination the cosine-squared distribution increases the beamwidth
by about sixty-five percent and reduces the gain by about 1.7 dB. Thus, to
achieve low sidelobes the beam scanning range (measured in beamwidths) will be
reduced. The effective beam scanning range is defined in terms of gain as
3dB below the boresight value. The location of the maximum of the cosine-
squared distribution on the phased array is a function of the beam scan angle.
This location is found in the computer program by choosing the center point
of the region in which signal is intercepted by the array in the receiving
case. Also, the breadth of the distribution is adjusted with beam scanning
to exclude shadowed areas where blockage occurs. This avoids sharp steps in
the illumination which would cause high sidelobes. The aperture efficiency
computation includes the losses due to this selective illumination. Note that
for a radar application this adaptive (with scan) amplitude control would
only be required on the receive beam since sidelobe control is for antijamm-
ing purposes and need not be done on the transmit beam.

The cosine-squared illumination was applied to a two-reflector system
with the following parameters:

$$D_1 = 300\lambda$$
$$D_2 = 120\lambda$$
$$D_3 = 120\lambda$$
$$f/D = 1.0$$
$$M = 2.5$$

array elements are 0.6λ horns. These parameters were selected to maximize the
steering range and to prevent the formation of grating lobes by the phased
array feed. Starting with this sytem the subreflector and phased array dia-
meters were increased (in ten percent increments) until spillover was mini-
mized. This was done by trial and error using the computer programs for this
system. The optimum diameters found were $D_2 = 168\lambda$ and $D_3 = 156\lambda$. These
correspond to a forty percent larger subreflector and a thirty percent larger
phased array. This new system is shown in Figure 3.1-27 for the symmetric
plane and Figure 3.1-28 for the offset plane. Note that the phased array is
stepped and follows the parabolic contour shown. The location of the control
points that adjust the primary reflector profile are shown as circles. A
practical implementation of this system would look like that shown in Fig.
3.1-29. The beam scanning performance of this system in terms of loss in
gain is shown in Figure 3.1-30. The results show that the scanning range is
approximately ± 37 beamwidths in the symmetric plane. Here the half-power
beamwidth is 0.28 degrees referred to boresight. In the offset plane the
beam scanning range is limited to -20 to +16 beamwidths. This is about one-

[11] R. C. Hansen (ed.), Microwave Scanning Antennas, Vol. I: Apertures,
Academic Press, New York, 1966, pg. 50.
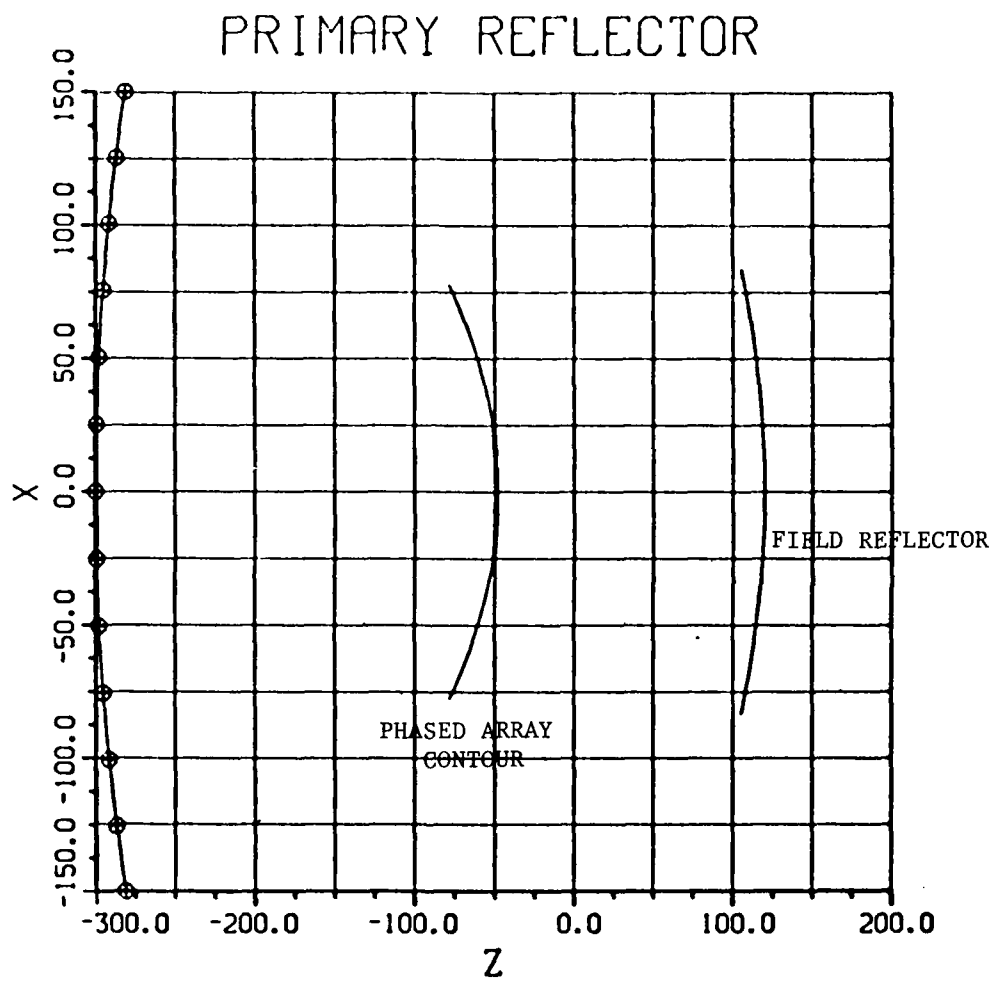
PRIMARY REFLECTOR

Figure 3.1-27   Symmetric plane of two-reflector
                 phased array fed system.

148

PRIMARY REFLECTOR
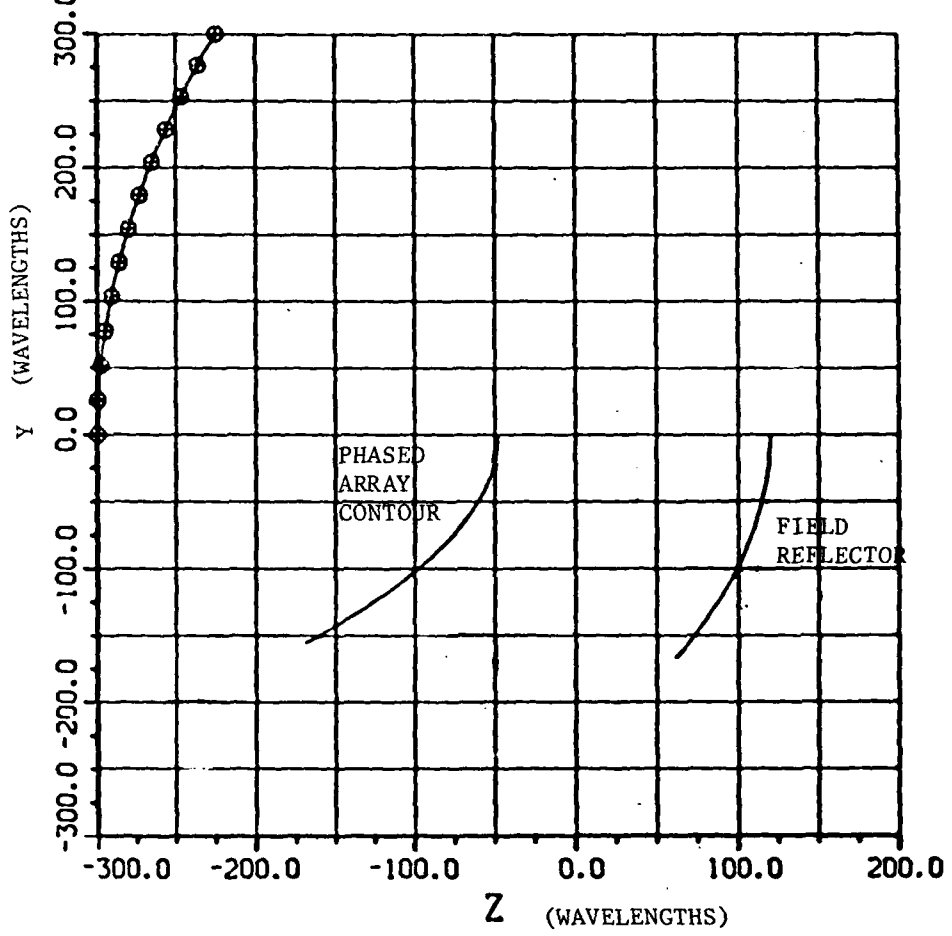
Figure 3.1-28   Offset plane of two-reflector phased array-fed system.

149
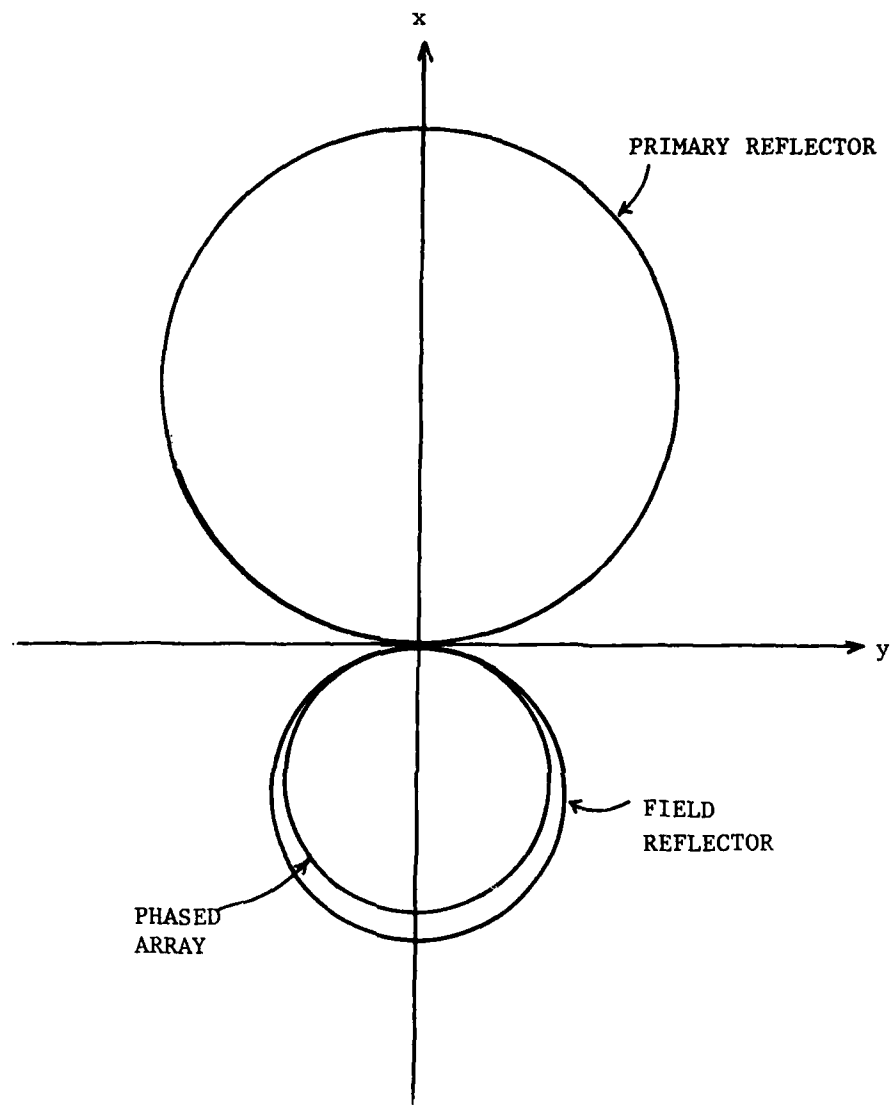
Figure 3.1-29   Rear view of a two reflector phased
                 array-fed system.

150
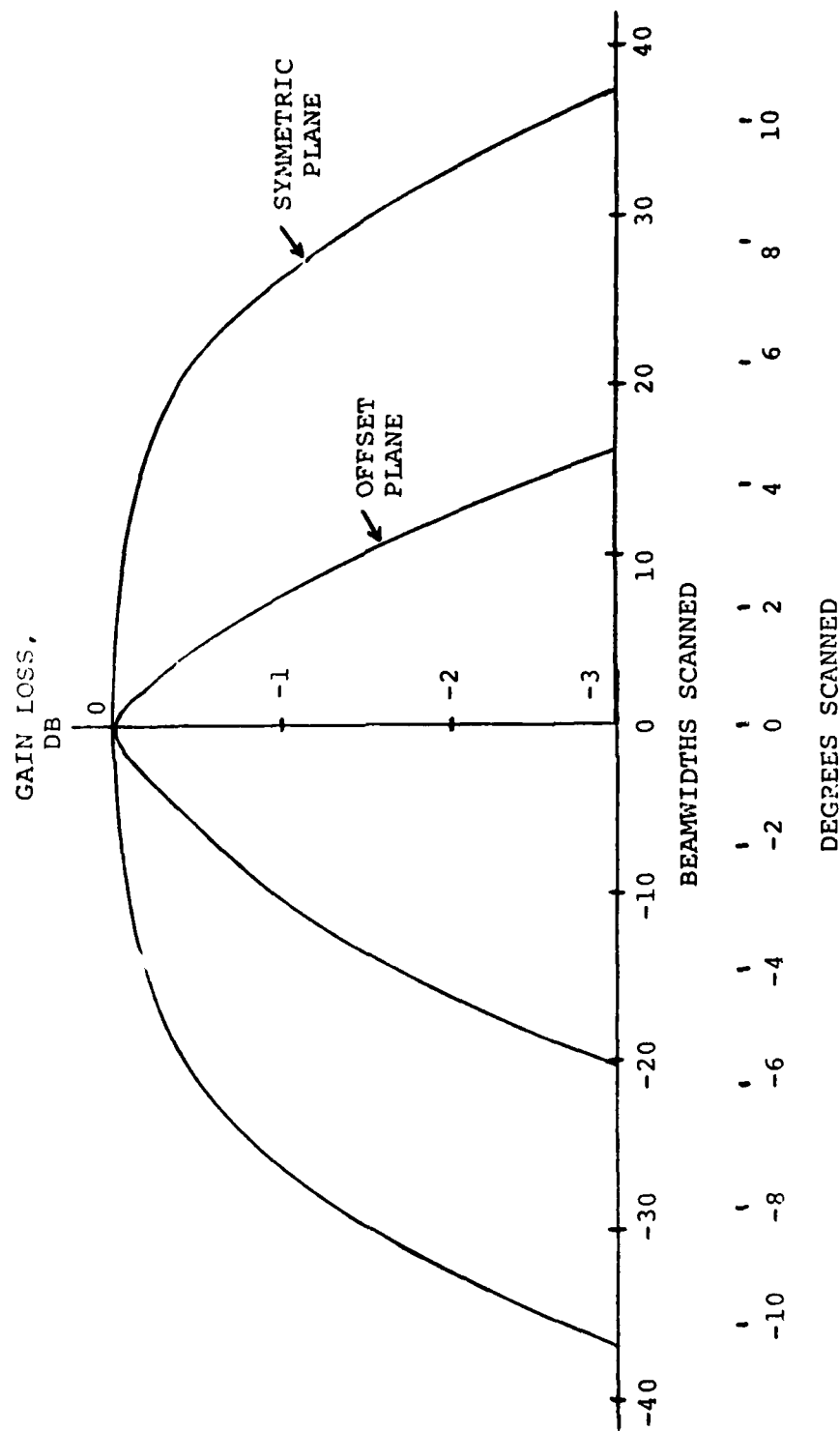
Figure 3.1-30   Beam Scanning Performance, Two-Reflector Antenna

151

half the range in the symmetric plane. The beam scanning results for the far-field pattern in the symmetric plane are given in Figures - 3.1-31 to 3.1-33. The boresight case shows that the 60 dB level is reached by the fifth sidelobe. For the cases of the beam scanned to 21 and 36 beamwidths the side-lobe level is raised to around the 40 to 50 dB level. Similar results are seen in Figures 3.1-34 to 3.1-39 for the offset plane.

3.1.3.4 Adaptive Nulling. In this section the procedure used for adaptive nulling is discussed and an example is given. Adaptive nulling is a method for placing a null at a desired location on any given antenna pattern. This is of particular interest in anti-jamming applications.

The basic adaptive nulling procedure is to combine two antenna patterns, via superposition, in such a way as to produce a null at some desired observation angle. One of the patterns is the desired pattern, with its main beam pointed in the desired direction, except that it does not have a null at the angle θ_n. The other pattern will be referred to as the sidelobe cancellation pattern and has its main beam peak located at the angle θ_n. By setting the amplitudes of the two patterns at the angle θ_n equal and the phases to be 180 degrees apart and adding them together a null is created. This is accomplished by adjusting and superimposing the amplitude and phase of the elements of the array. The factor by which the amplitude of the sidelobe cancellation excitation is multiplied by is expressed as

$$A = \frac{A_d}{A_{s.c.}} \tag{3.1-9}$$

where A_d is the amplitude of the desired pattern at $\theta = \theta_n$

$A_{s.c.}$ is the amplitude of the sidelobe cancellation pattern at $\theta = \theta_n$

The phase shift that is added to the sidelobe cancellation excitation is given by

$$\phi = (\phi_{s.c.} - \phi_d) - 180^\circ \tag{3.1-10}$$

where ϕ_d is the phase in degrees of the desired pattern at $\theta = \theta_n$

$\phi_{s.c.}$ is the phase in degrees of the sidelobe cancellation pattern at $\theta = \theta_n$.

Equations 3.1-9 and 3.1-10 are the required relations for generating a null. These equations will now be applied to an example.

Consider the 21 and 36 beamwidth patterns of the previous section shown in Figures 3.1-32 and 3.1-33, respectively. The 21 beamwidth pattern is taken to be the desired pattern. Suppose a null is reuqired at the peak of the 36 beamwidth patterns ($\theta = 10^\circ$). The computed pattern amplitude of the 21 beamwidth pattern at the angle is

$A_d = 0.00006099873$.

The corresponding pattern phase is
$\phi_d = 168.1398^\circ$.

FAR-FIELD PATTERN
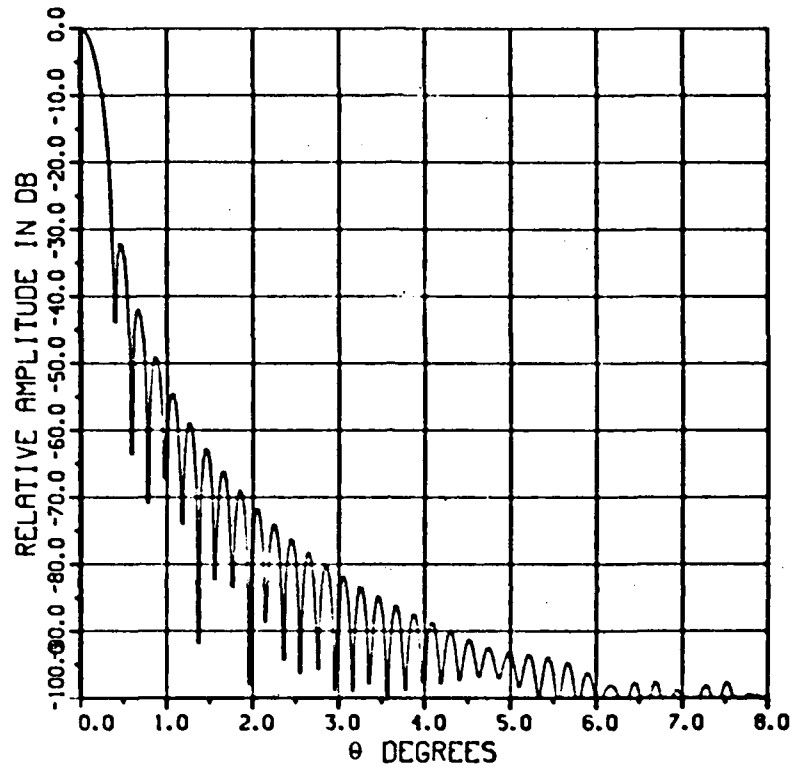
$$D_1 = 300\lambda$$
$$D_2 = 168\lambda$$
$$D_3 = 156\lambda$$

Figure 3.1-31   Radiation Pattern, Symmetric Plane, Two-Reflector Antenna, Tapered Illumination, On-Axis

153

FAR-FIELD PATTERN

$$D_1 = 300\lambda$$
$$D_2 = 168\lambda$$
$$D_3 = 156\lambda$$

Figure 3.1-32   Radiation Pattern, Symmetric Plane, Two-
Reflector Antenna, Tapered Illumination,
Scanned 21 Beamwidths

154

FAR-FIELD PATTERN
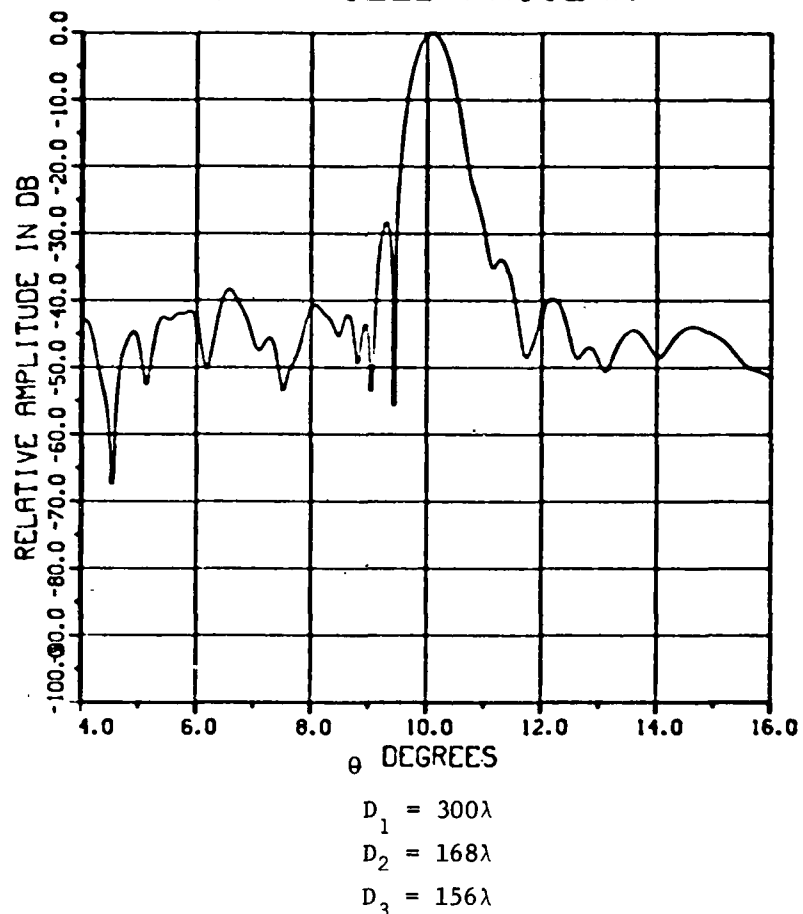
$$D_1 = 300\lambda$$
$$D_2 = 168\lambda$$
$$D_3 = 156\lambda$$

Figure 3.1-33   Radiation Pattern, Symmetric Plane, Two-Reflector Antenna, Tapered Illumination, Scanned 36 Beamwidths.

FAR-FIELD PATTERN
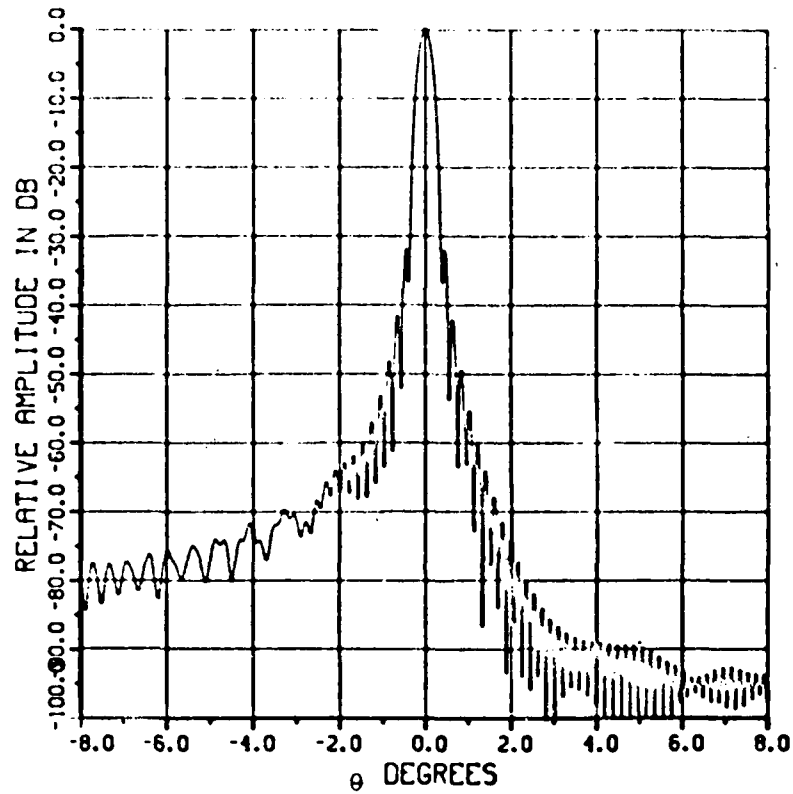
$D_1 = 300\lambda$

$D_2 = 168\lambda$

$D_3 = 156\lambda$

Figure 3.1-34　Radiation Pattern, Offset Plane,Two-Reflector Antenna, Tapered Illumination, On-Axis.

FAR-FIELD PATTERN
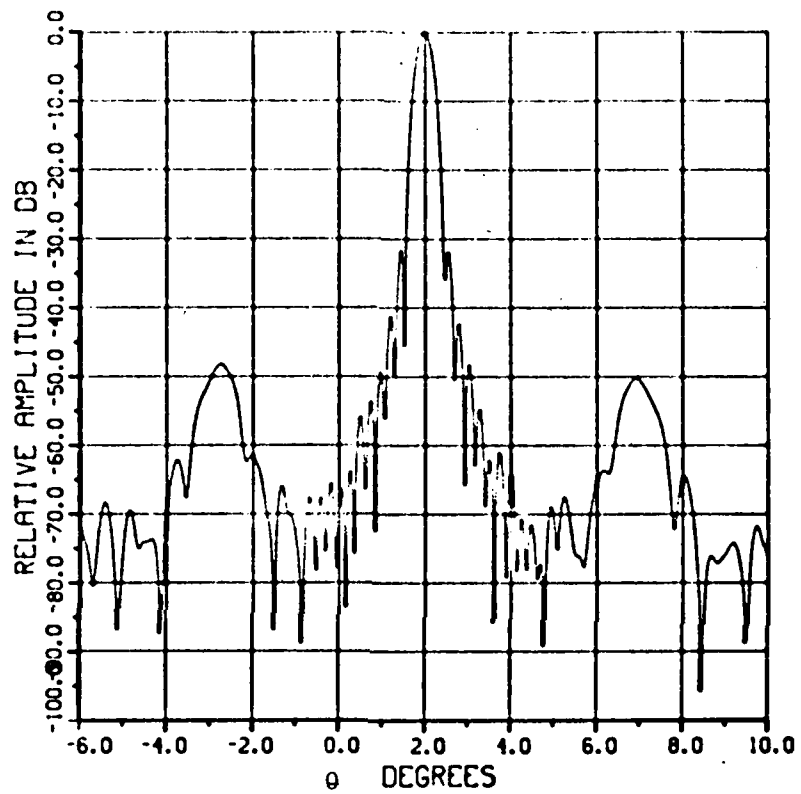
$D_1 = 300\lambda$

$D_2 = 168\lambda$

$D_3 = 156\lambda$

Figure 3.1-35   Radiation Pattern, Offset Plane, Two-
Reflector Antenna, Tapered Illumination,
Scanned + 7 Beamwidths.

157
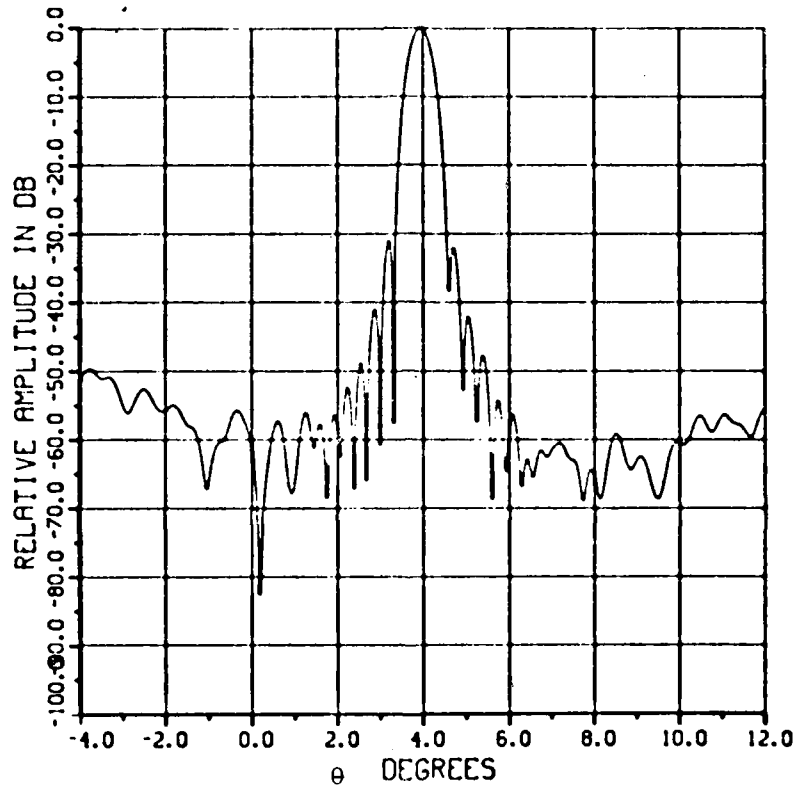
FAR-FIELD PATTERN

$$D_1 = 300\lambda$$
$$D_2 = 168\lambda$$
$$D_3 = 156\lambda$$

Figure 3.1-36   Radiation Pattern, Offset Plane,
Two-Reflector Antenna, Tapered
Illumination, Scanned +14 Beamwidths.

158

FAR-FIELD PATTERN
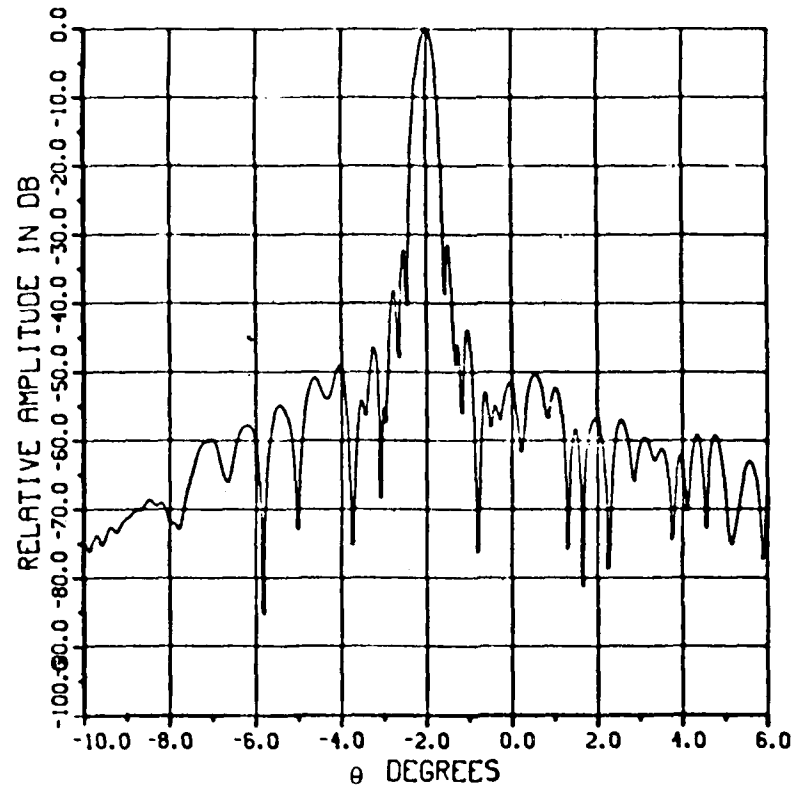
$D_1 = 300\lambda$

$D_2 = 168\lambda$

$D_3 = 156\lambda$

Figures 3.1-37   Radiation Pattern, Offset Plane,
Two-Reflector Antenna, Tapered
Illumination, Scanned -7 Beamwidths.

159
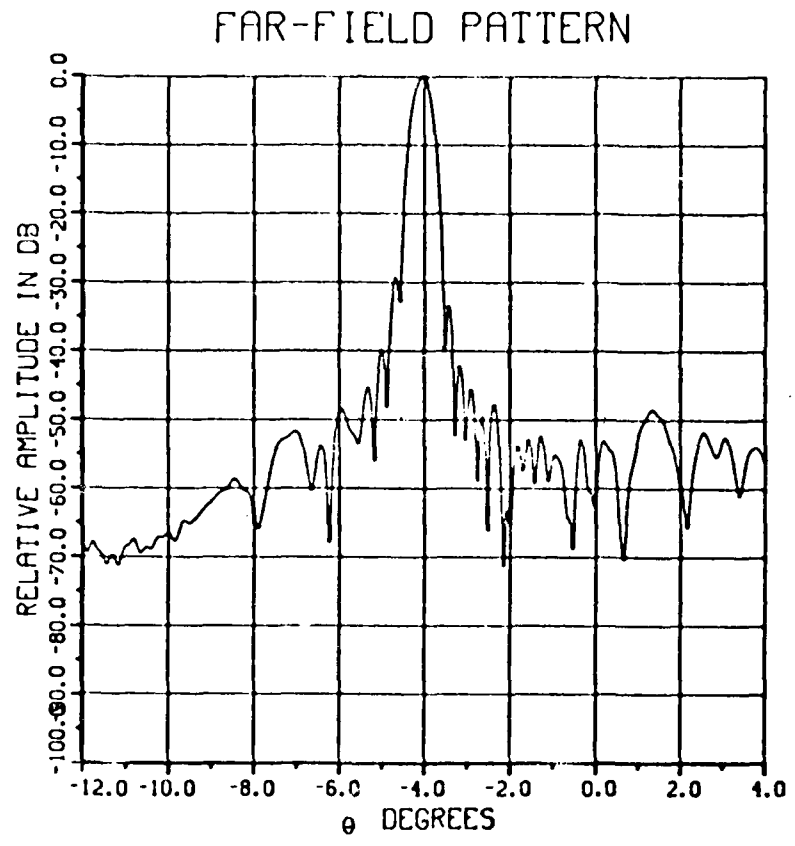
FAR-FIELD PATTERN

$D_1 = 300\lambda$

$D_2 = 168\lambda$

$D_3 = 156\lambda$

Figure 3.1-38   Radiation Pattern, Offset Plane, Two-
Reflector Antenna, Tapered Illumination,
Scanned -14 Beamwidths.

160

FAR-FIELD PATTERN
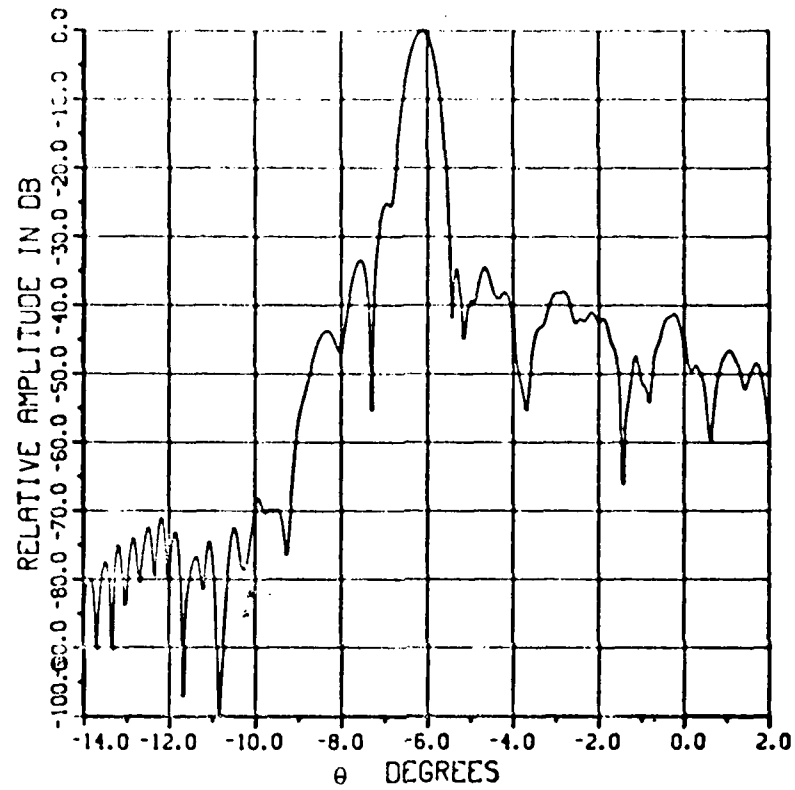
$D_1 = 300\lambda$

$D_2 = 168\lambda$

$D_3 = 156\lambda$

Figures 3.1-39   Radiation Pattern, Offset Plane,
Two-Reflector Antenna, Tapered
Illumination, Scanned -21 Beamwidths.

161

Now take the 36 beamwidth pattern to be the sidelobe cancellation pattern.
At $\theta = \theta_n$ the amplitude and phase are

$A_{s.c} = 0.0099379280$

$\emptyset_{s.c} = 271.3642^{\circ}$

From Equation 3.1-9 the required amplitude excitation factor is

$A = 0.006137972624$

and from Equation 3.1-10 the required phase excitation fractor is

$\emptyset = -76.7756^{\circ}$.

Using this information in the adaptive nulling computer program (listed in
Appendix C) a 106 dB null is generated at $\theta = 10^{\circ}$ as shown in Figure 3.1-40.
Note that the pattern shape away from the null is unchanged. The magnitude
of the null that can be achieved is constrained by the accuracy with which
the amplitude and phase of the array elements can be controlled. In practice,
adaptive nulling is usually achieved iteratively, using a closed loop null-
ing system. This computation demonstrates that any of the techniques used
for adaptive nulling in conventional phased arrays [2] can be applied to the
two-reflector system.

162

FAR-FIELD PATTERN
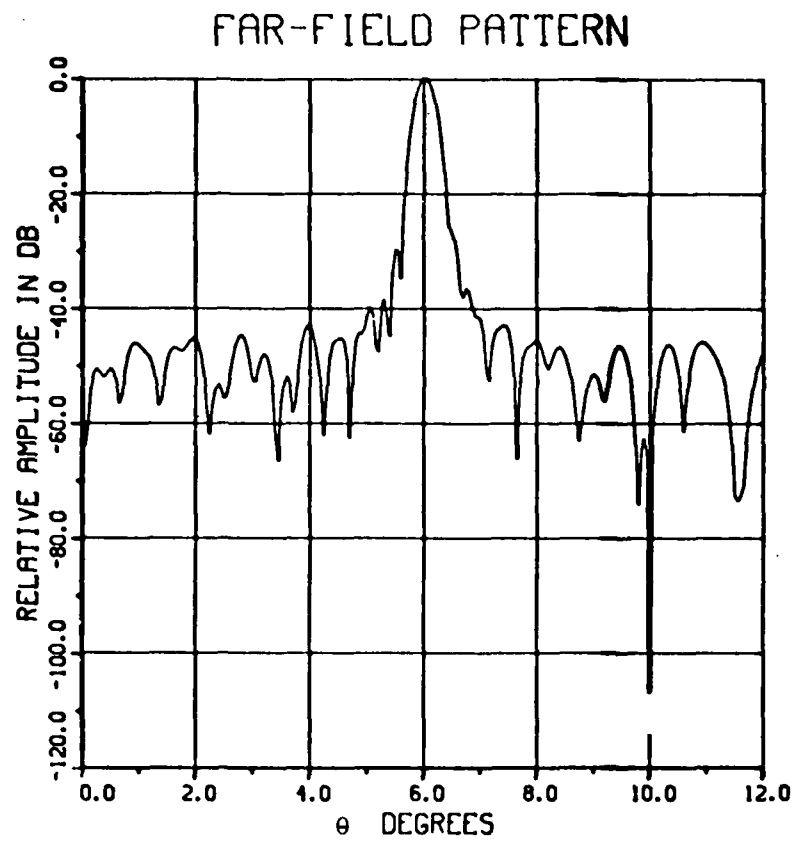
Figure 3.1-40   Radiation Pattern, Symmetric Plane,
                 Scanned 21 Beamwidths, Adaptive Null
                 Formed at +10°.

163

3.2   Structural Systems Performance Analysis

Three mission configurations were evaluated for STS Orbiter packaging, orbit transfer, mass, stiffness, thermal, and operational scenario. The first system is a low earth orbit (5000 n.mi.) two reflector space based radar. The main reflector is 70m. (227.5 ft) diameter and the field reflector and phased array are 28 m (91 ft) in diameter. The second system is a low earth orbit (5000 n.mi.) reflectarray. The reflector diameter is 91m. (300 ft) and the feed is located at an F/D = 0.5. The third system is a synchronous orbit two reflector space based radar. The main reflector is 305m (1000 ft) diameter and the field reflector and phased array are 30.5 (100 ft) in diameter.

3.2.1   Packaging in Orbiter. The objective of this task was to define a packaging and restraint system which will minimize the impact of the Orbiter-induced loads. A reuseable cradle approach that was developed on the SAMSO On-Orbit Assembly program is proposed.

The antenna & S/C is carried aloft, supported in a restraining cradle. This cradle interfaces with the shuttle cargo bay structure. The loads induced in the structural array by flight are transmitted through the cradle into the shuttle in a determinant manner and the cradle isolates the structure from the shuttle cargo bay deflections.

The cradle that supports the structure from Earth to orbit must meet the following requirements:

1. Load transfer interfaces with the shuttle must be limited in location and number so that all load paths are determinant. (Shuttle Payload Users Guide Volume 14.)

2. The cradle must capture and restrain the folded structure in a manner that prevents damage by straining and allows for induced deflections.

3. The cradle will also support the stage adapter which is attached to the rear of the structure.

4. The cradle will release all restraints on the structure and stage adapter, on remote command. The restaining mechanisms retract to a position that will permit the structure and stage adapter to rotate up and out of the cradle and shuttle cargo bay.

5. All extended restraining devices on the cradle will be capable of reclosing and relocking, for return to Earth aboard the shuttle.

6. The cradle will be refurbishable for additional subsequent flight operations.

7. The cradle will be made the lightest weight possible that is consistent with the functions to be performed.

164

← Fwd

Typical Linear
Actuator Pin
Puller

Adapter
Support Points

$Z_0 = 414.0$

$X_0 = 935.27$

Linear Actuator
Pin Puller

Linear Actuator

Typical
Spacers

Jointed Ring-
Half, Deployed

Latch

Linear
Actuator

Linear
Actuator
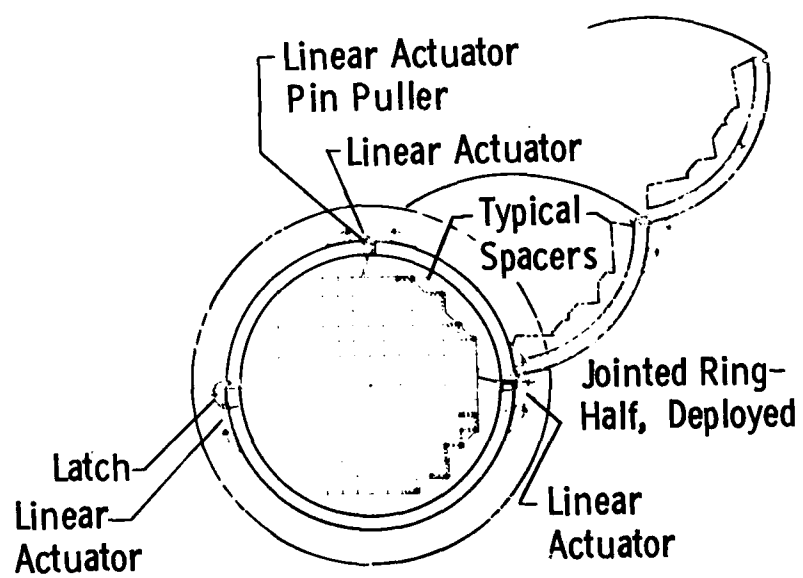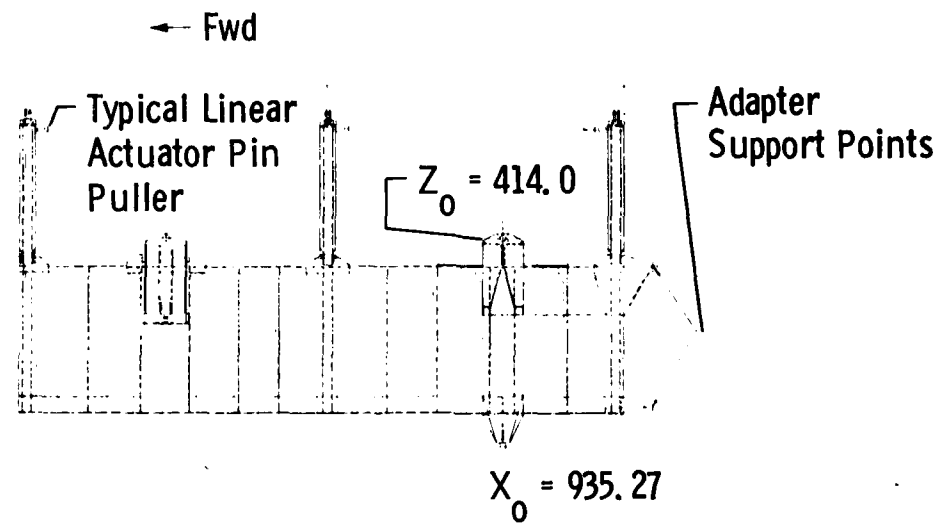
Figure 3.2-1   Cradle Support Structure In Orbiter

8. All axial (longitudinal) loads from the structure will be taken out at the stage adapter end of the cradle. No axial loads will be taken out anywhere else between the structure and cradle.

The cradle is a semicylindrical, thick walled, semi monocoque structure, with three segments semicircular rings that, together, form a circular enclosure around the structural array. The two side beams and the bottom keel beam extend out to pick up and support the stage adapter (See Figure 3.2-1).

The loads at the cradle adapter end, are introduced through trunnion and keel fittings directly to the shuttle spacecraft. The loads at the forward (opposite) end of the cradle are first passed to a hydraulic load leveling system mounted on the cradle or an an auxiliary cradle ring. This auxiliary ring then interfaces with the shuttle spacecraft through trunnion and keel fittings, thru which the loads are reacted.

The encircling rings are hinged at the side beams and at the top center. At the junction with the other side beam there is a releasable/re-engageable joint for each ring half. This arrangement permits the two ring quadrants to be swung out, clear of the structural array deployment path, on the cargo bay side opposite the manipulator arm. The folding and unfolding of the ring quadrants are powered by small linear actuators. Locking is also accomplished by linear actuators.

Inside each encircling ring (full circle) are expandable pneumatic tubes which thrust spacer blocks against a series of interlocking end and/or hinge fittings on the structure. This retains the structure in a rattle-free configuration for flight. Changes in axial length of the array (due to flexing or thermal gradients) are accommodated at the three encircling rings by rolling the pneumatic tube.

The cradle is reusable and refurbishable. The expanding tubes compensate for small manufacturing differences and tolerance buildups between assembled structural arrays. The hydraulic load leveling system keeps the load path relationship to the shuttle spacecraft determinant. All the cradle release mechanisms and movable parts are capable of restoring themselves to a landing configuration. The cradle weight will be minimized by using materials with a high strength to weight ratio such as aluminum, titanium, and high heat treat steels. All the design and manufacturing techniques are 'state of the art' with air-frames industries.

3.2.2   Orbit Transfer. During this task, the ability of three orbit transfer vehicles to meet the three mission requirements was evaluated; IUS, low thrust liquid (LTL) and solar electric propulsion (SEP). IUS is not acceptable due to its high thrust-to-weight ratio and low ISP. The storable propellant stage can be tailored to the desired thrust-to-weight (see Figure 3.2-2) but with the relatively low ISP ($\approx$ 305), the allowable payloads are too low (See Table 3.2-1). The optimum chemical stage is a cryogenic low thrust as shown in Figure 3.2-3. The stage that has the maximum payload to orbit is SEP. However the trip times to geosynchronous are much longer (months) than cryognics (hours). Typical SEP trip times are

Table 3.2-1   Payloads For Various OTV Configurations

CASE	ORBITER 1 PAYLOAD WT	ORBITER 1 PAYLOAD LENGTH	ORBITER 1 STAGE TYPE	ORBITER 2 STAGE TYPE	MAX g's
1	10,000	32 FT	CR-RD-TOR	-	<0.05
2	13,000	31	CR-CEN-TOR	-	0.70
3	29,200	35	CR-RD-TOR	CR-RD-CON	<0.03
4	32,000	36	CR-RD-TOR	CR-CEN-CON	0.24
5	33,700	34	CR-CEN-TOR	CR-CEN-CON	0.38
6	17,200	50	-	CR-RD-CON	<0.07
7	22,100	50	-	CR-CEN-CON	0.47
8	1,400	38	STO-MX-CL	-	0.18
9	2,000	50	-	STO-MX-CL	0.16
10	12,900	39	STO-MX-CL	STO-MX-CL	0.11
11	22,000*	24	EP	-	0
12	37,000*	39	-	EP	0
13	50,000**	50	-	EP	0

STAGE CODES:

FUEL

			I_{SP}
CR	=	CRYOGENIC	400 SEC
STO	=	STORABLE	305
EP	=	ELECTRIC PROPULSION	3000

ENGINES

CEN	=	CENTAUR
RD	=	ROCKETDYNE
MX	=	AXIAL PRESSURE FED

PROPELLANT TANKS

CON	=	CONVENTIONAL
TOR	=	TOROIDAL
CL	=	CLUSTERED

NOTES: 65000 LBM ORBITER PAYLOAD
PAYLOAD IS TO GEOSYNCHRONOUS EQUATORIAL
PAYLOAD CRADLE WT (LARGE STAGE OR PAYLOAD = 5000 LBM, SMALL STAGE = 3000 LBM
STAGE AND S/C ADAPTER = 3000 LBM
ALLOWABLE PAYLOAD LENGTH = 50 FT (4 FT EVA CLEARANCE, 1 FT AFT CLEARANCE,
        5 FT STAGE & S/C ADAPTER)

167
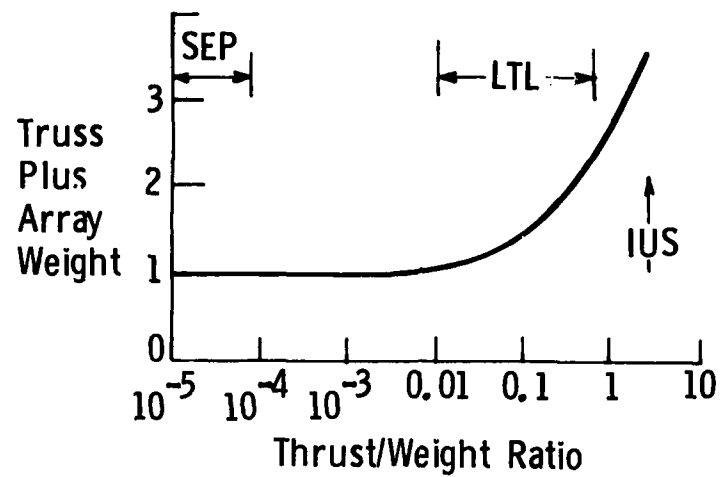
Figure 3.2-2   Impact Of OTV Thrust Load On Truss Structure
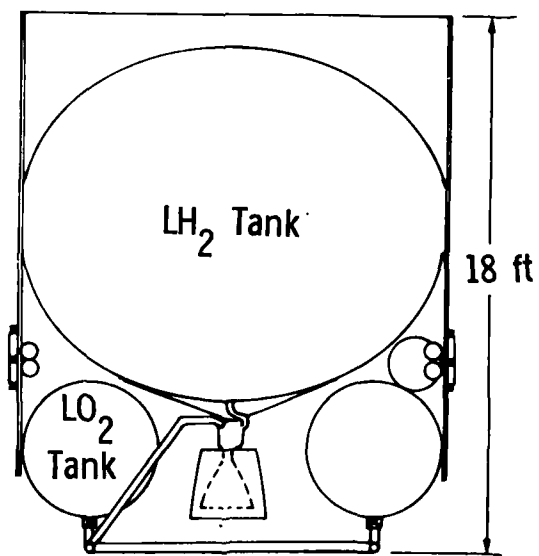
Figure 3.2-3   Cryogenic Low Thrust Liquid OTV

168

- $I_{SP} = 3000$
- STAGE WEIGHTS ARE FOR 700 DAY TRIPS. FOR SHORTER TRIPS WITH SMALLER PAYLOADS, DEDUCT 4% FROM STAGE WEIGHT FOR EACH 10% PAYLOAD REDUCTION
- DRY STAGE WEIGHT INCREASES LINEARLY WITH POWER
- SHORTER TRIPS AT HIGHER POWER AND LOWER I_{SP} ARE POSSIBLE (BUT STAGE GETS HEAVIER)

1 MEGAWATT, 240 K LB STAGE

500 KW, 120 K LB STAGE

250 KW, 60 K LB STAGE

150 KW, 36 K LB STAGE

100 KW, 24 K LB STAGE

50 KW, 12 K LB STAGE

GEOSYNCH. PAYLOAD, K LB.

TRIP TIME, DAYS

Figure 3.2-4 Electric Propulsion OTV
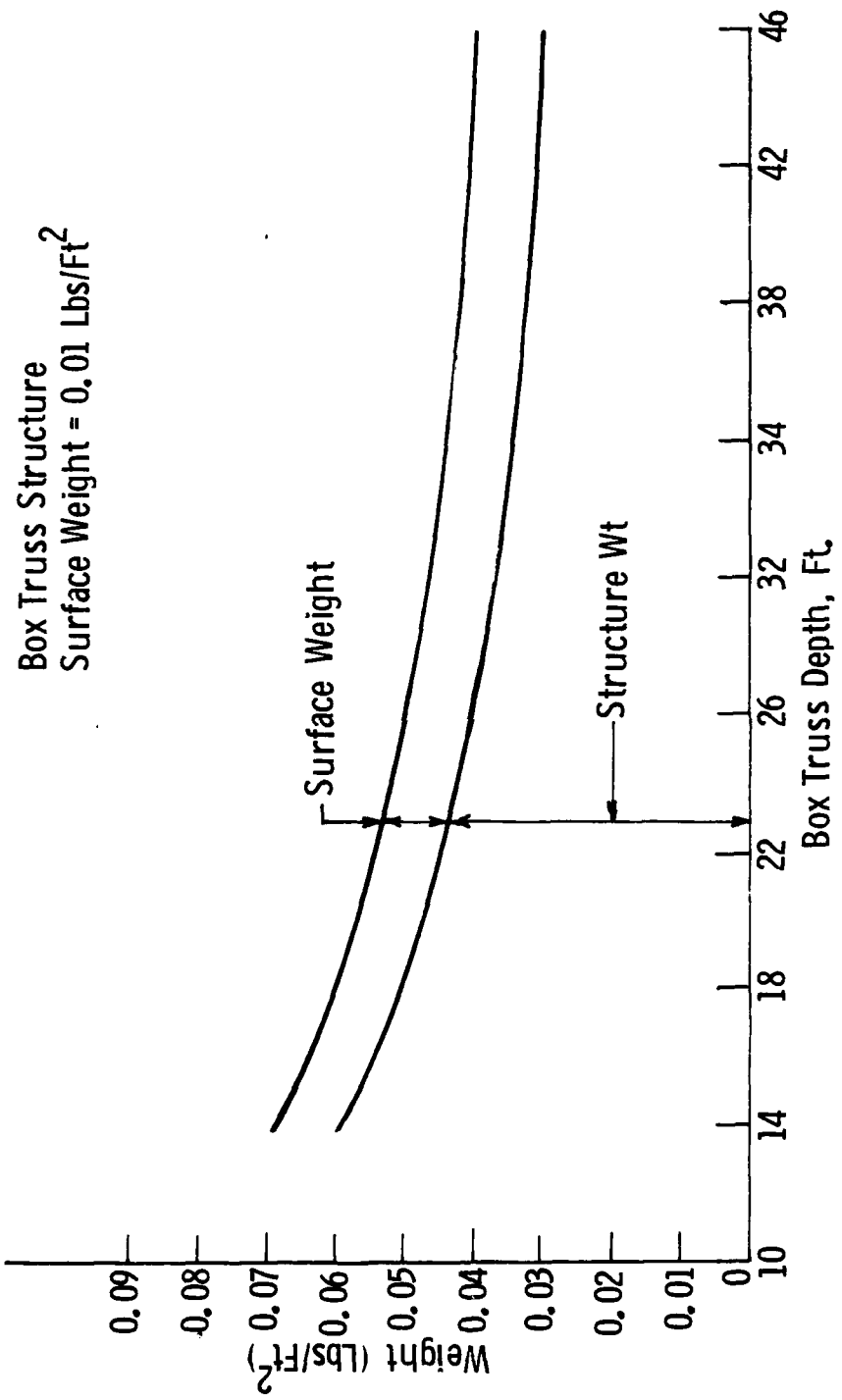
Figure 3.2.5   Effect Of Truss Depth On Antenna Weight

170

shown in Figure 3.2-4.

Three configurations were analyzed to determine the maximum payload for each upper stage. The first configuration has the antenna packaged with its upper stage in the orbiter bay. For this configuration, the antenna plus upper stage occupies the total orbiter bay. The optimum antenna depth/ upper stage length is determined, based on achieving the maximum diameter within the orbiter payload and envelope constraints. When the antenna and upper stage are transported to LEO in one Shuttle, the maximum truss depth is determined by the stage, truss/stage adapter, mesh lengths, and EVA and aft clearances. The mesh stowed length was assumed to be 0.15 times the truss depth.

In addition to affecting antenna size, the truss depth affects the number of cubes and weight required for a given diameter (See Figure 3.2-5). This is a reliability consideration because the number of cubes relates directly to the number of parts and deployment steps. Minimizing both parts. and steps will lead to maximum reliability. Therefore, maximizing truss depth is a design goal.

The second configuration has the antenna packaged in the total orbiter bay. This allows a truss depth of approximately 50 ft. For this configuration, the upper stage is brought up in a separate orbiter and docked to the antenna in LEO. The allowable antenna system weight is defined as the payload capability of the upper stage that can be carried in one separate orbiter.

To determine the maximum size that can be transported to geosynchronous orbit on each upper stage, two parameters are determined--the allowable weight of the antenna, and the allowable package envelope of the antenna. These were determined from orbiter constraints (orbiter payload, volume, and cg) and upper stage constraints (upper stage performance). Within these constraints, an optimum upper stage size was selected.

The maximum weight of the upper stage payload was specified to be 57,000 lb (8000 lb were specified for orbiter attachment and deployment structure). The maximum length of the payload was specified to be 55 ft. A 4-ft EVA clearance was allocated at the front of the orbiter bay and a 1-ft clearance was assumed at the rear. The antenna is packaged in a 13.5-ft-diameter envelope leaving space for support structure.

The third configuration is a two stage vehicle which has a small stage packaged with the S/C in Orbiter 1 and a large 60,000 lbs stage in Orbiter 2 that is docked to the small stage to produce a two stage orbit transfer vehicle. As can be seen in Table 3.2-1, large payload increases can be achieved. The technique for attaching the payload to the upper stage is shown in Figure 3.2-6. The stage is hard mounted to a structural hard point on the truss and reaction straps are deployed to provide pitch-yaw-roll stabilization.

In addition to the geosynchronous orbit transfer vehicle comparison,

171
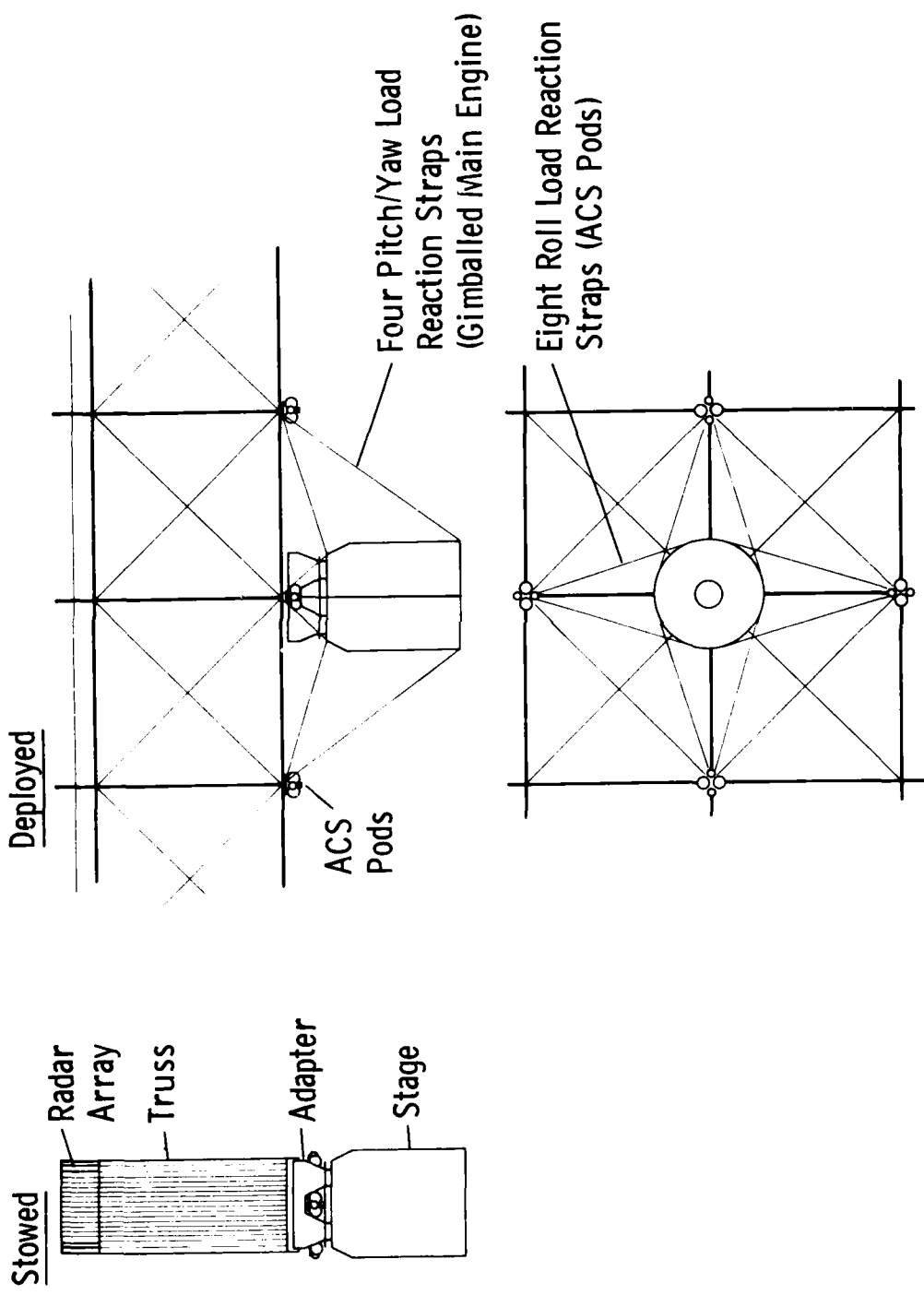
Figure 3.2-6   Antenna/OTV Interface

172

cryogenic stage to 5000 n.mi. x 65° inclination was evaluated. Three modes were evaluated (See Table 3.2-2).

Table 3.2-2   Transfer Modes To 5000 n.mi x 65°

Mode	Launch Site	Incl.	Max.Allow-ble Wt.	Plane Ch Deg	ΔV_p	ΔV_a Circ	P.Ch.	Total ΔV
1	KSC	28.5°	65,000	36.5	4600	3700	5700	14000
2	KSC	55°	55,000	10	4600	3700	800	9100
3	VAFB	65	48,000	9	4600	3700	0	8300
			@ 200 nmi					

NOTE: Toroidal LO_2 tank, clustered APS Thrusters
MF=.87 I_{sp} = 400

The results show that Mode 1 capability is 14750 lbs, Mode 2 is 19300 lbs, and Mode 3 is 18000 lbs.

3.2.3   Two Reflector LEO Radar Mission. The two reflector LEO radar configuration is shown in Figure 3.2-7. The 70m (227.5 ft) main reflector has a graphite epoxy box truss structure which supports a gold plated molybdenum wire tricot mesh. The box truss provides a stiff and thermally stable reflector structure. The platform that provides the attachments for the Astromasts, solar arrays, feed, S/C, and gravity gradient boom is a continuous extension of the reflector truss structure. The field reflector and phased array are also fabricated using a graphite epoxy box truss. The four Astromast which provide the separation between reflectors and array are stabilized in bending and torsion with graphite/epoxy tapes. The gravity gradient boom is an Astromast without guyline stabilizers. The antenna axes and orientation are shown in Figure 3.2-8. The gravity gradient boom is located along the yaw axis.

Table 3.2-3 presents a summary of the radar antenna size and weight. The total is 11500 lbs and the total stowed length is 36 ft.

The packaged configuration in the Orbiter consists of the trusses stowed, stacked and supported in a cradle similar to that shown in Figure 3.2-1. Each stowed box truss reflector has three jointed clamping rings to support and restrain the S/C. The cradle will then have a total of 9 rings. The stage is independently supported in its own cradle to provide a determinent attachment to the Orbiter. After a achieving shutter orbit, the attachments between the S/C and stage (See Figure 3.2-6) are made and the total system rotated out of the cargo bay.

The stage for transport from Shuttle orbit to 5000 n.mi. is a short cryogenic LTL stage (Figure 3.2-3) which has a thrust of 400 lbs. The stage
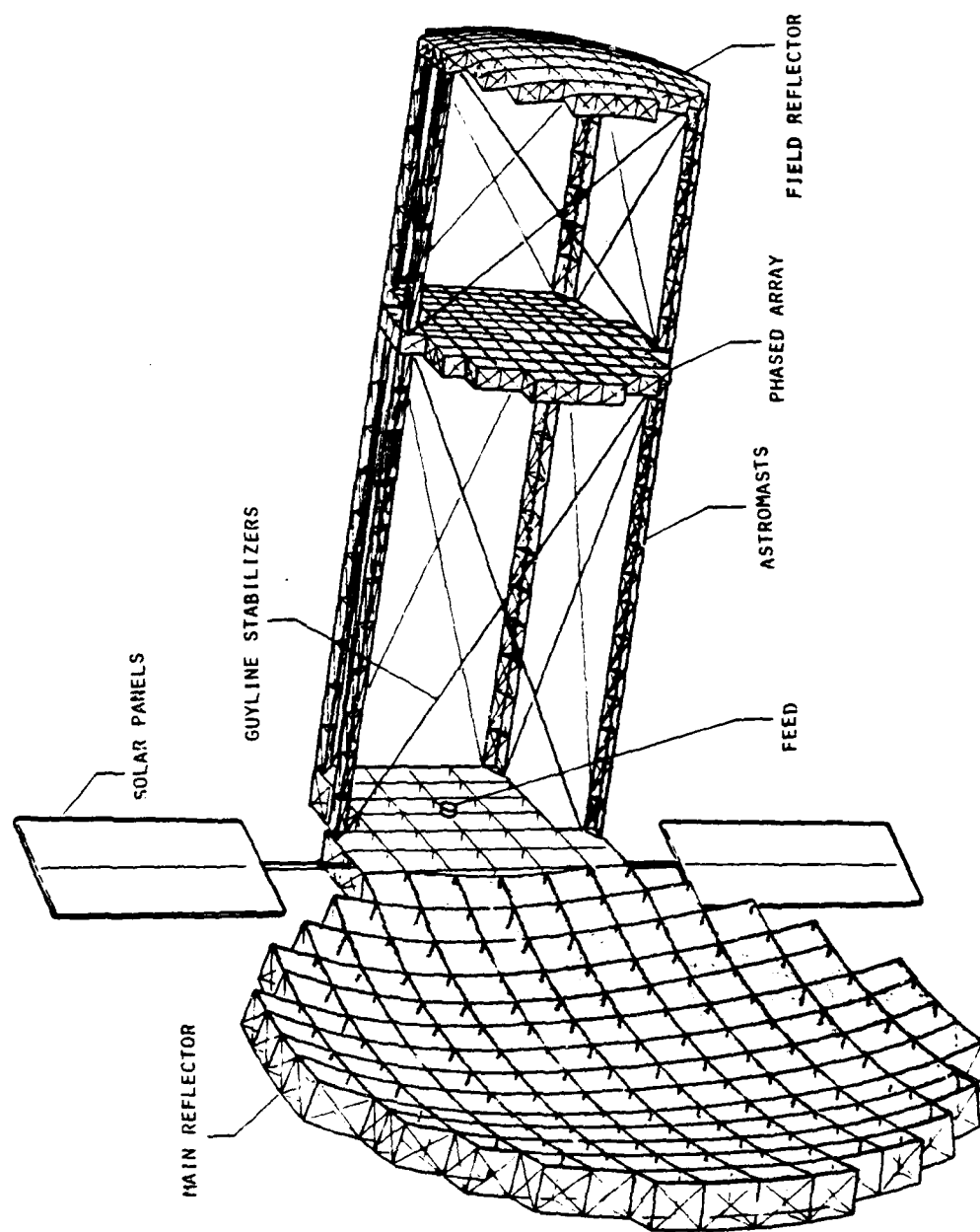
Figure 3.2-7 LEO RADAR ANTENNA CONFIGURATION

174
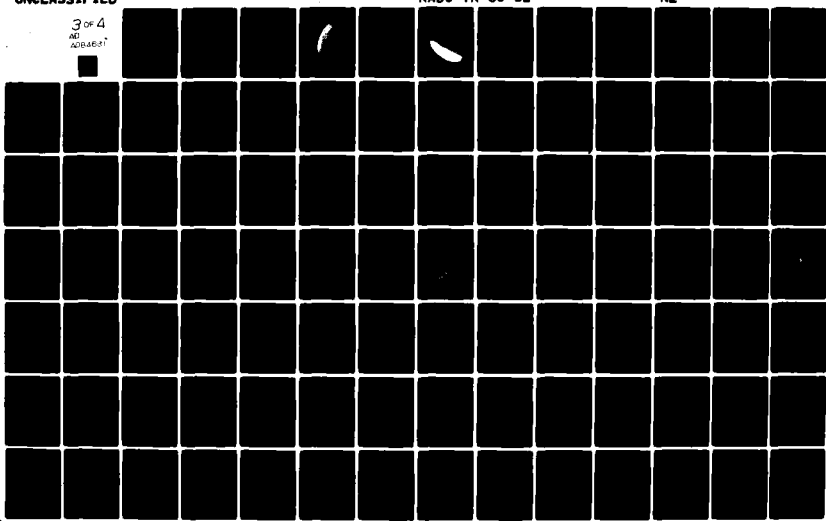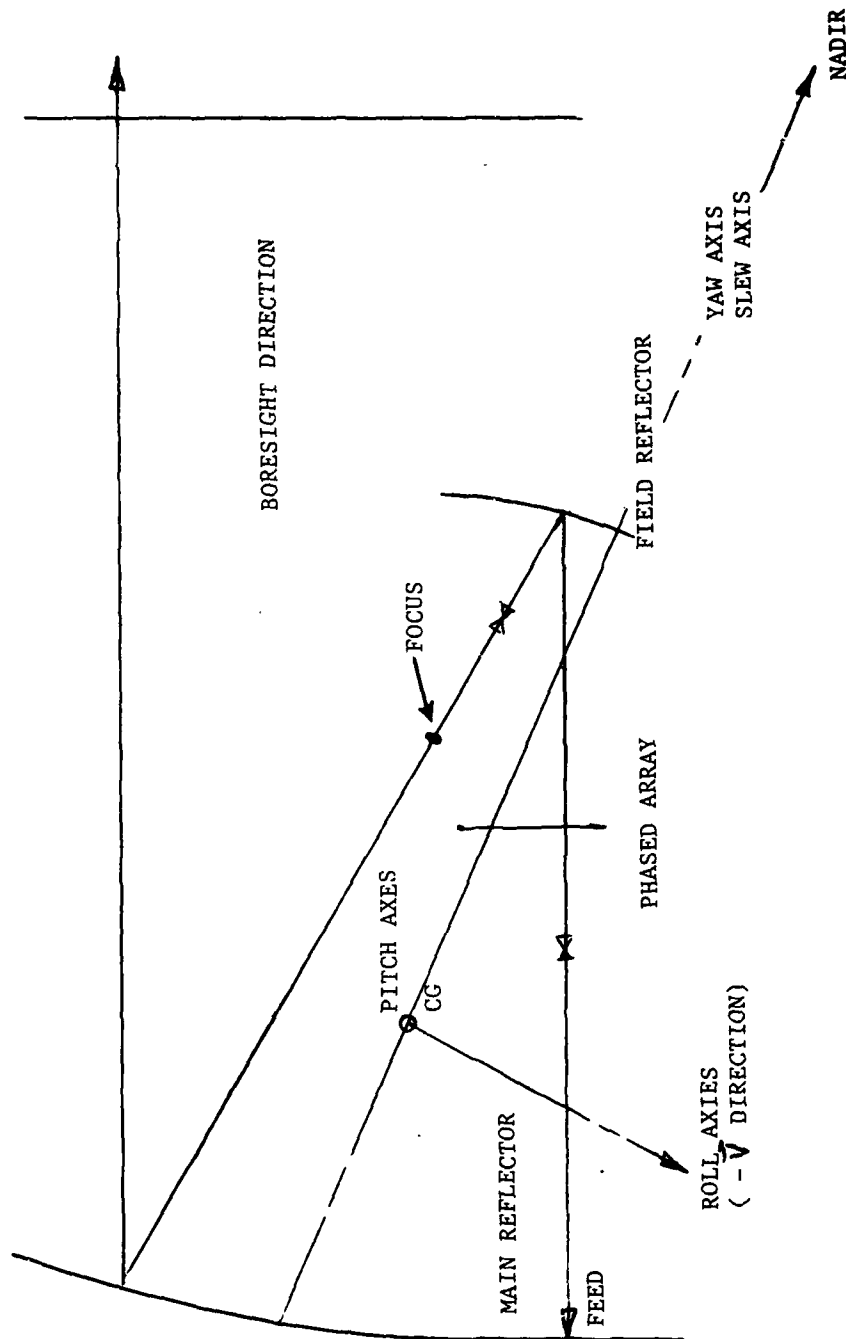
Figure 3.2-8 RADAR ANTENNA AXES AND ORIENTATION

175

Table 3.2-3 Radar Antenna Size and Weight (LEO)

Main Reflector

  Diameter = 70M (227.5 ft.)
  Depth = 16.2 ft.
  Weight = 2850 lbs.

Structural Platform Weight = 600 lbs.

Feed Weight = 100 lbs.

S/C Weight = 3000 lbs.

Phased Array

  Diameter = 28M (91 ft.)
  Depth = 7.6 ft.
  Weight = 1150 lbs.

Field Reflector

  Diameter = 28M (91 ft.)
  Depth = 6.6 ft.
  Weight = 900 lbs.

Astromast and Cannister (4)

  Length = 350 ft.
  Diameter = 2.0 ft.
  Weight (4) = 1050 lbs.

Solar Array (500 ft.^{2}) Weight = 500 lbs.

Gravity Gradient Boom Weight = 1350 lbs.

Summary: Total Weight = 11500 lbs.   Stowed Length = 36 ft.
           Single Orbiter

---

length is 14 ft which can be packaged with the 36 ft long S/C plus 5 ft long S/C and adapter for a total package length of 55 ft. The stage performances are shown in Table 3.2-2 for three modes of transport to 5000 n.mi. The combined manufacturing and orbital thermal distortion is summarized in Table 3.2-4.

Table 3.2-4 Thermal Distortion

Main Reflector RMS = 0.1 inch
Phased Array RMS = 0.06 inch
Field Reflector RMS = 0.06 inch

ΔL Between Field & Main = 0.12 inch
ΔH Between Field & Main = 0.17 inch

$\Delta \theta_1$ Between Field & Main = 0.0020
$\Delta \theta_2$ Between Field & Main = 0.0170
ΔL Between Phased Array & Main = 0.09 inch

ΔH Between Phased Array & Main = 0.14 inch
$\Delta \theta_1$ Between Phased Array & Main = 0.001°
$\Delta \theta_2$ Between PHased Array & Main = 0.013°

NOTE: ΔL = Distance Change Between Reflectors
$\Delta \theta_1$ = Torsion Rotation of Reflectors
$\Delta \theta_2$ = Canting Rotation of Reflectors
ΔH = Lateral Shift of Reflectors

3.2.4 Reflectarray LEO Radar Mission. The reflectarray LEO radar configuration is shown in Figure 3.2-9. The 91.4 m (300 ft) reflector has a graphite epoxy box truss structure which supports a reflectarray surface. The structure is thermally stable such that the required surface accuracy can be achieved without active control. The feed and S/C are supported utilizing four 2 ft. diameter graphite epoxy continuous longeron Astromasts. The two 6.25 KW solar arrays are located on the opposite ends of two of the feed support booms. However, they also could be attached to the S/C depending on the shadowing effects. The S/C body is assumed to be a 8 ft. diameter octagon structure by 5 ft. long weighing 3,000 lbs.

Table 3.2-5 presents a summary of the radar antenna size and weight. The total weight in 15370 lbs. and total length is 34.75 ft.

The packaged configuration in the Orbiter consisted of the truss and S/C stowed and supported in a cradle similar to that shown in Figure 3.2-1. The stage is independently supported in its own cradle to provide a determinant attachment to the orbiter.

The stage for transport to 5000 n.mi. is a short cryogenic stage utilized in mode 2 or 3 (see Table 3.2-2). Mode 1 is not acceptable since its payload capability is only 14750 lbs. The stage length is 14 ft. which can be packaged with the 34.75 ft. in the allowable 55 ft. of orbiter cargo bay.

177
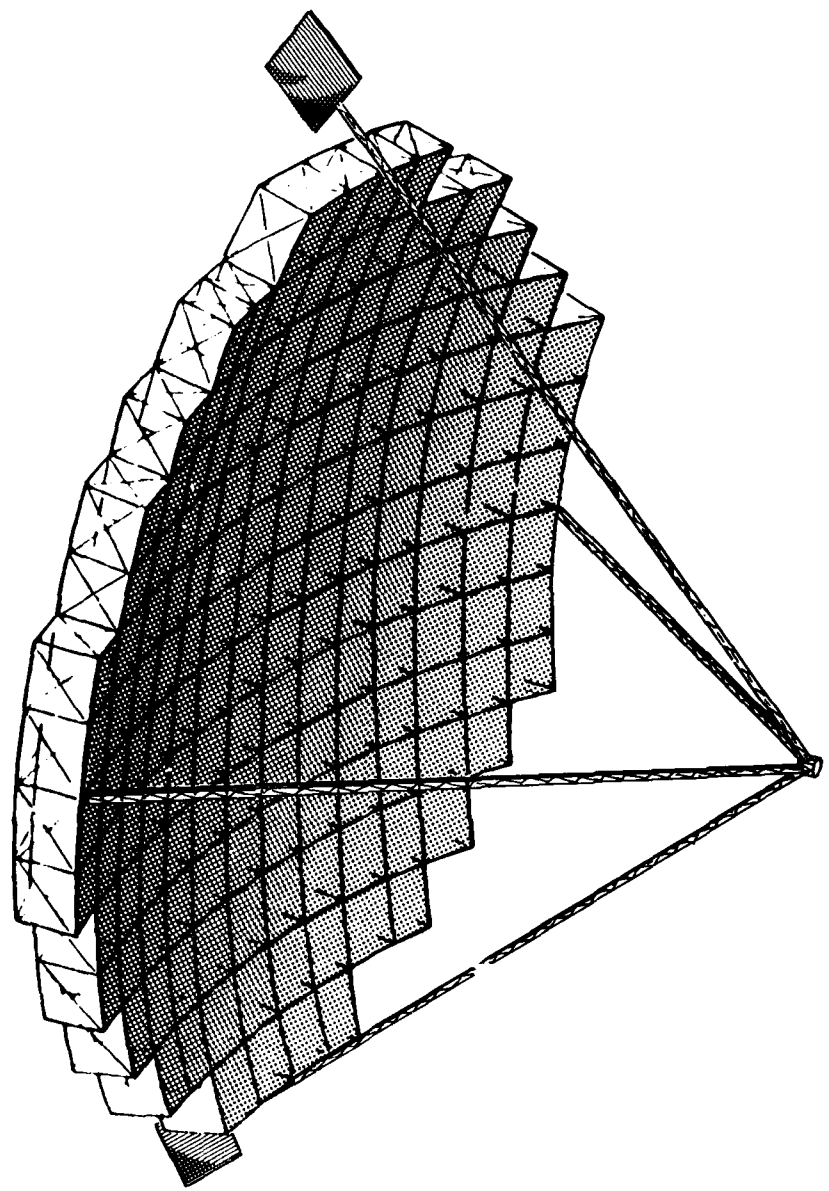
Figure 3.2-9   REFLECTARRAY LEO RADAR MISSION

178

Table 3.2-5 Reflectarray Size and Weight (LEO)

---

300 ft. Diameter - 16 bay (truss 18.75 ft. + 5 ft. surface)
- Structure (0.07 lbs/ft^2) = 5000 lbs.
- Phased Array (.07 lbs/ft^2) = 5000 lbs.

Astromast (4) (220 ft. long x 1 ft. dia.)
- Mast (0.5 lbs/ft) = 440 lbs.
- Canister (50 lbs/each) = 200 lbs.

Feed = 200 lbs.

S/C = 3000 lbs.

Solar Array 25 KW (2500 ft.^{2})

  Weight (30 watts/lb.) = 850 lbs.
  Cabling = 880 lbs.

Total S/C Weight = 15,370 lbs.

Total S/C Length = 34.75 ft.

Stage Length = 14.0 ft.

The combined manufacturing and orbital thermal distortion is summarized in Table 3.2-6.

Table 3.2-6 Thermal Distortion

Main Reflector RMS = 0.14 inch

Lateral Feed Shift = 0.08 inch

Feed Defocus = 0.10 inch

3.2.5 Two Reflector HEO Radar Mission. The two reflector HEO radar configuration is shown in Figure 3.2-10. The 305 m. (1000 ft.) diameter main reflector has a graphite epoxy box truss structure which supports a gold plated molybdenum wire tricot knit mesh. The mast, which is 350 m. (1150 ft.) long, must be both dynamically and thermally stable. Two mast designs were evaluated. The first was scaled up version of a continuous longeron Astromast which was 8 ft. in diameter. The properties of the mast are summarized in Table 3.2-7.

The second mast that was evaluated was a 50 ft. square deployable box truss beam. The primary advantage of a box truss beam is that the allowable diameter is 50 ft. while the Astromast is limited to the diameter of the

179
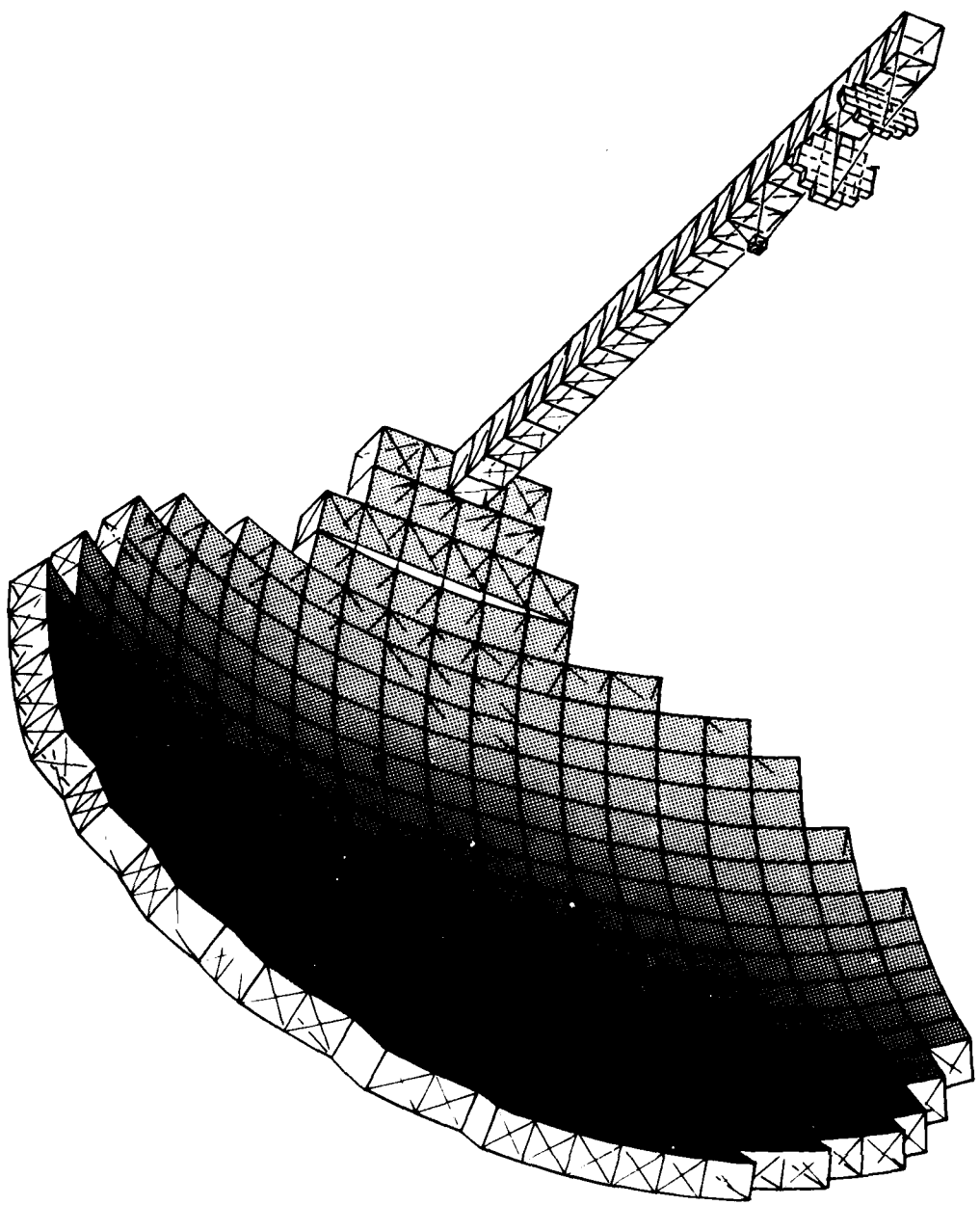
Figure 3.2-10   TWO REFLECTOR HEO RADAR MISSION

180

Orbiter cargo bay. The properties of the box truss mast are summarized in Table 3.2-8.

Table 3.2-7 Deployable Astromast Parameters

Stowed Envelope - 94 in. dia. by 110 in. long

Weight, lb. 1875

Length, ft. = 1150 (125:1 expansion)

Radius, in. = 47

Stiffness - EI, lb-in.^{2} = 2.3 x 10^{10}

Deployment Precision - Lateral, in. $\pm$ 3.2

Table 3.2-8 Deployable Box Truss Parameters

Stowed Envelope = 1.5 ft. x 9 ft. x 50 ft. long

Weight, lb. = 2875

Length, ft. = 1150

Section Dimensions, ft. = 50 x 50

Stiffness = EI, lb-in.^{2} = 9.0 x 10^{11}

Deployment Precision - Lateral, in. = $\pm$ 12

Deployed Operational Precision - Lateral, in. = $\pm$ 2.9

A comparison of the deployed stiffness shows that the box truss mast is 40 times stiffer than the Astromast while weighing only 1000 lbs. more. If the box truss was reduced in weight equivalent to the Astromast, the stiffness of the box truss beam would be 3.2 x 10^{11} lb-in.^{2} or 14 times as stiff.

The phased array and field reflector are both 100 ft. diameter six bay 16.5 ft. deep truss structures. They are attached to the beam at their edge and stabilized by four guylines. The S/C and feed are supported from a boom that is attached to the mast and stabilized by guylines. The size and weight summary is shown in Table 3.2-9.

The upper stage candidates are limited due to the large mass of this system. The only realistic transfer vehicle is a SEP stage which has the capability of payloads greater than 50000 lbs. (see Table 3.2-1). Referring to Figure 3.2-4, a 150 KW, 36000 lb. stage will transport to geosynchronous orbit in 425 days; while a 100 KW, 24000 lb. stage will transport to geosynchronous orbit in 575 days.

Table 3.2-9   Radar Antenna Size and Weight (HEO)

Main Reflector

  Diameter = 1000 ft.
  Truss = 50 ft.
  Weight = 31400 lbs.

Structural Platform Weight = 2000 lbs.

Feed Weight = 400 lbs.

S/C Weight = 5000 lbs.

Phased Array

  Diameter = 100 ft.
  Truss Depth = 16.5 ft.
  Weight = 500 lbs.

Field Reflector

  Diameter = 100 ft.
  Truss Depth = 16.5 ft.
  Weight = 400 lbs.

Box Truss Mast

  Length = 1150 ft.
  Diameter = 50 ft.
  Weight = 2875 lbs.

Solar Array (2000 ft.^{2}) Weight = 2000 lbs.

Gravity Gradient Boom Weight = 5425 lbs.

Summary: Total Weight = 50,000 lbs.   First Orbiter = Main Reflector
          Second Orbiter = Remainder of S/C   Third Orbiter = SEPS Stage

---

The combined manufacturing and orbital thermal distortion is summarized in Table 3.2-10.

Table 3.2-10   Thermal Distortion

Main Reflector RMS = 0.70 inch

Phased Array RSM = 0.06 inch

Field Reflector RMS = 0.06 inch

 L Between Field and Main = 0.3 inch

 H Between Field and Main = 14.9 inch*

L = Distance Change between Reflectors
H = Lateral Shift of Reflectors
* 12.0 inch Deployment Repeatability

4. TASK 3, SPECIFIC MISSION DESIGNS

4.1 Space-Based Radar, 5000 N.Mi. Orbit

4.1.1 RF System Design. The two-reflector system described in section 3.1 and sketched in Figures 3.1-27 and 28 is used for the radar antenna system, with some modifications. We have assumed a 70 meter primary reflector, which makes the field reflector and phased array feeds 28 meters in diameter or slightly larger. This means that all three components (primary reflector, field reflector, and array feed) must be spaced-deployable. The stepped-parabolic contour for the array feed shown in Figure 3.1-28 is more appropriate for an array of horns on a fixed substructure, and could not readily be space-deployed. We have changed the feed to a planar phased array with 0.6λ element spacing (dipole elements) for the radar mission. This can be done while still maintaining the basic properties of the system for beam scanning by changing the contour of the field reflector from a parabola to a contour that images the planar array onto the primary reflector surface. This contour can be computed. It is very close to a sphere (see Reference [5]). A space-fed lens-array was assumed for the feed. Its design would be essentially identical to the full-aperture array now being carried as the baseline system for the space-based radar mission. A crossection of the antenna layout is shown in figure 4.1-1. Figure 4.1-2 shows a perspective drawing of the antenna as realized using box truss structures for the elements of the antenna system.

The pattern data and steering range data presented in section 3.1 (Figures 3.1-30 through 39) were calculated under the assumption that the primary reflector diameter was 300λ. Applying this to our 70 meter reflector gives an operating frequency of 1.286 GHz. We have assumed this operating frequency, which is within the band of interest for the program, so the figures cited above apply directly to the mission design. The steering range curve (Figure 3.1-30) is repeated here as Figure 4.1-3 for convenience. The total number of active modules required for this array feed is approximately 30,000, or less than 1/4 the number required for the full-aperture phased array. Following the baseline design, the total radiated power should be around 4 kw average. This implies that each module must deliver around 130mw average RF power. We assume that uniform illumination would be used in the transmit mode for maximum efficiency and tapered illumination would be used in the receive mode for sidelobe control.

The scan range shown in figure 4.1-3 is 20° in the symmetric plane and 11° in the offset plane. This is not adequate for instantaneous full-earth visibility at a 5000 n.mi. oribt altitude, which has been taken as a mission requirement. This requires a scan range of around 40°. However, it is possible to define the mission so that the area of interest for surviellance on any given orbital pass is confined to a much smaller region than the whole visible earth. For example, a radar fence mission can be defined in this way. With this type of mission definition it is possible to orient the satellite attitude to boresight the center of the region of interest and then use the agile scan range shown in figure 4.1-3 to do the radar mission. Our structural and attitude control concept will allow a reorientation of the boresight with only a few minutes lost time for vibrational damping of the structure

183
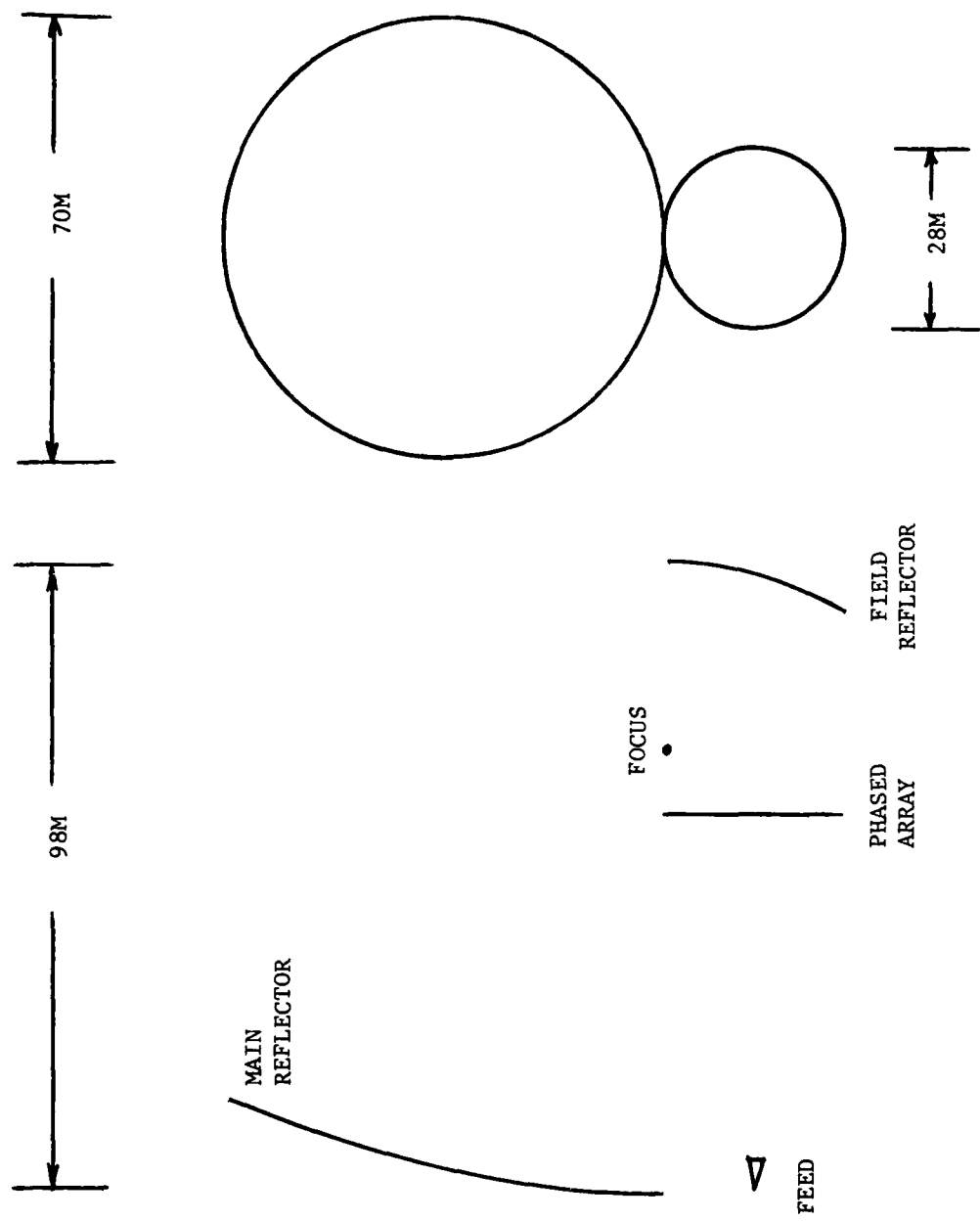
Figure 4.1-1   Radar Antenna Layout

184

SOLAR PANELS

GUYLINE STABILIZERS

FIELD REFLECTOR

PHASED ARRAY

ASTROMASTS

FEED

MAIN REFLECTOR
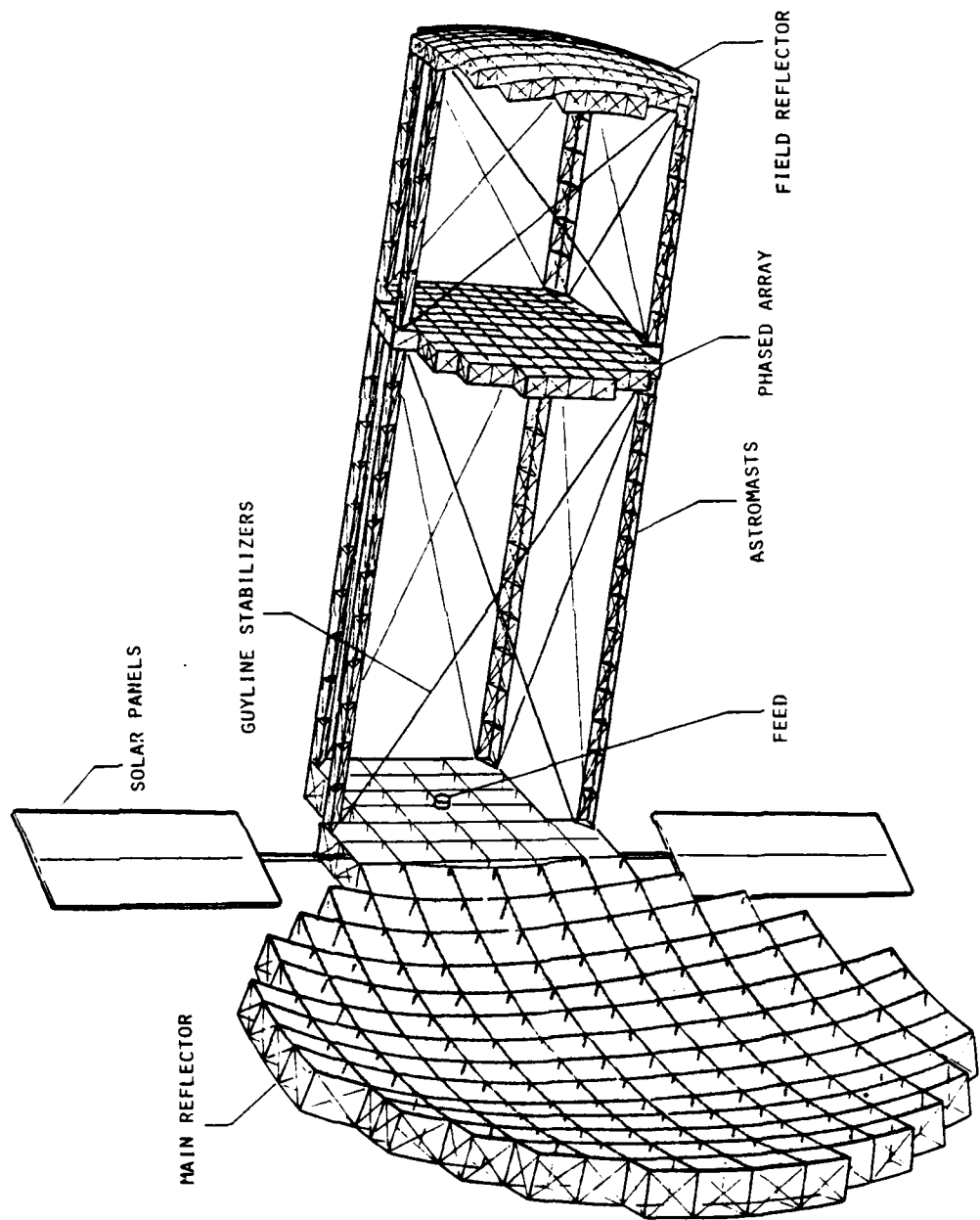
Figure 4.1-2   Radar Antenna

185

ON-AXIS BEAMWIDTH, 0.28°

GAIN LOSS,
DB

SYMMETRIC PLANE

OFFSET PLANE

BEAMWIDTHS SCANNED

DEGREES SCANNED
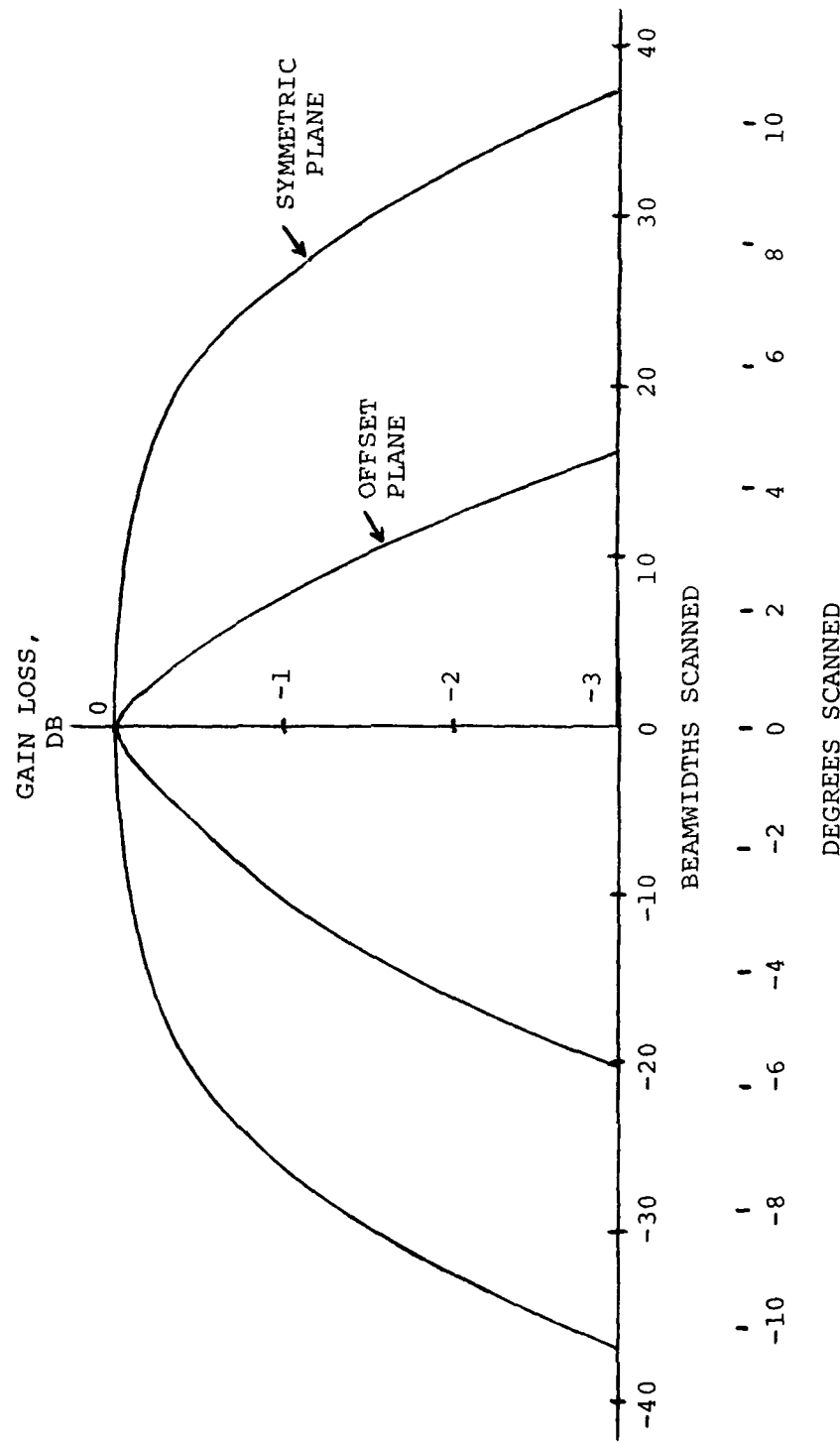
Figure 4.1-3   Scanning Range, Radar Antenna
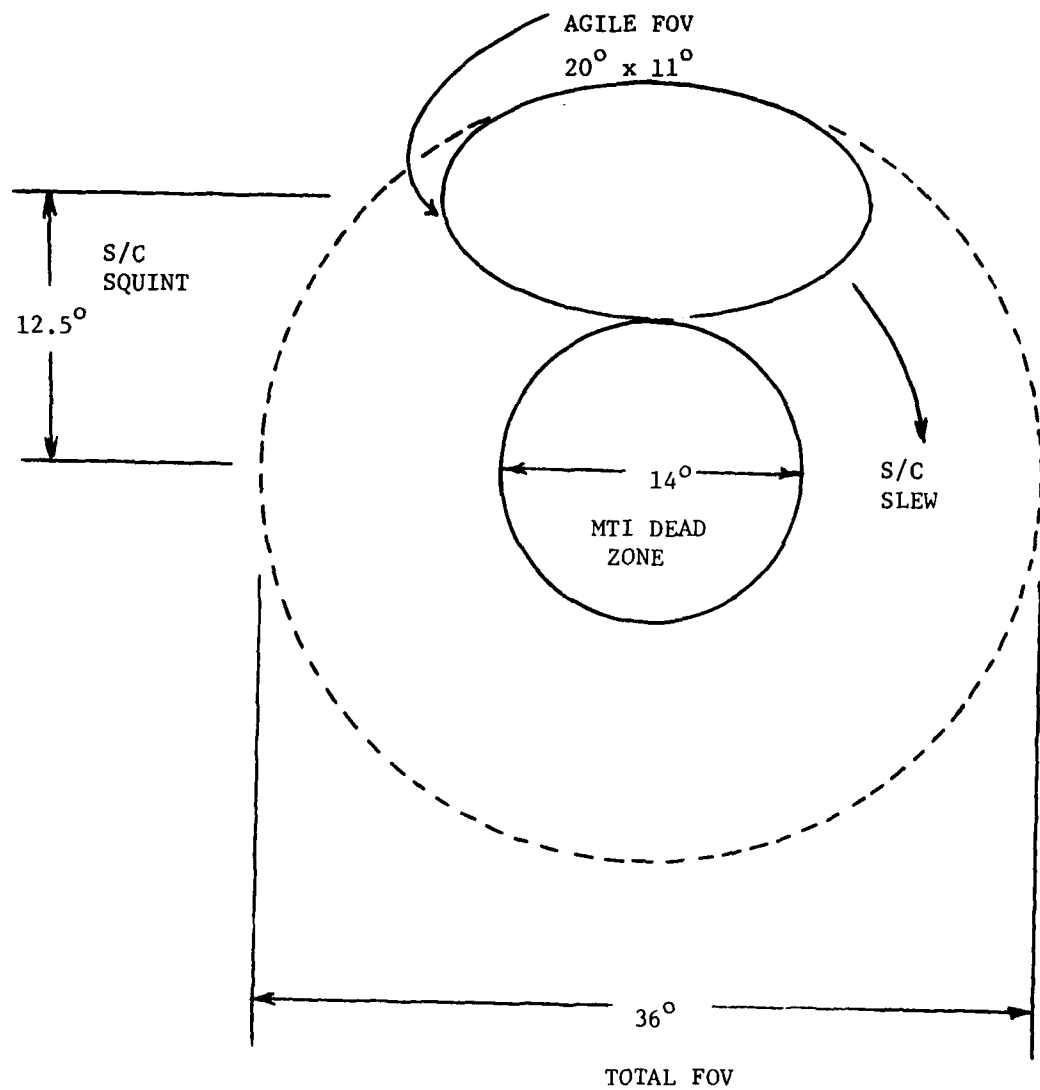
Figure 4.1-4   Coverage Plot, Space-Based Radar, 5000 n.mi.
                 Orbit

down to levels acceptable for its use as an antenna.

Our coverage approach can be explained by referring to figure 4.1-4. The MTI radar has a nadir blind spot of around 14° diameter. This blind spot exists for any MTI radar regardless of the type of antenna it uses, so there is nothing to be gained by providing coverage in this region. Our 11° x 20° agile beam steering zone is squinted away from nadir by 12.5° so that it falls wholly outside the blind spot. It can be moved to anywhere in the annular region bounded by the 14° and 36° circles centered on nadir by rotating the vehicle about the nadir axis. This gives coverage of the complete area of interest by a combination of electronic and mechanical steering. The 12.5° squint away from nadir places the antenna structure in an attitude that is very close to its natural gravity-gradient orientation. This is used to advantage in the attitude control system, described in section 4.1.3.

The anticipated manufacturing and thermal distortions for the antenna structure are quite small relative to an RF wavelength. This is discussed in section 2.2.4. There should be no need for an adaptive figure control system. It would be desirable to make an initial post-deployment check of the system as a receiver using a cooperating ground-based emitter for illumination of the antenna. It would be possible to adjust for distortions if necessary by adjusting the phase settings at the individual modules as discussed in Section 3.1.32.

4.1.2   Truss Blockage. One major concern associated with the use of a truss structure for a space-fed lens-array is blockage of the feed radiation falling on the back array by the truss structure. This assumes that a single membrane is used, containing both the back and the front array and mounted on the front surface of the truss. This blockage occurs for a full-aperture array and would also occur in the space-fed feed array used in our two-reflector design.

A typical truss design uses a 25 ft. deep truss, with the array on standoffs 2.5 ft. in front of the truss. The tubular truss members are 2.5 inches in diameter and are composed of graphite-epoxy. We have found from measurements that for the purpose of direct blockage loss, graphite-epoxy is essentially the same as metal. We have used this assumption in our calculations.

An example calculation was made assuming the full-aperture space-fed array shown in figure 4.1-5 which has an aperture diameter of 225 ft. and a focal length 577.5 ft. Results would be nearly the same for the radar antenna shown in figure 4.1-2, which uses a space-fed array feed.

The elements of the top plane of the truss cast one set of shadows on the array back surface and those on the bottom plane cast another set of shadows which don't exactly coincide with the shadow from the top plane. The shadows were computed assuming a wavelength of 1 ft. An example for one of the top plane elements is shown in figure 4.1-6. It is around 15" wide and the field strength at its center only 1.5% below the unperturbed level. The shadow from the bottom plane are similar to this. This is the shadow for parallel(to the truss member) polarization. The shadow for cross-

188

MAXIMUM FEED
MOVEMENT, 2'.

550'

225'
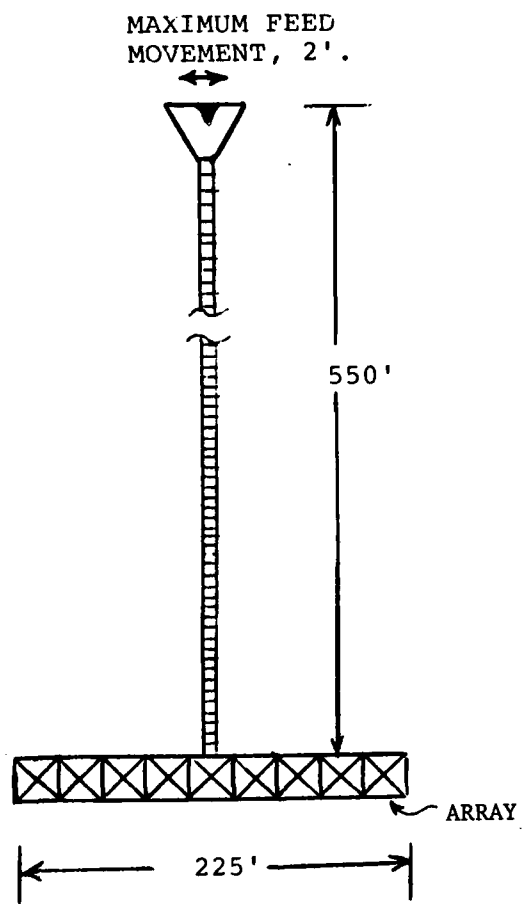
ARRAY

Figure 4.1-5   Space-Fed Array With Truss Blockage
Of Array Back Surface

189

WORST-CASE GRATING LOBES DUE TO SHADOWING, -64 dB.

SHADOW
DOUBLET
PATTERN

SHADOW,   SHADOW
2.5" TUBE   SHIFTED 1.2"

1.000
FIELD
STRENGTH

0.985

DIPOLE
LOCATIONS
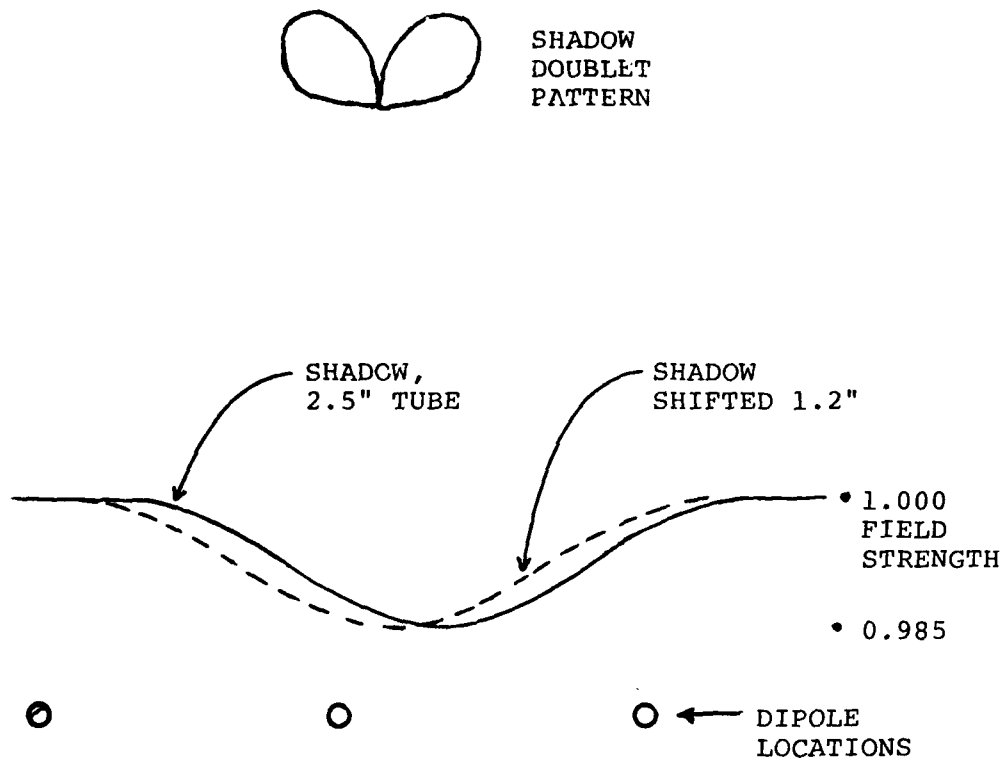
Figure 4.1-6   Truss Blockage Effects On Array Performance

polarization is much weaker.

These shadows are very nearly equi-spaced so they would form grating lobes rather than random lobes. If no corrections were made for them, the grating lobes would be around 20 dB below the antenna main lobe, which is unacceptably high. Our approach would be to determine the location and depth of these shadows on the back array and adjust the gain of the affected modules to compensate for the lower illumination of the back elements. The resulting distribution on the array front face would ideally be free of distortion. The errors in this correction would occur due to distortions in the feed support tower due to thermal effects and deployment errors. This would move the shadows away from their nominal location and cause the adjusted module gains to be incorrect. This effect is sketched in figure 4.1-6. A very conservative worst-case estimate for the feed location error in the configuration sketched in figure 4.1-5 is 2 ft. This will move the shadows due to the top plane members by 1.2". Movement of the shadows due to the bottom plane elements would be negligibly small. As shown in figure 4.1-6, 1 or 2 modules on the side of the nominal shadow center in the direction of the shadow movement will have reduced signal while those on the other side will have increased signal. This gives a plus/minus doublet relative to the nominal illumination, which generates a difference pattern having a null on axis and peaks around $\pm 45°$ off-axis as sketched in figure 4.1-6. This is the element pattern of the shadow array which is multiplied by the array grating lobe pattern to get the composite radiation pattern of the shadow array. The resulting lobes will be vanishingly small close to the antenna boresight and will rise to their peak levels at the element peak gain region $\pm 45°$ from boresight. The peak value of these lobes for the 1.2" shadow shift was computed to be 64 db below the antenna main beam gain. This is a negiligble value, so the shadowing problem can be solved by our proposed approach.

4.1.3   Stability, Pointing and Control.   The radar antenna will employ a system consisting of sensors, controllers and on-board processing to stabilize the antenna as a flexible body while pointing its boresight axis in the direction of the target area in the presence of disturbing torques.

The requirements which the assumed mission imposes upon the Stability Pointing and Control System are as follows.

4.1.3.1   Requirements:

Lifetime: 5 years

Weight and Power: Not Critical

Knowledge of Position In Space: ± 0.1 nm

Knowledge of Boresight Direction: $\pm .02°$, 1σ

Slewing: $\pm 10°$ to $15°$, cross-track

Surface Control: Not required

Feed Position Control: Not required

The operational orbit is assumed to be 5000 nm altitude, circular, inclined 70°. In the nominal case the antenna will fly with it's yaw axis along the nadir, as depicted in figure 4.1-7 , and it's bore sight direction (which lies in the plane formed by the yaw roll axis) squinted ahead of the yaw axis in the orbital plane by 12.5°. The antenna could be called upon to slew it's bore sight direction out of the orbital plane by as much as 15° in order to cover the required target search area.

4.1.3.2 Sensors. To achieve the required pointing accuracy of .02° necessitates the use of a star tracker mounted on rigid structure of the radar antenna. Other types of attitude sensing instrumentation are not applicable, either due to accuracy considerations, (horizon sensors and solar aspect angle sensors) or lack of sufficient radar antenna motion to support a scanning operation (star scanners).

Although the star tracker itself can be expected to be accurate enough to achieve the requiement (for instance, the NASA Standard Tracker made by BBRC is accurate to within 10 sec of arc, 1σ in each axis) there will be other large errors. These errors will be due to: (1) incertanties in the mounting of the tracker to the antenna structure; (2) uncertanties in the attitude of that particular piece of structure with respect to the theoretical boresight direction of the antenna; (3) differences between the actual and theoretical boresight direction. These errors could be expected to accure to a magnitude of one degree or so, and will vary under changing thermal conditions. They can be eliminated thru an inflight calibration procedure wherein the radar antenna is locked to a known target from a known position in space while a stellar fix is performed. Beam pointing would then be corrected electronically using the capabilities of the phased array feed.

The star tracker must be augmented by a 3 axis attitude reference system for short term attitude memory between stellar fixes. This requirement can be satisfied by employing the gyro package associated with the IRU (Inertial Reference Unit) which can be assumed to be on board by virtue of the fact that it's use was necessary to provide the navigational data for the boost phase of the mission; i.e. the orbital transfer from the Orbiter's low earth orbit to the radar antenna's 5000 NM orbit.

The radar antenna's mission requirement of knowledge of it's own position in inertial space to within .1 NM can be achieved by incorporating the DOD version of the GPS receiver into the radar antenna's compliment of airborne equipment. This will provide position information accurate to within 12 meters.

4.1.3.3   Controllers. Stabilization and pointing along the Nadir can be achieved by the gravity gradient method augmented by momentum wheels. The principal axis along which the satellite would stabilize (i.e., the axis of greatest moment of inertia) could be fixed by adjusting the location

192

ANTENNA BORESIGHT

MAIN REFLECTOR

FOCUS

C.G.

PHASED ARRAY

YAW AXIS

12.50

NADIR

FIELD REFLECTOR

ROLL AXIS

ARRAY FEED
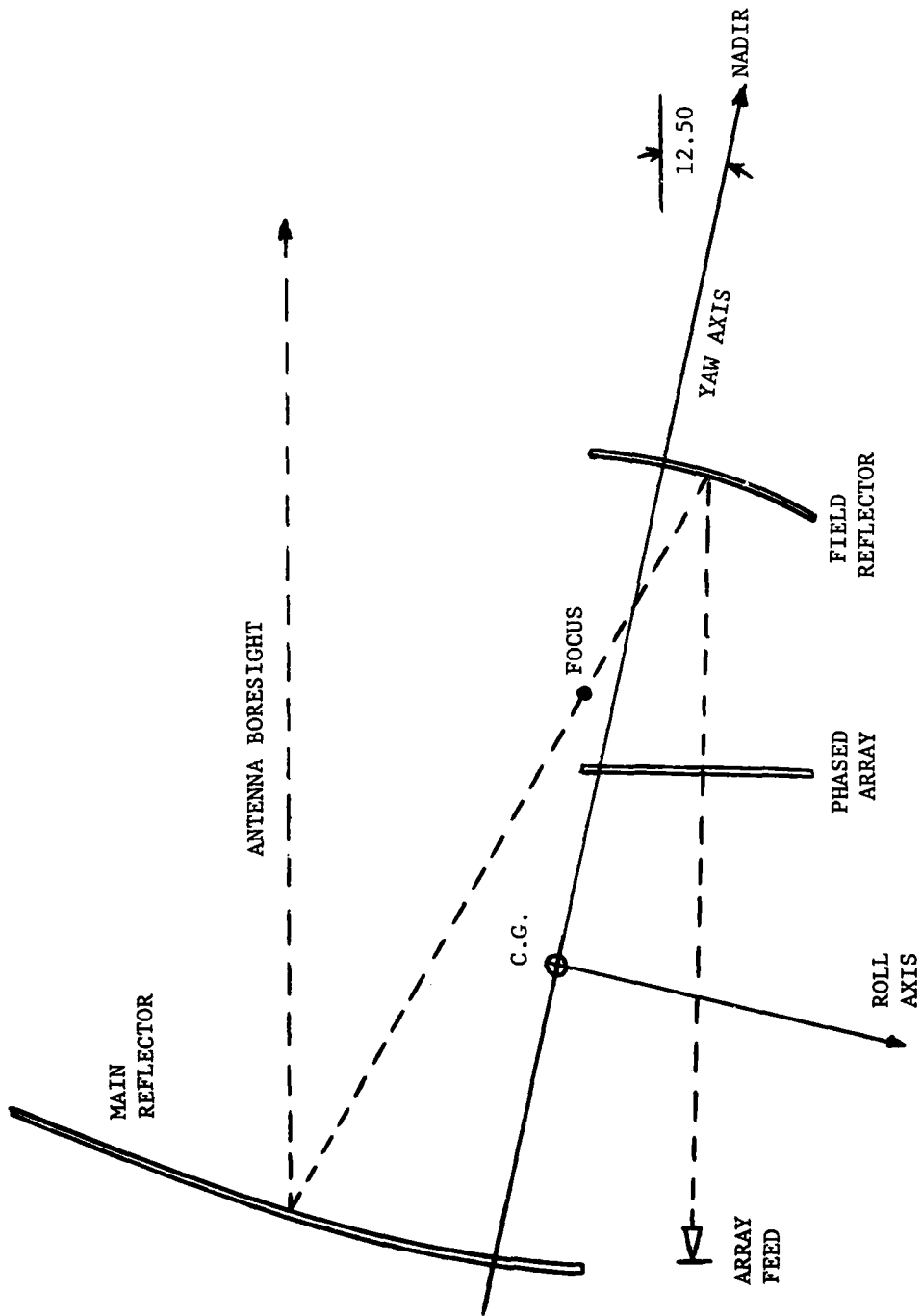
Figure 4.1-7   RADAR ATNENNA PRINCIPAL AXES

193

of masses such as the central spacecraft body so that it gives the desired 12.5° forward squint to the antenna boresight. However, due to the low ratios of the moments of inertia about the 3 principal axes, gravity gradient stabilization will be marginal with the present antenna configuration. This situation can be alleviated by moving the solar arrays from the location shown in figure 4.1-2 to a location where they constitute the tip weight on the end of a gimballed boom several hundred feet long extended out the yaw axis of the antenna.

Since gravity gradient stabilization alone will not provide the pointing accuracy required, due to the undamped nature of the oscillation about the vertical, characteristic of gg oriented space vehicles, the system must be augmented by semi passive control moment gyros, active control moment gyro's or reaction wheels. The long boom with it's tip mass, mentioned above, is also a part of the gg stabilization system. In fact, by using the gimballed boom, momentum wheel combination in what is called the gravity anchor configuration we may be able to greatly reduce if not eliminated the need for attitude control reaction jets to keep the momentum wheels from saturating. In this configuration the boom is suspended as an attitude anchor in the gravity field. The boom is gimballed about two axis and torqueable enabling the antenna to torque against the boom. Pitch and roll momentum wheels effectively damp out the libration (gg oscillation). Other disturbing torques (e.g. solar pressure) will be present and can also be eliminated by torquing against the gravitational field as described above. This controller system will be realtively reliable and long lived, requiring little if any attitude control propellant. However, to expect .02° pointing accuracy from it is pushing the state of the art. Considerable analysis and design, concentrating on the selection of the type of momentum wheels and their mechanical and electrical characteristics must be undertaken to achieve it. A preferable approach would be to relax the physical pointing accuracy requirement (but not the pointing knowledge), and make the boresight corrections electronically, using the phased array feed.

Additional problems exists due to the requirement to slew the antenna away from nadir. However, since the boresight direction of the antenna is offset from the yaw axis of the antenna by about 12.5° the slewing requirement can be met by rotating the antenna about it's yaw axis which is the nadir direction. In this case the controller system described above will suffice.

4.1.4   Structural Design. The structural design of the 5000 n.mi. orbit radar system (see Figure 4.1-2) consists of two box truss/gold plated molybdenum wire tricot knit mesh reflectors and a box truss/phased array lens connected by Astromasts and guyline stabilizers. A box truss support platform is provided which is an integral part of the main reflector and supports the feed, spacecraft, solar arrays, and provides the attachment points for the Astromasts.

The main reflector is 227.5 ft diameter and is constructed of 19 ft box trusses twelve across the diameter. The platform also has 28- 19 ft box trusses. The total weight of the main reflector and platform is 3450 lbs. The truss structure is fabricated utilizing graphite epoxy tubular and tape

194

material. Graphite epoxy was selected to minimize the weight and operational thermal distortions while maximizing the stiffness of the deployed structure. Typical tubular members are 2.0 inch diameter by 0.020 inch thick and typical diagonal tape truss members are 1" wide by 0.030 inch thick.

The phased array lens is 91ft diameter and is constructed of 7.6 ft box trusses, twelve across the diameter. It was assumed that the phased array surface weighed 0.05 lbs/ft for a total weight of 330 lbs.   The truss structure has a weight of 0.12 lbs/ft for a total weight of 820 lbs. The pahsed array lens also utilizes graphite epoxy.

The field reflector is a 91 ft diameter deployable box truss with a gold plated tricot knit mesh. The field reflector truss structure is identical to the phased array structure except the truss is formed into a curved reflector. The structure weight is 820 lbs while the mesh weight is 80 lbs. The field reflector also utilizes graphite epoxy.

The Astromasts are 2.0 ft diameter continuous longeron lattice masts. These masts are automatically deployable utilizing the strain energy of the coiled longerons Because the masts are extremely flexible in bending, guyline stabilizes are provided to increase both the torsional and bending structural modes of the overall system. The combination of the Astromasts and the guyline stabilizers provide a stiff and thermally stable structure for connecting the reflectors and phased array.

The steps of deployment after achieving the shuttle orbit are:

1 - Deploy Astromasts Simultaneously
(The masts are sufficiently strong and stiff to resist any forces produced by subsequent truss deployments).

2 - Deploy the three box structures simultaneously in the pitch axis box direction.

3 - Deploy the three box structure simultaneously in the roll axis direction (See Figure 4.1-7)

4 - Tension guyline stabilizers.

4.2   Space-Based Radar, Synchoronous Orbit

4.2.1   System Design. The basic antenna system is similar to that used in the 5000 mi. orbit system and shown in Figures 4.1-1 and -2 except that the primary reflector is scaled in size by a factor of 4.35, giving a primary reflector diameter of 1000 ft. The system would be designed to give a beam scanning range of approximately $4^{\circ} \times 7^{\circ}$. The attitude control system would also be similar to that described for the 5000 mi. orbit system, with the boresight squinted away from nadir by gravity-gradient stabilization to miss the MTI dead zone and the vehicle slewed about nadir to cover the annular region surrounding the MTI dead zone. The coverage plot is shown in Figure 4.2-1. The outer scan limits just cover the 17° earth disc. This requires a boresight squint of 6.5° rather than the 12.5° squint used for the 5000 mi orbit vehicle. This can be accomplished by suitable rearrangement of the vehicle masses to place the principal axis 6.5° away from the antenna boresight.

We estimate that, for this limited scan angle requirment, the antenna magnification factor M could be increased to 10, giving the configuration shown in Figure 4.2-2. The total number of array active modules and the total radiated RF power requirement would remain approximately the same as in the 5000 mi. design.

The system design for the synchronous orbit mission was given a relatively low priority in the expenditure of the limited program funds, so no patterns were computed for the M = 10 case. The sidelobe performance near the scan limits should be about the same as shown for the M = 2.5 case near its scan limit.

The worst-case RMS surface distortion of the 1000 ft. primary reflector is estimated to be on the order of 0.7" or around $\lambda/15$. (See the discussion in section 2.2.4) This level of distortion can readily be corrected electronically or could even be neglected. Another concern is the deployment and thermal errors in the truss mast that is used to position the feed and field reflector relative to the primary reflector. Lateral displacement of this assembly from its nominal location in deployment is estimated to be 12" worst case. Thermal distortion is estimated at 3" maximum. Axial (length) distortion is very small, 0.5" or less. The lateral displacement will cause a worst-case beam pointing error of 0.08°. This may be an acceptable error for the mission. If not, it could be calibrated out or adjusted mechanically by using some kind of an optical surveying system to measure the angular departure of the feed from the primary reflector principal axis. This could be a one-time correction, just to remove the initial deployment errors.

4.2.2   Structural Design. The geosynchronous orbit radar configuration (shown in Figure 3.2-10) consists of a large 1000 ft. diameter main reflector, 100 ft diameter field reflector, 100 ft diameter phased array, gravity gradient boom, feed spacecraft and a 1150 ft long boom connecting the major subsystems. The total system weight is 50,000 lbs.

The main reflector consists of a deployable box truss structure with a gold plated molybdenum wire tricot knit reflective mesh. The box truss structure is 20 bay 50 ft deep and fabricated from graphite epoxy for high

196
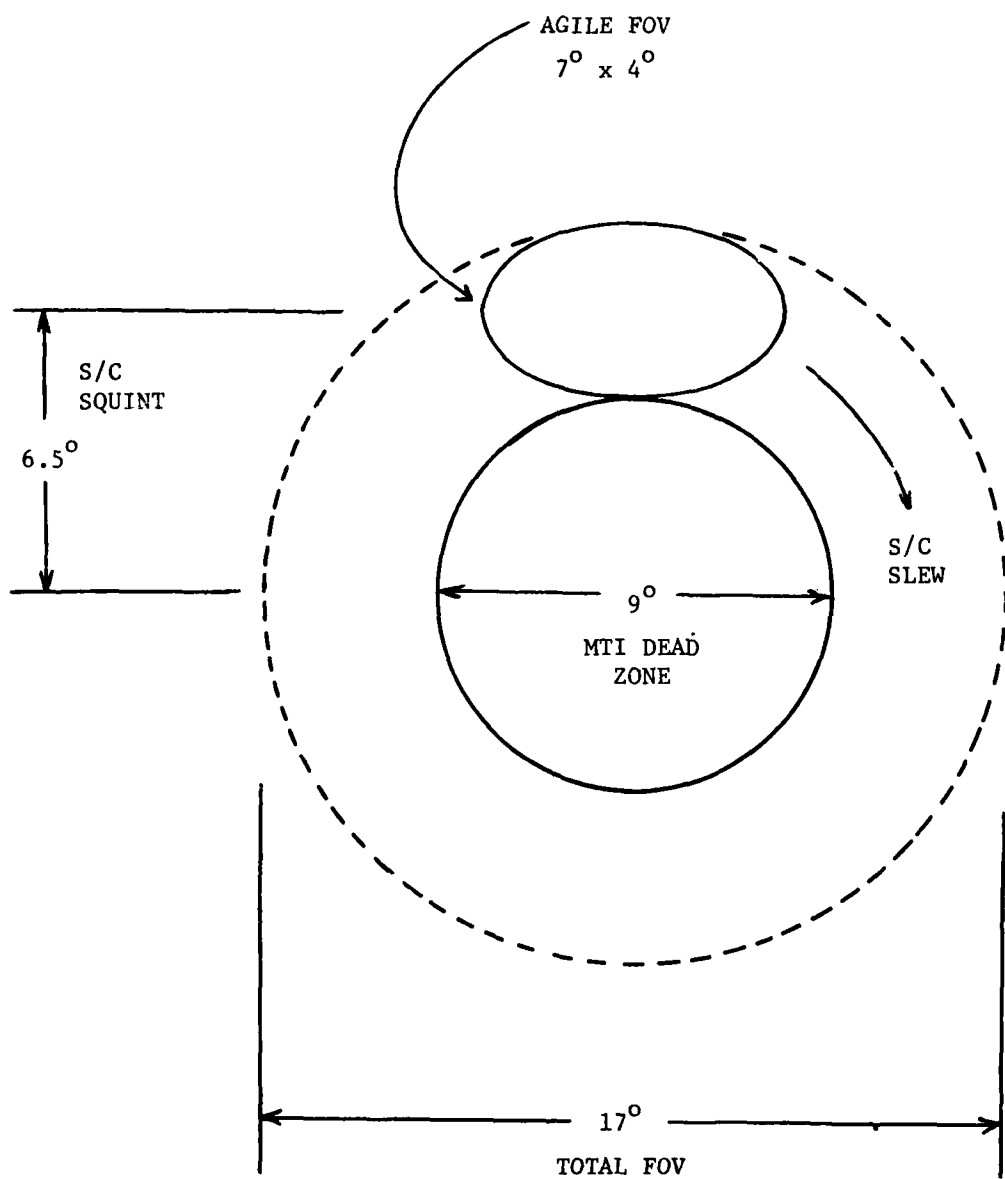
Figure 4.2-1   Coverage Plot, Space-Based Radar, Synchronous Orbit
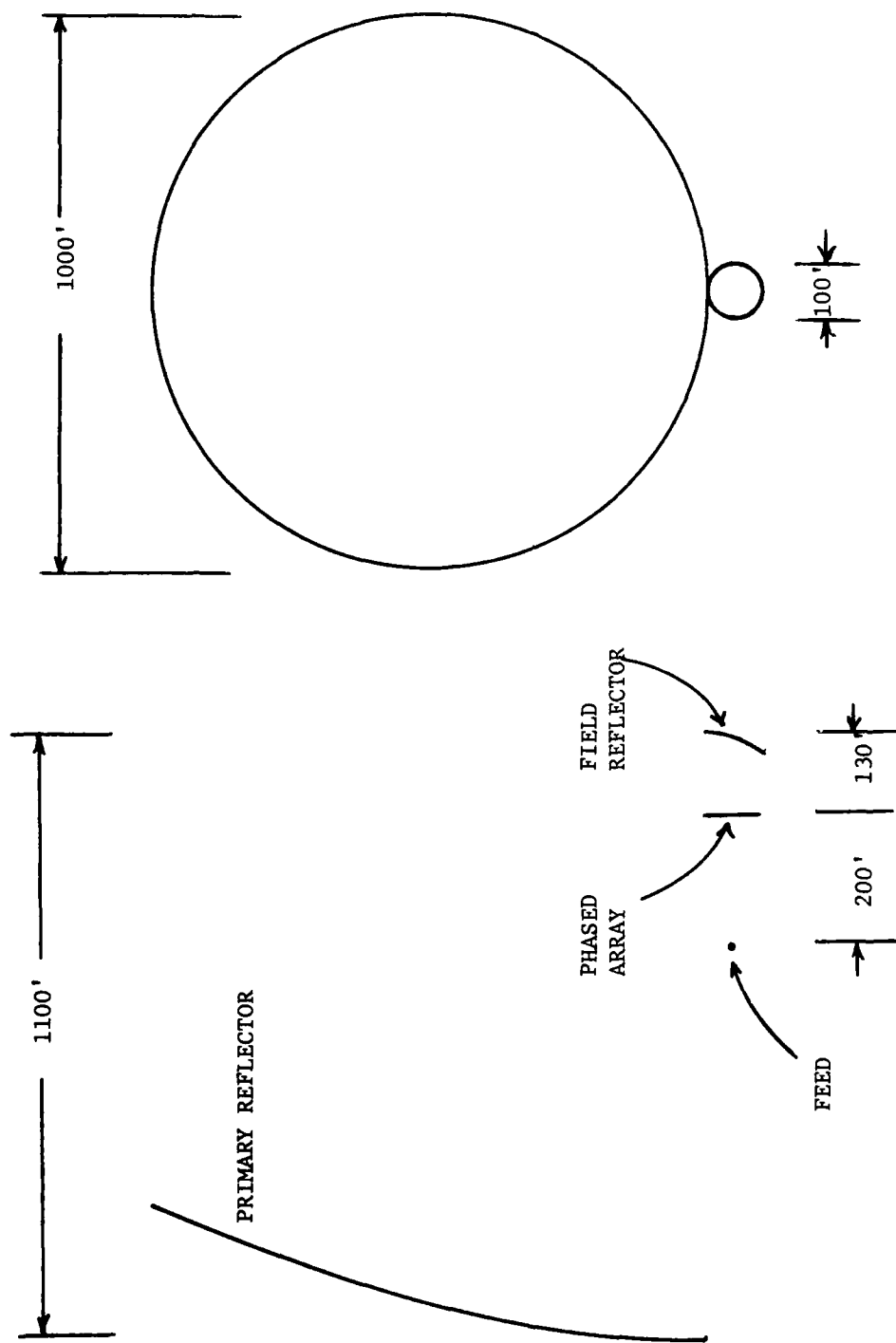
Figure 4.2-2.   Two-Reflector Antenna, Space-Based Radar, Synchronous Orbit

198

stiffness, low weight and low thermal distortion. The structural platform which is the attachment support for the mast is an integral part of the main reflector box truss structure. The stowed main reflector and platform occupy the total volume of one orbiter and weigh 33,000 lbs. The remaining subsystems (mast, S/C, feed, phased array, field reflector) are brought up in a second orbiter.

The phased array and field reflector are both 100 ft diameter systems with a box truss graphite epoxy structure. They are attached to the support mast and stabilized by guylines. The box truss structures are a 6 bay 16.5 ft deep truss. The feed and S/C are supported from the mast in a similar manner (see Figure 3.2-10).

The mast system requires a light weight, high stiffness, thermally stable structure that packages very efficiently. Two systems are potential candidates, Astromast and box truss beam. The Astromast was not selected due to the fact that the Astromast is orbiter packaging limited to 15 ft diameter while the box truss goes to 50 ft. Maximum diameter is required to achieve maximum deployed stiffness. The gravity gradient boom is also a box truss mast of approximately 3000 ft long.

A third orbiter is required to bring up the propulsion stage required for transfer to geosynchromous oribt. A SEPS stage has been selected to minimize propellant weight and to provide the low thrust required by the very large deployed structure.

The assembly process consists of:

1 - Deploy the main reflector.
2 - Rendezvous and dock second orbiter and attach stowed mass.
3 - Initiate deployment of mast while attached to orbiter.
4 - At appropriate bay, deploy field reflector and attach to mast.
5 - Continue deploying mast and at appropriate bay, deploy phased
    array and attach to mast.
6 - Continue deploying mast and at appropriate bay, attach S/C and feed.
7 - Complete mast deployment.
8 - Attach gravity gradient boom and deploy.
9 - Bring up and attach SEPS stage.
10 - Transfer to geosynchronous orbit.

4.3 Millimeter Wave Mapping Radiometer (MWR) Mission

4.3.1 Summary. The primary objective of the MWR mission is to map land areas with sufficient detail to detect construction activity, aircraft on the ground, and military vehicles such as tanks and trucks. Secondary missions include the location of ships and aircraft in flight. A bonus mission would be the detection of any emitters in the frequency band being used by the radiometer. The MWR is capable of penetrating cloud cover, and this is its principal advantage over visible and IR mappers. Compared to radar mappers it derives some advantages (both political and operational)from being passive and it has some anti-jamming advantage over typical radars because of its large bandwidth.

This is a very difficult mission to realize. The resolution requirements force a large aperture size (much larger than that of a SAR) even at low orbit. Minimum orbit height is fixed by atmospheric drag considerations. The high operating frequency imposes a severe surface figure requirement on the reflector. This in turn imposes the requirement for a high-quality adaptive figure control system for the reflectors. The mesh reflectors used at microwave frequencies cannot be used. Continuous panel or membrane reflectors must be used. Another major problem is the achievement of a very wide field-of-view (FOV) for the reflector system in order to do the mapping in an efficient manner. The large diameter/high surface figure requirement is the driving technology requirement for this mission. However, it is considered to be a feasible (though expensive) mission using current and near-term technology.

4.3.2 Mission Constraints. The sensitivity requirement for the mission is fixed by the requirement to detect military vehicles such as tanks. Other targets of interest require less sensitivity. The three system variables that impact the sensitivity are operating frequency, aperture size, and orbit altitude. Frequency selection options are confined to the atmospheric windows centered on 35 GHz, 95 GHz, 140 GHz, and higher bands. The 95 GHz band is the preferred choice. It is a relatively wide window and is less sensitive to clouds and weather effects than the higher bands. It allows the use of a substantially smaller antenna than would be required at 35 GHz. The minimum orbit altitude is fixed by atmospheric drag considerations at around 400 n.mi.

The FOV specification for the mission is impacted by the desire to map a relatively wide swath with one pass. This is bounded mainly by system complexity constraints such as number of receivers and downlink data rates.

There are two general ways to carry out a mapping mission. The simplest of these is the "pushbroom" mode, in which the mapping antenna is pointed to nadir and sweeps out a swath along the orbit track. The antenna provides a linear array of contiguous beams normal to the orbit track across the swath. In the "spotlight" mode, the vehicle is tasked to map certain specific areas that are not necessarily in the orbit track, though they cannot be too far away from it because of the foot-print-spreading effect given by an oblique look angle. This gives it considerably more flexibility than the pushbroom mode. In the pushbroom mode, dwell time is fixed by the footprint size and

the orbit velocity. The spotlight mode does not have this limitation and can control dwell time by nodding the antenna. The antenna design is similar for both systems but the pushbroom mode maintains a fixed nadir pointing of the antenna while the spotlight mode requires capability for frequent antenna attitude changes. We have assumed the pushbroom mode for our design. The spotlight mode would take considerably more attitude control and slew rate capability. It also raises the question of the damping time of the vibrational modes introduced by the frequent attitude changes. This could be a major concern for the very large structure required for the antenna system.

4.3.3   Antenna Design. The three performance factors that drive the antenna design for the mm wave mission are sensitivity, resolution, and field of view (FOV). Sensitivity requirements determine the effective aperture area and resolution determines the dimensions of the antenna system. These two are of course tied together if the primary aperture is a single reflector. A sparse array can be considered if the resolution requirement dictates a larger aperture than the sensitivity requirement. However, there are ways to trade excess sensitivity for resolution, which will be discussed below. If these techniques are used, a filled aperture becomes more attractive for this mission than an unfilled or sparse aperture.

Several possible multiple-reflector antenna systems were considered for wide FOV performance. The best performance, by a wide margin, was given by a reflective Schmidt telescope. This system, diagrammed in Figure 4.3-1, consists of a spherical primary reflector and a spherical feed cluster at the focus. In front of this, at twice the focal length from the primary, is the corrector plate. This is nominally flat, with undulations designed to remove the aberrations from the spherical system.

A spot design was made for a 100 meter primary with a F/D of 1.5 operating at a wavelength of 3 mm. The classic corrector plate design described in handbooks only corrects aberations out to the 3rd order. This design was refined for higher-order aberrations (up to 11th order) until the RMS wavefront error at 3 mm was less than $\lambda/60$. This gives essentially the diffraction-limited gain for the aperture. Scanning performance was then investigated. Figure 4.3-2 shows scanning loss out to beyond 5000 beamwidths off-axis and Figures 4.3-3 through 6 show typical radiation patterns. FOV is a function of F/D. This relationship is shown in Figure 4.3-7. These results are all for uniform illumination of the primary aperture since this was the only way to exercise the computer program used to make the design. Scanning performance would be somewhat better, and sidelobes would be lower, if a tapered illumination were used. This would be investigated in a more detailed system design, but it need not be done for this first look at the system.

The selection of F/D of around 1.5 appears close to optimum. Longer systems would be harder to deploy, and a scan range of $\pm$ 5000 beamwidths appears to be as large as could reasonably be handled due to the complexity of the electronics required to utilize it. If employed in a conventional "pushbroom" mode, for example, it would require 10,000 receivers. The design could be scaled upward to a larger diameter for improved resolution and sensitivity. The FOV measured in beamwidths would remain the same but it

201
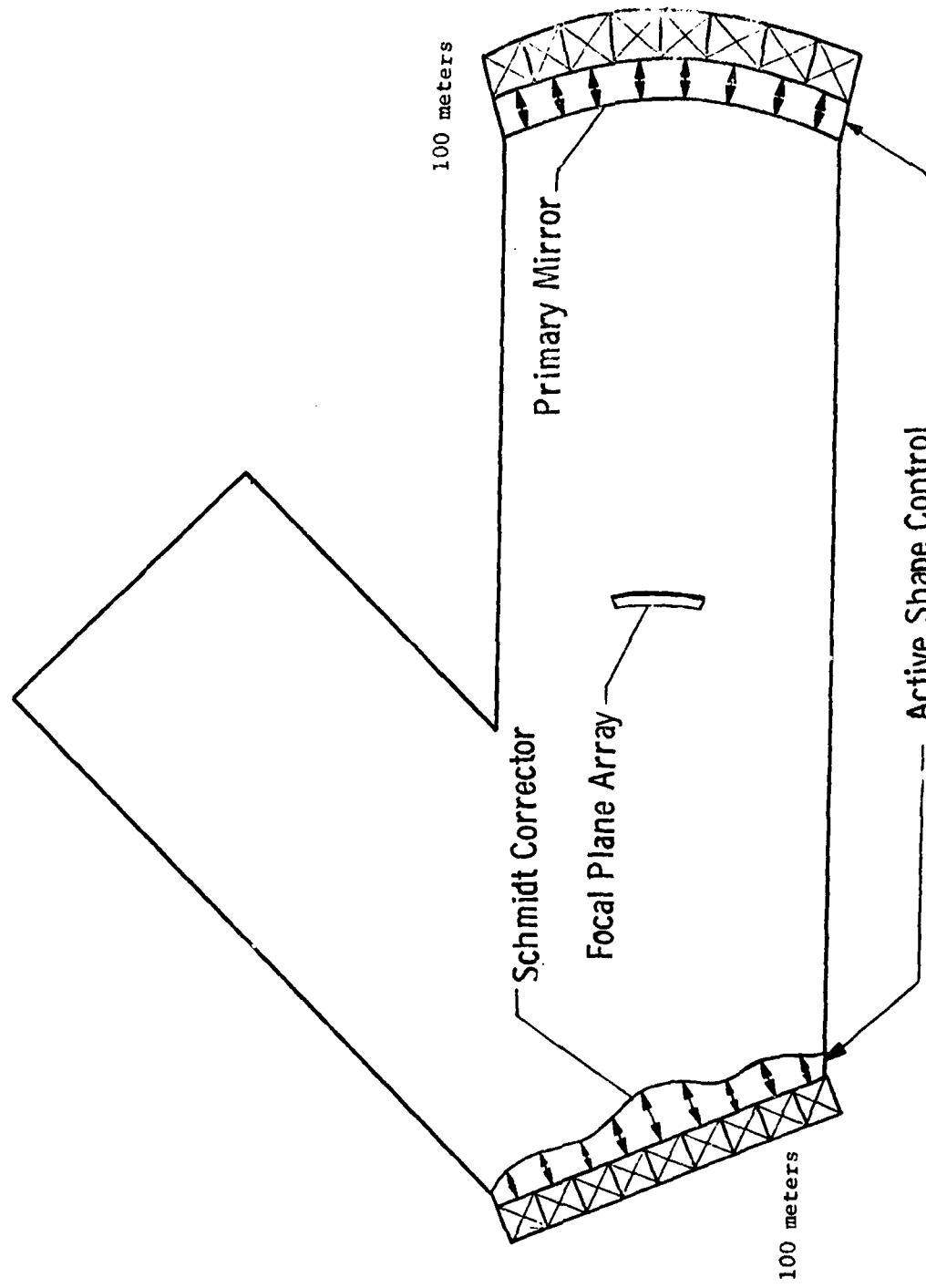
FIGURE 4.3-1   REFLECTIVE SCHMIDT TELESCOPE

Primary Mirror

Schmidt Corrector

Focal Plane Array

Active Shape Control

100 meters

100 meters

DIAMETER = 100 METERS
WAVELENGTH = 3 MM
f/D = 1.5

Figure 4.3-2   BEAM STEERING LOSS,
SCHMIDT TELESCOPE

DISTANCE OFF AXIS

BEAMWIDTHS

DEGREES

Loss

db

203

DIAMETER = 100 METERS
WAVELENGTH = 3 MM
f/D = 1.5
3DB BEAMWIDTH = .00175°
DIFFRACTION - LIMITED

SPOT SIZE FROM
400 N. MI. = 74 FT.

DEGREES/1000

GAIN DB
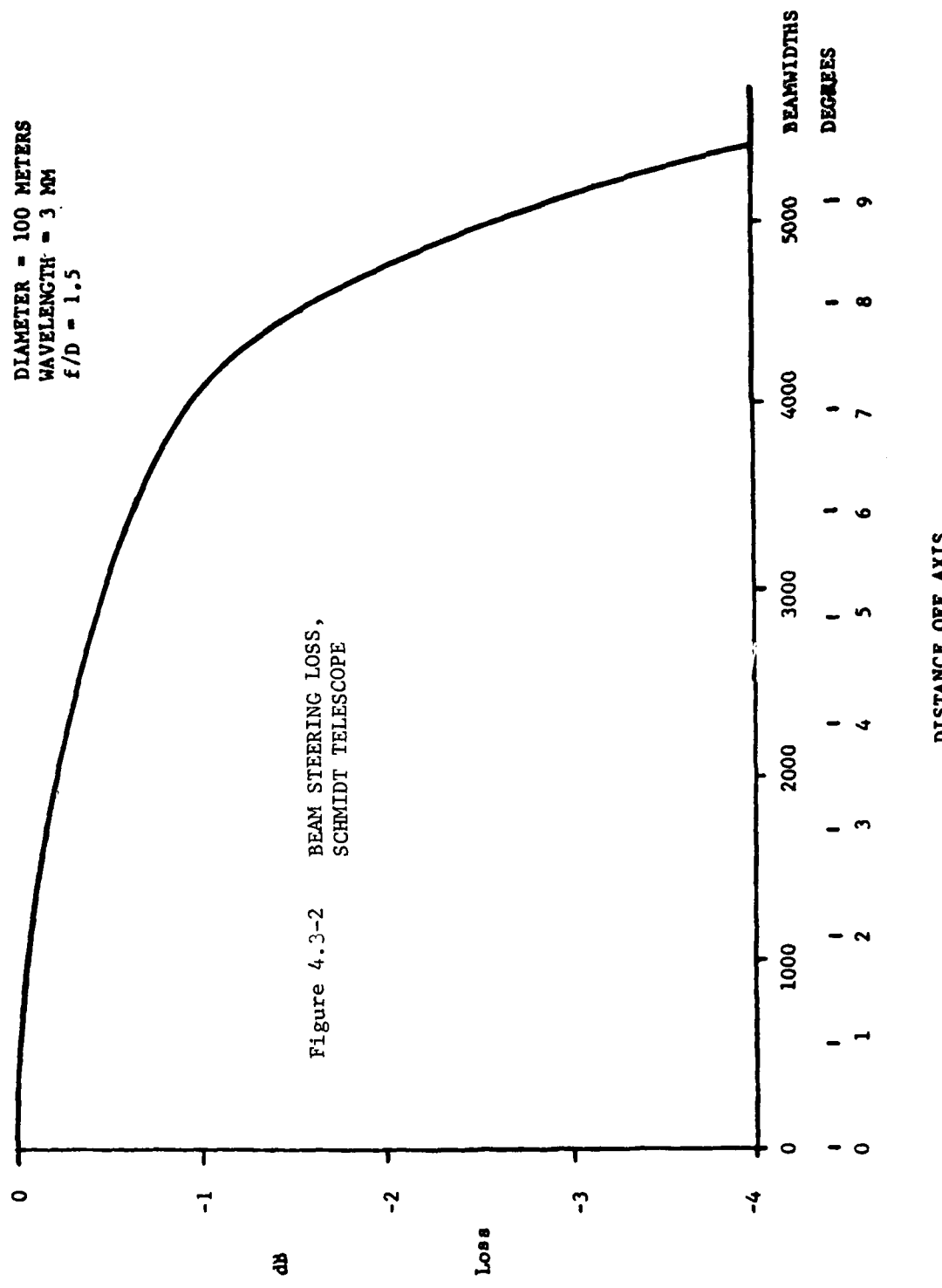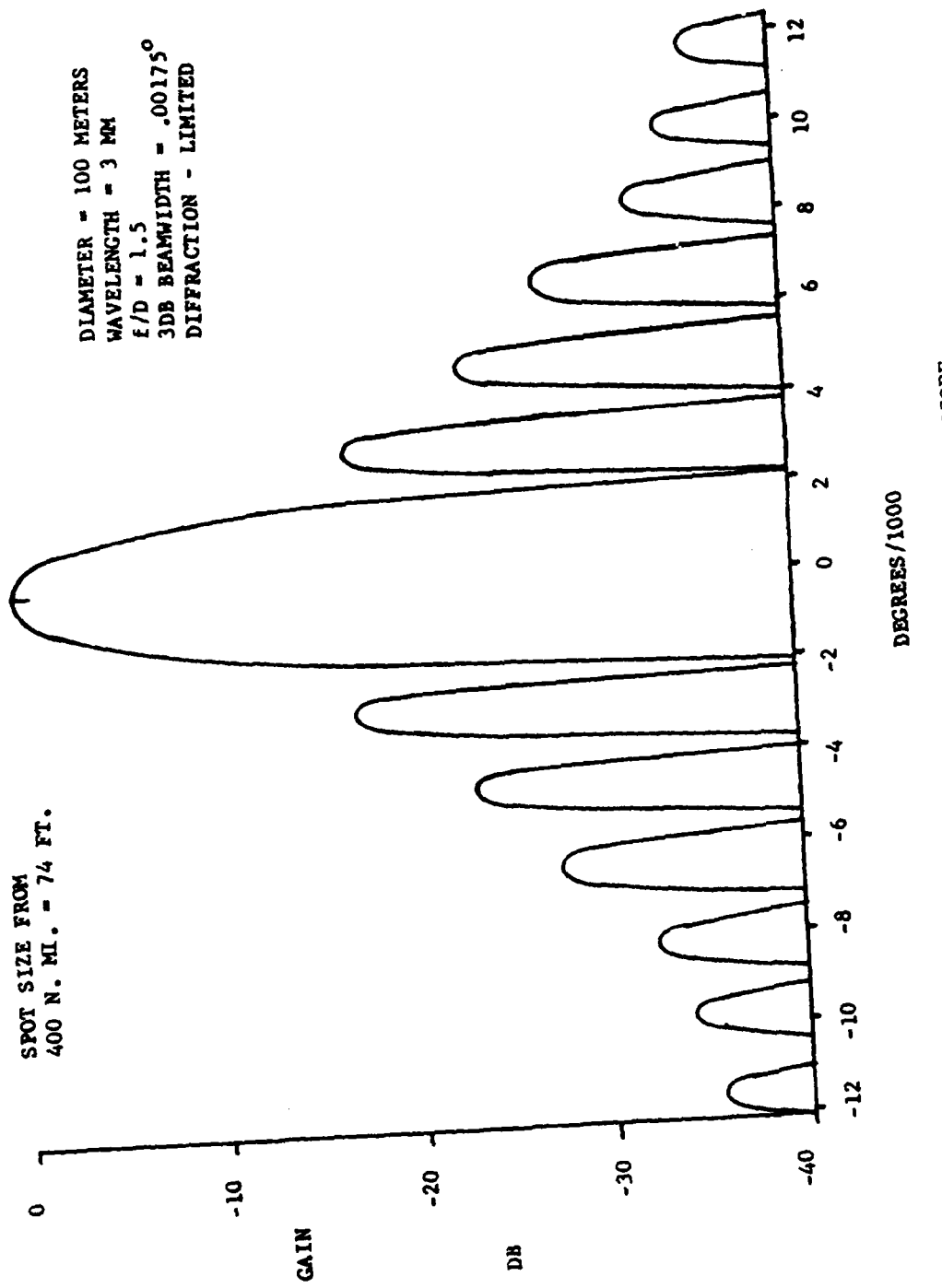
FIGURE 4.3-3 ON-AXIS RADIATION PATTERN, SCHMIDT TELESCOPE

204

DIAMETER = 100 METERS
WAVELENGTH = 3 MM
f/D = 1.5
BEAMWIDTHS SCANNED = 3548.
SCANNING LOSS = 0.65 dB

DEGREES/1000
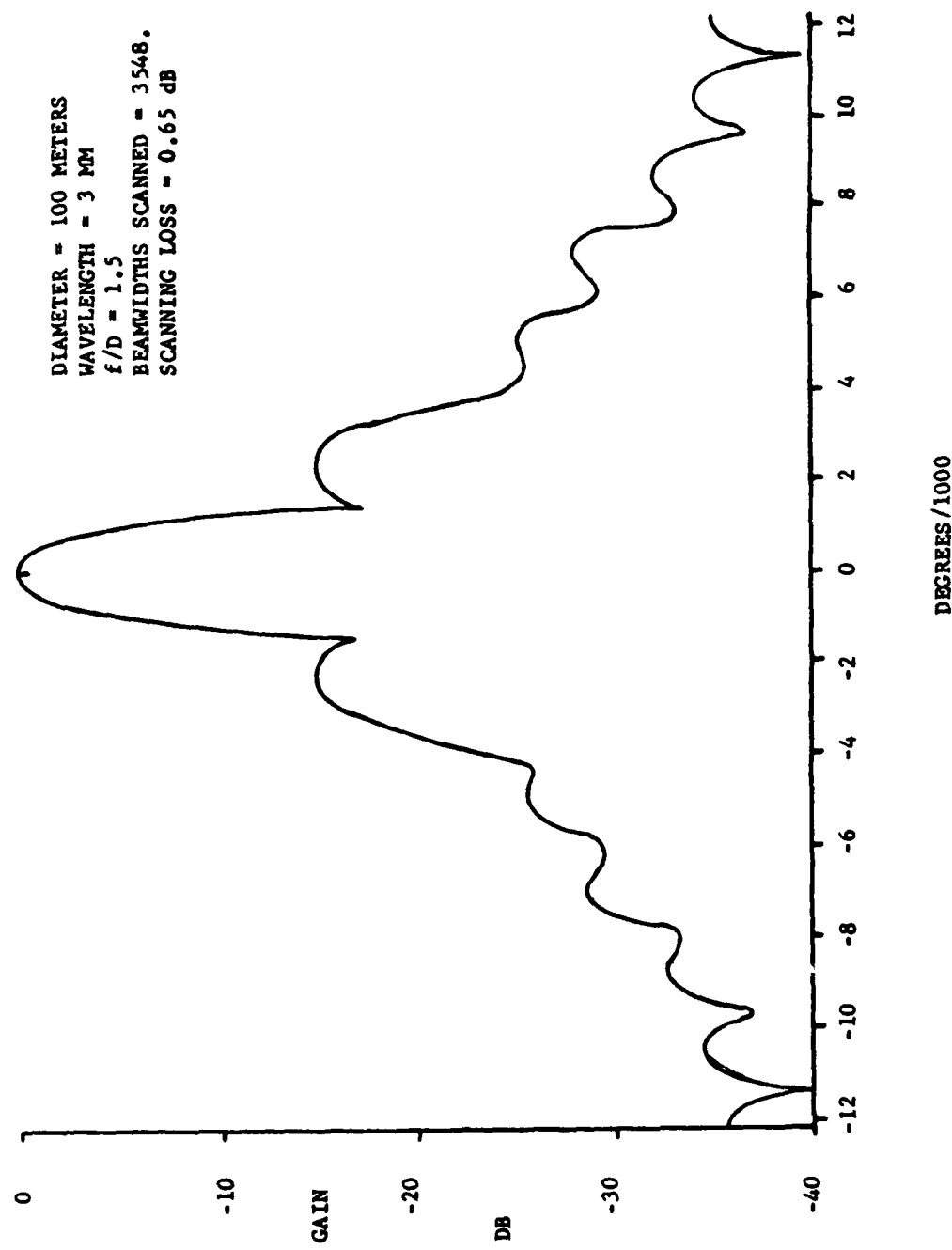
FIGURE 4.3-4   RADIATION PATTERN, SCHMIDT TELESCOPE, BEAM SCANNED 6.22°

205

DIAMETER = 100 METERS
WAVELENGTH = 3MM
f/D = 1.5
BEAMWIDTHS SCANNED = 4731
SCANNING LOSS = 1.96 dB

DEGREES/1000

GAIN

DB
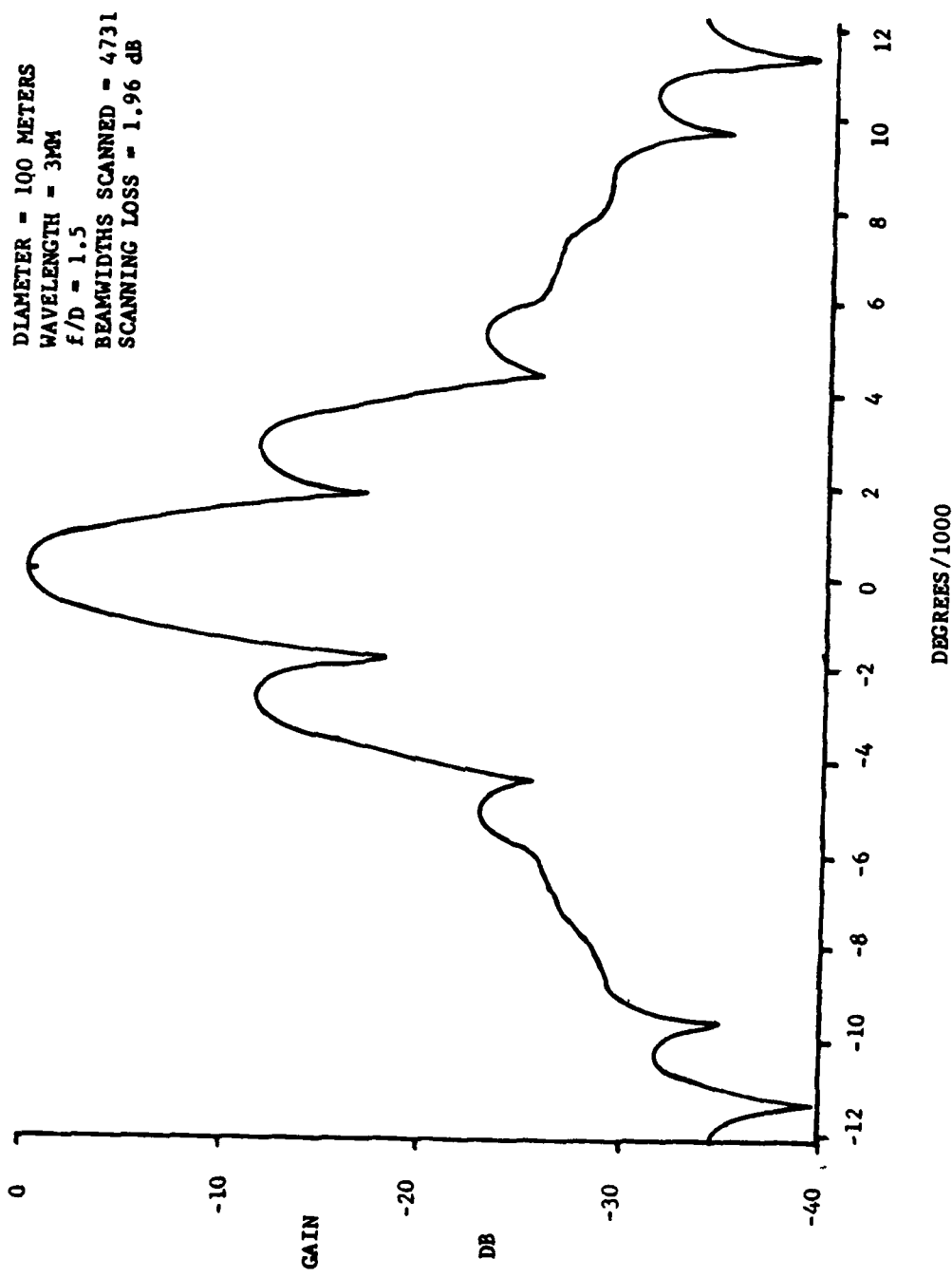
FIGURE 4.3-5   RADIATION PATTERN, SCHMIDT TELESCOPE, BEAM SCANNED 8.30°

206

DIAMETER, 100 METERS
WAVELENGTH, 3MM
f/D = 1.5
BEAMWIDTHS SCANNED = 5914
SCANNING LOSS = 6.82 dB
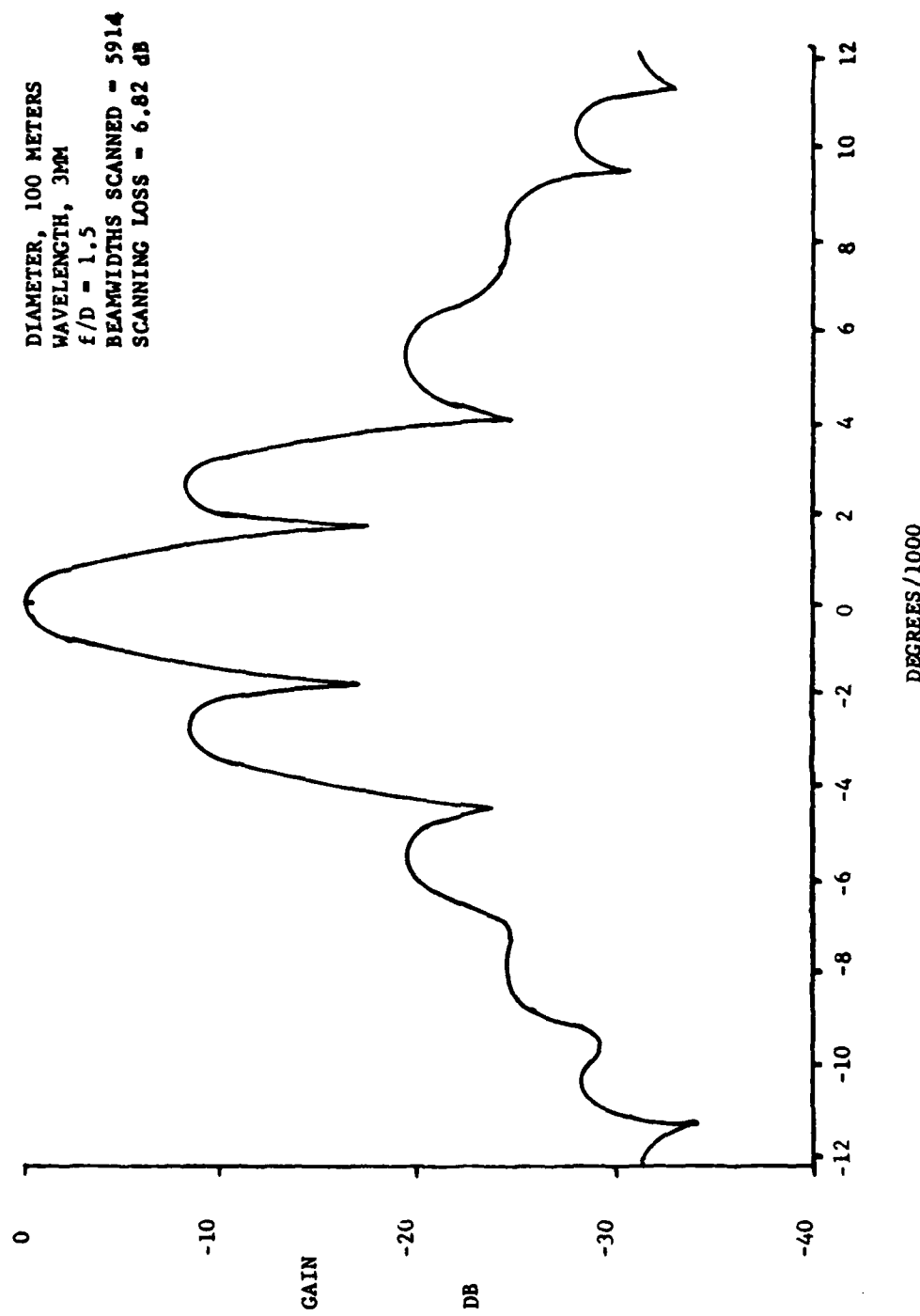
FIGURE 4.3-6   RADIATION PATTERN, SCHMIDT TELESCOPE, BEAM SCANNED 10.37°
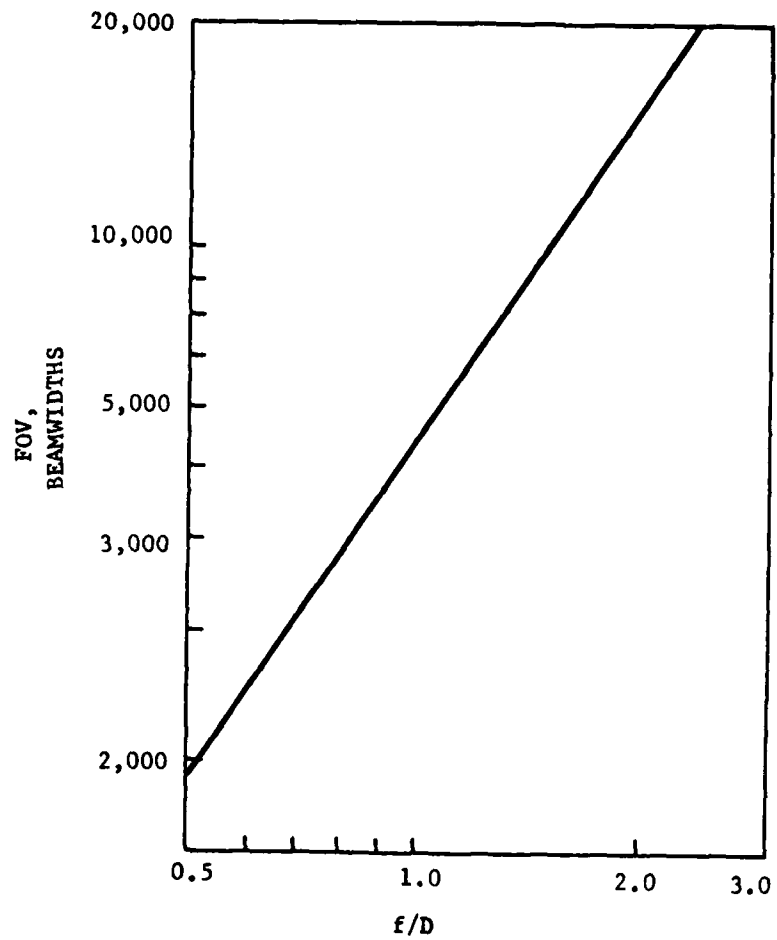
FIGURE   4.3-7   FIELD OF VIEW, SCHMIDT TELESCOPE

would scale inversely with primary reflector diameter if measured in spatial angles. The FOV in our example design (18°) sweeps out a 125 n.mi. swath from a 400 n.mi. orbit.

The 3 dB beamwidth for a 100 meter aperture and a 3 mm wavelength is $.00175^\circ$. This gives a 74' footprint on the ground from an orbit altitude of 400 n.mi. If the footprint diameter is taken as the resolution then it is clear that an enormous aperture would be required for a resolution of a few feet. Fortunately, there are techniques to improve the resolution to much better than that given by the footprint diameter. The original high-resolution scene can in principle be reconstructed by deconvolving the antenna beam shape out of the scene recorded by the antenna as the pushbroom scans the surface being mapped. The accuracy of this deconvolution is limited by SNR effects and also by the rather smooth shape of the beam pattern. Considerable improvement in resolving power can be realized by using sum-difference monopulse patterns and processing the data to take advantage of the sharp null provided by the difference pattern. Resolution as high as 1/50 beamwidth can be realized if the SNR is + 30 dB. 1/10 beamwidth can be realized with a SNR of 16 dB. Assuming that targets of interest will have a SNR of 16 dB or greater, the resolution of the system described above will be on the order of 7.4 feet or better, which should be adequate for sensing and defining targets down to the size of tanks and trucks.

The resolution given by the pattern deconvolution operation is only realized along the track of the pushbroom scan unless some method is devised to create the effect of a scan that also dithers the patterns back and forth in the cross-track direction. This could be done with mechanical or electronic scanning. Alternately, multiple rows of feeds staggered in position in the cross-track direction could be used. Scanning gives fewer receivers but it reduces the effective dwell time somewhat. Assuming a two-axis monopulse (cross-track and along track), three receivers per resolution cell would be required. The 10,000 beam FOV system described above would require 30,000 receivers. While this might appear prohibitive, the additional receiver costs incurred by going to a monopulse system would be much less expensive than trying to get the resolution by making the antenna dimensions larger.

A 400 n.mi. orbit altitude has been selected. This was selected as a result of a tradeoff of atmospheric drag vs. image resolution. An example calculation of the sensitivity of this system for the detection of a military tank is given below.

The SNR for detectability against receiver noise is given by

$$SNR = \Delta T_T \ \frac{\Omega_T}{\Omega_A} \ \alpha_{ATM} \ \frac{\sqrt{\beta} \ \sqrt{\tau} \ POST}{\gamma \ T_R}$$

where

ΔT_T = Target temperature contrast against its background

$\dfrac{\Omega_T}{\Omega_A}$ = Beam filling factor, equal to (Target area)/(Antenna foot print area)

α_{ATM} = Atmospheric absorption factor

β = Receiver predetection bandwidth

τ_{POST}= Post detection integration time

γ = Receiver duty cycle factor

T_R = Receiver front end noise temperature.

ΔT_T can ideally be as much as 290°K with a clean metal target on a clear day. However, a military tank is covered with paint and possibly some dirt, and clear weather is not guaranteed. A conservative value to use for ΔT_T is 200°K.

Assuming a 74 ft diameter circular footprint and a typical tank size of 30' x 12', the beam fill factor is 0.083.

α_{ATM} with heavy clouds but no rain can be taken as 0.5.

τ_{POST} depends on the mode of operation. Assuming a pushbroom scan, it cannot be larger than the time it takes the 74' footprint to sweep across a point target. This is dictated by the velocity of the subsatellite point which is fixed by the orbital period. This is computed to be 3.34×10^{-3} sec. for a 400 n.mi. orbit and a 74' footprint.

β depends on the state-of-the art (SOA) in receiver design. Typically, in a superhetrodyne receiver used for radiometry, both the upper and lower mixing sidebands can be retained. This gives an effective β that is twice the actual receiver IF bandwidth. If this is done, β = 10 GHz should be possible in the near future. There is little reason to expand it beyond this value since the width of the 90-100 GHz window is not much greater than 10 GHz.

The classic Dicke-switch radiometer switches between a calibrated temperature reference and its antenna with a duty cycle γ = 0.5. However, for a mapping mission absolute temperature is not as important as contrast, so calibration could be relatively infrequent. We will assume γ = 1.0.

The predicted near-term SOA receiver noise temperature for a mixer cooled to 100°K in the 90-100 GHz band is 500°K.

Combining all of these numbers gives SNR $\simeq$ 20 dB. This does not include the effects of background clutter or variability in the temperature of the background. A good value to assume for this clutter is difficult to estimate since insufficient measurement data exists. However, assuming

spectral filtering and other advanced processing techniques, it should not degrade the SNR very much under most circumstances. The conclusion is that tanks could be mapped with good reliability and reasonably good resolution (~7 ft) under all but the most adverse weather conditions. Heavy rain would drop the SNR by 10 dB or more. This would give marginal or no detectability. Larger targets such as aircraft and ships would be easily detected in the absence of rain and would usually be detectable even with rain.

The downlink data rate can be estimated as follows. The post-detection integration time τ_{POST}, defined above, was found to be 3.34×10^{-3} sec. Each receiver delivers a pixel once each τ_{POST} in a classic radiometer, but about 5 times this number would be required for the beam deconvolution operation. 12-bit quantization will be required for high-resolution mapping data. There will be 30,000 receivers. The downlink data rate is therefore equal to $\frac{5 \times 12 \times 30,000}{3.34 \times 10^{-3}} \approx 540$ megabits/sec. This is not an impossibly high rate by today's standards, but it is much too high for a store-and-dump mode. This means that the vehicle must continuously transmit data to a ground station during the operational part of its orbit. Since it is in a low orbit, this is most easily done by relaying through a synchronous-orbit comsat.

4.3.4   Grating Lobes Due To Reflector Panel Edges. The preferred reflector deployment approach uses solid graphite-epoxy honeycomb panels of a size that can be stowed in the Shuttle bay, mounted on a backup truss. The mounting will include mechanical actuators for adjustment of the reflector surface figure. The mechanical concept is described in the following sections. In this section we address the problem of possible sidelobe and grating lobe effects that might arise from the discontinuities or gaps in the reflector surface at the panel edges.

Since the panels are all nominally of the same size, the spacing between edges has some regularity, which leads to the formation of relatively strong grating lobes rather than random lobes. This would be true if the panels were deployed on a flat surface. The fact that they are deployed on a curved surface mitigates the grating lobe effect. Computations were made to determine the magnitude of this effect. The configuration sketched in Figure 4.3-8 was used. This is a 260 ft reflector composed of 10' x 10' panels. A parabolic surface, f/D = .46, with uniform illumination, was assumed. The assumed frequency was 95 GHz. Figure 4.3-9 shows the main axial lobe of the gap array. This will coincide with the desired main lobe of the antenna, but will be of opposite sense and many dB below the main antenna lobe. It accounts for the loss in gain of the antenna due to the presence of the gaps.

The magnitude of this lobe can be estimated as follows. The loss in gain is approximately proportional to the area occupied by the gaps relative to the total area of the reflector. There are some secondary effects for very narrow gaps. Figure 4.3-10 shows the total scattering crossection for thin metal strips as a function of width and polarization. This is the dual of gaps in a metal sheet (the reflector). As shown, for a strip (or gap) width greater than $\lambda/2$, the effective electrical width of the strip is essentially equal to its actual width, and essentially independent of polarization. So for gaps larger than around 1/16" at the frequency of interest,

211
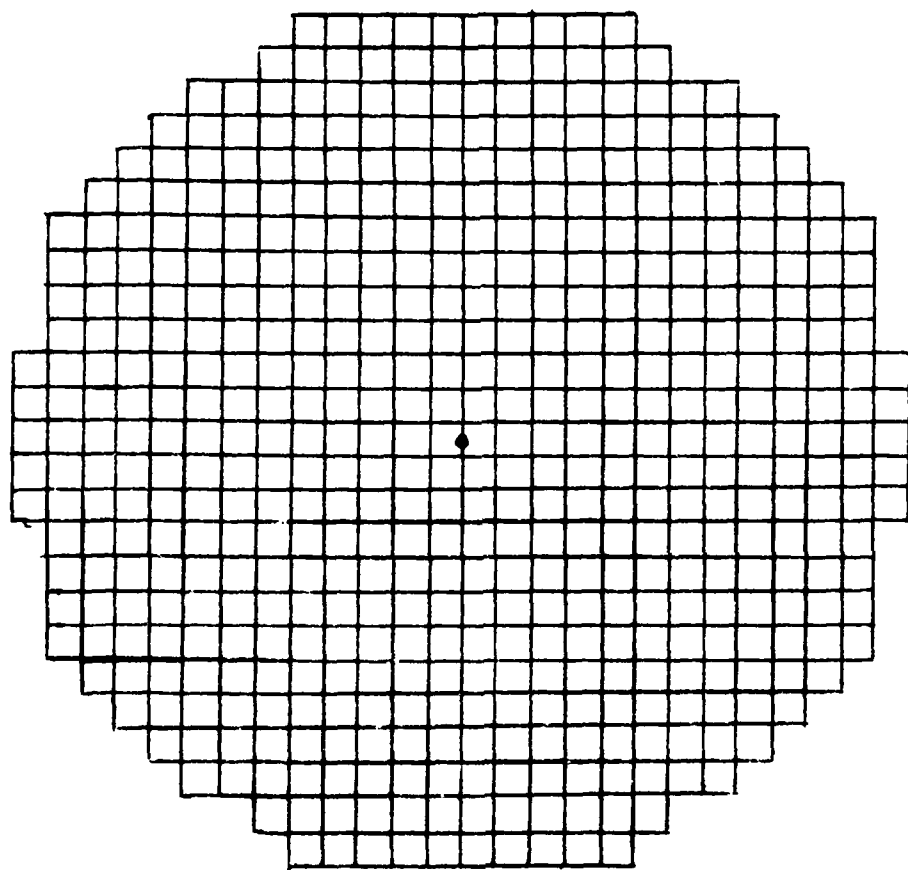
10' X 10' SEGMENTS

Figure 4.3-8   SEGMENTED REFLECTOR
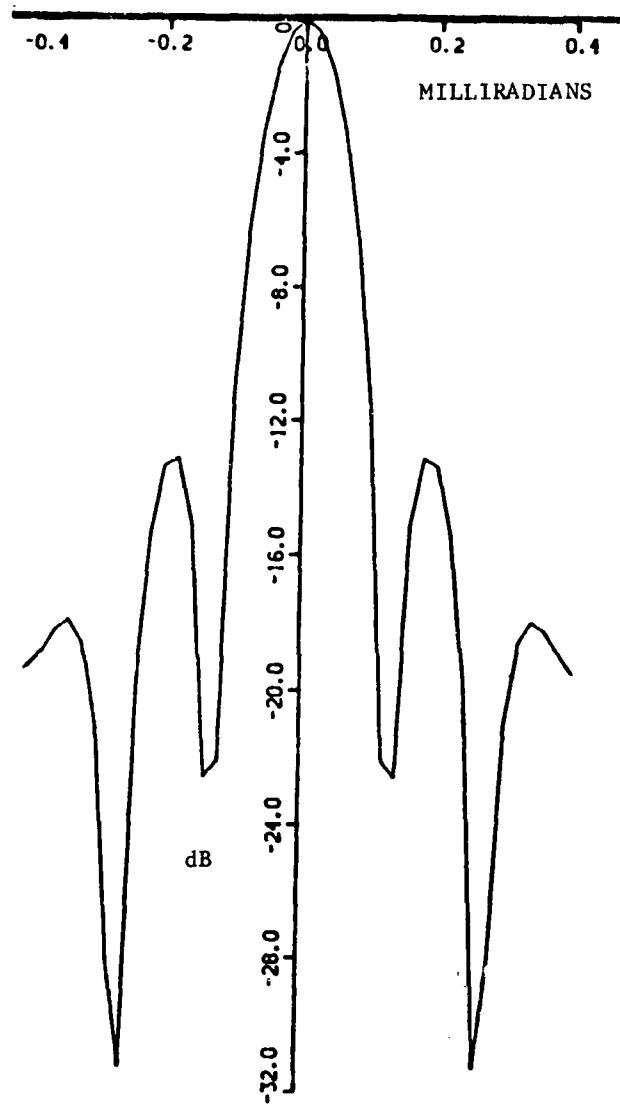
Figure 4.3-9   MAIN LOBE, SEGMENT GAP ARRAY

213

REF: MEI AND VAN BLADEL,   IEEE TRANSACTIONS AP-11, PG 188
        MARCH, 1963

STRIP WIDTH = D
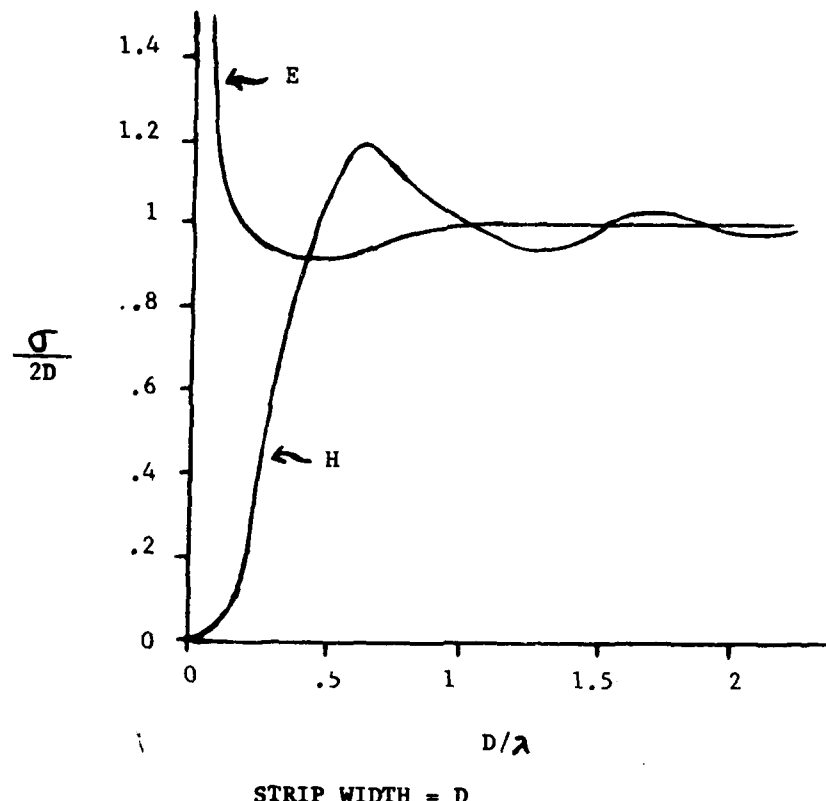
Figure 4.3-10   TOTAL SCATTERING CROSSECTION, METALLIC STRIPS

the relative physical area lost to the gaps is a good measure of the gain of the gap array main lobe relative to the gain of the ideal antenna main lobe. For example, 10 ft panels with a 1/8" gap gives a gap lobe down 27.8 dB from the antenna main lobe. It seems unlikely that the gaps could be made much smaller than this without excessively complicating the fabrication of the reflector.

The first and second grating lobes were then computed. They are shown in Figures 4.3-11 and -12. As shown, the first lobe dropped 12 dB and the second lobe 17 dB relative to the gap array main lobe. This is due to the curvature of the reflector surface. The computer program used to compute these patterns, entitled GRATE2, is listed in Appendix C.

These computations were made early in the program, before the Schmidt reflector concept was selected. The gaps in the Schmidt primary mirror will generate a set of grating lobe pointing generally upward, which can be ignored. The gaps in the corrector plate will also generate a set of grating lobes which will point downward. Since this plate is nearly flat the height of these grating lobes will not fall off very fast, and the first several lobes will be at about the same level as the gap array main lobe, i.e., around 28 dB below the main antenna lobe providing the gap breadth can be held to around 1/8". Lobes of this level are probably acceptable for the radiometer mission, but they should not be allowed to go much higher than this. This poses a mechanical design problem for the fabrication of the reflector. It could be mitigated by using somewhat rendomized dimensions for the panels.

4.3.5   Structural Approaches For The Schmidt Reflector. The Schmidt reflector places a unique requirement on the design of the spacecraft structure. Due to the high operating frequency, a deployable mesh reflector system is not adequate. The reflecting surface must be a continuous surface (i.e. aluminized Kapton or mylar sheets or aluminized honeycomb panels.

Four structural approaches were identified for the Schmidt reflector. The first two concepts utilize rigid honeycomb panels that are supported by a truss structure. The third concept is the Electrostatic Controlled Membrane Mirror (ECMM) approach of General Research Corporation. The fourth approach utilizes expandable air mats that are rigidized after deployment. Both the ECMM and the air mat approach utilize a deployable truss structure for support. All four of the approaches would require some degree of adaptive surface contouring capability to control the reflector surface figure.

Each of the four approaches have limitations and concerns that require substantially more investigation. The rigid honeycomb panels supported by a truss structure (deployable or erectable) require substantial assembly in low earth orbit. Such things as dexterity requirements placed on the remote manipulator system (RMS) or assembly aid, required assembly time, electrical and RF connections, mechanical attachment design, ground validation of both the assembly technique and the deployed precision, and lighting and power requirements must be investigated in order to show concept feasibility.

The feasibility of the ECMM approach rests on the successful demonstra-

215
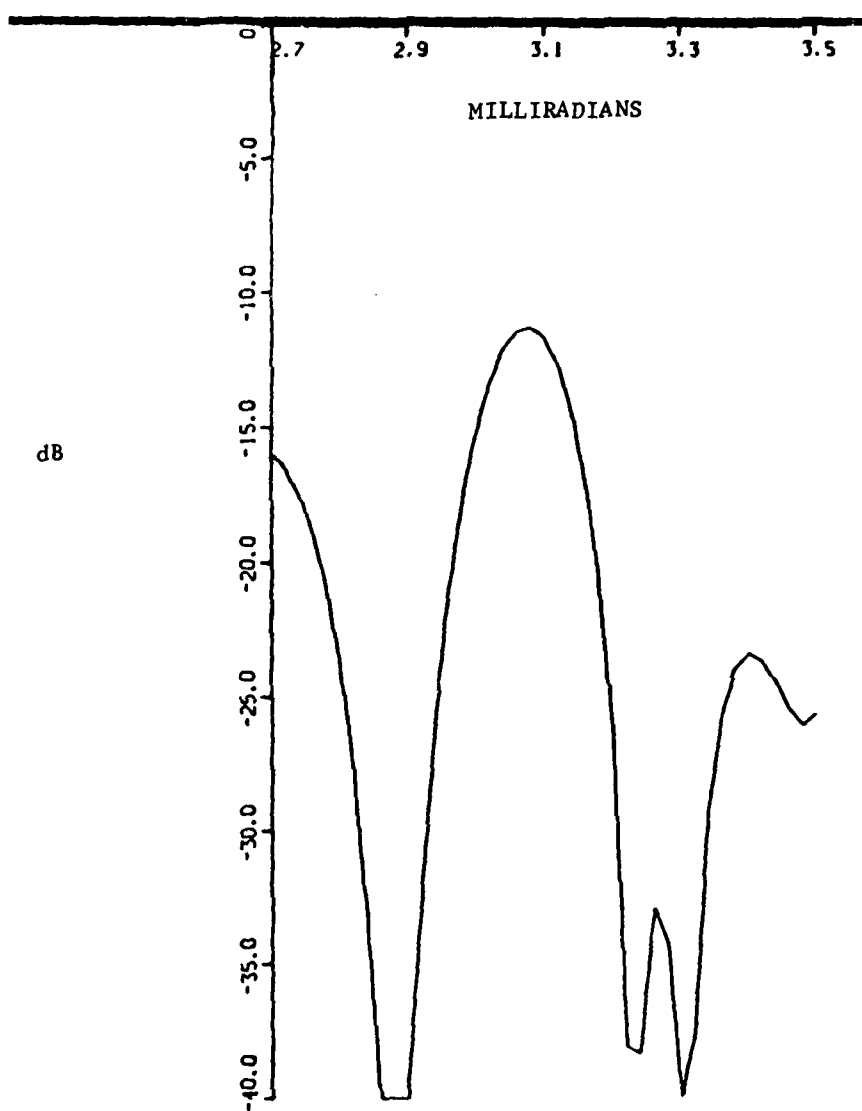
Figure 4.3-11   FIRST GRATING LOBE, SEGMENT CAP ARRAY

216
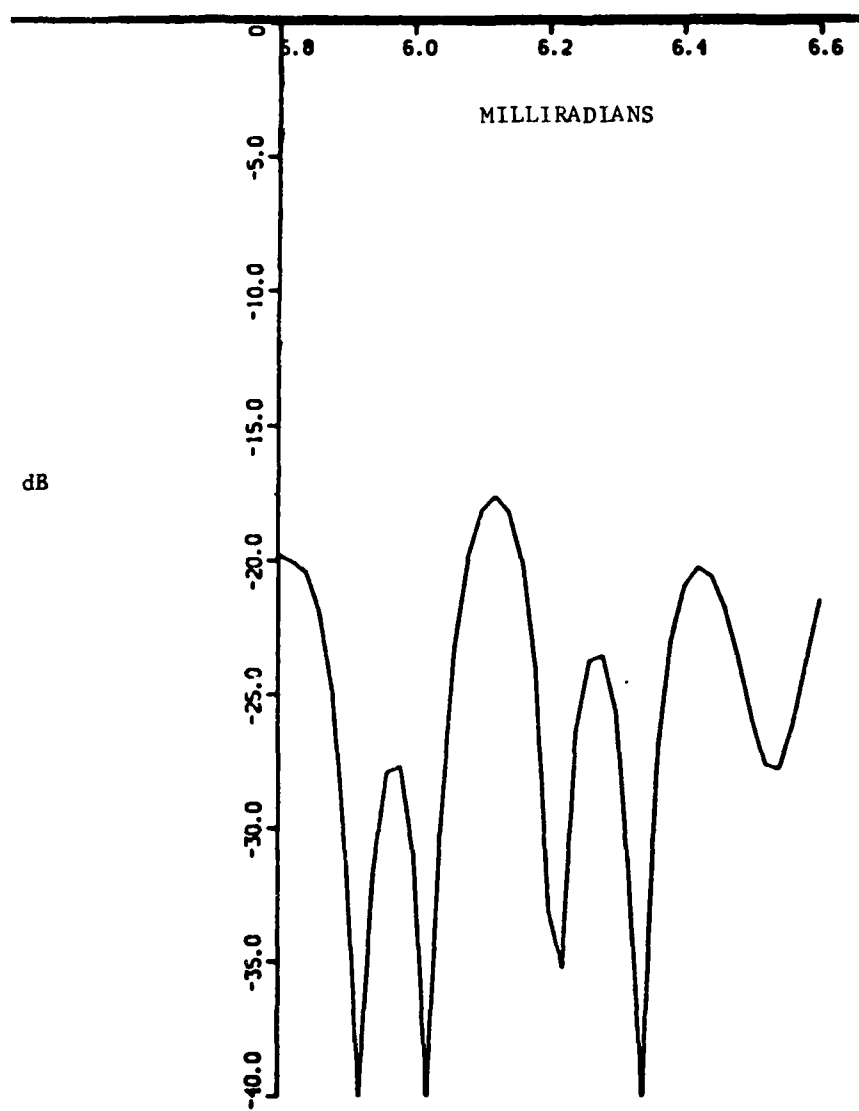
Figure 4.3-12   SECOND GRATING LOBE, SEGMENT GAP ARRAY

tion of the closed loop control of the electrostatic membrane. General Research is in the process of demonstrating the feasibility of the ECMM. Since the reflective surface is a membrane, it can be stowed on a deployable truss, thereby minimizing the required orbital operations. However, as in all deployable structures, failure identification, isolation, and repair must be investigated.

The air mat concept, being studied at Draper Labs, is an old approach being applied to a new requirement (high precision); therein lies the problem with the air mat. The ultra-tight tolerances place a severe constraint on the air mat design. Also, the dimensional stability with time is a question. Like the previous three concepts, significant work needs to be performed to demonstrate feasibility. It appears to be the least promising of the approaches studied.

4.3.5.1 Rigid Panels and Astro-Cell Structure* Approach. This approach consists of individual modules that are stowed in the Orbiter bay similar to a stack of records in a juke box, individually deployed, and then assembled into a reflector platform (See Figure 4.3-13).
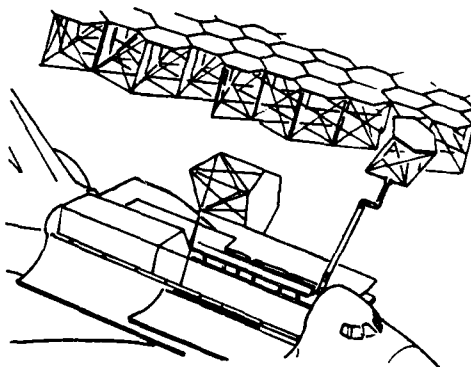
Figure 4.3-13   Assembly Technique

Each module consists of three parts, 1) a 14 ft diameter hexagonal reflector panel, 2) a deployable triangular truss, and 3) a set of three linear adjustment actuators for surface alignment. The cabling is incorporated into

---

*Astro-Cell concept Jointly developed by Dr. John Hedgepeth (Astro Research Corp) and Martin Mikulus (NASA Langley)

the structure and cable connections are automatically made when the modules are connected.

The support truss on each module is similar to the articulated astromast.

A module of the Astrocell structure with the payload panel removed is shown in Figure 4.3-14. Note that the structure consists of the upper and lower triangular frames and the diagonals. The curved "longerons" are not part of the primary structure; they are prebuckled and therefore supply the forces necessary to pretension the diagonals. The module is capable of carry-
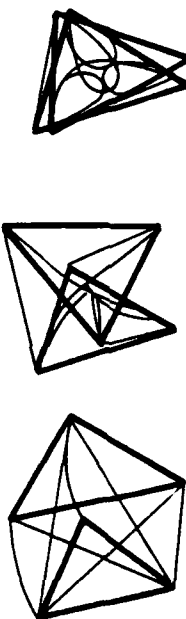
Figure 4.3-14   Deployable Truss Structure

ing compression with full stiffness. The design of the hinges and other attachments has been carefully thought out so as to achieve maximum compact-ness. The depth of the packaged module is just the sum of the triangular-frame thicknesses. The deployment motion is quite similar to that of one bay of an Astromast lattice column.

The joints between modules must provide a good structural tie. They must also provide for electrical connections. One attractive concept, de-

veloped by Astro Research, for meeting these requirements is shown in Figure 4.3-15. The probe-and-drogue arrangement facilitates engagement, and a torqued fastener on the end of the probe precompresses the joint to cement the marriage. Full modularity is enhanced by providing the universal triangular transition piece in which the variations in electrical circuitry can be accommodated.
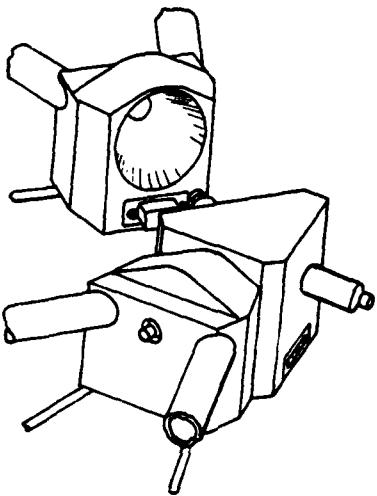
Figure 4.3-15   Attachment Method*

The fully assembled system is shown in Figure 4.3-16. An analysis was performed to determine the number of Orbiters required to assemble a reflector system which has 300 ft diameter reflectors and an overall length between reflectors of 900 ft. Table 4.3-1 summarizes these results. Analysis showed that one Orbiter is required to transport each 300 ft diameter reflector to earth orbit. The reflector requires 470 modules at 14 ft diameter each. The total weight of the system is 44650 lb. However this violates the weight and cg envelope of the Orbiter. To bring the cg within the envelope, the 15000 lb cradle has its cg biased aft.

After the two reflector systems are assembled, a third orbiter transports the feed, spacecraft, and deployable masts and guylines to orbit. The feed and masts are attached to the two reflectors and deployment is initiated.

---

*Developed by Astro Research

220

NUMBER OF ORBITERS: THREE (1 FOR SPHERICAL REFL, 1 FOR FLAT REFL.,
                       1 FOR S/C, MASTS, FEED, ETC.)

NUMBER OF CELLS: 470 @ 14 FT DIA.

TRUSS DEPTH: 13 FT

CELL PACKAGING: 470 @ 1.43 IN. = 56 FT

PANEL DESIGN   WEIGHT (LBS)

 FACE SHEETS (0.020 GR/E)   51.9

 HONEYCOMB (3 LBS/FT^3, 0.3 IN THICK)   11.2

 REFLECTING SKIN (0.001 IN AL)   2.2

 BOND LINES (0.002 IN EPOXY)   5.2

                       TOTAL   70.5

TRUSS DESIGN

 TUBES (0.5 IN. DIA. X 0.1 IN.   4.6 lbm
       THICK)

 END FITTINGS (TITANIUM - 0.2 lbm   1.2
               EACH)

 DIAGONALS (GR/E - 0.2 lbm EACH)   1.8

 ACTUATORS (2 lbm EACH)   6.0

 CABLING (.04 lbm/FT)   1.5

 CONNECTORS (.33 lbm EACH)   1.0

                       TOTAL   16.1 lbm

CONTINGENCY   8.4 lbm

                 TOTAL CELL WT. 95   lbm

                 TOTAL PAY-
                 LOAD WT.   44650   lbm (FOR ONE 300 FT. REFLECTOR)

Table 4.3-1   SUMMARY OF CONCEPT UTILIZING HEXAGONAL PANELS AND
               TRIANGULAR TRUSS

221
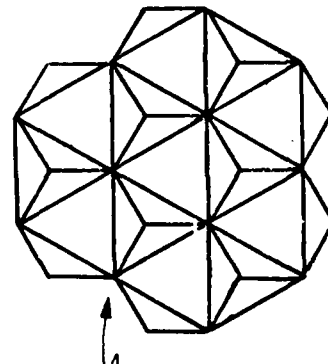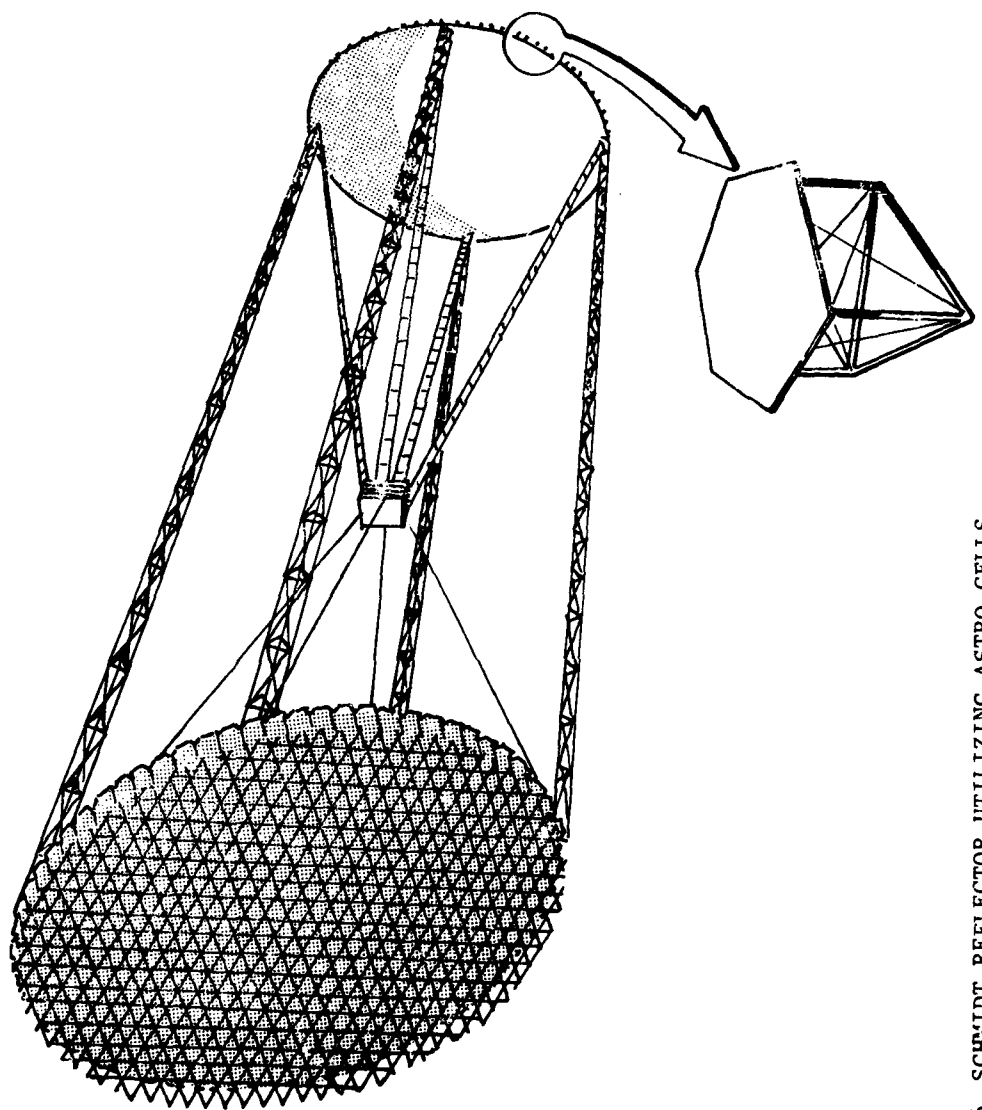
FIGURE   4.3-16   SCHMIDT REFLECTOR UTILIZING ASTRO-CELLS

4.3.5.2 Rigid Panels and Box Truss Structure Approach. This approach consists of individual rectangular panels that are stowed in approximately half the length of the Orbiter bay. A deployable box truss structure is stowed in the rest of the cargo bay. The stowed configuration is shown in Figure 4.3-17.

The heavier panels are stowed in the aft end of the cargo bay to bias the cg aft. No support cradle bias is required. 248 panels are required. This reduces the amount of assembly required. The assembly sequence is as follows:

1. The box truss structure is removed from the Orbiter bay with the RMS.

2. Deployment of the truss is initiated.

3. The panels are individually attached to the rectangular boxes of the box truss.

For this concept the panel adjustment actuators are incorporated into the box truss (as well as the electrical and RF cabling). Only mechanical attachments are required between the panels and the structures.

A plan view of the assembled reflector is shown in Figure 4.3-18. The panels are rectangular in shape with a constant length of 25.83 ft and varying width from 7 ft to 13.5 ft. This facilitates packaging the panels in the Orbiter. The assembly sequence after the reflectors are completed is identical to the Astro Cell concpet. The completed S/C is shown in Figure 4.3-19. The box truss configuration also must have a varying shape compatible with the panel sizes. This is accomplished by varying the surface tube lengths of the truss. Table 4.3-2 summarizes the results of the design. It can be seen that this approach allows thicker reflector panels and a deeper truss. The thicker panels and deeper truss provide improved dynamic performance and also improved deployed precision. It is assumed for both of the rigid panel approaches that the surface figure of the individual panels remains essentially perfect with temperature cycling. The requirement for adaptive surface control arises from distortions in the supporting truss.

4.3.5.3 ECMM Approach. The ECMM approach differs significantly from the previous two approaches. Because the reflective surface is a membrane, the total reflector system can be deployed without on-orbit assembly. In fact, the total S/C can be launched in only one Orbiter. The stowed configuration is shown in Figure 4.3-20. Two 20 ft deep box trusses are packaged in the Orbiter. The support mast canisters are packaged outside the periphery of the truss. The cannisters actually are part of the truss structure and replace the typical vertical member in the structure. A cradle is utilized to support the trusses, feed and S/C. No structural attachments are required after release from the Orbiter. The deployment sequence is as follows:

1. Release from Orbiter

6-7 FT
6-8 FT
PACKAGED IN ORBITER
14 FT
8-9 FT
8-10 FT
8-10.5 FT
10-11 FT
10-12 FT
10-12.5 FT
10-13 FT
24-13.5 FT
24-14 FT
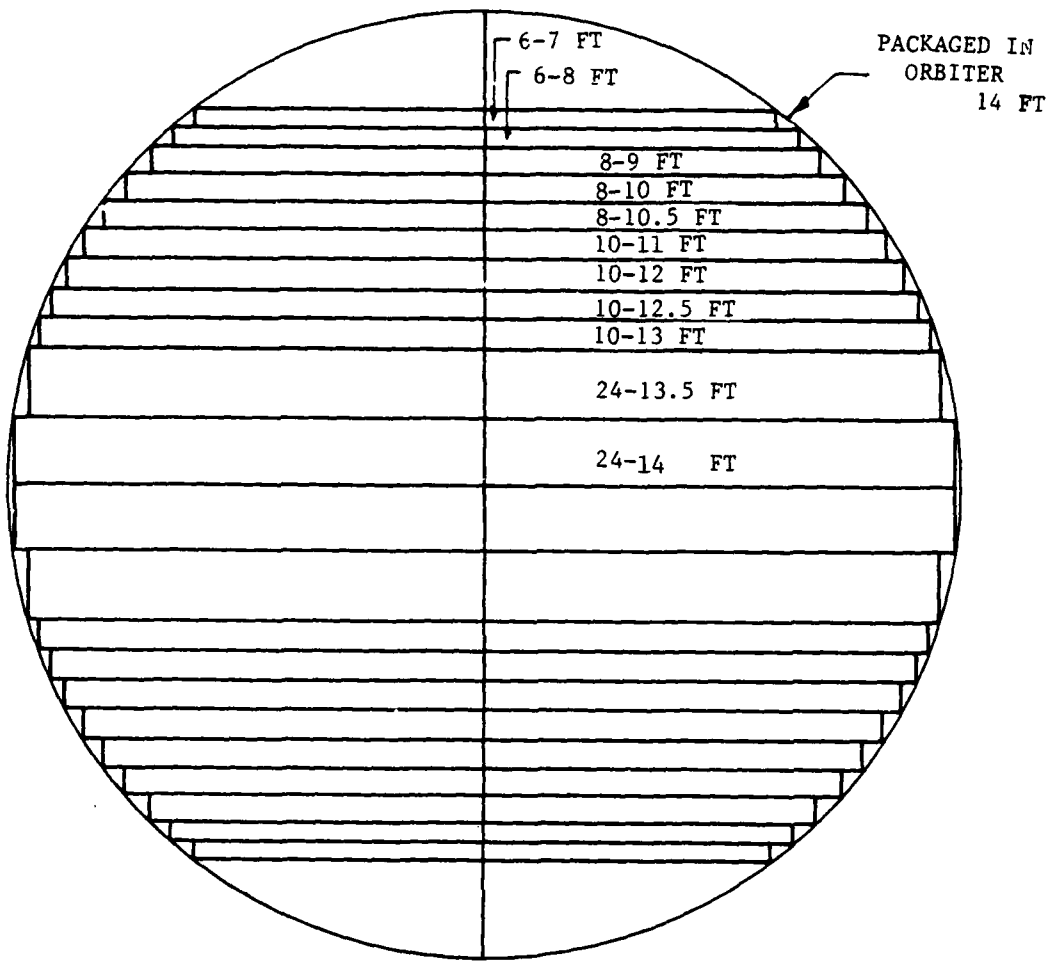
Figure 4.3-17   STOWED CONFIGURATION, RIGID PANELS
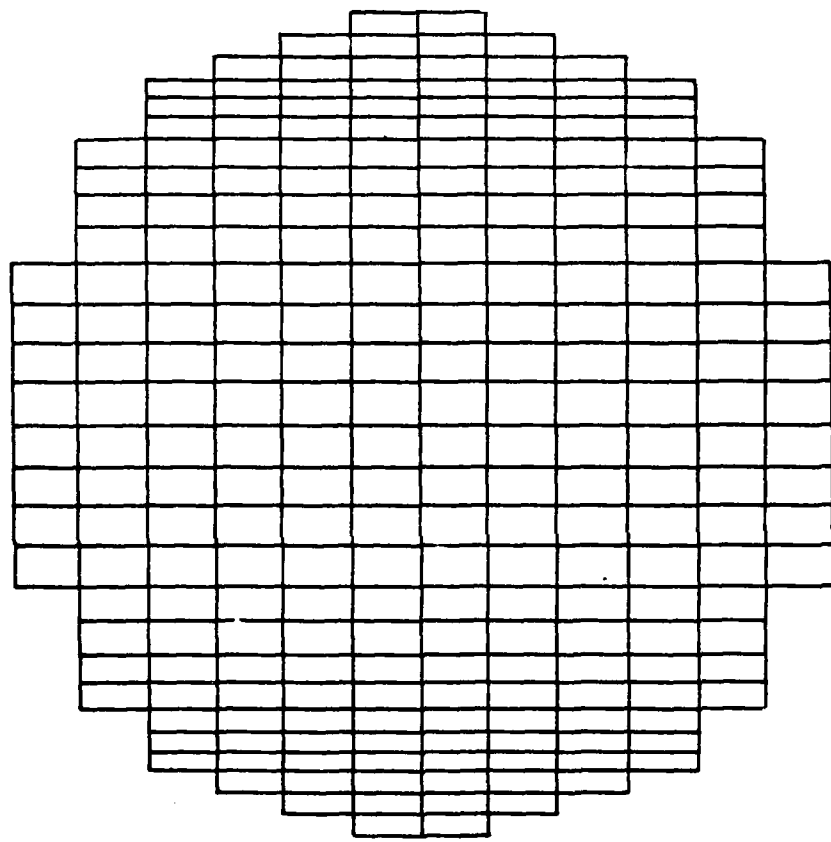
Figure 4.3-18   DEPLOYED REFLECTOR, 300 FT DIA.
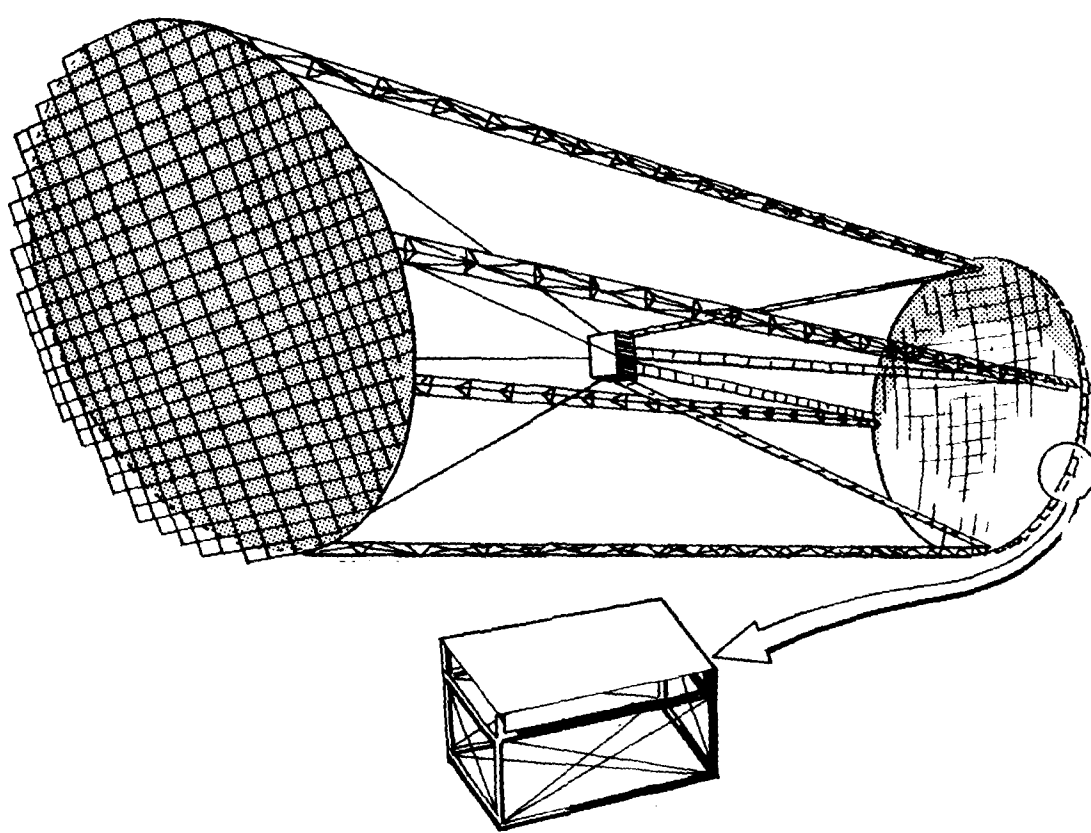
Figure 4.3-19   SCHMIDT REFLECTOR UTILIZING RECTANGULAR PANELS

226

```
NUMBER OF ORBITERS:    THREE (1 FOR SPHERICAL REFL., 1 FOR FLAT REFL.,
                       1 FOR S/C, MASTS, FEED, ETC.)


NUMBER OF PANELS:      248

TRUSS DEPTH:          25.83 FT

CELL PACKAGING:       PANELS ARE 25.83 FT LONG BY 7 →14 FT BY 0.6 INCH


PANEL DESIGN                                   WEIGHT (1 bm)

      FACE SHEETS (0.020 GR/E)                 25000

      HONEYCOMB (3 lbm/FT³, 0.375 IN. THICK)    6700

      REFLECTING SKIN (0.001 IN AL)             1000

      BOND LINES (0.002 EPOXY)                  2500

         TOTAL                                          35200 lbm

TRUSS DESIGN (0.10 lbm/FT²)                              7200 lbm

      TUBES (2.0 IN X 0.030 IN)

      END FITTINGS (TITANIUM)

      DIAGONALS (GR/E)

CABLING (.04 lbm/FT)                                    2200 lbm

ACTUATORS (2 lbm EACH)                                  1500 lbm

         TOTAL PAYLOAD WT (FOR  ONE  300 FT REFLECTOR)  46100 lbm
```

Table 4.3-2   SUMMARY OF CONCEPT UTILIZING RECTANGULAR PANELS
               AND BOX TRUSS

2. Simultaneously deploy the two reflectors row by row, column by column.

3. Deploy the masts.

The unique features of the ECMM integrated with a box truss allow the total S/C package to be launched in one Orbiter with no required orbital assembly. Details of the packaging support method and subsequent deployment dynamics need to be addressed in a future study.

One major concern is the deployment of high voltage cabling to the electrostatic control points on the membrane. The number of distinct control points (and cables) required for a 300 ft reflector is estimated by GRC to be a minimum of 2000.
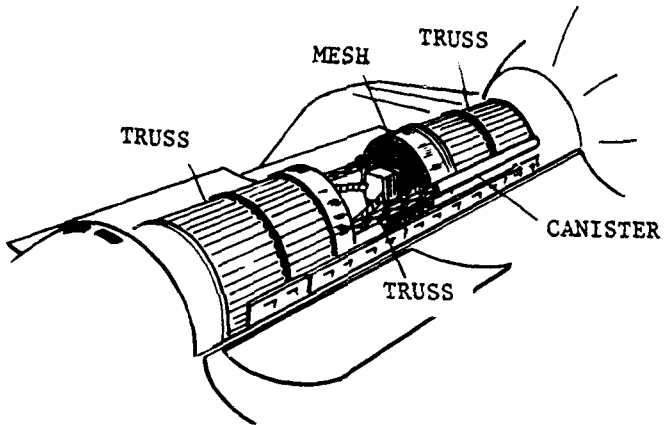
Figure 4.3-20   STOWED CONFIGURATION, ECMM ANTENNA

4.3.6   Stability, Pointing and Control. The purpose of the Stability, Pointing, and Control System is to point the antenna in the desired direction, to stabilize it as a flexible body, and to coordinate the control the motions of the various parts of the antenna so that the geometric properties of the structure and primary reflector surface are held to within the tolerances necessary for it's successful operation as a millimeter-wave radiometer.

The GN&C system requirements are:

Lifetime: 5-10 years; WT & Power: Low, but not critical; Navigation Accuracy: Position knowledge not required on board; Attitude Accuracy: Knowledge of direction of principal axis of antenna required to $\pm 1^o$ (i.e. knowledge of bore sight direction with respect to nadir required to $\pm 1^o$, geopositioning accuracy of the radiometer image map will be refined by

228

landmark map matching); Slewing: Required at initialization only; none during operation. Command Direction: Nadir pointing only; Surface Control: $\pm$ 1 mm to "best fit"; Feed Control: $\pm$ 1 mm to focal point.

The following discussion sets forth a stability pointing and control concept which is applicable to the reflecting Schmidt antenna for low earth orbit use. The control required is:

1. Control of direction of principal axis of antenna in space.

2. Flexible Body Stability & Mode Suppression

3. Figure control of reflector surface (see section 2.3)

4. Control of location of feed

These control loops are coupled which can create the potential for an unstable situation between loops. Hence the control problem must be treated in an integrated manner. A strawman concept for such an integrated control system for the Schmidt antenna is shown in Figure 4.3-21. The sensors, controllers and significant disturbances are broken out in Table 4.3-3.

4.3.6.1 Sensors. The concept involves mounting the primary sensing package consisting of a 3 axis strapdown gyro package, horizon sensor(s) sun sensor and local microprocessor below the lower structure in such a manner that the earth disk is not occulted. A laser beam then would run from the feed thru the lower structure to the attitude sensing package; constituting a columnated light source, defining the focal direction and, tyeing together the feed and the attitude sensing package. The gyro package acts as a mechanical attitude memory between Horizon Sensor-Sun Sensor optical updates and also as a sensor providing data on the attitude and attitude rates necessary for the stabilization loop which maintain rigid and flexible body control.

Systems of sensors to detect flexible body motion are also required on the upper structure and each of the support beams.

4.3.6.2 Controllers. The antenna principal axis is offset by a small angle from the boresight of the antenna due to a tilt in the corrector plate to avoid blockage by the primary reflector. This angle is approximately 19° for the selected design (f/D = 1.5). Gravity-gradient stabilization can be used if the antenna boresight is allowed to shift away from nadir by this angle. Gravity gradient stabilization is highly desirable since it results in a marked simplification and weight reduction of the ACS. The penalty for this small shift in boresight direction is an increased antenna footprint diameter in the shifted axis. The increase is only 12%, so it is acceptable.

While gravity-gradient is recommended for the primary ACS, there will be disturbing torques that can best be controlled by an auxiliary system of momentum wheels (Control Moment Gyros or Reaction Wheels) and reaction jets. The momentum wheels provide fine pointing control, modal suppression and com-

229
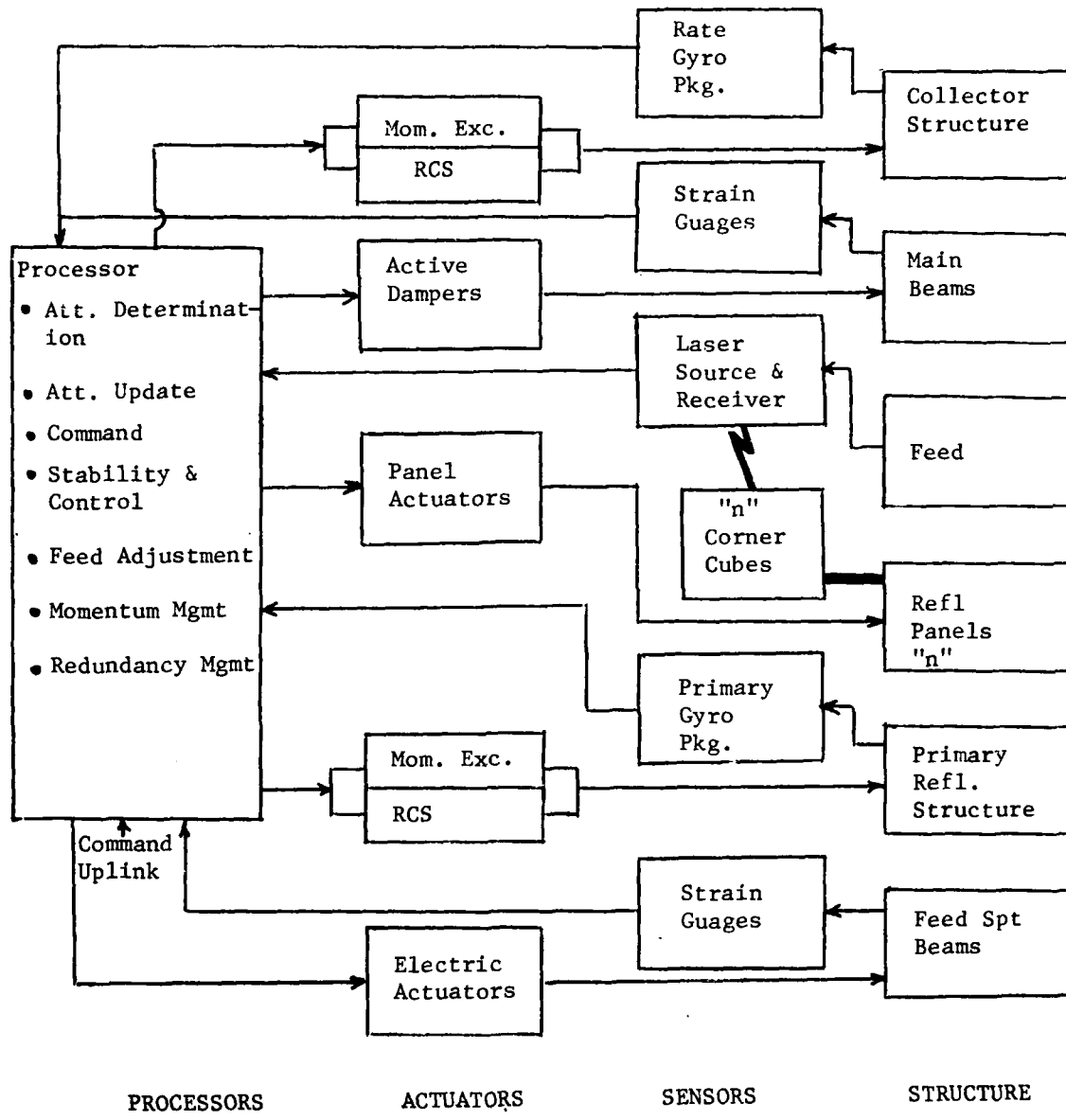
Figure 4.3-21   Integrated Control System For Schmidt
                 Reflector Antenna

230

TABLE 4.3-3   Principal Aspects Of Control Of The
Reflecting Schmidt Antenna

Control　　　　Principal Factors	Sensors	Controllers	Disturbances
Principal Axis Pointing	Hor Sensor ⎞ Primary Sun Sensor ⎬ Sensor Gyro Pkg ⎠ Set Rate Gyros; Strain 　　　　　　Gauges	CMG & RCS	Solar torques (Induced Thermal) Aero torques
Flexible Body Control	Gyro Pkg Rate Gyros Strain Gauges	CMG's	Desaturation RCS Firings
Figure Control	Laser & Corner Cubes	Local Surface Actuators	(Induced Thermal) De- saturation Firings
Feed Location Control	Laser & Corner Cubes Collimated Laser Source	3 DOF Actuators On Feed Support Beams	g.g. effects RCS Firings Solar Torques

231

pensation for most disturbing torques. The reaction jets are used for the initial slewing, to overcome large distrubing torques, compensate for drag and non-cyclic solar pressure, and to desaturate the momentum wheels. The reaction jets will be mecury ion thrusters with ISP of 3000 and thrust of .025 lbs. Due to the nature of the structure of the Schmidt reflector the system of momentum exchange devices should probably be split between the collector plate and the primary reflector. Also since the mission lifetime is 5 to 10 years the system of momentum exchange devices must be redundant. One of the most difficult control problems is the control of the location of the feed to within 1 mm of the "best fit" focus to the reflective surface. This can be achieved by adjusting the position of the feed via actuators between the feed and it's support beams using the laser mentioned above as the sensing element.

4.3.6.3 Disturbing Torques and Forces. Significant disturbing torques will arise from two sources; aerodynamic pressure and solar pressure. Aerodynamic pressure is on the order of 10^{-7} lbs per sq. ft. of solid surface, producing adverse effects at 400 nm altitude. Solar pressure results in disturbance of the same order of magnitude.

Solar pressure and aerodynamic drag are also disturbing forces, producing translational effects which alter the orbit parameters. By careful choice of the location of the reaction jets on the antenna structure it is possible to ameliorate the adverse effects of these disturbing forces while eliminating totally the attitude error caused by the disturbing torques.

5. CONCLUSIONS

5.1 Conclusions, Space-Based Radar Mission. The principal option to the baseline full-aperture space-fed array studied by us was the two-reflector system using a phased array feed. This concept has four primary disadvantages relative to the baseline system. These are listed below.

- Its electronic scanning range is smaller, though this disadvantage can be mitigated by a mission design using some mechanical scanning via attitude control of the spacecraft.

- It is heavier and more complex structurally, and more difficult to deploy, though the 5000 n.mi. orbit vehicle can be packaged in a single shuttle.

- The modules require electronically variable gain control in the receive mode to optimize the sidelobe performance with beam scanning.

- The sidelobe control with beam scanning appears to be inherently poorer than that of the baseline system, though sidelobes of -45 to -50 dB can be achieved.

The two-reflector system has one very big advantage over the baseline system. The total number of electronic modules required can be reduced by a factor of 4 to 6. However, since the total transmitted RF power must remain the same, each module must deliver proportionately more power in the transmit mode. This is not a major concern for the module design or for the mdoule cost, since the module RF power outputs are not high, around 0.1 watts average. The per module cost represents the largest cost risk in the space-based radar program. The two-reflector system offers the possibility of a marked reduction in this cost risk. Therefore, it is our recommendation that it be carried on the program as an option to be used in the event that the module cost cannot be held to the target value.

Another option, the full-aperture reflectarray, was not studied to any depth on this program, but it does have some attractive features. Its primary advantage over the baseline lens-array is that it can use a much shorter focal length for the same bandwidth constraints if it is deployed on a parabolic surface. This gives a lighter and stiffer structure. We also recommend that further study be done on this concept.

5.2 Conclusions, Millimeter Wave Radiometer Mission. The antenna size and surface precision requirements of this mission would make it an extremely difficult and costly mission to carry out. While it may have some advantages over a synthetic aperture mapping radar (SAR) in terms of jamming, a radar giving equivalent resolution has a much smaller and simpler antenna, and could operate in the microwave frequency band. It appears that, at least for present-generation technology, the SAR is the better choice.

However, in the event that the millimeter wave radiometer mission is carried forward at some future date, we believe that the atnenna system selected by us, the reflective Schmidt telescope, is the best choice for

the mission because of its very wide FOV and the simplicity of its feed
system.

6. RECOMMENDATIONS, CRITICAL TECHNOLOGIES

Our general mission-related conclusions and recommendations are presented in Section 5. This section addresses specific technology areas where additional work should be done, assuming that the program recommended in section 5 is carried forward.

6.1 <u>Antenna Performance Analysis</u>. The analysis done on this program was not carried to great depth, primarily because of the limited funding of the program. All of the computed performance data was based on a two-dimensional analysis. This should be expanded to a full 3-dimensional analysis. The tradeoff of the various antenna parameters vs. performance should be carried to greater depth. The parameters include magnification (M), primary reflector f/D, feed array element spacing, field reflector oversizing factor, and illumination taper. Also, the configuration using a planar phased array feed should be modelled. It would also be desirable to carry out a scale model build and test program.

6.2 <u>Deployable Structures</u>. The development of the deployable box truss concept is proceeding, mainly under an in-house IR&D program. The work could of course be accelerated with some contract support. The next phase of the effort will be a detailed mechanical design followed by a feasibility model build and ground verification program. This should be followed by a flight experiment to demonstrate the space deployment and determine the tolerances achieved.

6.3 <u>Attitude and Figure Control of Flexible Bodies</u>. It is recommended that a flexible body stability analysis be performed on either a selected antenna or an artificial design, combining structural bending, mast dynamics, mesh dynamics and figure control so that the problems associated with an integrated control system can be surfaced. It is further recommended that the problem of achieving reasonable reliability for lifetimes over 5 years be attacked.

Adaptive figure control does not appear to be necessary for the radar mission. However, if further work is to be done in this area, the technology of the various laser surveying systems described in Section 2.3 would have to be developed to the operational level.

APPENDIX A

RAY TRACING: DISTORTED PRIMARY REFLECTOR
TO SUBREFLECTOR

In this appendix a fourth order polynomial is derived which locates points of incidence on the subreflector due to some incident ray on the distorted primary reflector. The two-reflector confocal parabolic system is shown in Figure A-1. The polynomial is found by setting the angle of incidence equal to the angle of reflection at the surface of the primary reflector. First, the unit normal for an undistorted parabola is derived. Then it is modified to include distortions by introducing a rotation factor. The reason that the equation will be a fourth order polynomial (with four roots) is that, geometrically, setting the angle of incidence equal to the angle of reflection corresponds to two lines intersecting with the equation of the subreflector. Each line has two solutions with the parabolic subreflector. The primary reflector is made up of N equal arc length segments supported at 2N points (one support at each segment edge). Individual segments are assumed to be free of distortion (i.e. they always remain parabolic) however, the supports can undergo a displacement Δz (forward or backward). Thus, any distortion may consist of displacement and/or rotation of a segment. The distortions are represented mathematically as a rotation in unit normal and a displacement Δz_1 at the desired reflection point on the primary reflector. The equation for a parabola (no distortion) is given by

$$z = a \frac{x^2}{4f} + z_o \qquad (A-1)$$

where $a = \pm 1$ (concave or convex)
 f is the focal point
 z_o is the shift from the origin.

The rectangular coordinate system used is shown in Figure A-1. The normal to the parabola can be found by using a parametric representation of Equation (1). This is done as follows [13]:

Let $\bar{R} = \hat{x}x + \hat{z}z$ (A-2) be a position vector and choose x=t, then
$z = a \frac{t^2}{4f} + z_o$.

Equation (2) then becomes

$$\bar{R}(t) = \hat{x}t + \hat{z}\left(\frac{at^2}{4f} + z_o\right). \qquad (A-3)$$

The unit tangent vector is defined by

$$\hat{t}(t) = \frac{d\bar{R}(t)}{dt} \bigg/ \left|\frac{d\bar{R}(t)}{dt}\right| \qquad (A-4)$$

236
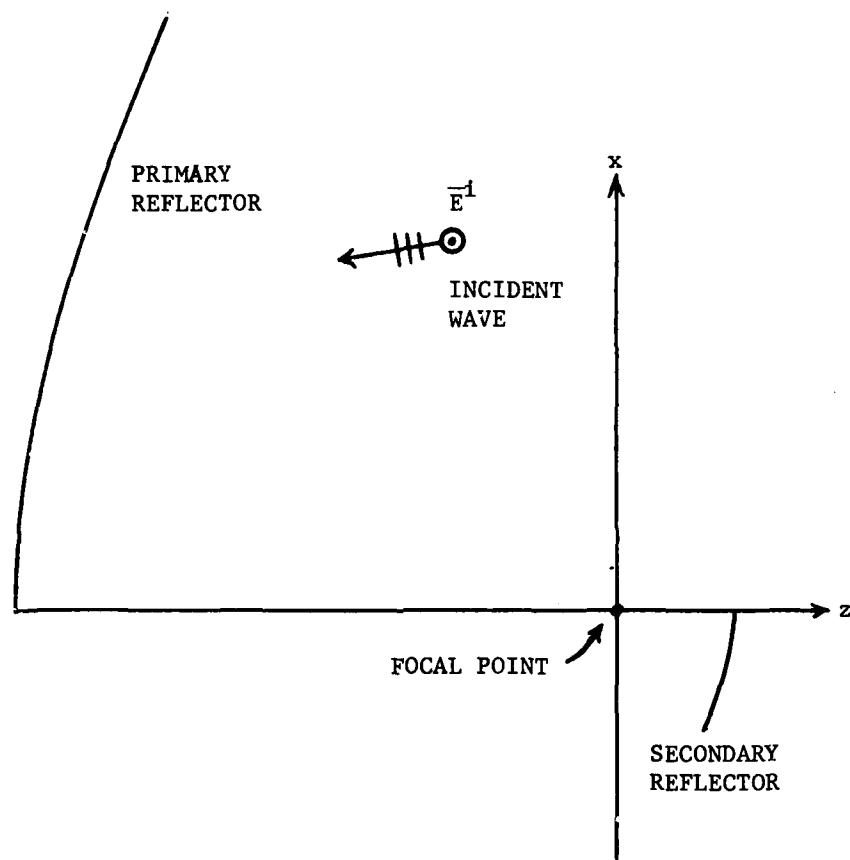
Figure A-1   Two reflector confocal parabolic system.

From Equation (3) it follows that

$$\hat{t}(t) = \frac{\hat{x} + \hat{z}\,\dfrac{at}{2f}}{\sqrt{1+(\dfrac{at}{2f})^2}} \tag{A-5}$$

The curvature is defined as

$$\overline{k} = \frac{d\hat{t}}{dt} \Bigg/ \left|\frac{d\overline{R}}{dt}\right| \tag{A-6}$$

Differentiating Equations (A-5) and (A-6) yields

$$\frac{d\hat{t}}{dt} = -\hat{x}c^2 t(1 + (ct)^2)^{-3/2} + \hat{z}c(1+(ct)^2)^{-3/2} \tag{A-7}$$

$$\left|\frac{d\overline{R}}{dt}\right| = (1+(ct)^2)^{\frac{1}{2}} \tag{A-8}$$

where $c = \dfrac{a}{2f}$ \qquad (A-9)

Thus $\overline{k} = c(1+(ct)^2)^{-2}\,(-\hat{x}ct + \hat{z})$ \qquad (A-10)

The unit normal is now defined as

$$\hat{n} = \frac{\overline{k}}{|\overline{k}|} \tag{A-11}$$

From Equation (A-10) it is clear that

$$\hat{n}(t) = \frac{c}{|c|}\,\frac{(-\hat{x}ct+\hat{z})}{\sqrt{1+(ct)^2}} \tag{A-12}$$

Note that

$$\frac{c}{|c|} = \begin{cases} +1 & a=1 \\ -1 & a=-1 \end{cases}$$

and since $x=t$ and $c = \dfrac{a}{2f}$ then

$$\hat{n}(x) = \begin{cases} \dfrac{-\hat{x}x + \hat{z}2f}{\sqrt{4f^2 + x^2}} & a = +1 \\[4mm] \dfrac{-\hat{x}x - \hat{z}2f}{\sqrt{4f^2 + x^2}} & a = -1 \end{cases} \tag{A-13}$$

238

The equation that describes the undistorted primary reflector is given by

$$z_1 = \frac{x_1^2}{4f_1} - f_1 \qquad (A-14)$$

where f is the focal distance of the primary reflector. From Equation (13) with $a = +1$ the unit normal to the primary reflector at the point x_1 is

$$\hat{n}_1(x_1) = \frac{-\hat{x}x_1 + \hat{z}2f_1}{\sqrt{4f_1^2 + x_1^2}} \qquad (A-15)$$

The determination of the new unit normal and the displacement due to a distortion is facilitated by use of two lines as follows: Let (x_a, z_a) and (x_b, z_b) be the coordinates of the two edges of any segment of the undistorted primary and let (x_a', z_a') and (x_b', z_b') be the coordinates of the same segment when it is distorted. Each set of points defines a line, ℓ_{ab} and ℓ_{ab}', as shown in Figure A-2. The unit normal to each line is given by

$$\hat{n}_{ab} = \frac{-\hat{x}(z_b - z_a) + \hat{z}(x_b - x_a)}{\sqrt{(z_b - z_a)^2 + (x_b - x_a)^2}} \qquad (A-16)$$

$$\hat{n}_{ab}' = \frac{-\hat{x}(z_b' - z_a') + \hat{z}(x_b' - x_a')}{\sqrt{(z_b' - z_a')^2 + (x_b' - x_a')^2}} \qquad (A-17)$$

The angle between n_{ab} and n_{ab}' designated as θ_3 gives the amount of rotation required to model the distortion. The undistorted unit normal vector $\hat{n}_1$ makes an angle designated θ_1 with respect to the z axis. When the segment is distorted the new unit normal vector $\hat{n}_1'$ makes an angle designated θ_2 with respect to the z axis. From Figure A-3 it is clear that

$$\theta_2 = \theta_1 + \theta_3 \qquad (A-18)$$

Taking the dot product of Equation (A-15) with $\hat{z}$ yields

$$\hat{n}_1 \cdot \hat{z} = \frac{2f_1}{\sqrt{4f_1^2 + x_1^2}} = \cos\theta_1 \qquad (A-19)$$

so

$$\theta_1 = \cos^{-1}\left(\frac{2f_1}{\sqrt{4f_1^2 + x_1^2}}\right) \qquad (A-20)$$

The sign of θ_1 is chosen positive (negative) if $\hat{z} \times \hat{n}_1$ yields $+\hat{y}$ $(-\hat{y})$.
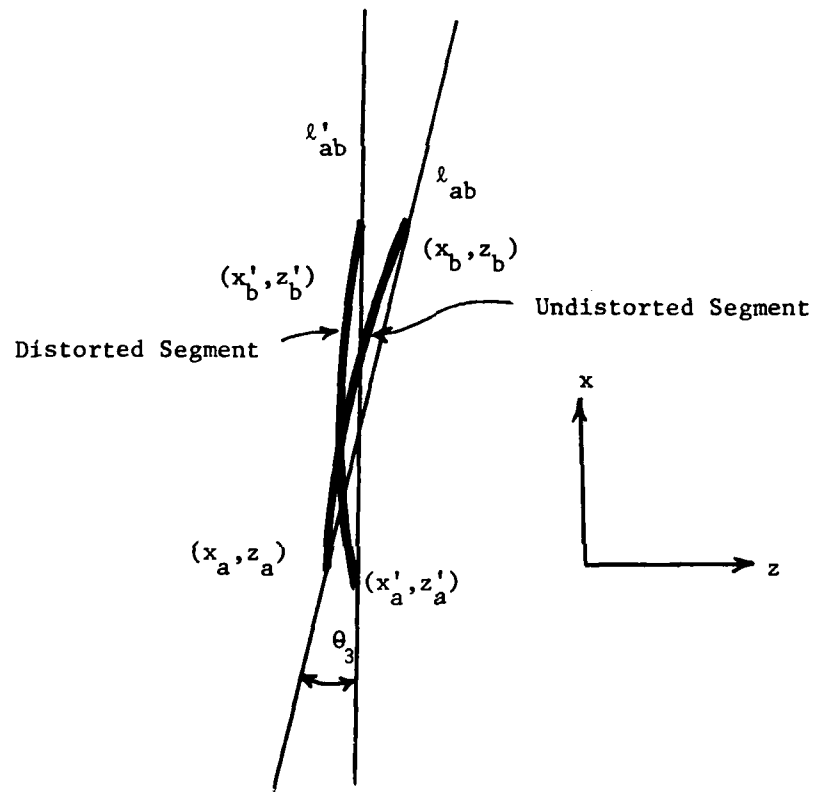
Figure A-2   Geometry relating distorted and
             undistorted segment.
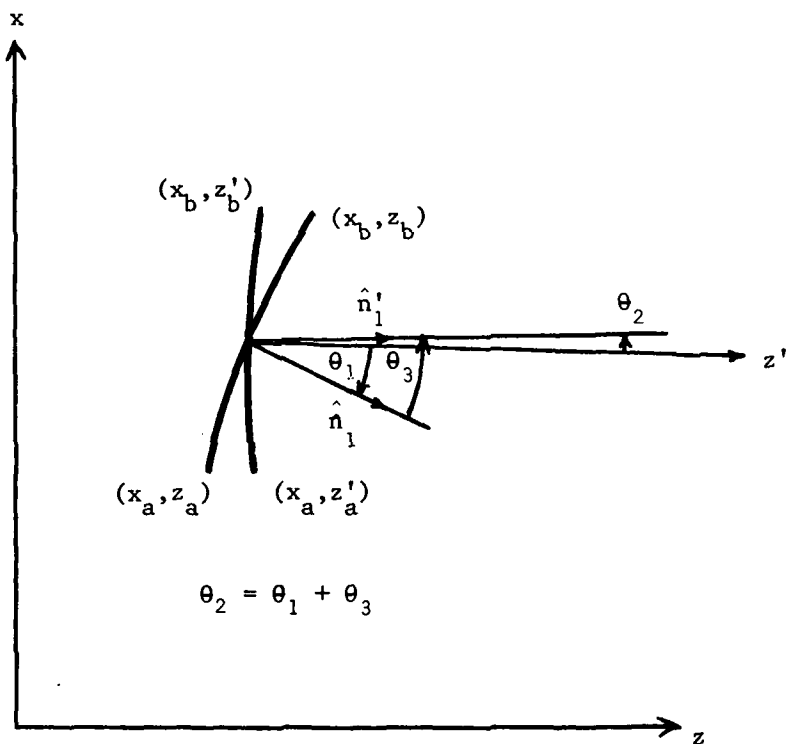
Figure A-3 Angles relating distorted and
undistorted segment.

241

By taking the dot product of Equations (A-16) and (A17) it follows that

$$\theta_3 = \cos^{-1}\left(\frac{(z_b-z_a)(z_b'-z_a') + (x_b-x_a)(x_b'-x_a')}{\sqrt{(z_b-z_a)^2 + (x_b-x_a)^2}\sqrt{(z_b'-z_a')^2 + (x_b'-x_a')^2}}\right) \tag{A-21}$$

The sign of θ_3 is chosen positive (negative) if $\hat{n}_1 \times \hat{n}_1'$ yields $+\hat{y}$ $(-\hat{y})$. The new unit normal is expressed in terms of θ_2 as

$$\hat{n}_1' = -\hat{x}\sin\theta_2 + \hat{z}\cos\theta_2 \tag{A-22}$$

Note that for the case where $\theta_3 = 0$ (no distortion) Equation (A-22) reduces to Equation (A-15) as it should.

The required displacement in the z direction due to a distortion can be determined from Figure A-3. At any point x_1 in the range (x_a, x_b) the z displacement between the distorted and undistorted segment is closely approximated by the z displacement between the lines ℓ_{ab} and ℓ_{ab}'. The equation for this displacement can be shown to be

$$\Delta z_1 = \left(\frac{x_1-x_b'}{m_n}\right) - \left(\frac{x_1-x_b}{m_o}\right) + \left(z_b' - z_b\right) \tag{A-23}$$

where

$$m_n = \frac{(x_b'-x_a')}{(z_b'-z_a')} \quad \text{is the slope of line } \ell_{ab}' \text{ and}$$

$$m_o = \frac{(x_b-x_a)}{(z_b-z_a)} \quad \text{is the slope of line } \ell_{ab}.$$

At any point x the location of the distorted **primary is given by**

$$z_1' = z_1 + \Delta z_1 \tag{A-24}$$

where z_1 is given by Equation (A-14)

Now that $\hat{n}_1'$ and z_1' have been specified, the condition that the angle of incidence equals the angle of reflection can be enforced.

Consider a ray incident at an angle θ from the axis of the two-reflector system as shown in Figure A-4. The direction of the incident ray is given by the unit vector

$$\hat{s}_1 = -\hat{x}\sin\theta - \hat{z}\cos\theta \tag{A-25}$$
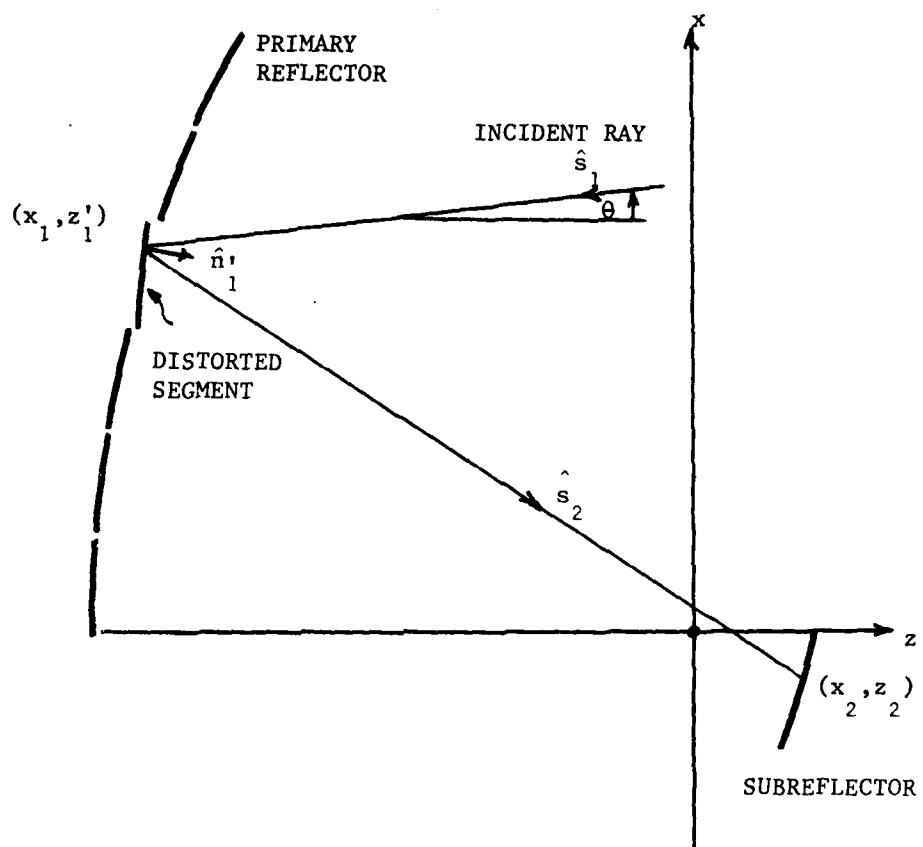
Figure A-4   Incident rag path from distorted primary
segment to subreflector.

243

The direction of the reflected ray at the point (x_1, z_1') in terms of (x_2, z_2) is given by

$$\hat{s}_2 = \frac{\hat{x}(x_2-x_1) + \hat{z}(z_2 - z_1')}{\sqrt{(x_2 - x_1)^2 + (z_2 - z_1')^2}}$$

(A-26)

The law of reflection requires that

$$-\hat{n}_1' \cdot \hat{s}_1 = \hat{n}_1' \cdot \hat{s}_2$$

(A-27)

be satisfied at the point (x_1, z_1'). From Equations (A-22 and (A-25) the left side of the above equality is

$$-\hat{n}_1' \cdot \hat{s}_1 = -\sin\theta_2\sin\theta + \cos\theta_2\cos\theta = A_2$$

(A-28)

The equation of the subreflector is given by

$$z_2 = f_2 - \frac{x_2^2}{4f_2}$$

(A-29)

where f_2 is the focal distance of the subreflector. Using Equations (A-14), (A-24) and (A-29) Equation (A-26) becomes

$$\hat{s}_2 = \frac{\hat{x}(x_2-x_1) + \hat{z}\left(A_1 - \frac{x_2^2}{4f_2}\right)}{\sqrt{(x_2 - x_1)^2 + \left(A_1 - \frac{x_2^2}{4f_2}\right)^2}}$$

(A-30)

where

$$A_1 = f_1 + f_2 - \frac{x_1^2}{4f_1} - \Delta z_1$$

(A-31)

The right side of Equation (A-27) is now found to be

$$\hat{n}_1' \cdot \hat{s}_2 = \frac{x_2\left(\sin\theta_2 + \frac{x_2}{4f_2}\cos\theta_2\right) + A_3}{\sqrt{(x_2 - x_1)^2 + \left(A_1 - \frac{x_2^2}{4f_2}\right)^2}}$$

(A-32)

where

$$A_3 = x_1\sin\theta_2 + A_1\cos\theta_2$$

(A-33)

Setting Equations (A-28) and (A-33) equal yields the following fourth order polynomial in the variable x_2

$$B_4 x_2^4 + B_3 x_2^3 + B_2 x_2^2 + B_1 x_2 + B_0 = 0$$

(A-34)

244

where

$$B_0 = A_3^2 - A_2^2 (A_1^2 + x_1^2) \quad , \tag{A-34}$$

$$B_1 = 2A_2^2 x_1 - 2A_3 S_2 \quad ,$$

$$B_2 = S_2^2 - \frac{C_2 A_3}{2f_2} - A_2^2 \left(1 - \frac{A_1}{2f_2}\right) \quad ,$$

$$B_3 = \frac{S_2 C_2}{2f_2^2} \quad ,$$

$$B_4 = \frac{C_2^2 - A_2^2}{16f_2^2} \quad ,$$

$$C_2 = \cos\theta_2 \quad , \text{ and } S_2 = \sin\theta_2 \quad .$$

The four roots in Equation (A-34) are found by using the Newton-Raphson iterative techniques. The computer program that does this is listed in Appendix C. The one correct root is chosen by comparing them against the range of possible values on the subreflector.

APPENDIX B

RAY TRACING: SUBREFLECTOR TO PRIMARY
REFLECTOR IMAGE SURFACE

In Appendix A a fourth order polynomial was found that locates points
of incidence on the subreflector for a ray reflected from the primary re-
flector. In this appendix another fourth order polynomial is found that
traces the ray from the subreflector to the phased array surface. This is
done by enforcing the law of reflection at the subreflector surface. For a
two-reflector confocal-parabolic system the primary image contour (eyepiece)
is a parabola whose equation is [14]

$$z_3 = -\frac{f_2^2}{f_1} - \frac{x_3^2}{4f_3} \tag{B-1}$$

where

$$f_3 = \frac{f_2}{\left(2 + \frac{f_2}{f_1}\right)} \tag{B-2}$$

This configuration is shown in Figure B-1. In a practical antenna system
the phased array will follow the ideal parabolic surface defined by Equation
(B-1) in steps. This configuration is shown in Figure 3.1-1. The fourth-
order polynomial found in this appendix finds the solution on the ideal para-
bolic surface. In the computer program given in Appendix C this solution
(x_3, z_3) (ideal) is referred to the stepped-parabolic surface to obtain the
desired solution (x_3, z_3) stepped. The normal to the subreflector is deter-
mined from Equations (A-13) and (A-29) to be

$$\hat{n}_2(x_2) = \frac{-\hat{x}x_2 - \hat{z}2f}{\sqrt{4f^2 + x_2^2}} \tag{B-3}$$

In Figure (B-1) the incident and reflected directions are given by

$$\hat{s}_2 = \frac{\hat{x}(x_2 - x_1) + \hat{z}(z_2 - z_1')}{\sqrt{(x_2 - x_1)^2 + (z_2 - z_1')^2}} \tag{B-4}$$

$$\hat{s}_3 = \frac{\hat{x}(x_3 - x_2) + \hat{z}(z_3 - z_2)}{\sqrt{(x_3 - x_2)^2 + (z_3 - z_2)^2}} \tag{B-5}$$

246
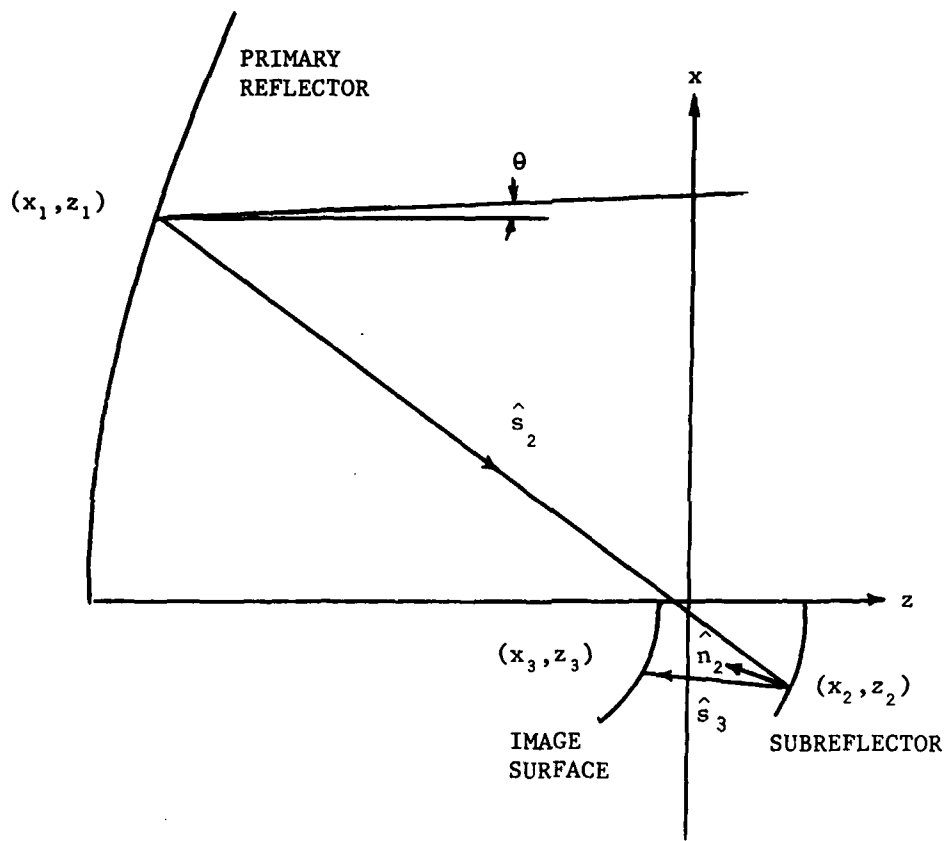
Figure B-1   Ray Path From Subreflector To Primary
              Reflector Image Surface.

Substituting Equations (A-29) and (B-1) into Equation (B-5) yields

$$\hat{s}_3 = \frac{x(x_3 - x_2) + z\left(D_1 - \frac{x_3^2}{4f_3}\right)}{\sqrt{(x_3 - x_2)^2 + \left(D - \frac{x_3^2}{4f_3}\right)^2}} \tag{B-6}$$

where

$$D_1 = \frac{-f_2^2}{f_1} - f_2 + \frac{x_2^2}{4f_2} \tag{B-7}$$

The law of reflection requires that

$$-\hat{s}_2 \cdot \hat{n}_2 = \hat{s}_3 \cdot \hat{n}_2 \tag{B-8}$$

be satisfied at the desired point (x_2, z_2). Using Equations (B-3) and (B-4) the left-hand side of Equation (B-8) is evaluated as

$$-\hat{s}_2 \cdot \hat{n}_2 = \frac{F}{\sqrt{4f_2^2 + x_2^2}} \tag{B-9}$$

where

$$F = \frac{x_2(x_2 - x_1) + 2f_2(z_2 - z_1)}{\sqrt{(x_2 - x_1)^2 + (z_2 - z_1)^2}} \tag{B-10}$$

The right-hand side of Equation (B-8) is evaluated using Equations (B-3) and (B-6) to be

$$\hat{s}_3 \cdot \hat{n}_2 = \frac{-x_3\left(x_2 - \frac{f_2}{2f_3}\right) + D_2}{\sqrt{(x_3 - x_2)^2 + \left(D_1 - \frac{x_3^2}{4f_3}\right)^2}\sqrt{4f_2^2 + x_2^2}} \tag{B-11}$$

where

$$D_2 = -2f_2 D_1 + x_2^2 \tag{B-12}$$

Setting Equations (B-9) and (B-11) equal yields the following fourth order polynomial involving the variable x_3

$$B_4 x_3^4 + B_3 x_3^3 + B_2 x_3^2 + B_1 x_3 + B_o = 0 \tag{B-13}$$

where

$$B_o = F^2(x_2^2 + D_1^2) - D_2^2 \ ,$$

$$B_1 = -2x_2 F^2 + 2D_2 x_2 \ ,$$

248

$$B_2 + F^2 \left(1 - \frac{D_1}{2f_3}\right) - x_2^2 - \frac{D_2 f_2}{f_3} \quad , \tag{B-13}$$

$$B_3 = \frac{x_2 f_2}{f_3}, \quad \text{and}$$

$$B_4 = \frac{F^2}{16f_3^2} - \left(\frac{f_2}{2f_3}\right)^2$$

The four roots in Equation (B-13) are found by using the Newton-Raphson iterative technique. The one correct root is chosen by comparing them against the range of possible values on the array.

APPENDIX C

Computer Program Listings

C.1   Program TRPPBB

```
      PROGRAM TRPPBE(INPUT,TAPE5,OUTPUT,TAPE6=OUTPUT,TAPE1,FR80)         000100
C**THIS PROGRAM CALCULATES THE ARRAY APERTURE DISTRIBUTION OF AN         000110
C**OFFSET TWO REFLECTOR (PARABOLIC-PARABOLIC CONFOCAL) SYSTEM            000120
C**PROGRAM WRITTEN BY ALAN FENN (MARTIN-MARIETTA)                        000130
C**MODIFIED TO RUN BATCH                                                 000140
      COMPLEX ESA(4000),ESI(500),EA                                      000150
      DIMENSION ZAPP(20),ZBPP(20),T(21),XS3(4000),SA3(500),INUMRY(500)   000160
      DIMENSION EMAG(500),EPHAD(500)                                     000170
      LOGICAL DPR                                                        000180
C     CALL CONNEC(5LINPUT)                                               000190
C**ESA AND XS3 DIMENSIONS ARE PROPORTIONAL TO THE NUMBER OF SAMPLES NPS. 000200
      ITIMES=0                                                           000210
      NSBGN=1                                                            000220
      READ(5,*)F1,F2                                                     000230
      READ(5,*)X1L,X1U,X2L,X2U                                           000240
      READ(5,*)X3L,X3U                                                   000250
      READ(5,*)NMDS                                                      000260
      NMDSM1=NMDS-1                                                      000270
      READ(5,*)DPR                                                       000280
      IF(DPR)711,811                                                     000290
811   DO 200 I=1,NMDSM1                                                 000300
      ZBPP(I)=0.0                                                        000310
      ZAPP(I)=0.0                                                        000320
200   CONTINUE                                                          000330
      GO TO 24                                                          000340
711   DO 23 I=1,NMDSM1                                                 000350
C     WRITE(5,7)I                                                       000360
7     FORMAT(1X,*SECTION#*,I3,2X,*INCREMENTAL DISTORTION FOR ZB=*)       000370
      READ(5,*)ZBPP(I)                                                   000380
C     WRITE(5,8)                                                         000390
8     FORMAT(1X,*INCREMENTAL DISTORTION FOR ZA=*)                        000400
      READ(5,*)ZAPP(I)                                                   000410
23    CONTINUE                                                          000420
24    READ(5,*)TD                                                       000430
      READ(5,*)SN                                                        000440
      READ(5,*)NDS                                                       000450
      DO 321 KTIM=1,NDS                                                  000460
      READ(5,*)NPS                                                       000470
      CALL SECOND(ACPUA1)                                                000480
      ITIMES=ITIMES+1                                                    000490
      F3=F2/(2.+F2/F1)                                                   000500
      ISPILS=0                                                           000510
      ISPILA=0                                                           000520
      IBLCPS=0                                                           000530
      IBLCSB=0                                                           000540
      X3BGN=0.0                                                          000550
      INUM=0                                                             000560
      CALL SECOND(ACPU1)                                                 000570
      CALL PARDIV(X1L,X1U,NMDS,F1,ST,T)                                  000580
3456  CONTINUE                                                          000590
      T(NMDS)=X1U                                                        000600
      X1UM1=X1U-.001                                                     000610
      X1UP1=X1U+.001                                                     000620
      ISKIP=0                                                            000630
      ICT=0                                                              000640
      T2=0.0                                                             000650
      DELX=(X1U-X1L)/(NPS-1)                                             000660
      DO 40 I=1,NMDSM1                                                   000670
      IP1=I+1                                                            000680
      XA=T(I)                                                            000690
      XB=T(IP1)                                                          000700
      ZA=XA*XA/(4.*F1)-F1                                                000710
      ZB=XB*XB/(4.*F1)-F1                                                000720
```

```
        IF(ISKIP.EQ.1)GO TO 912                                  000730
99      CALL PRILC2(ICT,DELX,T1,T2)                              000740
        X1=T1                                                    000750
        IF(X1.GT.X1UM1.AND.X1.LT.X1UP1)X1=X1UM1                  000760
912     IF(X1.LE.XB)ZBP=ZB+ZBPP(I)                               000770
        IF(X1.LE.XB)ZAP=ZA+ZAPP(I)                               000780
        IF(X1.GT.XB)ISKIP=1                                      000790
        IF(X1.GT.XB)GO TO 40                                     000800
        ISKIP=0                                                  000810
        CALL SUBRFD(TD,X1,F1,F2,XA,XB,ZA,ZB,ZAP,ZBP,X2L,X2U,Z1,X2,IRTFS) 000820
        IF(IRTFS.EQ.0)ISPILS=ISPILS+1                            000830
        IF(IRTFS.EQ.2)IBLCSB=IBLCSB+1                            000840
        IF(IRTFS.EQ.0.AND.TD.LT.0.0)X3BGN=X3                     000850
        WRITE(6,7576)IRTFS,X3BGN                                 000860
7576    FORMAT(1X,*IRTFS=*,I4,2X,*X3BGN=*,F12.5)                 000870
        IF(IRTFS.NE.1)GO TO 99                                   000880
        Z2=F2-X2*X2/(4.*F2)                                      000890
        CALL PARRAY(X1,Z1,X2,F1,F2,X3L,X3U,X3,IRTFA)             000900
        I3=X3/SN-1                                               000910
        X3MIN=I3*SN                                              000920
        X3MAX=X3MIN+SN                                           000930
        X3I=(X3MAX+X3MIN)/2.                                     000940
        Z3=-F2*F2/F1-X3I*X3I/(4.*F3)                             000950
        RL21=SQRT((X2-X1)**2+(Z2-Z1)**2)                         000960
        RL32=SQRT((X3-X2)**2+(Z3-Z2)**2)                         000970
        IF(IRTFA.EQ.0)ISPILLA=ISPILLA+1                          000980
        IF(IRTFA.EQ.2)IBLCPS=IBLCPS+1                            000990
        IF(IRTFA.NE.1)GO TO 99                                   001000
        INUM=INUM+1                                              001010
        IF(INUM.EQ.1)X3BGN=X3                                    001020
        GO TO 9871                                               001030
7198    CONTINUE                                                 001040
9871    CALL PROJCS(F1,F2,F3,X2,X3,P)                            001050
        CALL EIARRY(TD,SN,X1,Z1,RL21,RL32,P,EA)                  001060
        EAMAG=CABS(EA)                                           001070
        EAPHAD=ATAN2(AIMAG(EA),REAL(EA))*180./3.14159265         001080
        WRITE(6,5765)X1,X2,X3,EA,RL21,RL32,EAMAG,EAPHAD          001090
5765    FORMAT(1X,*X1=*,F9.4,2X,*X2=*,F9.4,2X,*X3=*,F9.4,2X,     001100
       2*EA=*,2E12.5,2X,*RL21=*,E12.6,2X,*RL32=*,F8.4,2X,E10.3,2X, 001110
       3F8.3)                                                    001120
        ESA(INUM)=EA                                             001130
        XS3(INUM)=X3                                             001140
        X3FINL=X3                                                001150
        GO TO 99                                                 001160
40      CONTINUE                                                 001170
        CALL SECOND(ACPUA2)                                      001180
        ACPU21=ACPUA2-ACPUA1                                     001190
        WRITE(6,1794)ACPU21                                      001200
1794    FORMAT(1X,*CPU FOR FIELD CONTRIBUTIONS=*,F14.3)          001210
        NCON=INUM                                                001220
        IAT=0                                                    001230
        CALL SECOND(ACPUB1)                                      001240
        DO 41 I=1,500                                            001250
        IAT=IAT+1                                                001260
        X3MX=-SN*(I-1)                                           001270
        X3MN=-SN*I                                               001280
        WRITE(6,1515)X3MX,X3MN                                   001290
1515    FORMAT(1X,*X3MX=*,F12.5,2X,*X3MN=*,F12.5)                001300
        IF(X3MN.LT.X3L)GO TO 33                                  001310
        SA3(IAT)=-(X3MX+X3MN)/2.                                 001320
        CALL SORTEA(IAT,X3MN,X3MX,NCON,XS3,ESA,ESI,INUMRY)       001330
41      CONTINUE                                                 001340
33      NAP=IAT-1                                                001350
```

253

```
          CALL SECOND(ACPUB2)                                           001360
          ACPU21=ACPUB2-ACPUB1                                          001370
          WRITE(6,1321)ACPU21                                           001380
1321      FORMAT(1X,*CPU FOR SORTING FIELD CONTRIBUTIONS=*,F14.3)       001390
          FAC=1.                                                        001400
          RNSBGN=NSBGN                                                  001410
          RNPS=NPS                                                      001420
          IF(ITIMES.GT.1)FAC=RNSBGN/RNPS                                001430
C         WRITE(5,6767)ITIMES,NSBGN,FAC                                 001440
6767      FORMAT(1X,*ITIMES=*,I5,2X,*NSBGN=*,I5,2X,*FAC=*,F12.5)        001450
          WRITE(6,71)F1,F2,F3                                           001460
71        FORMAT(1X,*F1=*,F12.3,2X,*F2=*,F12.3,2X,*F3=*,F12.5)          001470
          WRITE(6,72)X1L,X1U,X2L,X2U                                    001480
72        FORMAT(1X,*X1L=*,F12.3,2X,*X1U=*,F12.3,2X,*X2L=*,F12.3,2X,*X2U=*, 001490
         2F12.3)                                                        001500
          WRITE(6,8364)X3L,X3U                                          001510
8364      FORMAT(1X,*X3L=*,F12.5,2X,*X3U=*,F12.5)                       001520
          WRITE(6,73)TD,SN,NPS,FAC                                      001530
73        FORMAT(1X,*TD=*,F10.4,2X,*SN=*,F12.4,2X,*NPS=*,I7,2X,*FAC=*,F12.4)001540
          WRITE(6,700)NAP,NCON                                          001550
700       FORMAT(1X,*NAP=*,I5,2X,*NCON=*,I5)                            001560
          BIGE=0.0                                                      001570
          DO 199 IE=1,NAP                                               001580
          EMG=CABS(ESI(IE))                                             001590
          IF(EMG.GT.BIGE)BIGE=EMG                                       001600
199       CONTINUE                                                      001610
          DO 42 I=1,NAP                                                 001620
          EMAG(I)=CABS(ESI(I))*FAC                                      001630
          IF(EMAG(I).EQ.0.)GO TO 9000                                   001640
          EPHAD(I)=ATAN2(AIMAG(ESI(I)),REAL(ESI(I)))*180./3.14159265    001650
          WRITE(6,50)I,SA3(I),EMAG(I),EPHAD(I),INUMRY(I)                001660
50        FORMAT(1X,I4,2X,*SA3=*,F14.4,2X,*EMAG=*,E15.5,2X,*EPHAD=*,F14.4 001670
         2,2X,*INUMRY=*,I5)                                             001680
9000      IF(EMAG(I).EQ.0.)WRITE(6,5000)I,SA3(I)                        001690
5000      FORMAT(1X,I4,2X,*SA3(I)=*,F14.4,2X,*EMAG=0      INUMRY(I)=0*)  001700
42        CONTINUE                                                      001710
          WRITE(6,74)ISPILS,ISPILA,IBLCPS                               001720
74        FORMAT(1X,*ISPILS=*,I5,2X,*ISPILA=*,I5,2X,*IBLCPS=*,I5)       001730
          WRITE(6,9515)IBLCSB                                           001740
9515      FORMAT(1X,*IBLCSB=*,I5)                                       001750
          DO 101 I=1,NMDSM1                                             001760
          WRITE(6,75)I,ZAPP(I),ZBPP(I)                                  001770
75        FORMAT(1X,*SECTION#*,I3,2X,*ZAPP(I)=*,F15.7,2X,*ZBPP(I)=*,F15.7) 001780
101       CONTINUE                                                      001790
          IF(ITIMES.EQ.1)NSBGN=NPS                                      001800
          EMAX=BIGE                                                     001810
C         CALL PLOTE(X3L,SA3,EMAG,EMAX,EPHAD,NAP)                       001820
          WRITE(1)NMDSM1,T                                              001830
          WRITE(1)SA3,ESI                                               001840
          WRITE(1)ZAPP,ZBPP                                             001850
          WRITE(1)F1,F2,F3                                              001860
          WRITE(1)X1L,X1U,X2L,X2U                                       001870
          WRITE(1)TD,SN,NAP,NCON                                        001880
          WRITE(1)X3L,X3U                                               001890
          WRITE(1)X3BGN,X3FINL                                          001900
321       CONTINUE                                                      001910
          CALL SECOND(ACPU2)                                            001920
          ACPU21=ACPU2-ACPU1                                            001930
          WRITE(6,52)ACPU21                                             001940
52        FORMAT(1X,*CPU FOR THIS RUN=*,F14.3)                          001950
          CALL EXIT                                                     001960
          END                                                          001970
          SUBROUTINE PARDIV(XMIN,XMAX,NMDS,F1,ST,T)                     001980
```

254

```
C****THIS SUBROUTINE DIVIDES A PARABOLA INTO (NMDS-1) EQUAL ARC LENGTH    001900
C****SEGMENTS                                                             002000
C****PROGRAM BY ALAN FENN                                                 002010
      DIMENSION T(21),IT(21)                                              002020
222   FORMAT(1X,2F15.5,I7,F15.5)                                          002030
      C=2.*F1                                                             002040
      CS=C*C                                                              002050
      Q1=1./(2.*C)                                                        002060
      T1=XMIN                                                             002070
      T2=XMAX                                                             002080
      T1S=T1*T1                                                           002090
      T2S=T2*T2                                                           002100
      Q2=T2*SQRT(CS+T2S)                                                  002110
      ARG2=T2+SQRT(CS+T2S)                                                002120
      Q3=CS*ALOG(ARG2)                                                    002130
      Q4=T1*SQRT(CS+T1S)                                                  002140
      ARG1=T1+SQRT(CS+T1S)                                                002150
      Q5=CS*ALOG(ARG1)                                                    002160
      ST=Q1*(Q2+Q3)-Q1*(Q4+Q5)                                           002170
      S=ST/(NMDS-1)                                                       002180
      T(1)=XMIN                                                           002190
      IT(1)=0                                                             002200
      DO 1 I=2,NMDS                                                       002210
      IT(I)=0                                                             002220
      IM1=I-1                                                             002230
      IM2=I-2                                                             002240
      T(I)=T(IM1)+S                                                       002250
      IF(I.GE.3) T(I)=T(IM1)+(T(IM1)-T(IM2))                             002260
      T1=T(IM1)                                                           002270
      T1S=T1*T1                                                           002280
7     CONTINUE                                                            002290
      IT(I)=IT(I)+1                                                       002300
      T2=T(I)                                                             002310
      T2S=T2*T2                                                           002320
      Q2=T2*SQRT(CS+T2S)                                                  002330
      ARG2=T2+SQRT(CS+T2S)                                                002340
      Q3=CS*ALOG(ARG2)                                                    002350
      Q4=T1*SQRT(CS+T1S)                                                  002360
      ARG1=T1+SQRT(CS+T1S)                                                002370
      Q5=CS*ALOG(ARG1)                                                    002380
      G2=Q1*(Q2+Q3)                                                       002390
      G1=Q1*(Q4+Q5)                                                       002400
      SP=G2-G1                                                            002410
C     WRITE(6,47)I,S,SP                                                   002420
47    FORMAT(1X,2HI=,I3,2X,2HS=,F15.7,2X,3HSP=,F15.7)                    002430
      IF(ABS(SP-S).LT.0.0001) GO TO 1                                     002440
      IF(SP.GT.S) T(I)=T(I)-(SP-S)                                        002450
      IF(SP.LT.S) T(I)=T(I)+(S-SP)                                        002460
      GO TO 7                                                             002470
1     CONTINUE                                                            002480
      DO 9 I=1,NMDS                                                       002490
      WRITE(6,12)I,IT(I),T(I)                                             002500
12    FORMAT(1X,3HIT(,I2,2H)=,1X,I7,2X,*T(I)=*,F15.5)                    002510
9     CONTINUE                                                            002520
      RETURN                                                             002530
      END                                                                002540
      SUBROUTINE PRILC2(ICT,DELX,T1,T2)                                   002550
      ICT=ICT+1                                                           002560
      T1=T2                                                               002570
      T2=DELX*ICT                                                         002580
      RETURN                                                             002590
      END                                                                002600
      SUBROUTINE SUBRFD(TD,X1,F1,F2,XA,XB,ZA,ZB,ZAP,ZBP,X2L,X2U,Z1,X2,  002610
```

255

```
      2IRTF)                                                               002820
C**THIS SUBROUTINE LOCATES POINTS OF REFLECTION ON THE SUB-REFLECTOR.      002830
      DIMENSION B(5),COF(5),ROOTR(4),ROOTI(4)                              002640
      TR=TD*3.14159265/180.                                                002650
      F1S=F1*F1                                                            002660
      F2S=F2*F2                                                            002670
      X1S=X1*X1                                                            002680
      XAP=XA                                                               002690
      XBP=XB                                                               002700
      XBA=XB-XA                                                            002710
      XBAP=XBP-XAP                                                         002720
      ZBA=ZB-ZA                                                            002730
      ZBAP=ZBP-ZAP                                                         002740
      PNUM=ZBA*ZBAP+XBA*XBAP                                               002750
      PDEN1=SQRT(ZBA*ZBA+XBA*XBA)                                          002760
      PDEN2=SQRT(ZBAP*ZBAP+XBAP*XBAP)                                      002770
      PABP=PNUM/PDEN1/PDEN2                                                002780
      IF(PABP.GT.1.0.AND.PABP.LT.1.01)PABP=1.0                             002790
      T3R=ACOS(PABP)                                                       002800
      ARG1=2.*F1/SQRT(4.*F1S+X1S)                                          002810
      T1R=ACOS(ARG1)                                                       002820
      T2R=T1R-T3R                                                          002830
      ZDIF1=ZBP-ZB                                                         002840
      ZDIF2=ZAP-ZA                                                         002850
      IF(ZDIF1.GT.ZDIF2)T2R=T1R+T3R                                        002860
      C2=COS(T2R)                                                          002870
      S2=SIN(T2R)                                                          002880
      A2=-S2*SIN(TR)+C2*COS(TR)                                            002890
      RMO=XBA/ZBA                                                          002900
      FMN=XBAP/ZBAP                                                        002910
      DELZ1=(X1-XBP)/RMN-(X1-XB)/RMO+ZBP-ZB                                002920
      Z1=X1S/(4.*F1)-F1+DELZ1                                              002930
      A1=F1+F2-X1S/(4.*F1)-DELZ1                                           002940
      A3=X1*S2+A1*C2                                                       002950
C     WRITE(6,76)A1,A2,A3,C2,S2                                            002960
76    FORMAT(1X,5E15.5)                                                    002970
      A1S=A1*A1                                                            002980
      A2S=A2*A2                                                            002990
      A3S=A3*A3                                                            003000
      B(1)=A3S-A2S*(A1S+X1S)                                               003010
      B(2)=2.*A2S*X1-2.*A3*S2                                              003020
      B(3)=S2*S2-C2*A3/(2.*F2)-A2S*(1.-A1/(2.*F2))                         003030
      B(4)=S2*C2/(2.*F2)                                                   003040
      B(5)=(C2*C2-A2S)/(16.*F2*F2)                                         003050
C     WRITE(6,78)B(1),B(2),B(3),B(4),B(5)                                  003060
78    FORMAT(1X,5E14.5)                                                    003070
      M=4                                                                  003080
      IF(B(5).LT.1.0E-12)M=3                                               003090
      IF(TR.EQ.0.AND.X1.EQ.0.AND.T3R.EQ.0.)X2=0.                           003100
      IF(TR.EQ.0.AND.X1.EQ.0.AND.T3R.EQ.0.)IRTF=1                          003110
      IF(TR.EQ.0.AND.X1.EQ.0.AND.T3R.EQ.0.)GO TO 29                        003120
      CALL POLRT(B,COF,M,ROOTR,ROOTI,IER)                                  003130
      X2=1.0                                                               003140
      IRTF=0                                                               003150
      DO 1 I=1,M                                                           003160
C     WRITE(6,3)I,ROOTR(I),ROOTI(I),IER                                    003170
3     FORMAT(1X,*X2(*,I1,*)=*,F15.5,3X,F15.5,1X,*  J*,*  IER=*,I2)         003180
      IF(ROOTI(I).NE.0.) GO TO 1                                           003190
      IF(ROOTR(I).GE.X2L.AND.ROOTR(I).LE.X2U) X2=ROOTR(I)                  003200
      IF(ROOTR(I).GE.X2L.AND.ROOTR(I).LE.X2U) IRTF=IRTF+1                  003210
1     CONTINUE                                                             003220
29    RETURN                                                               003230
      END                                                                  003240
```

```
      SUBROUTINE ETARRY(TD,SN,X1,Z1,RL21,RL32,P,EA)           003250
C**THIS SUBROUTINE CALCULATES THE E FIELD INCIDENT ON THE ARRAY  003260
      COMPLEX J,EO,SP21,SP32,EA                                003270
      PI=3.14159265                                            003280
      B=2.*PI                                                  003290
      TR=TD*PI/180.                                            003300
      J=(0.,1.)                                                003310
      EO=CEXP(J*B*(X1*SIN(TR)+Z1*COS(TR)))                     003320
      SP21=CEXP(-J*B*RL21)                                     003330
      SP32=CEXP(-J*B*RL32)                                     003340
      PTR=P*P                                                  003350
      IF(SN.LT.0.8)PTR=P                                       003360
      EA=EO*SP21*SP32*PTR                                      003370
      RETURN                                                   003380
      END                                                      003390
      SUBROUTINE SORTEA(ICT,X3L,X3U,NCON,XS3,ESA,EI,INUMRY)    003400
C**THIS SUBROUTINE CALCULATES E FIELD CONTRIBUTIONS TO EACH APERTURE  003410
      COMPLEX ESA(1),EI(1)                                     003420
      DIMENSION XS3(1),INUMRY(1)                               003430
      EI(ICT)=(0.,0.)                                          003440
      INUMRY(ICT)=0                                            003450
      DO 77 I=1,NCON                                           003460
      IF(XS3(I).LE.X3U.AND.XS3(I).GE.X3L)EI(ICT)=EI(ICT)+ESA(I)  003470
      IF(XS3(I).LE.X3U.AND.XS3(I).GE.X3L)INUMRY(ICT)=INUMRY(ICT)+1  003480
77    CONTINUE                                                 003490
      RETURN                                                   003500
      END                                                      003510
      SUBROUTINE POLRT(XCOF,COF,M,ROOTR,ROOTI,IER)             003520
      DIMENSION XCOF(1),COF(1),ROOTR(1),ROOTI(1)               003530
      DOUBLE PRECISION XO,YO,X,Y,XPR,YPR,UX,UY,V,YT,XT,U,XT2,YT2,SUMSQ,  003540
     2DX,DY,TEMP,ALPHA                                         003550
      ITWO=2                                                   003560
      IFIT=0                                                   003570
      N=M                                                      003580
      IER=0                                                    003590
      IF(XCOF(N+1))10,25,10                                    003600
10    IF(N)15,15,32                                            003610
15    IER=1                                                    003620
20    RETURN                                                   003630
25    IER=4                                                    003640
      GO TO 20                                                 003650
30    IER=2                                                    003660
      GO TO 20                                                 003670
32    IF(N-36)35,35,30                                         003680
35    NX=N                                                     003690
      NXX=N+1                                                  003700
      N2=1                                                     003710
      KJ1=N+1                                                  003720
      DO 40 L=1,KJ1                                            003730
      MT=KJ1-L+1                                               003740
40    COF(MT)=XCOF(L)                                          003750
45    XO=.00500101                                             003760
      YO=0.01000101                                            003770
      IN=0                                                     003780
50    X=XO                                                     003790
      XO=-10.0*YO                                              003800
      YO=-10.0*X                                               003810
      X=XO                                                     003820
      Y=YO                                                     003830
      IN=IN+1                                                  003840
      GO TO 59                                                 003850
      IFIT=1                                                   003860
      XPR=X                                                    003870
```

257

```
        YPR=Y                                          003060
59      ICT=0                                          003990
60      UX=0.0                                         003900
        UY=0.0                                         003910
        V=0.0                                          003920
        YT=0.0                                         003930
        XT=1.0                                         003940
        U=COF(N+1)                                     003950
        IF(U)65,130,65                                 003900
65      DO 70 I=1,N                                    003970
        L=N-I+1                                        003980
        TEMP=COF(L)                                    003990
        XT2=X*XT-Y*YT                                  004000
        YT2=X*YT+Y*XT                                  004010
        U=U+TEMP*XT2                                   004020
        V=V+TEMP*YT2                                   004030
        FI=I                                           004040
        UX=UX+FI*XT*TEMP                               004050
        UY=UY-FI*YT*TEMP                               004060
        XT=XT2                                         004070
70      YT=YT2                                         004060
        SUMSQ=UX*UX+UY*UY                              004090
        IF(SUMSQ)75,110,75                             004100
75      DX=(V*UY-U*UX)/SUMSQ                           004110
        X=X+DX                                         004120
        DY=-(U*UY+V*UX)/SUMSQ                          004130
        Y=Y+DY                                         004140
78      IF(DABS(DY)+DABS(DX)-1.0D-05)100,80,80         004150
80      ICT=ICT+1                                      004160
        IF(ICT-500)60,85,85                            004170
85     'IF(IFIT)100,90,100                             004180
90      IF(IN-5)50,95,95                               004190
95      IER=3                                          004200
        GO TO 20                                       004210
100     DO 105 L=1,NXX                                 004220
        MT=KJ1-L+1                                     004230
        TEMP=XCOF(MT)                                  004240
        XCOF(MT)=COF(L)                                004250
105     COF(L)=TEMP                                    004260
        ITEMP=N                                        004270
        N=NX                                           004280
        NX=ITEMP                                       004290
        IF(IFIT)120,55,120                             004300
110     IF(IFIT)115,50,115                             004310
115     X=XPR                                          004320
        Y=YPR                                          004330
120     IFIT=0                                         004340
122     IF(DABS(Y)-1.0D-4*DABS(X))135,125,125          004350
125     ALPHA=X+X                                      004360
        SUMSQ=X*X+Y*Y                                  004370
        N=N-2                                          004330
        GO TO 140                                      004390
130     X=0.0                                          004400
        NX=NX-1                                        004410
        NXX=NXX-1                                      004420
135     Y=0.0                                          004430
        SUMSQ=0.0                                      004440
        ALPHA=X                                        004450
        N=N-1                                          004460
140     COF(ITWO)=COF(ITWO)+ALPHA*COF(1)               004470
145     DO 150 L=2,N                                   004480
150     COF(L+1)=COF(L+1)+ALPHA*COF(L)-SUMSQ*COF(L-1)  004490
155     ROOTI(N2)=Y                                    004500
```

258

```
          ROOTR(N2)=X                                                    004510
          N2=N2+1                                                        004520
          IF(SUMSQ)160,165,160                                           004530
160       Y=-Y                                                           004540
          SUMSQ=0.0                                                      004550
          GO TO 155                                                      004560
165       IF(N)20,20,45                                                  004570
          END                                                            004580
          SUBROUTINE PLOTE(X3L,S3,EMAG,EMAX,EPHAD,NPNTS)                 004590
          DIMENSION S3(1),EMAG(1),EPHAD(1)                               004600
          LOGICAL PLOT,HARDC,WPLOTA                                      004610
          XMX=ABS(X3L)                                                   004620
C         WRITE(5,22)                                                    004630
22        FORMAT(1X,*WANT TO PLOT? T.OR.F*)                              004640
          READ(5,*)PLOT                                                  004650
          IF(PLOT)7,88                                                   004660
7         CALL TEKTRN(960)                                               004670
99        CALL BGNPL(1)                                                  004680
          CALL PHYSOR(2.5,1.0)                                           004690
          CALL TITLE(10HPHASE OF E,10,17HLOCATION ON ARRAY,17,          004700
         215HPHASE (DEGREES),15,4.,3.)                                   004710
          CALL XTICKS(4)                                                 004720
          CALL YTICKS(2)                                                 004730
          CALL GRAF(0.,"SCALE",XMX,-180.,90.,180.)                      004740
          CALL GRID(1,1)                                                 004750
          CALL MARKER(10)                                                004760
          CALL CURVE(S3,EPHAD,NPNTS,-1)                                  004770
          CALL ENDGR(1)                                                  004780
          CALL BGNPL(2)                                                  004790
          CALL OREL(0.,4.)                                               004800
          CALL TITLE(14HMAGNITUDE OF E,14,17HLOCATION ON ARRAY,17,      004810
         211HMAGNITUDE E,11,4.,3.)                                       004820
          CALL XTICKS(4)                                                 004830
          CALL YTICKS(2)                                                 004840
          CALL GRAF(0.,"SCALE",XMX,0.,"SCALE",EMAX)                     004850
          CALL GRID(1,1)                                                 004860
          CALL MARKER(10)                                                004870
          CALL CURVE(S3,EMAG,NPNTS,-1)                                   004880
          CALL ENDPL(2)                                                  004890
C88       WRITE(5,23)                                                    004900
23        FORMAT(1X,*WANT HARD COPY? T.OR.F*)                            004910
88        READ(5,*)HARDC                                                 004920
          IF(HARDC)12,77                                                 004930
12        CALL FR80(3)                                                   004940
          GO TO 99                                                       004950
C77       WRITE(5,24)                                                    004960
24        FORMAT(1X,*WANT TO PLOT AGAIN? T.OR.F*)                        004970
77        READ(5,*)WPLOTA                                                004980
          IF(WPLOTA)7,42                                                 004990
42        RETURN                                                         005000
          END                                                            005010
C***THIS SUBROUTINE CALCULATES POINTS OF INCIDENCE ON THE PHASED        005020
C***ARRAY WHICH WAS PARABOLIC BUT REPLACED BY STRAIGHT LINE SEGMENTS    005030
          SUBROUTINE PARPST(X1,Z1,X2,F1,F2,F3,X3MIN,X3MAX,Z3I,X3,IRTF,RL21, 005040
         2RL32)                                                         005050
          DIMENSION X3R(2)                                               005060
          X2S=X2*X2                                                      005070
          Z2=F2-X2S/(4.*F2)                                             005080
          BI=Z3I-Z2                                                      005090
          BIS=BI*BI                                                      005100
          X23=X2S*X2                                                     005110
          X24=X23*X2                                                     005120
          F2S=F2*F2                                                      005130
```

```
            Z0=-F2S/F1                                           005140
            D1=Z0-F2+X2S/(4.*F2)                                 005150
            FNUM=X2*(X2-X1)+2.*F2*(Z2-Z1)                        005160
            FDEN=SQRT((X2-X1)**2+(Z2-Z1)**2)                     005170
            IF(X1.EQ.0.AND.X2.EQ.0)X3=0.0                        005180
            IF(X1.EQ.0.AND.X2.EQ.0)IRTF=1                        005190
            IF(X1.EQ.0.AND.X2.EQ.0)GO TO 88                      005200
            F=FNUM/FDEN                                          005210
            FS=F*F                                               005220
            A=FS-X2S                                             005230
            B=2.*X23-4.*F2*X2*BI-2.*FS*X2                        005240
            C=FS*(X2S+BIS)-X24+4.*F2*X2S*BI-4.*F2S*BIS           005250
            BS=B*B                                               005260
            DIS=BS-4.*A*C                                        005270
            IF(DIS.LT.0.)GO TO 55                                005280
            X3R(1)=(-B+SQRT(DIS))/(2.*A)                         005290
            X3R(2)=(-B-SQRT(DIS))/(2.*A)                         005300
            IF(X3R(1).LT.0.AND.X3R(2).LT.0.)IRTF=2               005310
            IF(X3R(1).LT.0.AND.X3R(2).LT.0.)GO TO 88             005320
            IRTF=0                                               005330
            DO 1 I=1,2                                           005340
            IF(X3R(I).LE.X3MAX.AND.X3R(I).GE.X3MIN)X3=X3R(I)     005350
            IF(X3R(I).LE.X3MAX.AND.X3R(I).GE.X3MIN)IRTF=IRTF+1   005360
     1      CONTINUE                                             005370
     55     IF(DIS.LT.0.)WRITE(6,12)                             005380
     12     FORMAT(1X,*ROOTS ARE COMPLEX*)                       005390
     88     Z3=Z3I                                               005400
            RL21=FDEN                                            005410
            RL32=SQRT((X3-X2)**2+(Z3-Z2)**2)                     005420
            RETURN                                               005430
            END                                                  005440
            SUBROUTINE PROJCS(F1,F2,F3,X2,X3,P)                  005450
C***THIS SUBROUTINE CALCULATES THE PROJECTION ON THE NORMAL TO THE 005460
C***PHASED ARRAY                                                 005470
            X3S=X3*X3                                            005480
            D1=-F2*F2/F1-F2+X2*X2/(4.*F2)                        005490
            RNUM=X3S/(4.*F3)-D1                                  005500
            DEN=SQRT((X3-X2)**2+(X3S/(4.*F3)-D1)**2)             005510
            P=RNUM/DEN                                           005520
            IF(P.GT.1.0.AND.P.LT.1.01)P=1.0                      005530
            RETURN                                               005540
            END                                                  005550
            SUBROUTINE PARRAY(X1,Z1,X2,F1,F2,X3L,X3U,X3,IRTF)    005560
C****THIS PROGRAM CALCULATES INCIDENT POINTS ON THE PHASED ARRAY SURFACE005570
C****PROGRAM BY ALAN FENN                                        005580
            DIMENSION B(5),COF(5),ROOTR(4),ROOTI(4)              005590
            F3=F2/(2.+F2/F1)                                     005600
            Z0=-F2**2/F1                                         005610
            X2S=X2*X2                                            005620
            D1=Z0-F2+X2S/(4.*F2)                                 005630
            Z2=F2-X2S/(4.*F2)                                    005640
            FNUM=X2*(X2-X1)+2.*F2*(Z2-Z1)                        005650
            FDEN=SQRT((X2-X1)**2+(Z2-Z1)**2)                     005660
            IF(X1.EQ.0.AND.X2.EQ.0.)X3=0.0                       005670
            IF(X1.EQ.0.AND.X2.EQ.0.)IRTF=1                       005680
            IF(X1.EQ.0.AND.X2.EQ.0.)GO TO 75                     005690
            F=FNUM/FDEN                                          005700
            FS=F**2                                              005710
            D2=-2.*F2*D1+X2S                                     005720
            B(1)=FS*(X2S+D1**2)-D2*D2                            005730
            B(2)=-2.*X2*FS+2.*D2*X2                              005740
            B(3)=FS-FS*D1/(2.*F3)-X2S-D2*F2/F3                   005750
            B(4)=X2*F2/F3                                        005760
```

260

```
        B(5)=FS/(16.*F3*F3)-(F2/(2.*F3))**2                              005770
C       WRITE(5,76)B(1),B(2),B(3),B(4),B(5)                              005780
76      FORMAT(1X,5E12.3,*COEFS IN PAR*)                                 005790
        M=4                                                              005800
        IF(B(5).LT.1.0E-10)M=3                                           005810
        CALL POLRT(B,COF,M,ROOTR,ROOTI,IER)                              005820
        X3=0.0                                                           005830
        IRTF=0                                                           005840
        DO 1 I=1,M                                                       005850
C       WRITE(5,3)I,ROOTR(I),ROOTI(I),IER                                005860
3       FORMAT(1X,*X3(*,I1,*)=*,E15.5,3X,E15.5,1X,*J*,2X,*IER=*,I2)      005870
        IF(ROOTI(I).NE.0.) GO TO 1                                       005880
        IF(ROOTR(I).GE.X3L.AND.ROOTR(I).LE.X3U) X3=ROOTR(I)              005890
        IF(ROOTR(I).GE.X3L.AND.ROOTR(I).LE.X3U) IRTF=IRTF+1              005900
1       CONTINUE                                                         005910
75      Z3=Z0-X3+X3/(4.*F3)                                              005920
        RETURN                                                           005930
        END                                                              005940
```

C.2   Program FFPTBB

```
C***PROGRAM BY ALAN FENN (MARTIN MARIETTA)                                000100
C***THIS PROGRAM COMPUTES THE APERTURE DISTRIBUTION AND FAR-FIELD         000110
C***PATTERN OF AN OFFSET TWO REFLECTOR ARRAY CLUSTER FEED SYSTEM.         000120
C***MODIFIED TO RUN BATCH (WAS FFPTR4,CY=2)                               000130
      PROGRAM FFPTBB(INPUT,TAPE5,OUTPUT,TAPE6=OUTPUT,TAPE1,FR80)          000140
C     2,TAPE2)                                                            000150
      COMPLEX J,ESI(500),ESUB(500),EL4(600),ECON,EPRI                     000160
      COMPLEX EFARF,EFF(500),SUME,ESID(500)                              000170
      DIMENSION SA3(500),X4L(600),EL4MAG(600),ELPHAD(600)                 000180
      DIMENSION T(21),ZAPP(20),ZBPP(20),ENORM(500),THETAD(500)           000190
      DIMENSION EMDIF(120),EPDIF(120)                                    000200
      LOGICAL WPLFF,WIDIS,WPLAPR,WCLFF                                   000210
C     CALL CONNEC(5LINPUT)                                               000220
      REWIND 1                                                           000230
C     REWIND 2                                                           000240
      READ(1)NMDSM1,T                                                    000250
      READ(1)SA3,ESI                                                     000250
      READ(1)ZAPP,ZBPP                                                   000270
      READ(1)F1,F2,F3                                                    000280
      READ(1)X1L,X1U,X2L,X2U                                             000290
      READ(1)TD,SN,NAP,NCON                                              000300
      READ(1)X3L,X3U                                                     000310
      READ(1)X3BGN,X3FINL                                                000320
C     READ(2)NMDSM1,T                                                    000330
C     READ(2)SA3,ESID                                                    000340
      IF(TD.EQ.-6.0)X3BGN=-50.0                                          000350
      IF(TD.EQ.-4.0)X3BGN=-30.0                                          000360
      IF(TD.EQ.-2.0)X3BGN=-14.0                                          000370
      NSBGN=1                                                            000380
C     WRITE(5,1)                                                         000390
1     FORMAT(1X,*# OF DATA SETS=*)                                       000400
      READ(5,*)NDS                                                       000410
      DO 321 II=1,NDS                                                    000420
C     WRITE(5,12)                                                        000430
12    FORMAT(1X,*WANT TO INPUT NEW DISTORTIONS? T.OR.F*)                 000440
      READ(5,*)WIDIS                                                     000450
      IF(WIDIS)17,18                                                     000460
17    DO 19 I=1,NMDSM1                                                   000470
C     WRITE(5,7)I                                                        000480
7     FORMAT(1X,*SECTION#*,I3,2X,*INCREMENTAL DISTORTION FOR ZB=*)       000490
      READ(5,*)ZBPP(I)                                                   000500
C     WRITE(5,8)                                                         000510
8     FORMAT(1X,*INCREMENTAL DISTORTION FOR ZA=*)                        000520
      READ(5,*)ZAPP(I)                                                   000530
19    CONTINUE                                                           000540
18    READ(5,*)NSAMS                                                     000550
C     WRITE(5,3)                                                         000560
3     FORMAT(1X,*# OF PRIMARY SAMPLES=*)                                 000570
      READ(5,*)NSAMP                                                     000580
      CALL SECOND(ACPU1)                                                 000590
      IBLCPA=0                                                           000600
      X3DIF=X3FINL-X3BGN                                                 000610
      X3AVE=(X3FINL+X3BGN)/2.                                            000620
      Z1U=X1U*X1U/(4.*F1)-F1                                             000630
      J=(0.,1.)                                                          000640
      PI=3.14159265                                                      000650
      B=2.*PI                                                            000660
      TR=TD*PI/180.                                                      000670
      DO 4242 I=1,NAP                                                    000680
      A3=COS(PI*(-SA3(I)-X3AVE)/(X3DIF-2.*SN))**2                        000690
      IF(-SA3(I).GT.X3BGN.OR.-SA3(I).LT.X3FINL)A3=0.0                    000700
      IF(CABS(ESI(I)).EQ.0.0)GO TO 4242                                  000710
      EPHR=ATAN2(AIMAG(ESI(I)),REAL(ESI(I)))                             000720
```

263

```
         ESI(I)=A3*CEXP(J*EPHR)                                          000730
C        WRITE(5,1000)I,ESI(I),SA3(I)                                    000740
1000     FORMAT(1X,*I=*,I3,2X,*ESI=*,2E12.5,2X,*SA3=*,F12.5)            000750
4242     CONTINUE                                                        000760
5555     CONTINUE                                                        000770
         ESI(1)=(0.,0.)                                                  000780
         ESI(2)=(0.,0.)                                                  000790
         ESI(NAP)=(0.,0.)                                                000300
         NAPM1=NAP-1                                                     000810
         ESI(NAPM1)=(0.,0.)                                              000820
C        WRITE(5,4646)                                                   000830
4646     FORMAT(1X,*WANT TO PLOT ARRAY FIELD DISTRIBUTION? T.OR.F*)     000840
         READ(5,*)WPLAPR                                                 000850
         IF(WPLAPR)33,34                                                 000860
33       EMAX=0.0                                                        000870
         GO TO 34                                                        000880
         DO 1913 I=1,NAP                                                 000890
         EMG=CABS(ESI(I))                                                000900
         EMGD=CABS(ESID(I))                                              000910
         IF(EMG.EQ.0.OR.EMGD.EQ.0)GO TO 8586                            000920
         EMDIF(I)=EMGD-EMG                                               000930
         IF(ABS(EMDIF(I)).GT.EMAX)EMAX=ABS(EMDIF(I))                    000940
         EPH=ATAN2(AIMAG(ESI(I)),REAL(ESI(I)))*180./PI                  000950
         EPHD=ATAN2(AIMAG(ESID(I)),REAL(ESID(I)))*180./PI              000960
         EPDIF(I)=EPHD-EPH                                               000970
         IF(EPHD.GT.-180..AND.EPHD.LT.-90..AND.EPH.GT.0.)EPDIF(I)=360.+ 000980
        2EPHD-EPH                                                        000990
         IF(EPH.GT.-180..AND.EPH.LT.-90..AND.EPHD.GT.0.)EPDIF(I)=EPHD-  001000
        2(360.+EPH)                                                      001010
         WRITE(6,2112)EPHD,EPH,EPDIF(I),EMDIF(I),EMGD,EMG              001020
2112     FORMAT(1X,*EPHD=*,F12.4,2X,*EPH=*,F12.4,2X,*EPDIF=*,F12.4,      001030
        22X,*EMDIF=*,F12.6,2X,*EMGD=*,F12.6,2X,*EMG=*,F12.6)           001040
8586     CONTINUE                                                        001050
1913     CONTINUE                                                        001060
         NDIF=1                                                          001070
         CALL PLOTE(X2L,X2U,SA3,EMDIF,EMAX,EPDIF,NAP,NDIF)             001080
34       NMDS=NMDSM1+1                                                   001090
         Z0=-F2*F2/F1                                                    001100
         DELXS=(X2U-X2L)/(NSAMS-1)                                       001110
         DO 44 I=1,NSAMS                                                 001120
         X2=-DELXS*(I-1)                                                 001130
         Z2=F2-X2*X2/(4.*F2)                                             001140
         ESUB(I)=(0.,0.)                                                 001150
         DO 100 JJ=1,NAP                                                 001160
         X3=-SA3(JJ)                                                     001170
         Z3=Z0-X3*X3/(4.*F3)                                            001180
C***BLOCKAGE IS INCLUDED IN PROGRAM TRPP6B                               001190
C        CALL BLOCK(X2,X3,Z0,Z2,Z3,F2,X51,X52,IBLOCK)                   001200
C        IF(IBLOCK.EQ.1)IBLCPA=IBLCPA+1                                 001210
C        IF(IBLOCK.EQ.1)GO TO 100                                       001220
         RL23=SQRT((X2-X3)**2+(Z2-Z3)**2)                               001230
         P=(Z2-Z3)/RL23                                                 001240
         PTR=P*P                                                         001250
         IF(SN.LT.0.8)PTR=P                                             001260
         ECON=CONJG(ESI(JJ))*CEXP(-J*B*RL23)*PTR/(B*RL23)              001270
C        WRITE(6,4499)X3,Z3,X2,Z2,ECON                                 001280
4499     FORMAT(1X,4F12.5,2X,*ECON=*,2E10.3)                           001290
         ESUB(I)=ESUB(I)+ECON                                           001300
100      CONTINUE                                                        001310
44       CONTINUE                                                        001320
         DO 1199 I=1,NSAMS                                               001330
         ESUBM=CABS(ESUB(I))                                            001340
         X2=-DELXS*(I-1)                                                001350
```

264

```
      WRITE(6,1177)I,X2,ESUBM                                    001360
1177  FORMAT(1X,*I=*,I4,2X,*X2=*,F12.5,2X,*ESUBM=*,E12.5)        001370
1199  CONTINUE                                                   001380
      X1UM1=X1U-.001                                             001390
      X1UP1=X1U+.001                                             001400
      ISKIP=0                                                    001410
      ICT=0                                                      001420
      T2=0.0                                                     001430
      DELXP=(X1U-X1L)/(NSAMP-1)                                  001440
      DXCENT=(X1U+X1L)/2.                                        001450
      DO 40 I=1,NMDSM1                                           001460
      IP1=I+1                                                    001470
      XA=T(I)                                                    001480
      XB=T(IP1)                                                  001490
      ZA=XA*XA/(4.*F1)-F1                                        001500
      ZB=XB*XB/(4.*F1)-F1                                        001510
      IF(ISKIP.EQ.1)GO TO 912                                    001520
99    ICT=ICT+1                                                  001530
      EL4(ICT)=(0.,0.)                                           001540
      T1=T2                                                      001550
      T2=DELXP*ICT                                               001560
      X1=T1                                                      001570
      IF(X1.GT.X1UM1.AND.X1.LT.X1UP1)X1=X1UM1                    001580
912   IF(X1.LE.XB)ZBP=ZB+ZBPP(I)                                001590
      IF(X1.LE.XB)ZAP=ZA+ZAPP(I)                                001600
      IF(X1.GT.XB)ISKIP=1                                        001610
      IF(X1.GT.XB)GO TO 40                                       001620
      ISKIP=0                                                    001630
      XAP=XA                                                     001640
      XBP=XB                                                     001650
      XBA=XB-XA                                                  001660
      XBAP=XBP-XAP                                               001670
      ZBA=ZB-ZA                                                  001680
      ZBAP=ZBP-ZAP                                               001690
      RMO=XBA/ZBA                                                001700
      RMN=XBAP/ZBAP                                              001710
      DELZ1=(X1-XBP)/RMN-(X1-XB)/RMO+ZBP-ZB                      001720
      Z1=X1*X1/(4.*F1)-F1+DELZ1                                  001730
      ZDIF=Z1U-Z1                                                001740
      X4L(ICT)=X1                                                001750
      DO 101 JJ=1,NSAMS                                          001760
      X2=-DELXS*(JJ-1)                                           001770
      Z2=F2-X2*X2/(4.*F2)                                        001780
      RL12=SQRT((X1-X2)**2+(Z1-Z2)**2)                           001790
      EPRI=ESUB(JJ)*CEXP(-J*B*(RL12+ZDIF))/(B*RL12)              001800
      EL4(ICT)=EL4(ICT)+EPRI                                     001810
C     WRITE(6,8877)X2,Z2,X1,Z1,EL4(ICT),ESUB(JJ)                001820
8877  FORMAT(1X,*X2,Z2,X1,Z1=*,4F12.5,2X,*EL4(ICT)=*,2E12.5,2X  001830
     2,*ESUB(JJ)=*,2E12.5)                                      001840
101   CONTINUE                                                   001850
      GO TO 99                                                   001860
40    CONTINUE                                                   001870
      FAC=1.0                                                    001880
      RNSBGN=NSBGN                                               001890
      RNSAMS=NSAMS                                               001900
      IF(IT.GT.1)FAC=RNSBGN/RNSAMS                               001910
      WRITE(6,6767)IT,NSBGN,FAC                                  001920
6767  FORMAT(1X,*IT=*,I5,2X,*NSBGN=*,I5,2X,*FAC=*,F12.5)         001930
      WRITE(6,71)F1,F2,F3                                        001940
71    FORMAT(1X,*F1=*,F12.3,2X,*F2=*,F12.3,2X,*F3=*,F12.5)       001950
      WRITE(6,72)X1L,X1U,X2L,X2U                                 001960
72    FORMAT(1X,*X1L=*,F12.3,2X,*X1U=*,F12.3,2X,*X2L=*,F12.3,2X, 001970
     2*X2U=*,F12.3)                                             001980
```

265

```
      WRITE(6,7487)X3L,X3U                                          001990
7487  FORMAT(1X,*X3L=*,F12.5,2X,*X3U=*,F12.5)                       002000
      WRITE(6,7488)X3BGN,X3FINL,X3AVE,X3DIF                         002010
7488  FORMAT(1X,*X3BGN,X3FINL,X3AVE,X3DIF=*,4F12.5)                 002020
      WRITE(6,73)TD,SN,NSAMP,FAC,NSAMS                              002030
73    FORMAT(1X,*TD=*,F10.4,2X,*SN=*,F12.4,2X,*NSAMP=*,I7,2X,*FAC=*, 002040
     2F12.4,2X,*NSAMS=*,I7)                                         002050
      WRITE(6,700)NAP,NCON                                          002060
700   FORMAT(1X,*NAP=*,I5,2X,*NCON=*,I5)                            002070
      DO 333 I=1,NMDS                                               002080
      WRITE(6,222)I,T(I)                                            002090
222   FORMAT(1X,*T(*,I3,*)=*,F15.5)                                 002100
333   CONTINUE                                                      002110
      DO 151 I=1,NAP                                                002120
      EMG=CABS(ESI(I))                                              002130
      IF(EMG.EQ.0.)GO TO 3681                                       002140
      EPH=ATAN2(AIMAG(ESI(I)),REAL(ESI(I)))*180./PI                 002150
      WRITE(6,159)SA3(I),EMG,EPH                                    002160
159   FORMAT(1X,*SA3=*,F14.4,2X,*EMG=*,E15.5,2X,*EPH=*,F14.5)       002170
3681  IF(EMG.EQ.0.)WRITE(6,4927)SA3(I)                             002180
4927  FORMAT(1X,*SA3=*,F14.4,2X,*EMG=0*)                           002190
151   CONTINUE                                                      002200
      DO 109 I=1,NMDSM1                                             002210
      WRITE(6,75)I,ZAPP(I),ZBPP(I)                                  002220
75    FORMAT(1X,*SECTION#*,I3,2X,*ZAPP(I)=*,F15.7,2X,*ZBPP(I)=*,F15.7) 002230
109   CONTINUE                                                      002240
      BIGEST=0.0                                                    002250
      DO 42 I=1,NSAMP                                               002260
      EL4MAG(I)=CABS(EL4(I))*FAC                                    002270
      IF(EL4MAG(I).EQ.0.)GO TO 4200                                 002280
      ELPHAD(I)=ATAN2(AIMAG(EL4(I)),REAL(EL4(I)))*180./PI           002290
      WRITE(6,50)I,X4L(I),EL4MAG(I),ELPHAD(I)                       002300
50    FORMAT(1X,*I=*,I5,2X,*X4L=*,F15.5,2X,*EL4MAG=*,E15.5,2X,      002310
     2*ELPHAD=*,F14.5)                                              002320
4200  IF(EL4MAG(I).EQ.0.)WRITE(6,5000)X4L(I)                       002330
5000  FORMAT(1X,*X4L=*,F15.5,2X,*EL4MAG=0*)                        002340
      IF(EL4MAG(I).GT.BIGEST)BIGEST=EL4MAG(I)                       002350
42    CONTINUE                                                      002360
      WRITE(6,74)IBLCPA                                             002370
74    FORMAT(1X,*IBLCPA=*,I5)                                       002380
      IF(IT.EQ.1)NSBGN=NSAMS                                        002390
      CALL PLOTE(X1L,X1U,X4L,EL4MAG,BIGEST,ELPHAD,NSAMP,0)          002400
C     WRITE(5,360)                                                  002410
360   FORMAT(1X,*WANT TO CACULATE FAR-FIELD PATTERN? T.OR.F*)       002420
      READ(5,*)WCLFF                                                002430
      IF(WCLFF)209,32                                               002440
C***THIS PART COMPUTES THE FAR-FIELD PATTERN                       002450
209   READ(5,*)TMIN,TMAX                                            002460
      READ(5,*)NPNTS                                                002470
      BIGE=0.0                                                      002480
      DINC=(TMAX-TMIN)/(NPNTS-1)                                    002490
      DO 59 K=1,NPNTS                                               002500
      THETAD(K)=TMIN+DINC*(K-1)                                     002510
      THETAR=THETAD(K)*PI/180.                                      002520
      STH=SIN(THETAR)                                               002530
      SUME=(0.,0.)                                                  002540
      DO 49 I=1,NSAMP                                               002550
      EFARF=EL4(I)*CEXP(J*B*(X4L(I)-DXCENT)*STH)                    002560
      SUME=SUME+EFARF                                               002570
49    CONTINUE                                                      002580
      EFF(K)=SUME                                                   002590
      IF(CABS(EFF(K)).GT.BIGE)BIGE=CABS(EFF(K))                     002600
59    CONTINUE                                                      002610
```

```
      DO 111 K=1,NPNTS                                               002620
      ENORM(K)=20.*ALOG10(CABS(EFF(K))/BIGE)                         002630
      EPHD=ATAN2(AIMAG(EFF(K)),REAL(EFF(K)))*180./PI                 002640
      WRITE(6,223)THETAD(K),ENORM(K),EPHD                            002650
223   FORMAT(1X,*THETAD=*,F14.5,2X,*ENORM=*,F15.5,2X,*EPHD=*,F10.3)  002660
111   CONTINUE                                                       002670
C     WRITE(5,37)                                                    002680
37    FORMAT(1X,*WANT TO CALL PATTERN PLOTTING SUBROUTINE? T.OR.F*)  002690
      READ(5,*)WPLFF                                                 002700
      IF(WPLFF)31,32                                                 002710
31    CALL PLOTFF(ENORM,THETAD,TMIN,TMAX,NPNTS)                      002720
32    CALL APEREF(NSAMP,EL4,TR,X4L,AEF)                              002730
      WRITE(6,25)AEF                                                 002740
25    FORMAT(1X,*APERTURE ILLUMINATION EFFICENCY=*,F15.5)            002750
321   CONTINUE                                                       002760
      CALL SECOND(ACPU2)                                             002770
      ACPU21=ACPU2-ACPU1                                             002780
      WRITE(6,52)ACPU21                                              002790
52    FORMAT(1X,*CPU FOR THIS RUN=*,F14.3)                           002800
      CALL EXIT                                                      002810
      END                                                            002820
      SUBROUTINE BLOCK(X2,X3,Z0,Z2,Z3,F2,X51,X52,IBLOCK)            002830
C***THIS SUBROUTINE DETERMINES IF THERE IS BLOCKAGE BY THE ARRAY    002840
      IBLOCK=0                                                       002850
      FNUM=X2*(X2-X3)+2.*F2*(Z2-Z3)                                  002860
      FDEN=SQRT((X2-X3)**2+(Z2-Z3)**2)                              002870
      F=FNUM/FDEN                                                    002880
      X2S=X2*X2                                                      002890
      FS=F*F                                                         002900
      A1=Z0-Z2                                                       002910
      A2=X2S-2.*F2*A1                                                002920
      A=FS-X2S                                                       002930
      B=2.*X2*(A2-FS)                                                002940
      C=FS*(A1*A1+X2S)-A2*A2                                         002950
      DIS=B*B-4.*A*C                                                 002960
      IF(DIS.LT.0.)WRITE(6,1)                                        002970
1     FORMAT(1X,*ROOTS ARE COMPLEX*)                                 002980
      X51=(-B+SQRT(DIS))/(2.*A)                                      002990
      X52=(-B-SQRT(DIS))/(2.*A)                                      003000
      IF(X51.LT.0.AND.X52.LT.0.)IBLOCK=1                             003010
      RETURN                                                         003020
      END                                                            003030
      SUBROUTINE PLOTFF(EMAG,THETAD,TMIN,TMAX,NPNTS)                 003040
C***THIS SUBROUTINE PLOTS THE FAR-FIELD PATTERN OF THE TWO          003050
C***REFLECTOR ARRAY CLUSTER SYSTEM.                                 003060
      DIMENSION EMAG(1),THETAD(1)                                    003070
      LOGICAL PLOT,HARDC,WPLOTA                                      003080
C     WRITE(5,22)                                                    003090
22    FORMAT(1X,*WANT TO PLOT? T.OR.F*)                             003100
      READ(5,*)PLOT                                                  003110
      IF(PLOT)7,88                                                   003120
7     CALL TEKTRN(960)                                               003130
99    CALL BGNPL(1)                                                  003140
      CALL BASALF("STANDARD")                                        003150
      CALL MIXALF("L/CGREEK")                                        003160
      CALL PAGE(10.897,14.103)                                       003170
      CALL GRACE(0.0)                                                003180
      CALL TITLE(17HFAR-FIELD PATTERN,17,11H(Q) DEGREES,11,          003190
     224HRELATIVE AMPLITUDE IN DB,24,5.,5.)                          003200
      CALL XTICKS(2)                                                 003210
      CALL YTICKS(2)                                                 003220
      CALL GRAF(TMIN,"SCALE",TMAX,-100.,10.,0.)                      003230
      CALL GRID(1,1)                                                 003240
```

```
        CALL MARKER(10)                                              003250
        CALL CURVE(THETAD,EMAG,NPNTS,0)                              003260
        CALL ENDPL(1)                                                003270
C88     WRITE(5,23)                                                  003280
23      FORMAT(1X,*WANT HARD COPY? T.OR.F*)                          003290
88      READ(5,*)HARDC                                               003300
        IF(HARDC)12,77                                               003310
12      CALL FR80(3)                                                 003320
        GO TO 99                                                     003330
C77     WRITE(5,24)                                                  003340
24      FORMAT(1X,*WANT TO PLOT AGAIN? T.OR.F*)                      003350
77      READ(5,*)WPLOTA                                              003360
        IF(WPLOTA)7,42                                               003370
42      RETURN                                                       003380
        END                                                          003390
        SUBROUTINE APEREF(N,E,TR,X,EFF)                              003400
C***THIS SUBROUTINE CALCULATES THE APERTURE ILLUMINATION EFFICIENCY  003410
        COMPLEX E(1),SUMC,J                                          003420
        DIMENSION X(1)                                               003430
        B=2.*3.14159265                                              003440
        J=(0.,1.)                                                    003450
        SUMR=0.0                                                     003460
        SUMC=(0.,0.)                                                 003470
        DO 1 I=1,N                                                   003480
        SUMC=SUMC+E(I)*CEXP(J*B*X(I)*SIN(TR))                        003490
        SUMR=SUMR+CABS(E(I))**2                                      003500
1       CONTINUE                                                     003510
        EFF=CABS(SUMC)**2/(N*SUMR)                                   003520
        RETURN                                                       003530
        END                                                          003540
        SUBROUTINE PLOTE(X1L,X1U,S3,EMAG,EMAX,EPHAD,NPNTS,NDIF)      003550
        DIMENSION S3(1),EMAG(1),EPHAD(1)                             003560
        LOGICAL PLOT,HARDC,WPLOTA                                    003570
        XMX=ABS(X1L)                                                 003580
        DO 1 I=1,NPNTS                                               003590
        WRITE(6,71)I,S3(I),EMAG(I),EPHAD(I)                          003600
71      FORMAT(1X,*I,S3,EMAG,EPHAD=*,I4,2X,3F12.4)                   003610
1       CONTINUE                                                     003620
C       WRITE(5,22)                                                  003630
22      FORMAT(1X,*WANT TO PLOT? T.OR.F*)                            003640
        READ(5,*)PLOT                                                003650
        IF(PLOT)7,88                                                 003660
7       CALL TEKTRN(960)                                             003670
99      CALL BGNPL(1)                                                003680
        CALL PAGE(10.897,14.103)                                     003690
        CALL GRACE(0.0)                                              003700
        CALL PHYSOR(2.5,1.0)                                         003710
        IF(NDIF.EQ.0)GO TO 61                                        003720
        CALL TITLE(1OHPHASE DIFFERENCE,16,17HLOCATION ON ARRAY,17,   003730
       215HPHASE (DEGREES),15,4.,3.)                                 003740
        GO TO 64                                                     003750
61      CALL TITLE(1OHPHASE OF E,10,20HLOCATION ON APERTURE,20,      003760
       215HPHASE (DEGREES),15,4.,3.)                                 003770
64      CALL XTICKS(4)                                               003780
        CALL YTICKS(2)                                               003790
        CALL GRAF(X1L,"SCALE",X1U,-180.,90.,180.)                    003800
        CALL GRID(1,1)                                               003810
        CALL MARKER(10)                                              003820
        CALL SCLPIC(0.5)                                             003830
        CALL CURVE(S3,EPHAD,NPNTS,0)                                 003840
        CALL ENDGR(1)                                                003850
        CALL BGNPL(2)                                                003860
        CALL GRACE(0.0)                                              003870
```

```
        CALL OREL(0.,4.)                                              003880
        IF(NDIF.EQ.0)GO TO 62                                         003890
        CALL TITLE(20HAMPLITUDE DIFFERENCE,20,17HLOCATION ON ARRAY,17, 003900
       2SHAMPLITUDE,9,4.,3.)                                          003910
        GO TO 65                                                      003920
62      CALL TITLE(14HMAGNITUDE OF E,14,20HLOCATION ON APERTURE,20,    003930
       211HMAGNITUDE E,11,4.,3.)                                      003940
65      CALL XTICKS(4)                                                003950
        CALL YTICKS(2)                                                003960
        IF(NDIF.EQ.0)GO TO 66                                         003970
        EMAXCS=-EMAX                                                  003980
        CALL GRAF(-X3U,"SCALE",XMX,EMAXCS,"SCALE",EMAX)               003990
        GO TO 67                                                      004000
66      CALL GRAF(X1L,"SCALE",X1U,0.,"SCALE",EMAX)                    004010
67      CALL GRID(1,1)                                                004020
        CALL MARKER(10)                                               004030
        CALL SCLPIC(0.5)                                              004040
        CALL CURVE(S3,EMAG,NPNTS,0)                                   004050
        CALL ENDPL(2)                                                 004060
C88     WRITE(5,23)                                                   004070
23      FORMAT(1X,*WANT HARD COPY? T.OR.F*)                           004080
88      READ(5,*)HARDC                                                004090
        IF(HARDC)12,77                                                004100
12      CALL FR80(3)                                                  004110
        GO TO 99                                                      004120
C77     WRITE(5,24)                                                   004130
24      FORMAT(1X,*WANT TO PLOT AGAIN? T.OR.F*)                       004140
77      READ(5,*)WPLOTA                                               004150
        IF(WPLOTA)7,42                                                004160
42      RETURN                                                        004170
        END                                                           004180
```

C.3   Program TGBATCH
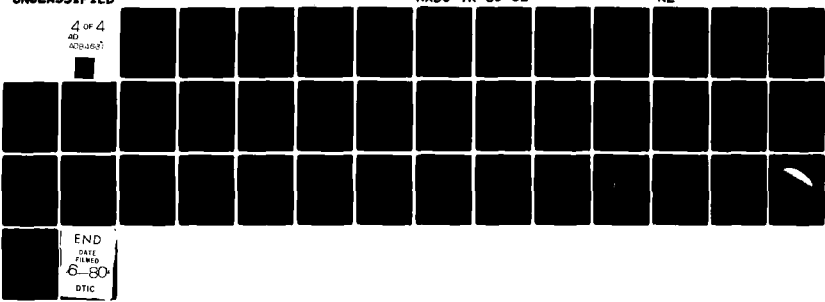
```
       PROGRAM TGDATCH(INPUT,TAPE5,OUTPUT,TAPE6=OUTPUT,TAPE1,FR80)      000100
C**THIS PROGRAM CALCULATES THE ARRAY APERTURE DISTRIBUTION OF A         000110
C**SYMMETRIC TWO REFLECTOR (PARABOLIC-PARABOLIC CONFOCAL) SYSTEM        000120
C**PROGRAM WRITTEN BY ALAN FENN (MARTIN-MARIETTA)                       000130
       COMPLEX ESA(4000),ESI(500),EA                                    000140
       DIMENSION ZAPP(20),ZBPP(20),T(21),XS3(4000),SA3(500),INUMRY(500) 000150
       DIMENSION EMAG(500),EPHAD(500)                                   000160
       LOGICAL DPR                                                      000170
C      CALL CONNEC(5LINPUT)                                             000180
C**ESA AND XS3 DIMENSIONS ARE PROPORTIONAL TO THE NUMBER OF SAMPLES NPS.000190
       ITIMES=0                                                         000200
       NSEGN=1                                                          000210
       READ(5,*)F1,F2                                                   000220
       WRITE(6,6664)F1,F2                                               000230
6664   FORMAT(1X,*F1=*,F12.5,2X,*F2=*,F12.5)                           000240
       READ(5,*)X1L,X1U,X2L,X2U                                         000250
       WRITE(6,6663)X1L,X1U,X2L,X2U                                     000260
6663   FORMAT(1X,*X1L,X1U,X2L,X2U=*,4F12.5)                            000270
       READ(5,*)X3L,X3U                                                 000280
       WRITE(6,6662)X3L,X3U                                             000290
6662   FORMAT(1X,*X3L=*,F12.5,2X,*X3U=*,F12.5)                         000300
       READ(5,*)NMDS                                                    000310
       WRITE(6,6661)NMDS                                                000320
6661   FORMAT(1X,*NMDS=*,I4)                                           000330
       NMDSM1=NMDS-1                                                    000340
       READ(5,*)DPR                                                     000350
       IF(DPR)711,811                                                   000360
811    DO 200 I=1,NMDSM1                                                000370
       ZBPP(I)=0.0                                                      000380
       ZAPP(I)=0.0                                                      000390
200    CONTINUE                                                         000400
       GO TO 24                                                         000410
711    DO 23 I=1,NMDSM1                                                 000420
C      WRITE(5,7)I                                                      000430
7      FORMAT(1X,*SECTION#*,I3,2X,*INCREMENTAL DISTORTION FOR ZB=*)     000440
       READ(5,*)ZBPP(I)                                                 000450
C      WRITE(5,8)                                                       000460
8      FORMAT(1X,*INCREMENTAL DISTORTION FOR ZA=*)                      000470
       READ(5,*)ZAPP(I)                                                 000480
23     CONTINUE                                                         000490
C24    WRITE(5,4)                                                       000500
4      FORMAT(1X,*ANGLE OF INCIDENCE=*)                                 000510
24     READ(5,*)TD                                                      000520
       PI=3.14159265                                                    000530
       TR=TD*PI/180.                                                    000540
C      WRITE(5,9)                                                       000550
9      FORMAT(1X,*ARRAY ELEMENT LENGTH=*)                               000560
       READ(5,*)SN                                                      000570
C      SN=1.0                                                           000580
C      WRITE(5,10)                                                      000590
10     FORMAT(1X,*# OF DATA SETS=*)                                     000600
       READ(5,*)NDS                                                     000610
       DO 321 KTIM=1,NDS                                                000620
C      WRITE(5,12)                                                      000630
12     FORMAT(1X,*# OF PRIMARY SAMPLES=*)                               000640
       READ(5,*)NPS                                                     000650
       CALL SECOND(ACPUA1)                                              000660
       ITIMES=ITIMES+1                                                  000670
       F3=F2/(2.+F2/F1)                                                 000680
       ISPILS=0                                                         000690
       ISPILA=0                                                         000700
       IBLCPS=0                                                         000710
       INUM=0                                                           000720
```

```
      CALL SECOND(ACPU1)                                            000730
      CALL PARDIV(X1L,X1U,NMDS,F1,ST,T)                             000740
3456  CONTINUE                                                      000750
      T(NMDS)=X1U                                                   000760
      X1UM1=X1U-.001                                                000770
      X1UP1=X1U+.001                                                000780
      ISKIP=0                                                       000790
      ICT=0                                                         000800
      DELX=(X1U-X1L)/(NPS-1)                                        000810
      DO 40 I=1,NMDSM1                                              000820
      IP1=I+1                                                       000830
      XA=T(I)                                                       000840
      XB=T(IP1)                                                     000850
      ZA=XA*XA/(4.*F1)-F1                                           000860
      ZB=XB*XB/(4.*F1)-F1                                           000870
      IF(ISKIP.EQ.1)GO TO 912                                       000880
99    ICT=ICT+1                                                     000890
      X1=DELX*(ICT-1)-X1U                                           000900
C     IF(X1.GT.-150)GO TO 321                                       000910
      IF(X1.GT.X1UM1.AND.X1.LT.X1UP1)X1=X1UM1                       000920
      IF(X1.GT.-X1UP1.AND.X1.LT.-X1UM1)X1=-X1UM1                    000930
912   IF(X1.LE.XB)ZBP=ZB+ZBPP(I)                                    000940
      IF(X1.LE.XB)ZAP=ZA+ZAPP(I)                                    000950
      IF(X1.GT.XB)ISKIP=1                                           000960
      IF(X1.GT.XB)GO TO 40                                          000970
      ISKIP=0                                                       000980
C***APPROXIMATE Z1 (EXACT FOR NO DISTORTION)                        000990
      Z1=X1*X1/(4.*F1)-F1                                           001000
      CALL LOCX2I(X1,Z1,F1,F2,TR,X2L,X2U,X2I)                       001010
      CALL SUBRFD(TR,X1,F1,F2,XA,XB,ZA,ZB,ZAP,ZBP,X2L,X2U,Z1,X2,IRTFS, 001020
     2X2I)                                                          001030
      IF(IRTFS.EQ.0)ISPILS=ISPILS+1                                 001040
      IF(IRTFS.NE.1)GO TO 99                                        001050
C     X3L=X2L                                                       001060
C     X3U=X2U                                                       001070
      Z2=F2-X2*X2/(4.*F2)                                           001080
C     CALL ACUCHP(X1,Z1,X2,Z2,F1,TR,TDIFPS)                         001090
C     WRITE(6,1785)TDIFPS                                           001100
1785  FORMAT(1X,*ANGLE REF-ANGLE INC (PRIMARY TO SUBREF)=*,E14.5)   001110
      CALL LOCX3I(X1,Z1,X2,Z2,F1,F2,F3,X3L,X3U,X3II)                001120
C     Z3I=-F2*F2/F1-X3I*X3I/(4.*F3)                                 001130
C     CALL ACUCHP(X1,Z1,X3I,Z3I,F1,TR,TDIFP)                        001140
C     WRITE(6,1853)TDIFP                                            001150
1853  FORMAT(1X,*ANGLE REF-ANGLE INC (PRIMARY TO ARRAY)=*,2X,E14.5) 001160
      CALL PARRAY(X1,Z1,X2,F1,F2,X3L,X3U,X3II,X3,IRTFA)             001170
      I3=X3/SN+1                                                    001180
      X3MAX=I3*SN                                                   001190
      X3MIN=X3MAX-SN                                                001200
      IF(X3.GT.0.)GO TO 4167                                        001210
      I3=X3/SN-1                                                    001220
      X3MIN=I3*SN                                                   001230
      X3MAX=X3MIN+SN                                                001240
4167  X3I=(X3MAX+X3MIN)/2.                                          001250
      Z3=-F2*F2/F1-X3I*X3I/(4.*F3)                                  001260
      RL21=SQRT((X2-X1)**2+(Z2-Z1)**2)                              001270
      RL32=SQRT((X3-X2)**2+(Z3-Z2)**2)                              001280
C     WRITE(6,1000)X1,X2,X3,IRTFA                                   001290
1000  FORMAT(1X,*X1,X2,X3,IRTFA=*,2X,3F12.5,2X,I5,*AFTER PARRAY*)   001300
      IF(IRTFA.EQ.0)ISPILLA=ISPILLA+1                               001310
C     IF(IRTFA.EQ.2)IBLCPS=IBLCPS+1                                 001320
      IF(IRTFA.NE.1)GO TO 99                                        001330
      INUM=INUM+1                                                   001340
      GO TO 9871                                                    001350
```

272

```
7198   CONTINUE                                                        001360
       I3=X3                                                           001370
       X3MAX=I3                                                        001380
       X3MIN=I3-1                                                      001390
       IF(X3.GT.0.)X3MIN=I3                                           001400
       IF(X3.GT.0.)X3MAX=I3+1                                         001410
       X3I=(X3MAX+X3MIN)/2.                                           001420
       Z3I=-F2*F2/F1-X3I*X3I/(4.*F3)                                  001430
       CALL PARPST(X1,Z1,X2,F1,F2,F3,X3MIN,X3MAX,Z3I,X3,IRTFA,RL21,RL32) 001440
       IF(IRTFA.EQ.1)GO TO 1111                                      001450
       X3MAX=I3-1                                                      001460
       X3MIN=I3-2                                                      001470
       IF(X3.GT.0.)X3MIN=I3+1                                         001480
       IF(X3.GT.0.)X3MAX=I3+2                                         001490
       X3I=(X3MAX+X3MIN)/2.                                           001500
       Z3I=-F2*F2/F1-X3I*X3I/(4.*F3)                                  001510
       CALL PARPST(X1,Z1,X2,F1,F2,F3,X3MIN,X3MAX,Z3I,X3,IRTFA,RL21,RL32) 001520
       IF(IRTFA.EQ.1)GO TO 1111                                      001530
       X3MAX=I3+1                                                      001540
       X3MIN=I3                                                        001550
       IF(X3.GT.0.)X3MIN=I3-1                                         001560
       IF(X3.GT.0.)X3MAX=I3                                           001570
       X3I=(X3MAX+X3MIN)/2.                                           001580
       Z3I=-F2*F2/F1-X3I*X3I/(4.*F3)                                  001590
       CALL PARPST(X1,Z1,X2,F1,F2,F3,X3MIN,X3MAX,Z3I,X3,IRTFA,RL21,RL32) 001600
       IF(IRTFA.EQ.1)GO TO 1111                                      001610
       IF(IRTFA.NE.1)WRITE(6,2222)                                    001620
C      IF(IRTFA.NE.1)WRITE(5,2222)                                    001630
2222   FORMAT(1X,*THERE IS A PROBLEM IN FINDING A SOLUTION*)          001640
1111   INUM=INUM+1                                                    001650
       IF(IRTFA.EQ.1)Z3=Z3I                                          001660
C      CALL ACUCHA(X1,Z1,X2,Z2,X3,Z3,F1,F2,F3,TDIF)                  001670
9871   CALL PROJCS(F1,F2,F3,X2,X3,P)                                 001680
       CALL EIARRY(TR,X1,Z1,SN,RL21,RL32,P,EA)                       001690
       EAMAG=CABS(EA)                                                001700
       EAPHAD=ATAN2(AIMAG(EA),REAL(EA))*180./PI                      001710
       WRITE(6,5765)X1,X2,X3,EA,RL21,RL32,EAMAG,EAPHAD               001720
5765   FORMAT(1X,*X1=*,F9.4,2X,*X2=*,F9.4,2X,*X3=*,F9.4,2X,          001730
      2*EA=*,2E12.5,2X,*RL21=*,E12.6,2X,*RL32=*,F8.4,2X,E10.3,2X,     001740
      3F8.3)                                                          001750
C      WRITE(6,3399)TDIF                                             001760
3399   FORMAT(1X,*ANGLE REF - ANGLE INC =*,2X,E14.5,2X,*DEGREES*)    001770
       ESA(INUM)=EA                                                   001780
       XS3(INUM)=X3                                                   001790
       X3RANG=X3                                                      001800
       GO TO 99                                                       001810
40     CONTINUE                                                       001820
       WRITE(6,7416)X3RANG                                            001830
7416   FORMAT(1X,*X3RANG=*,F12.5)                                     001840
       CALL SECOND(ACPUA2)                                           001850
       ACPU21=ACPUA2-ACPUA1                                          001860
       WRITE(6,1794)ACPU21                                           001870
1794   FORMAT(1X,*CPU FOR FIELD CONTRIBUTIONS=*,F14.3)               001880
       NCON=INUM                                                      001890
       IAT=0                                                          001900
       CALL SECOND(ACPUB1)                                           001910
       DO 41 I=1,500                                                  001920
       IAT=IAT+1                                                      001930
       X3MX=-SN*(I-1)+X3U                                            001940
       X3MN=-SN*I+X3U                                                001950
       WRITE(6,1515)X3MX,X3MN                                        001960
1515   FORMAT(1X,*X3MX=*,F12.5,2X,*X3MN=*,F12.5)                     001970
       IF(X3MN.LT.X3L)GO TO 33                                       001980
```

273

```
          SA3(IAT)=(X3MX+X3MN)/2.                                            001990
          CALL SORTEA(IAT,X3MN,X3MX,NCON,XS3,ESA,ESI,INUMRY)                 002000
41        CONTINUE                                                          002010
33        NAP=IAT-1                                                         002020
          CALL SECOND(ACPUB2)                                               002030
          ACPU21=ACPUB2-ACPUB1                                              002040
          WRITE(6,1321)ACPU21                                               002050
1321      FORMAT(1X,*CPU FOR SORTING FIELD CONTRIBUTIONS=*,F14.3)           002060
          FAC=1.                                                            002070
          RNSBGN=NSBGN                                                      002080
          RNPS=NPS                                                          002090
          IF(ITIMES.GT.1)FAC=RNSBGN/RNPS                                    002100
C         WRITE(5,6767)ITIMES,NSBGN,FAC                                     002110
6767      FORMAT(1X,*ITIMES=*,I5,2X,*NSBGN=*,I5,2X,*FAC=*,F12.5)            002120
          WRITE(6,71)F1,F2,F3                                               002130
71        FORMAT(1X,*F1=*,F12.3,2X,*F2=*,F12.3,2X,*F3=*,F12.5)              002140
          WRITE(6,72)X1L,X1U,X2L,X2U,X3L,X3U                                002150
72        FORMAT(1X,*X1L=*,F12.3,2X,*X1U=*,F12.3,2X,*X2L=*,F12.3,2X,*X2U=*, 002160
         2F12.3,2X,*X3L=*,F12.3,2X,*X3U=*,F12.3)                            002170
          WRITE(6,73)TD,SN,NPS,FAC                                          002180
73        FORMAT(1X,*TD=*,F10.4,2X,*SN=*,F12.4,2X,*NPS=*,I7,2X,*FAC=*,F12.4)002190
C         WRITE(5,700)NAP,NCON                                              002200
          WRITE(6,700)NAP,NCON                                              002210
700       FORMAT(1X,*NAP=*,I5,2X,*NCON=*,I5)                                002220
          BICE=0.0                                                          002230
          DO 199 IE=1,NAP                                                   002240
          EMG=CABS(ESI(IE))                                                 002250
          IF(EMG.GT.BIGE)BIGE=EMG                                           002260
199       CONTINUE                                                          002270
          DO 42 I=1,NAP                                                     002280
          EMAG(I)=CABS(ESI(I))*FAC                                          002290
          IF(EMAG(I).EQ.0.)GO TO 9000                                       002300
          EPHAD(I)=ATAN2(AIMAG(ESI(I)),REAL(ESI(I)))*180./PI               002310
          WRITE(6,50)I,SA3(I),EMAG(I),EPHAD(I),INUMRY(I)                    002320
50        FORMAT(1X,I4,2X,*SA3=*,F14.4,2X,*EMAG=*,E15.5,2X,*EPHAD=*,F14.4   002330
         2,2X,*INUMRY=*,I5)                                                 002340
9000      IF(EMAG(I).EQ.0.)WRITE(6,5000)I,SA3(I)                           002350
5000      FORMAT(1X,I4,2X,*SA3(I)=*,F14.4,2X,*EMAG=0      INUMRY(I)=0*)     002360
42        CONTINUE                                                          002370
          WRITE(6,74)ISPILS,ISPILA                                         002380
74        FORMAT(1X,*ISPILS=*,I5,2X,*ISPILA=*,I5)                           002390
          DO 101 I=1,NMDSM1                                                 002400
          WRITE(6,75)I,ZAPP(I),ZBPP(I)                                     002410
75        FORMAT(1X,*SECTION#*,I3,2X,*ZAPP(I)=*,F15.7,2X,*ZBPP(I)=*,F15.7)  002420
101       CONTINUE                                                         002430
          IF(ITIMES.EQ.1)NSBGN=NPS                                         002440
          EMAX=BIGE                                                        002450
C         CALL PLOTE(X3L,SA3,EMAG,EMAX,EPHAD,NAP)                          002460
          WRITE(1)NMDSM1,T                                                 002470
          WRITE(1)SA3,ESI                                                  002480
          WRITE(1)ZAPP,ZBPP                                                002490
          WRITE(1)F1,F2,F3                                                 002500
          WRITE(1)X1L,X1U,X2L,X2U                                          002510
          WRITE(1)TD,SN,NAP,NCON                                           002520
          WRITE(1)X3L,X3U,X3RANG                                           002530
321       CONTINUE                                                         002540
          CALL SECOND(ACPU2)                                               002550
          ACPU21=ACPU2-ACPU1                                               002560
          WRITE(6,52)ACPU21                                                002570
52        FORMAT(1X,*CPU FOR THIS RUN=*,F14.3)                             002580
          CALL EXIT                                                        002590
          END                                                             002600
          SUBROUTINE PARDIV(XMIN,XMAX,NMDS,F1,ST,T)                        002610
```

```
C****THIS SUBROUTINE DIVIDES A PARABOLA INTO (NMDS-1) EQUAL ARC LENGTH    002620
C****SEGMENTS                                                             002630
C****PROGRAM BY ALAN FENN                                                 002640
      DIMENSION T(21),IT(21)                                              002650
222   FORMAT(1X,2F15.5,I7,F15.5)                                          002660
      C=2.*F1                                                             002670
      CS=C*C                                                              002680
      Q1=1./(2.*C)                                                        002690
      T1=XMIN                                                             002700
      T2=XMAX                                                             002710
      T1S=T1*T1                                                           002720
      T2S=T2*T2                                                           002730
      Q2=T2*SQRT(CS+T2S)                                                  002740
      ARG2=T2+SQRT(CS+T2S)                                                002750
      Q3=CS*ALOG(ARG2)                                                    002760
      Q4=T1*SQRT(CS+T1S)                                                  002770
      ARG1=T1+SQRT(CS+T1S)                                                002780
      Q5=CS*ALOG(ARG1)                                                    002790
      ST=Q1*(Q2+Q3)-Q1*(Q4+Q5)                                           002800
      S=ST/(NMDS-1)                                                       002810
      T(1)=XMIN                                                           002820
      IT(1)=0                                                             002830
      DO 1 I=2,NMDS                                                       002840
      IT(I)=0                                                             002850
      IM1=I-1                                                             002860
      IM2=I-2                                                             002870
      T(I)=T(IM1)+S                                                       002880
      IF(I.GE.3) T(I)=T(IM1)+(T(IM1)-T(IM2))                             002890
      T1=T(IM1)                                                           002900
      T1S=T1*T1                                                           002910
7     CONTINUE                                                            002920
      IT(I)=IT(I)+1                                                       002930
      T2=T(I)                                                             002940
      T2S=T2*T2                                                           002950
      Q2=T2*SQRT(CS+T2S)                                                  002960
      ARG2=T2+SQRT(CS+T2S)                                                002970
      Q3=CS*ALOG(ARG2)                                                    002980
      Q4=T1*SQRT(CS+T1S)                                                  002990
      ARG1=T1+SQRT(CS+T1S)                                                003000
      Q5=CS*ALOG(ARG1)                                                    003010
      G2=Q1*(Q2+Q3)                                                       003020
      G1=Q1*(Q4+Q5)                                                       003030
      SP=G2-G1                                                            003040
C     WRITE(6,47)I,S,SP                                                   003050
47    FORMAT(1X,2HI=,I3,2X,2HS=,F15.7,2X,3HSP=,F15.7)                    003060
      IF(ABS(SP-S).LT.0.0001) GO TO 1                                     003070
      IF(SP.GT.S) T(I)=T(I)-(SP-S)                                        003080
      IF(SP.LT.S) T(I)=T(I)+(S-SP)                                        003090
      GO TO 7                                                             003100
1     CONTINUE                                                            003110
      DO 9 I=1,NMDS                                                       003120
      WRITE(6,12)I,IT(I),T(I)                                             003130
12    FORMAT(1X,3HIT(,I2,2H)=,1X,I7,2X,*T(I)=*,F15.5)                    003140
9     CONTINUE                                                            003150
      RETURN                                                              003160
      END                                                                 003170
      SUBROUTINE PRILC2(ICT,DELX,T1,T2)                                   003180
      ICT=ICT+1                                                           003190
      T1=T2                                                               003200
      T2=DELX*ICT                                                         003210
      RETURN                                                              003220
      END                                                                 003230
      SUBROUTINE SUBRFD(TR,X1,F1,F2,XA,XB,ZA,ZB,ZAP,ZBP,X2L,X2U,Z1,X2,   003240
```

275

```
      2 IRTF,X2I) ·                                                        003250
C**THIS SUBROUTINE LOCATES POINTS OF REFLECTION ON THE SUB-REFLECTOR.      003260
      DIMENSION B(5),COF(5),ROOTR(4),ROOTI(4)                              003270
C     IF(X1.GT.-210)WRITE(6,4232)TR,X1,X2I                                 003280
4232  FORMAT(1X,*TR,X1,X2I=*,3F12.5)                                       003290
      X2IM1=X2I-.01                                                        003300
      X2IP1=X2I+.01                                                        003310
      IF(A3S(TR).LE..009)GO TO 75                                          003320
      X2IM1=X2I-.1                                                         003330
      X2IP1=X2I+.1                                                         003340
75    F1S=F1*F1                                                            003350
      F2S=F2*F2                                                            003360
      X1S=X1*X1                                                            003370
      XAP=XA                                                               003380
      XBP=XB                                                               003390
      XBA=XB-XA                                                            003400
      XBAP=XBP-XAP                                                         003410
      ZBA=ZB-ZA                                                            003420
      ZBAP=ZBP-ZAP                                                         003430
      FNUM=ZBA*ZBAP+XBA*XBAP                                               003440
      FDEN1=SQRT(ZBA*ZBA+XBA*XBA)                                          003450
      PDEN2=SQRT(ZBAP*ZBAP+XBAP*XBAP)                                      003460
      PABP=FNUM/PDEN1/PDEN2                                                003470
      IF(PABP.GT.1.0.AND.PABP.LT.1.01)PABP=1.0                             003480
      T3R=ACOS(PABP)                                                       003490
      ARG1=2.*F1/SQRT(4.*F1S+X1S)                                          003500
      T1R=ACOS(ARG1)                                                       003510
      IF(X1.LT.0.)T1R=-T1R                                                 003520
      T2R=T1R-T3R                                                          003530
      ZDIF1=ZBP-ZB                                                         003540
      ZDIF2=ZAP-ZA                                                         003550
      IF(ZDIF1.GT.ZDIF2)T2R=T1R+T3R                                        003560
      C2=COS(T2R)                                                          003570
      S2=SIN(T2R)                                                          003580
      A2=-S2*SIN(TR)+C2*COS(TR)                                            003590
      RMO=XBA/ZBA                                                          003600
      RMN=XBAP/ZBAP                                                        003610
      DELZ1=(X1-XBP)/RMN-(X1-XB)/RMO+ZBP-ZB                                003620
      Z1=X1S/(4.*F1)-F1+DELZ1                                              003630
      A1=F1+F2-X1S/(4.*F1)-DELZ1                                           003640
      A3=X1*S2+A1*C2                                                       003650
C     WRITE(6,76)A1,A2,A3,C2,S2                                            003660
76    FORMAT(1X,5E15.5)                                                    003670
      A1S=A1*A1                                                            003680
      A2S=A2*A2                                                            003690
      A3S=A3*A3                                                            003700
      B(1)=A3S-A2S*(A1S+X1S)                                               003710
      B(2)=2.*A2S*X1-2.*A3*S2                                              003720
      B(3)=S2*S2-C2*A3/(2.*F2)-A2S*(1.-A1/(2.*F2))                         003730
      B(4)=S2*C2/(2.*F2)                                                   003740
      B(5)=(C2*C2-A2S)/(16.*F2*F2)                                         003750
C     WRITE(6,78)B(1),B(2),B(3),B(4),B(5)                                  003760
78    FORMAT(1X,5E14.5,*  COEFS IN SUBRFD*)                                003770
      M=4                                                                  003780
      IF(B(5).LT.1.0E-12)M=3                                               003790
      IF(TR.EQ.0.AND.X1.EQ.0.AND.T3R.EQ.0.)X2=0.                           003800
      IF(TR.EQ.0.AND.X1.EQ.0.AND.T3R.EQ.0.)IRTF=1                          003810
      IF(TR.EQ.0.AND.X1.EQ.0.AND.T3R.EQ.0.)GO TO 29                        003820
      CALL POLRT(B,COF,M,ROOTR,ROOTI,IER)                                  003830
      X2=1.0                                                               003840
      IRTF=0                                                               003850
      DO 1 I=1,M                                                           003860
C     WRITE(6,3)I,ROOTR(I),ROOTI(I),IER                                    003870
```

276

```
3         FORMAT(1X,*X2(*,I1,*)=*,F15.5,3X,F15.5,1X,* J*,* IER=*,I2)      003880
          IF(ROOTI(I).NE.0.) GO TO 1                                      003890
          IF(ROOTR(I).GE.X2L.AND.ROOTR(I).LE.X2U.AND.(ROOTR(I).LT.        003900
         2X21M1.OR.ROOTR(I).GT.X2IP1))X2=ROOTR(I)                         003910
          IF(X2.EQ.ROOTR(I))IRTF=IRTF+1                                   003920
C         IF(ROOTR(I).GE.X2L.AND.ROOTR(I).LE.X2U) IRTF=IRTF+1             0C3930
1         CONTINUE                                                        003940
          IF(IRTF.EQ.0.OR.IRTF.EQ.1)GO TO 29                             003950
          DO 49 I=1,M                                                     G03960
          TIMES=RCOTR(I)*X2I                                              003970
          IF(TIMES.LE.0.AND.ROOTR(I).GE.X2L.AND.ROOTR(I).LE.X2U)X2=ROOTR(I) 003980
          IF(X2.EQ.ROOTR(I))IRTF=1                                        003990
49        CONTINUE                                                        004000
C         WRITE(6,7454)X2                                                 004010
7454      FORMAT(1X,*X2=*,F12.5,*  !!!!!!*)                               004020
29        RETURN                                                          004030
          END                                                            004040
          SUBROUTINE EIARRY(TR,X1,Z1,SN,RL21,RL32,P,EA)                   004050
C**THIS SUBROUTINE CALCULATES THE E FIELD INCIDENT ON THE ARRAY          004060
          COMPLEX J,E0,SP21,SP32,EA                                       004070
          PI=3.14159265                                                   004080
          B=2.*PI                                                         004090
          J=(0.,1.)                                                       004100
          PTR=P*P                                                         004110
          IF(SN.LT.0.8)PTR=P                                              004120
          E0=CEXP(J*B*(X1*SIN(TR)+Z1*COS(TR)))                           004130
          SP21=CEXP(-J*B*RL21)                                            004140
          SP32=CEXP(-J*B*RL32)                                            004150
          EA=E0*SP21*SP32*PTR                                             004160
          RETURN                                                         004170
          END                                                            004180
          SUBROUTINE SORTEA(ICT,X3L,X3U,NCON,XS3,ESA,EI,INUMRY)          004190
C**THIS SUBROUTINE CALCULATES E FIELD CONTRIBUTIONS TO EACH APERTURE     004200
          COMPLEX ESA(1),EI(1)                                            004210
          DIMENSION XS3(1),INUMRY(1)                                      004220
          EI(ICT)=(0.,0.)                                                 004230
          INUMRY(ICT)=0                                                   004240
          DO 77 I=1,NCON                                                  004250
          IF(XS3(I).LE.X3U.AND.XS3(I).GE.X3L)EI(ICT)=EI(ICT)+ESA(I)       004260
          IF(XS3(I).LE.X3U.AND.XS3(I).GE.X3L)INUMRY(ICT)=INUMRY(ICT)+1    004270
77        CONTINUE                                                        004280
          RETURN                                                         004290
          END                                                            004300
          SUBROUTINE POLRT(XCOF,COF,M,ROOTR,ROOTI,IER)                    004310
          DIMENSION XCOF(1),COF(1),ROOTR(1),ROOTI(1)                      004320
          DOUBLE PRECISION XO,YO,X,Y,XPR,YPR,UX,UY,V,YT,XT,U,XT2,YT2,SUMSQ, 004330
         2DX,DY,TEMP,ALPHA                                                004340
          ITWO=2                                                          004350
          IFIT=0                                                          004360
          N=M                                                             004370
          IER=0                                                           004380
          IF(XCOF(N+1))10,25,10                                           004390
10        IF(N)15,15,32                                                   004400
15        IER=1                                                           004410
20        RETURN                                                         004420
25        IER=4                                                           004430
          GO TO 20                                                        004440
30        IER=2                                                           004450
          GO TO 20                                                        004460
32        IF(N-36)35,35,30                                                004470
35        NX=N                                                            004480
          NXX=N+1                                                         004490
          N2=1                                                            004500
```

```
          KJ1=N+1                                             004510
          DO 40 L=1,KJ1                                       004520
          MT=KJ1-L+1                                          004530
40        COF(MT)=XCOF(L)                                     004540
45        XO=.00500101                                        004550
          YO=0.01000101                                       004560
          IN=0                                                004570
50        X=XO                                                004580
          XO=-10.0*YO                                         004590
          YO=-10.0*X                                          004600
          X=XO                                                004610
          Y=YO                                                004620
          IN=IN+1                                             004630
          GO TO 59                                            004640
55        IFIT=1                                              004650
          XPR=X                                               004660
          YPR=Y                                               004670
59        ICT=0                                               004680
60        UX=0.0                                              004690
          UY=0.0                                              004700
          V=0.0                                               004710
          YT=0.0                                              004720
          XT=1.0                                              004730
          U=COF(N+1)                                          004740
          IF(U)65,130,65                                      004750
65        DO 70 I=1,N                                         004760
          L=N-I+1                                             004770
          TEMP=COF(L)                                         004780
          XT2=X*XT-Y*YT                                       004790
          YT2=X*YT+Y*XT                                       004800
          U=U+TEMP*XT2                                        004810
          V=V+TEMP*YT2                                        004820
          FI=I                                                004830
          UX=UX+FI*XT*TEMP                                    004840
          UY=UY-FI*YT*TEMP                                    004850
          XT=XT2                                              004860
70        YT=YT2                                              004870
          SUMSQ=UX*UX+UY*UY                                   004880
          IF(SUMSQ)75,110,75                                  004890
75        DX=(V*UY-U*UX)/SUMSQ                                004900
          X=X+DX                                              004910
          DY=-(U*UY+V*UX)/SUMSQ                               004920
          Y=Y+DY                                              004930
78        IF(DABS(DY)+DABS(DX)-1.0D-05)100,80,80              004940
80        ICT=ICT+1                                           004950
          IF(ICT-500)60,85,85                                 004960
85        IF(IFIT)100,90,100                                  004970
90        IF(IN-5)50,95,95                                    004980
95        IER=3                                               004990
          GO TO 20                                            005000
100       DO 105 L=1,NXX                                      005010
          MT=KJ1-L+1                                          005020
          TEMP=XCOF(MT)                                       005030
          XCOF(MT)=COF(L)                                     005040
105       COF(L)=TEMP                                         005050
          ITEMP=N                                             005060
          N=NX                                                005070
          NX=ITEMP                                            005080
          IF(IFIT)120,55,120                                  005090
110       IF(IFIT)115,50,115                                  005100
115       X=XPR                                               005110
          Y=YPR                                               005120
120       IFIT=0                                              005130
```

```
122     IF(DABS(Y)-1.0D-4*DABS(X))135,125,125              005140
125     ALPHA=X+X                                          005150
        SUMSQ=X*X+Y*Y                                      005160
        N=N-2                                              005170
        GO TO 140                                          005180
130     X=0.0                                              005190
        NX=NX-1                                            005200
        NXX=NXX-1                                          005210
135     Y=0.0                                              005220
        SUMSQ=0.0                                          005230
        ALPHA=X                                            005240
        N=N-1                                              005250
140     COF(ITWO)=COF(ITWO)+ALPHA*COF(1)                   005260
145     DO 150 L=2,N                                       005270
150     COF(L+1)=COF(L+1)+ALPHA*COF(L)-SUMSQ*COF(L-1)      005280
155     ROOTI(N2)=Y                                        005290
        ROOTR(N2)=X                                        005300
        N2=N2+1                                            005310
        IF(SUMSQ)160,165,160                               005320
160     Y=-Y                                               005330
        SUMSQ=0.0                                          005340
        GO TO 155                                          005350
165     IF(N)20,20,45                                      005360
        END                                                005370
        SUBROUTINE PLOTE(X3L,S3,EMAG,EMAX,EPHAD,NPNTS)     005380
        DIMENSION S3(1),EMAG(1),EPHAD(1)                   005390
        LOGICAL PLOT,HARDC,WPLOTA                          005400
        XMX=ABS(X3L)                                       005410
C       WRITE(5,22)                                        005420
22      FORMAT(1X,*WANT TO PLOT? T.OR.F*)                  005430
        READ(5,*)PLOT                                      005440
        IF(PLOT)7,88                                       005450
7       CALL TEKTRN(960)                                   005460
99      CALL BGNPL(1)                                      005470
        CALL PHYSOR(2.5,1.0)                               005480
        CALL TITLE(10HPHASE OF E,10,17HLOCATION ON ARRAY,17, 005490
       215HPHASE (DEGREES),15,4.,3.)                       005500
        CALL XTICKS(4)                                     005510
        CALL YTICKS(2)                                     005520
        CALL GRAF(0.,"SCALE",XMX,-180.,90.,180.)           005530
        CALL GRID(1,1)                                     005540
        CALL MARKER(10)                                    005550
        CALL CURVE(S3,EPHAD,NPNTS,-1)                      005560
        CALL ENDGR(1)                                      005570
        CALL BGNPL(2)                                      005580
        CALL OREL(0.,4.)                                   005590
        CALL TITLE(14HMAGNITUDE OF E,14,17HLOCATION ON ARRAY,17, 005600
       211HMAGNITUDE E,11,4.,3.)                           005610
        CALL XTICKS(4)                                     005620
        CALL YTICKS(2)                                     005630
        CALL GRAF(0.,"SCALE",XMX,0.,"SCALE",EMAX)          005640
        CALL GRID(1,1)                                     005650
        CALL MARKER(10)                                    005660
        CALL CURVE(S3,EMAG,NPNTS,-1)                       005670
        CALL ENDPL(2)                                      005680
C88     WRITE(5,23)                                        005690
23      FORMAT(1X,*WANT HARD COPY? T.OR.F*)                005700
88      READ(5,*)HARDC                                     005710
        IF(HARDC)12,77                                     005720
12      CALL FR80(3)                                       005730
        GO TO 99                                           005740
C77     WRITE(5,24)                                        005750
24      FORMAT(1X,*WANT TO PLOT AGAIN? T.OR.F*)            005760
```

279

```
77      READ(5,*)WPLOTA                                                   005770
        IF(WPLOTA)7,42                                                    005780
42      RETURN                                                            005790
        END                                                               005800
C***THIS SUBROUTINE CALCULATES POINTS OF INCIDENCE ON THE PHASED         005810
C***ARRAY WHICH WAS PARABOLIC BUT REPLACED BY STRAIGHT LINE SEGMENTS     005820
        SUBROUTINE PARPST(X1,Z1,X2,F1,F2,F3,X3MIN,X3MAX,Z3I,X3,IRTF,RL21, 005830
       2RL32)                                                             005840
        DIMENSION X3R(2)                                                  005850
        X2S=X2*X2                                                         005860
        Z2=F2-X2S/(4.*F2)                                                 005870
        BI=Z3I-Z2                                                         005880
        BIS=BI*BI                                                         005890
        X23=X2S*X2                                                        005900
        X24=X23*X2                                                        005910
        F2S=F2*F2                                                         005920
        Z0=-F2S/F1                                                        005930
        D1=Z0-F2+X2S/(4.*F2)                                              005940
        FNUM=X2*(X2-X1)+2.*F2*(Z2-Z1)                                     005950
        FDEN=SQRT((X2-X1)**2+(Z2-Z1)**2)                                  005960
        IF(X1.EQ.0.AND.X2.EQ.0)X3=0.0                                     005970
        IF(X1.EQ.0.AND.X2.EQ.0)IRTF=1                                     005980
        IF(X1.EQ.0.AND.X2.EQ.0)GO TO 88                                   005990
        F=FNUM/FDEN                                                       006000
        FS=F*F                                                            006010
        A=FS-X2S                                                          006020
        B=2.*X23-4.*F2*X2*BI-2.*FS*X2                                     006030
        C=FS*(X2S+BIS)-X24+4.*F2*X2S*BI-4.*F2S*BIS                        006040
C       WRITE(6,78)A,B,C                                                  006050
78      FORMAT(1X,*A,B,C=*,3E12.5,2X,*INSIDE PARPST*)                     006060
        BS=B*B                                                            006070
        DIS=BS-4.*A*C                                                     006080
        IF(DIS.LT.0.)GO TO 55                                             006090
        X3R(1)=(-B+SQRT(DIS))/(2.*A)                                      006100
        X3R(2)=(-B-SQRT(DIS))/(2.*A)                                      006110
C       WRITE(6,41)X3R(1),X3R(2)                                          006120
41      FORMAT(1X,*X3R(1),X3R(2)=*,2F12.5,2X,*INSIDE PARPST*)             006130
C       IF(X3R(1).LT.0.AND.X3R(2).LT.0.)IRTF=2                            006140
C       IF(X3R(1).LT.0.AND.X3R(2).LT.0.)GO TO 88                          006150
        IRTF=0                                                            006160
        DO 1 I=1,2                                                        006170
        IF(X3R(I).LE.X3MAX.AND.X3R(I).GE.X3MIN)X3=X3R(I)                  006180
        IF(X3.EQ.X3R(I))IRTF=1                                            006190
C       IF(X3R(I).LE.X3MAX.AND.X3R(I).GE.X3MIN)IRTF=IRTF+1                006200
C       WRITE(6,9988)X3,Z3I,X3R(I),X3MAX,X3MIN,IRTF                       006210
9988    FORMAT(1X,*X3,Z3I,X3R(I),X3MAX,X3MIN,IRTF=*,5F10.3,2X,I4)         006220
1       CONTINUE                                                          006230
55      IF(DIS.LT.0.)WRITE(6,12)                                          006240
12      FORMAT(1X,*ROOTS ARE COMPLEX*)                                    006250
88      Z3=Z3I                                                            006260
        RL21=FDEN                                                         006270
        RL32=SQRT((X3-X2)**2+(Z3-Z2)**2)                                  006280
        RETURN                                                            006290
        END                                                               006300
        SUBROUTINE PROJCS(F1,F2,F3,X2,X3,P)                               006310
C***THIS SUBROUTINE CALCULATES THE PROJECTION ON THE NORMAL TO THE       006320
C***PHASED ARRAY                                                         006330
        X3S=X3*X3                                                         006340
        D1=-F2*F2/F1-F2+X2*X2/(4.*F2)                                     006350
        RNUM=X3S/(4.*F3)-D1                                               006360
        DEN=SQRT((X3-X2)**2+(X3S/(4.*F3)-D1)**2)                          006370
        P=RNUM/DEN                                                        006380
        IF(P.GT.1.0.AND.P.LT.1.01)P=1.0                                   006390
```

280

```
        RETURN                                                      006400
        END                                                         006410
        SUBROUTINE PARRAY(X1,Z1,X2,F1,F2,X3L,X3U,X3I,X3,IRTF)       006420
C****THIS PROGRAM CALCULATES INCIDENT POINTS ON THE PHASED ARRAY SURFACE006430
C****PROGRAM BY ALAN FENN                                           006440
        DIMENSION B(5),COF(5),ROOTR(4),ROOTI(4)                     006450
C       WRITE(6,5)X1,X2,X3I                                         006460
5       FORMAT(1X,*X1,X2,X3I=*,3F12.5,2X,*INSIDE PARRAY*)           006470
        X3IM1=X3I-.01                                               006480
        X3IP1=X3I+.01                                               006490
        F3=F2/(2.+F2/F1)                                            006500
        Z0=-F2**2/F1                                                006510
        X2S=X2*X2                                                   006520
        D1=Z0-F2+X2S/(4.*F2)                                        006530
        Z2=F2-X2S/(4.*F2)                                           006540
        FNUM=X2*(X2-X1)+2.*F2*(Z2-Z1)                               006550
        FDEN=SQRT((X2-X1)**2+(Z2-Z1)**2)                            006560
        IF(X1.EQ.0.AND.X2.EQ.0.)X3=0.0                              006570
        IF(X1.EQ.0.AND.X2.EQ.0.)IRTF=1                              006580
        IF(X1.EQ.0.AND.X2.EQ.0.)GO TO 75                            006590
        F=FNUM/FDEN                                                 006600
        FS=F**2                                                     006610
        D2=-2.*F2*D1+X2S                                            006620
        B(1)=FS*(X2S+D1**2)-D2*D2                                   006630
        B(2)=-2.*X2*FS+2.*D2*X2                                     006640
        B(3)=FS-FS*D1/(2.*F3)-X2S-D2*F2/F3                          006650
        B(4)=X2*F2/F3                                               006660
        B(5)=FS/(16.*F3*F3)-(F2/(2.*F3))**2                         006670
C       WRITE(6,76)B(1),B(2),B(3),B(4),B(5)                        006680
76      FORMAT(1X,5E12.3,2X,*COEFS IN PARRAY*)                      006690
        M=4                                                         006700
        IF(B(5).LT.1.0E-10)M=3                                      006710
        CALL POLRT(B,COF,M,ROOTR,ROOTI,IER)                         006720
        X3=0.0                                                      006730
        IRTF=0                                                      006740
        DO 1 I=1,M                                                  006750
C       WRITE(6,3)I,ROOTR(I),ROOTI(I),IER                          006760
3       FORMAT(1X,*X3(*,I1,*)=*,E15.5,3X,E15.5,1X,*J*,2X,*IER=*,I2) 006770
        IF(ROOTI(I).NE.0.) GO TO 1                                  006780
        IF(ROOTR(I).GE.X3L.AND.ROOTR(I).LE.X3U.AND.(ROOTR(I).LT.    006790
     2X3IM1.OR.ROOTR(I).GT.X3IP1))X3=ROOTR(I)                       006800
        IF(X3.EQ.ROOTR(I))IRTF=IRTF+1                               006810
C       IF(ROOTR(I).GE.X3L.AND.ROOTR(I).LE.X3U) IRTF=IRTF+1         006820
1       CONTINUE                                                    006830
        IF(IRTF.EQ.0.OR.IRTF.EQ.1)GO TO 75                          006840
        DO 49 I=1,M                                                 006850
        TIMES=ROOTR(I)*X3I                                          006860
        IF(TIMES.LE.0.AND.ROOTR(I).GE.X3L.AND.ROOTR(I).LE.X3U)X3=ROOTR(I) 006870
        IF(X3.EQ.ROOTR(I))IRTF=1                                    006880
49      CONTINUE                                                    006890
75      RETURN                                                      006900
        END                                                         006910
        SUBROUTINE LOCX3I(X1,Z1,X2,Z2,F1,F2,F3,X3MIN,X3MAX,X3I)     006920
C***THIS SUBROUTINE CALCULATES POINTS OF INCIDENCE ON THE ARRAY     006930
        DIMENSION X3R(2)                                            006940
C       WRITE(6,429)X1,Z1,X2,Z2,F1,F2,F3,X3MIN,X3MAX               006950
429     FORMAT(1X,*X1,Z1,X2,Z2,F1,F2,F3,X3MIN,X3MAX=*,9F10.3)       006960
        Z0=-F2*F2/F1                                                006970
        RM=(X1-X2)/(Z1-Z2)                                          006980
        IF(RM.EQ.0.)X3I=X1                                          006990
        IF(RM.EQ.0.)GO TO 2                                         007000
        A=RM/(4.*F3)                                                007010
        C=-(X1+RM*(Z0-Z1))                                          007020
```

281

```
C       WRITE(6,576)A,C                                                   007030
576     FORMAT(1X,*A,C=*,2F12.5,2X,*INSIDE LOCX3I*)                       007040
        DIS=1.-4.*A*C                                                     007050
        IF(DIS.LT.0)WRITE(6,1)                                            007060
1       FORMAT(1X,*THE ROOTS IN LOCX3I ARE IMAGINARY*)                    007070
        IF(DIS.LT.0)X3I=1.0E10                                            007080
        IF(DIS.LT.0)GO TO 2                                               007090
        X3R(1)=(-1.+SQRT(DIS))/(2.*A)                                     007100
        X3R(2)=(-1.-SQRT(DIS))/(2.*A)                                     007110
C       WRITE(6,333)X3R(1),X3R(2)                                         007120
333     FORMAT(1X,*X3R(1),X3R(2)=*,2F12.5,2X,*INSIDE LOCX3I*)             007130
        DO 3 I=1,2                                                        007140
        IF(X3R(I).LE.X3MAX.AND.X3R(I).GE.X3MIN)X3I=X3R(I)                 007150
3       CONTINUE                                                          007160
2       RETURN                                                            007170
        END                                                              007180
        SUBROUTINE LOCX2I(X1,Z1,F1,F2,TR,X2MIN,X2MAX,X2I)                 007190
C***THIS SUBROUTINE LOCATES POINTS OF INCIDENCE ON SUBREFLECTOR          007200
        DIMENSION X2R(2)                                                  007210
        IRTF=0                                                            007220
        RM=TAN(TR)                                                        007230
        IF(RM.EQ.0.)X2I=X1                                                007240
        IF(RM.EQ.0.)GO TO 2                                               007250
        A=RM/(4.*F2)                                                      007260
        C=RM*(Z1-F2)-X1                                                   007270
        DIS=1.-4.*A*C                                                     007280
        IF(DIS.LT.0)WRITE(6,1)                                            007290
1       FORMAT(1X,*THE ROOTS IN LOCX2I ARE IMAGINARY*)                    007300
        IF(DIS.LT.0)GO TO 2                                               007310
        X2R(1)=(-1.+SQRT(DIS))/(2.*A)                                     007320
        X2R(2)=(-1.-SQRT(DIS))/(2.*A)                                     007330
        DO 3 I=1,2                                                        007340
        IF(X2R(I).LE.X2MAX.AND.X2R(I).GE.X2MIN)X2I=X2R(I)                 007350
        IF(X2I.EQ.X2R(I))IRTF=1                                           007360
3       CONTINUE                                                          007370
        IF(IRTF.EQ.0)X2I=0.0                                              007380
2       RETURN                                                            007390
        END                                                              007400
        SUBROUTINE ACUCHA(X1,Z1,X2,Z2,X3,Z3,F1,F2,F3,TDIF)               007410
C***THIS SUBROUTINE CHECKS THE ACCURACY OF X1,X2,X3 IN TERMS OF THE      007420
C***DIFFERENCE BETWEEN THE ANGLE OF INCIDENCE AND ANGLE OF REFLECTION.   007430
C       Z3=-X3*X3/(4.*F3)-F2*F2/F1                                       007440
        RNUM21=X2*(X2-X1)+2*F2*(Z2-Z1)                                   007450
        RNUM32=-X2*(X3-X2)-2.*F2*(Z3-Z2)                                 007460
        DEN1=SQRT(4.*F2*F2+X2*X2)                                        007470
        DEN2=SQRT((X2-X1)**2+(Z2-Z1)**2)                                 007480
        DEN3=SQRT((X3-X2)**2+(Z3-Z2)**2)                                 007490
        PROJ2=RNUM21/DEN1/DEN2                                           007500
        PROJ3=RNUM32/DEN1/DEN3                                           007510
        IF(PROJ2.GT.1.0.AND.PROJ2.LT.1.01)PROJ2=1.0                      007520
        IF(PROJ3.GT.1.0.AND.PROJ3.LT.1.01)PROJ3=1.0                      007530
        T2D=ACOS(PROJ2)*180./3.14159265                                  007540
        T3D=ACOS(PROJ3)*180./3.14159265                                  007550
        TDIF=T3D-T2D                                                     007560
C       WRITE(6,1)X1,Z1,X2,Z2,X3,Z3                                      007570
1       FORMAT(1X,*X1,Z1,X2,Z2,X3,Z3=*,6F9.3)                           007580
C       WRITE(6,2)F1,F2,F3,T2D,T3D,TDIF                                 007590
2       FORMAT(1X,*F1,F2,F3,T2D,T3D,TDIF=*,6F9.3)                       007600
        RETURN                                                          007610
        END                                                            007620
        SUBROUTINE ACUCHP(X1,Z1,X3,Z3,F1,TR,TDIF)                       007630
C***THIS SUBROUTINE CHECKS THE ACCURACY OF X1,X3 IN TERMS OF THE        007640
C***DIFFERENCE BETWEEN THE ANGLE OF INCIDENCE AND ANGLE OF REFLECTION   007650
```

282

```
C***AT THE PRIMARY.                                              007660
      RNUM1=-X1*SIN(TR)+2.*F1*COS(TR)                            007670
      RNUM3=-X1*(X3-X1)+2.*F1*(Z3-Z1)                            007680
      DEN1=SQRT(4.*F1*F1+X1*X1)                                  007690
      DEN3=SQRT((X3-X1)**2+(Z3-Z1)**2)                           007700
      PROJ1=RNUM1/DEN1                                           007710
      PROJ2=RNUM3/DEN1/DEN3                                      007720
      IF(PROJ1.GT.1.0.AND.PROJ1.LT.1.01)PROJ1=1.0               007730
      IF(PROJ2.GT.1.0.AND.PROJ2.LT.1.01)PROJ2=1.0               007740
      T1D=ACOS(PROJ1)*180./3.14159265                           007750
      T2D=ACOS(PROJ2)*180./3.14159265                           007760
      TDIF=T2D-T1D                                               007770
      RETURN                                                     007780
      END                                                        007790
```

C.4   Program PTBATCH

```
C***PROGRAM BY ALAN FENN (MARTIN MARIETTA)                              000100
C***THIS PROGRAM COMPUTES THE APERTURE DISTRIBUTION AND FAR-FIELD       000110
C***PATTERN OF A SYMMETRIC TWO REFLECTOR ARRAY CLUSTER FEED SYSTEM.     000120
      PPOGRAM PTBATCH(INPUT,TAPE5,OUTPUT,TAPE6=OUTPUT,TAPE1,FR80)       000130
C***THIS PROGRAM HAS BEEN MODIFIED TO RUN BATCH                         000140
C***THE ARRAY USES A SHIFTED COSINE-SQUARED DISTRIBUTION                000150
      COMPLEX J,ESI(500),ESUB(700),EL4(2000),ECON,EPRI                  000160
      COMPLEX EFARF,EFF(300),SUME                                       000170
      DIMENSION SA3(500),X4L(2000),EL4MAG(2000),ELPHAD(2000)            000180
      DIMENSION T(21),ZAPP(20),ZBPP(20),ENORM(300),THETAD(300)          000190
      LOGICAL WPLFF,WIDIS,WPLAPR                                        000200
C     CALL CONNEC(5LINPUT)                                              000210
      REWIND 1                                                          000220
      REWIND 5                                                          000230
      READ(1)NMDSM1,T                                                   000240
      READ(1)SA3,ESI                                                    000250
      READ(1)ZAPP,ZBPP                                                  000260
      READ(1)F1,F2,F3                                                   000270
      READ(1)X1L,X1U,X2L,X2U                                            000280
      READ(1)TD,SN,NAP,NCON                                             000290
      READ(1)X3L,X3U,X3RANG                                             000300
      NSBGN=1                                                           000310
C     WRITE(5,1)                                                        000320
1     FORMAT(1X,*# OF DATA SETS=*)                                      000330
      READ(5,*)NDS                                                      000340
      DO 321 IT=1,NDS                                                   000350
C     WRITE(5,12)                                                       000360
12    FORMAT(1X,*WANT TO INPUT NEW DISTORTIONS? T.OR.F*)                000370
      READ(5,*)WIDIS                                                    000380
      IF(WIDIS)17,18                                                    000390
17    DO 19 I=1,NMDSM1                                                  000400
C     WRITE(5,7)I                                                       000410
7     FORMAT(1X,*SECTION#*,I3,2X,*INCREMENTAL DISTORTION FOR ZB=*)      000420
      READ(5,*)ZBPP(I)                                                  000430
C     WRITE(5,8)                                                        000440
8     FORMAT(1X,*INCREMENTAL DISTORTION FOR ZA=*)                       000450
      READ(5,*)ZAPP(I)                                                  000460
19    CONTINUE                                                          000470
C18   WRITE(5,2)                                                        000480
2     FORMAT(1X,*# OF SUBREFLECTOR SAMPLES=*)                           000490
18    READ(5,*)NSAMS                                                    000500
C     WRITE(5,3)                                                        000510
3     FORMAT(1X,*# OF PRIMARY SAMPLES=*)                                000520
      READ(5,*)NSAMP                                                    000530
      CALL SECOND(ACPU1)                                                000540
      IBLCPA=0                                                          000550
      RMAG=F1/F2                                                        000560
      X3LIM=X1U/RMAG                                                    000570
      Z1U=X1U*X1U/(4.*F1)-F1                                            000580
      PI=3.14159265                                                     000590
      J=(0.,1.)                                                         000600
      X3AVE=(X3U+X3RANG)/2.                                             000610
      IF(TD.LT.0.)X3AVE=(X3L+X3RANG)/2.                                 000620
      IF(TD.EQ.0.0)X3AVE=0.0                                            000630
      DO 4242 I=1,NAP                                                   000640
C     A3=COS(PI*SA3(I)/(2.*(X3U-2*SN)))**2                             000650
      A3=COS(PI*(SA3(I)-X3AVE)/(X3U-X3RANG-2.*SN))**2                   000660
      IF(TD.EQ.0.0)A3=COS(PI*SA3(I)/(2.*(X3LIM-2.*SN)))**2             000670
      IF(TD.EQ.0.0.AND.SA3(I).GT.X3LIM)A3=0.0                           000680
      IF(SA3(I).LT.X3RANG)A3=0.0                                        000690
      IF(CABS(ESI(I)).EQ.0.)GO TO 4242                                  000700
      EPH=ATAN2(AIMAG(ESI(I)),REAL(ESI(I)))                            000710
      ESI(I)=A3*CEXP(J*EPH)                                             000720
```

285

```
C        WRITE(5,2765)A3,EPH                                            000730
2765     FORMAT(1X,*A3,EPH=*,2E12.5)                                    000740
C        WRITE(5,1000)I,ESI(I),SA3(I)                                   000750
1000     FORMAT(1X,*I=*,I3,2X,*ESI=*,2E12.5,2X,*SA3=*,F12.5)            000760
C3993    IF(CABS(ESI(I)).EQ.0.)WRITE(5,3333)I                          000770
3333     FORMAT(1X,*I=*,I4,2X,*ESI(I)=0.0*)                            000780
4242     CONTINUE                                                       000790
5555     CONTINUE                                                       000800
         ESI(1)=(0.,0.)                                                 000810
         ESI(2)=(0.,0.)                                                 000820
         ESI(NAP)=(0.,0.)                                               000830
         NAPM1=NAP-1                                                    000840
         ESI(NAPM1)=(0.,0.)                                             000850
         B=2.*PI                                                        000860
         TR=TD*PI/180.                                                  000870
         NMDS=NMDSM1+1                                                  000880
         Z0=-F2*F2/F1                                                   000890
         DELXS=(X2U-X2L)/(NSAMS-1)                                      000900
         DO 44 I=1,NSAMS                                                000910
         X2=X2U-DELXS*(I-1)                                             000920
         Z2=F2-X2*X2/(4.*F2)                                            000930
         ESUB(I)=(0.,0.)                                                000940
         DO 100 JJ=1,NAP                                                000950
         X3=SA3(JJ)                                                     000960
         Z3=Z0-X3*X3/(4.*F3)                                            000970
         IF(X2U.NE.0.)GO TO 87                                          000980
         CALL BLOCK(X2,X3,Z0,Z2,Z3,F2,X51,X52,IBLOCK)                   000990
         IF(IBLOCK.EQ.1)IBLCPA=IBLCPA+1                                 001000
         IF(IBLOCK.EQ.1)GO TO 100                                       001010
87       RL23=SQRT((X2-X3)**2+(Z2-Z3)**2)                              001020
         P=(Z2-Z3)/RL23                                                 001030
         PTR=P*P                                                        001040
         IF(SN.LT.0.8)PTR=P                                             001050
C        EPH=ATAN2(AIMAG(ESI(JJ)),REAL(ESI(JJ)))                       001060
C        ESI(JJ)=A3*CEXP(J*EPH)                                         001070
C        WRITE(5,9181)JJ,A3,EPH                                         001080
9181     FORMAT(1X,*JJ,A3,EPH=*,2X,I4,2X,2F12.5)                        001090
         ECON=CONJG(ESI(JJ))*CEXP(-J*B*RL23)*PTR/(8*RL23)              001100
C        WRITE(6,4499)X3,Z3,X2,Z2,ECON                                  001110
4499     FORMAT(1X,4F12.5,2X,*ECON=*,2E10.3)                            001120
         ESUB(I)=ESUB(I)+ECON                                           001130
100      CONTINUE                                                       001140
44       CONTINUE                                                       001150
         DO 7474 I=1,NSAMS                                              001160
         X2=X2U-DELXS*(I-1)                                             001170
         ESUBM=CABS(ESUB(I))                                            001180
         WRITE(6,5272)I,X2,ESUBM                                        001190
5272     FORMAT(1X,*I=*,I4,2X,*X2=*,F12.5,2X,*ESUBM=*,E12.5)            001200
7474     CONTINUE                                                       001210
         X1UM1=X1U-.001                                                 001220
         X1UP1=X1U+.001                                                 001230
         ISKIP=0                                                        001240
         ICT=0                                                          001250
         DELXP=(X1U-X1L)/(NSAMP-1)                                      001260
         DXCENT=(X1U+X1L)/2.                                            001270
         DO 40 I=1,NMDSM1                                               001280
         IP1=I+1                                                        001290
         XA=T(I)                                                        001300
         XB=T(IP1)                                                      001310
         ZA=XA*XA/(4.*F1)-F1                                            001320
         ZB=XB*XB/(4.*F1)-F1                                            001330
         IF(ISKIP.EQ.1)GO TO 912                                        001340
99       ICT=ICT+1                                                      001350
```

286

```
         EL4(ICT)=(0.,0.)                                              001360
         X1=DELXP*(ICT-1)+X1L                                          001370
         IF(X1.GT.X1UM1.AND.X1.LT.X1UP1)X1=X1UM1                       001380
912      IF(X1.LE.XB)ZBP=ZB+ZBPP(I)                                    001390
         IF(X1.LE.XB)ZAP=ZA+ZAPP(I)                                    001400
         IF(X1.GT.XB)ISKIP=1                                           001410
         IF(X1.GT.XB)GO TO 40                                          001420
         ISKIP=0                                                       001430
         XAP=XA                                                        001440
         XBP=XB                                                        001450
         XBA=XB-XA                                                     001460
         XBAP=XBP-XAP                                                  001470
         ZBA=ZB-ZA                                                     001480
         ZBAP=ZBP-ZAP                                                  001490
         RMO=XBA/ZBA                                                   001500
         RMN=XBAP/ZBAP                                                 001510
         DELZ1=(X1-XBP)/RMN-(X1-XB)/RMO+ZBP-ZB                         001520
         Z1=X1*X1/(4.*F1)-F1+DELZ1                                     001530
         ZDIF=Z1U-Z1                                                   001540
         X4L(ICT)=X1                                                   001550
         DO 101 JJ=1,NSAMS                                             001560
         X2=X2U-DELXS*(JJ-1)                                           001570
         Z2=F2-X2*X2/(4.*F2)                                           001580
         RL12=SQRT((X1-X2)**2+(Z1-Z2)**2)                              001590
         EPRI=ESUB(JJ)*CEXP(-J*B*(RL12+ZDIF))/(B*RL12)                 001600
         EL4(ICT)=EL4(ICT)+EPRI                                        001610
C        WRITE(6,8877)X2,Z2,X1,Z1,EL4(ICT),ESUB(JJ)                    001620
8877     FORMAT(1X,*X2,Z2,X1,Z1=*,4F12.5,2X,*EL4(ICT)=*,2E12.5,2X      001630
        2,*ESUB(JJ)=*,2E12.5)                                          001640
101      CONTINUE                                                      001650
         GO TO 99                                                      001660
40       CONTINUE                                                      001670
         FAC=1.0                                                       001680
         RNSBGN=NSBGN                                                  001690
         RNSAMS=NSAMS                                                  001700
         IF(IT.GT.1)FAC=RNSBGN/RNSAMS                                  001710
C        WRITE(5,6767)IT,NSBGN,FAC                                     001720
6767     FORMAT(1X,*IT=*,I5,2X,*NSBGN=*,I5,2X,*FAC=*,F12.5)            001730
         WRITE(6,71)F1,F2,F3                                           001740
71       FORMAT(1X,*F1=*,F12.3,2X,*F2=*,F12.3,2X,*F3=*,F12.5)          001750
         WRITE(6,72)X1L,X1U,X2L,X2U,X3L,X3U                            001760
72       FORMAT(1X,*X1L=*,F12.3,2X,*X1U=*,F12.3,2X,*X2L=*,F12.3,2X,    001770
        2*X2U=*,F12.3,2X,*X3L=*,F12.3,2X,*X3U=*,F12.3)                 001780
         WRITE(6,73)TD,SN,NSAMP,FAC,NSAMS                              001790
73       FORMAT(1X,*TD=*,F10.4,2X,*SN=*,F12.4,2X,*NSAMP=*,I7,2X,*FAC=*,001800
        2F12.4,2X,*NSAMS=*,I7)                                         001810
         WRITE(6,700)NAP,NCON                                          001820
700      FORMAT(1X,*NAP=*,I5,2X,*NCON=*,I5)                            001830
         WRITE(6,8354)X3RANG,X3AVE                                     001840
8354     FORMAT(1X,*X3RANG=*,F12.5,2X,*X3AVE=*,F12.5)                  001850
         DO 333 I=1,NMDS                                               001860
         WRITE(6,222)I,T(I)                                            001870
222      FORMAT(1X,*T(*,I3,*)=*,F15.5)                                 001880
333      CONTINUE                                                      001890
         DO 151 I=1,NAP                                                001900
         EMG=CABS(ESI(I))                                              001910
         IF(EMG.EQ.0.)GO TO 3681                                       001920
         EPH=ATAN2(AIMAG(ESI(I)),REAL(ESI(I)))*180./PI                 001930
         WRITE(6,159)SA3(I),EMG,EPH                                    001940
159      FORMAT(1X,*SA3=*,F14.4,2X,*EMG=*,E15.5,2X,*EPH=*,F14.5)       001950
3681     IF(EMG.EQ.0.)WRITE(6,4927)SA3(I)                             001960
4927     FORMAT(1X,*SA3=*,F14.4,2X,*EMG=0*)                           001970
151      CONTINUE                                                      001980
```

```
      DO 109 I=1,NMDSM1                                            001990
      WRITE(6,75)I,ZAPP(I),ZBPP(I)                                002000
75    FORMAT(1X,*SECTION#*,I3,2X,*ZAPP(I)=*,F15.7,2X,*ZBPP(I)=*,F15.7) 002010
109   CONTINUE                                                    002020
      BIGEST=0.0                                                  002030
      DO 42 I=1,NSAMP                                             002040
      EL4MAG(I)=CABS(EL4(I))*FAC                                  002050
      IF(EL4MAG(I).EQ.0.)GO TO 4200                              002060
      ELPHAD(I)=ATAN2(AIMAG(EL4(I)),REAL(EL4(I)))*180./PI        002070
      WRITE(6,50)I,X4L(I),EL4MAG(I),ELPHAD(I)                    002080
50    FORMAT(1X,*I=*,I5,2X,*X4L=*,F15.5,2X,*EL4MAG=*,E15.5,2X,    002090
     2*ELPHAD=*,F14.5)                                            002100
4200  IF(EL4MAG(I).EQ.0.)WRITE(6,5000)X4L(I)                     002110
5000  FORMAT(1X,*X4L=*,F15.5,2X,*EL4MAG=0*)                      002120
      IF(EL4MAG(I).GT.BIGEST)BIGEST=EL4MAG(I)                    002130
42    CONTINUE                                                    002140
      WRITE(6,74)IBLCPA                                           002150
74    FORMAT(1X,*IBLCPA=*,I5)                                     002160
      IF(IT.EQ.1)NSBGN=NSAMS                                      002170
C     WRITE(5,3131)                                               002180
3131  FORMAT(1X,*WANT TO CALL APERTURE PLOTTING ROUTINE? T.OR.F*) 002190
      READ(5,*)WPLAPR                                             002200
      IF(WPLAPR)9787,9788                                         002210
9787  CALL PLOTE(X1L,X1U,X4L,EL4MAG,BIGEST,ELPHAD,NSAMP,0)       002220
C***THIS PART COMPUTES THE FAR-FIELD PATTERN                      002230
C9788 WRITE(5,4121)                                               002240
4121  FORMAT(1X,*PATTERN RANGE...TMIN=,TMAX=*)                   002250
9788  READ(5,*)TMIN,TMAX                                          002260
C     WRITE(5,4836)                                               002270
4836  FORMAT(1X,*NUMBER OF POINTS=*)                             002280
      READ(5,*)NPNTS                                              002290
      BIGE=0.0                                                    002300
      DINC=(TMAX-TMIN)/(NPNTS-1)                                 002310
      DO 59 K=1,NPNTS                                            002320
      THETAD(K)=TMIN+DINC*(K-1)                                  002330
      THETAR=THETAD(K)*PI/180.                                   002340
      STH=SIN(THETAR)                                            002350
      SUME=(0.,0.)                                               002360
      DO 49 I=1,NSAMP                                            002370
      EFARF=EL4(I)*CEXP(J*B*(X4L(I)-DXCENT)*STH)                002380
      SUME=SUME+EFARF                                            002390
49    CONTINUE                                                    002400
      EFF(K)=SUME                                                 002410
      IF(CABS(EFF(K)).GT.BIGE)BIGE=CABS(EFF(K))                 002420
59    CONTINUE                                                    002430
      DO 111 K=1,NPNTS                                           002440
      ENORM(K)=20.*ALOG10(CABS(EFF(K))/BIGE)                     002450
      EPHD=ATAN2(AIMAG(EFF(K)),REAL(EFF(K)))*180./PI            002460
      WRITE(6,223)THETAD(K),ENORM(K),EPHD                       002470
223   FORMAT(1X,*THETAD=*,F14.5,2X,*ENORM=*,F15.5,2X,*EPHD=*,F10.3) 002480
111   CONTINUE                                                    002490
C     WRITE(5,37)                                                 002500
37    FORMAT(1X,*WANT TO CALL PATTERN PLOTTING SUBROUTINE? T.OR.F*) 002510
      READ(5,*)WPLFF                                              002520
      IF(WPLFF)31,32                                              002530
31    CALL PLOTFF(ENORM,THETAD,TMIN,TMAX,NPNTS)                  002540
32    CALL APEREF(NSAMP,EL4,TR,X4L,AEF)                         002550
C     WRITE(5,25)AEF                                              002560
      WRITE(6,25)AEF                                              002570
25    FORMAT(1X,*APERTURE ILLUMINATION EFFICENCY=*,F15.5)        002580
321   CONTINUE                                                    002590
      CALL SECOND(ACPU2)                                          002600
      ACPU21=ACPU2-ACPU1                                          002610
```

```
      WRITE(6,52)ACPU21                                              002620
52    FORMAT(1X,*CPU FOR THIS RUN=*,F14.3)                           002630
      CALL EXIT                                                      002640
      END                                                            002650
      SUBROUTINE BLOCK(X2,X3,Z0,Z2,Z3,F2,X51,X52,IBLOCK)            002660
C***THIS SUBROUTINE DETERMINES IF THERE IS BLOCKAGE BY THE ARRAY    002670
      IBLOCK=0                                                       002680
      FNUM=X2*(X2-X3)+2.*F2*(Z2-Z3)                                  002690
      FDEN=SQRT((X2-X3)**2+(Z2-Z3)**2)                              002700
      F=FNUM/FDEN                                                    002710
      X2S=X2*X2                                                      002720
      FS=F*F                                                         002730
      A1=Z0-Z2                                                       002740
      A2=X2S-2.*F2*A1                                                002750
      A=FS-X2S                                                       002760
      B=2.*X2*(A2-FS)                                                002770
      C=FS*(A1*A1+X2S)-A2*A2                                         002780
      DIS=B*B-4.*A*C                                                 002790
C     IF(DIS.LT.0.)WRITE(5,1)                                       002800
1     FORMAT(1X,*ROOTS ARE COMPLEX*)                                002810
      X51=(-B+SQRT(DIS))/(2.*A)                                     002820
      X52=(-B-SQRT(DIS))/(2.*A)                                     002830
      IF(X51.LT.0.AND.X52.LT.0.)IBLOCK=1                            002840
      RETURN                                                        002850
      END                                                           002860
      SUBROUTINE PLOTFF(EMAG,THETAD,TMIN,TMAX,NPNTS)               002870
C***THIS SUBROUTINE PLOTS THE FAR-FIELD PATTERN OF THE TWO          002880
C***REFLECTOR ARRAY CLUSTER SYSTEM.                                 002890
      DIMENSION EMAG(1),THETAD(1)                                   002900
      LOGICAL PLOT,HARDC,WPLOTA                                     002910
C     WRITE(5,22)                                                   002920
22    FORMAT(1X,*WANT TO PLOT? T.OR.F*)                             002930
      READ(5,*)PLOT                                                 002940
      IF(PLOT)7,88                                                  002950
7     CALL TEKTRN(960)                                              002960
99    CALL BGNPL(1)                                                 002970
      CALL BASALF("STANDARD")                                       002980
      CALL MIXALF("L/CGREEK")                                       002990
      CALL PAGE(10.89,11.0)                                         003000
      CALL GRACE(0.0)                                               003010
      CALL TITLE(17HFAR-FIELD PATTERN,17,11H(Q) DEGREES,11,        003020
     224HRELATIVE AMPLITUDE IN DB,24,5.,5.)                        003030
      CALL XTICKS(2)                                                003040
      CALL YTICKS(2)                                                003050
      CALL GRAF(TMIN,"SCALE",TMAX,-100.,10.,0.)                    003060
      CALL GRID(1,1)                                                003070
      CALL MARKER(10)                                               003080
      CALL CURVE(THETAD,EMAG,NPNTS,0)                              003090
      CALL ENDPL(1)                                                 003100
C88   WRITE(5,23)                                                   003110
23    FORMAT(1X,*WANT HARD COPY? T.OR.F*)                          003120
88    READ(5,*)HARDC                                               003130
      IF(HARDC)12,77                                                003140
12    CALL FR80(3)                                                  003150
      GO TO 99                                                      003160
C77   WRITE(5,24)                                                   003170
24    FORMAT(1X,*WANT TO PLOT AGAIN? T.OR.F*)                      003180
77    READ(5,*)WPLOTA                                              003190
      IF(WPLOTA)7,42                                                003200
42    RETURN                                                        003210
      END                                                           003220
      SUBROUTINE APEREF(N,E,TR,X,EFF)                              003230
C***THIS SUBROUTINE CALCULATES THE APERTURE ILLUMINATION EFFICIENCY 003240
```

289

```
        COMPLEX E(1),SUMC,J,F(600)                                      003250
        DIMENSION X(1)                                                  003260
        B=2.*3.14159265                                                 003270
        J=(0.,1.)                                                       003280
        SUMR=0.0                                                        003290
        SUMC=(0.,0.)                                                    003300
        DO 1 I=1,N                                                      003310
        F(I)=E(I)*CEXP(J*B*X(I)*SIN(TR))                                003320
        SUMC=SUMC+E(I)*CEXP(J*B*X(I)*SIN(TR))                           003330
        SUMR=SUMR+CABS(E(1))**2                                         003340
   C    WRITE(6,74)I,F(I),SUMC,SUMR                                     003350
   74   FORMAT(1X,*I,F(I),SUMC,SUMR=*,I5,2X,5F17.7)                     003360
   1    CONTINUE                                                        003370
        EFF=CABS(SUMC)**2/(N*SUMR)                                      003380
        RETURN                                                          003390
        END                                                             003400
        SUBROUTINE PLOTE(X1L,X1U,S3,EMAG,EMAX,EPHAD,NPNTS,NDIF)         003410
        DIMENSION S3(1),EMAG(1),EPHAD(1)                                003420
        LOGICAL PLOT,HARDC,WPLOTA                                       003430
        XMX=ABS(X1L)                                                    003440
        DO 1 I=1,NPNTS                                                  003450
        WRITE(6,71)I,S3(I),EMAG(I),EPHAD(I)                             003460
   71   FORMAT(1X,*I,S3,EMAG,EPHAD=*,I4,2X,F12.4,2X,E12.4,2X,F12.4)     003470
   1    CONTINUE                                                        003480
   C    WRITE(5,22)                                                     003490
   22   FORMAT(1X,*WANT TO PLOT? T.OR.F*)                               003500
        READ(5,*)PLOT                                                   003510
        IF(PLOT)7,88                                                    003520
   7    CALL TEKTRN(960)                                                003530
   99   CALL BGNPL(1)                                                   003540
        CALL PAGE(10.897,14.103)                                        003550
        CALL GRACE(0.0)                                                 003560
        CALL PHYSOR(2.5,1.0)                                            003570
        IF(NDIF.EQ.0)GO TO 61                                           003580
        CALL TITLE(16HPHASE DIFFERENCE,16,17HLOCATION ON ARRAY,17,      003590
       215HPHASE (DEGREES),15,4.,3.)                                    003600
        GO TO 64                                                        003610
   61   CALL TITLE(10HPHASE OF E,10,20HLOCATION ON APERTURE,20,         003620
       215HPHASE (DEGREES),15,4.,3.)                                    003630
   64   CALL XTICKS(4)                                                  003640
        CALL YTICKS(2)                                                  003650
        CALL GRAF(X1L,"SCALE",X1U,-180.,90.,180.)                       003660
        CALL GRID(1,1)                                                  003670
        CALL MARKER(10)                                                 003680
        CALL SCLPIC(0.5)                                                003690
        CALL CURVE(S3,EPHAD,NPNTS,0)                                    003700
        CALL ENDGR(1)                                                   003710
        CALL BGNPL(2)                                                   003720
        CALL GRACE(0.0)                                                 003730
        CALL OREL(0.,4.)                                                003740
        IF(NDIF.EQ.0)GO TO 62                                           003750
        CALL TITLE(20HAMPLITUDE DIFFERENCE,20,17HLOCATION ON ARRAY,17,  003760
       29HAMPLITUDE,9,4.,3.)                                            003770
        GO TO 65                                                        003780
   62   CALL TITLE(14HMAGNITUDE OF E,14,20HLOCATION ON APERTURE,20,     003790
       211HMAGNITUDE E,11,4.,3.)                                        003800
   65   CALL XTICKS(4)                                                  003810
        CALL YTICKS(2)                                                  003820
        IF(NDIF.EQ.0)GO TO 66                                           003830
        EMAXCS=-EMAX                                                    003840
        CALL GRAF(-X3U,"SCALE",XMX,EMAXCS,"SCALE",EMAX)                 003850
        GO TO 67                                                        003860
   88   CALL GRAF(X1L,"SCALE",X1U,0.,"SCALE",EMAX)                      003870
```

```
67       CALL GRID(1,1)                                003880
         CALL MARKER(10)                               003890
         CALL SCLPIC(0.5)                              003900
         CALL CURVE(S3,EMAG,NPNTS,0)                   003910
         CALL ENDPL(2)                                 003920
C88      WRITE(5,23)                                   003930
23       FORMAT(1X,*WANT HARD COPY? T.OR.F*)           003940
88       READ(5,*)HARDC                                003950
         IF(HARDC)12,77                                003960
12       CALL FR80(3)                                  003970
         GO TO 99                                      003930
C77      WRITE(5,24)                                   003990
24       FORMAT(1X,*WANT TO PLOT AGAIN? T.OR.F*)       004000
77       READ(5,*)WPLOTA                               004010
         IF(WPLOTA)7,42                                004020
42       RETURN                                        004030
         END                                           004040
```

C.5   Program PTNUL2

```
C***PROGRAM BY ALAN FENN (MARTIN MARIETTA)                           000100
C***THIS PROGRAM COMPUTES THE APERTURE DISTRIBUTION AND FAR-FIELD    000110
C***PATTERN OF A SYMMETRIC TWO REFLECTOR ARRAY CLUSTER FEED SYSTEM.  000120
      PROGRAM PTNUL2(INPUT,TAPE5,OUTPUT,TAPE6=OUTPUT,TAPE1,FR80,     000130
     2TAPE2)                                                         000140
C***THIS PROGRAM HAS BEEN MODIFIED TO RUN BATCH                      000150
C***THE ARRAY USES A SHIFTED COSINE-SQUARED DISTRIBUTION             000160
C***ADAPTIVE NULLING HAS BEEN ADDED TO THIS PROGRAM                  000170
      COMPLEX J,ESI(500),ESUB(700),EL4(1000),ECON,EPRI              000180
      COMPLEX EFARF,EFF(300),SUME,ESI2(500),FACNUL                  000190
      DIMENSION SA3(500),X4L(1000),EL4MAG(1000),ELPHAD(1000)        000200
      DIMENSION T(21),ZAPP(20),ZBPP(20),ENORM(300),THETAD(300)      000210
      DIMENSION TT(21),SA32(500)                                    000220
      LOGICAL WPLFF,WIDIS,WPLAPR                                    000230
C     CALL CONNEC(5LINPUT)                                          000240
      REWIND 1                                                      000250
      REWIND 2                                                      000260
      REWIND 5                                                      000270
      READ(1)NMDSM1,T                                               000280
      READ(1)SA3,ESI                                                000290
      READ(1)ZAPP,ZBPP                                              000300
      READ(1)F1,F2,F3                                               000310
      READ(1)X1L,X1U,X2L,X2U                                        000320
      READ(1)TD,SN,NAP,NCON                                         000330
      READ(1)X3L,X3U,X3RANG                                         000340
      READ(2)KNDSM1,TT                                              000350
      READ(2)SA32,ESI2                                              000360
      NSBGN=1                                                       000370
C     WRITE(5,1)                                                    000380
1     FORMAT(1X,*# OF DATA SETS=*)                                  000390
      READ(5,*)NDS                                                  000400
      DO 321 IT=1,NDS                                               000410
C     WRITE(5,12)                                                   000420
12    FORMAT(1X,*WANT TO INPUT NEW DISTORTIONS? T.OR.F*)            000430
      READ(5,*)WIDIS                                                000440
      IF(WIDIS)17,18                                                000450
17    DO 19 I=1,NMDSM1                                              000460
C     WRITE(5,7)I                                                   000470
7     FORMAT(1X,*SECTION#*,I3,2X,*INCREMENTAL DISTORTION FOR ZB=*)  000480
      READ(5,*)ZBPP(I)                                              000490
C     WRITE(5,8)                                                    000500
8     FORMAT(1X,*INCREMENTAL DISTORTION FOR ZA=*)                   000510
      READ(5,*)ZAPP(I)                                              000520
19    CONTINUE                                                      000530
C18   WRITE(5,2)                                                    000540
2     FORMAT(1X,*# OF SUBREFLECTOR SAMPLES=*)                       000550
18    READ(5,*)NSAMS                                                000560
C     WRITE(5,3)                                                    000570
3     FORMAT(1X,*# OF PRIMARY SAMPLES=*)                            000580
      READ(5,*)NSAMP                                                000590
      CALL SECOND(ACPU1)                                            000600
      IBLCPA=0                                                      000610
      RMAG=F1/F2                                                    000620
      X3LIM=X1U/RMAG                                                000630
      Z1U=X1U*X1U/(4.*F1)-F1                                        000640
      PI=3.14159265                                                 000650
      J=(0.,1.)                                                     000660
      X3AVE=(X3U+X3RANG)/2.                                         000670
      IF(TD.LT.0.)X3AVE=(X3L+X3RANG)/2.                             000680
      IF(TD.EQ.0.0)X3AVE=0.0                                        000690
C     FACNUL=0.0060375*CEXP(-J*1.27409)                             000700
      FACNUL=0.006137972624*CEXP(-J*1.339987)                       000710
      X350RN=-18.71215                                              000720
```

```
         X350AV=29.71215
         DO 4343 I=1,NAP
         A3=COS(PI*(SA32(I)-X350AV)/(X3U-X350RN-2.*SN))**2
         IF(SA32(I).LT.X350RN)A3=0.0
         IF(CABS(ESI2(I)).EQ.0.0)GO TO 4343
         EPH=ATAN2(AIMAG(ESI2(I)),REAL(ESI2(I)))
         ESI2(I)=A3*CEXP(J*EPH)*FACNUL
4343     CONTINUE
         DO 4242 I=1,NAP
C        A3=COS(PI*SA3(I)/(2.*(X3U-2*SN)))**2
         A3=COS(PI*(SA3(I)-X3AVE)/(X3U-X3RANG-2.*SN))**2
         IF(TD.EQ.0.0)A3=COS(PI*SA3(I)/(2.*(X3LIM-2.*SN)))**2
         IF(TD.EQ.0.0.AND.SA3(I).GT.X3LIM)A3=0.0
         IF(SA3(I).LT.X3RANG)A3=0.0
         IF(CABS(ESI(I)).EQ.0.)GO TO 4242
         EPH=ATAN2(AIMAG(ESI(I)),REAL(ESI(I)))
         ESI(I)=A3*CEXP(J*EPH)
C        WRITE(5,2765)A3,EPH
2765     FORMAT(1X,*A3,EPH=*,2E12.5)
C        WRITE(5,1000)I,ESI(I),SA3(I)
1000     FORMAT(1X,*I=*,I3,2X,*ESI=*,2E12.5,2X,*SA3=*,F12.5)
C3993     IF(CABS(ESI(I)).EQ.0.)WRITE(5,3333)I
3333     FORMAT(1X,*I=*,I4,2X,*ESI(I)=0.0*)
4242     CONTINUE
5555     CONTINUE
         DO 7673 I=1,NAP
         ESI(I)=ESI(I)+ESI2(I)
7673     CONTINUE
         ESI(1)=(0.,0.)
         ESI(2)=(0.,0.)
         ESI(NAP)=(0.,0.)
         NAPM1=NAP-1
         ESI(NAPM1)=(0.,0.)
         B=2.*PI
         TR=TD*PI/180.
         NMCS=NMDSM1+1
         Z0=-F2*F2/F1
         DELXS=(X2U-X2L)/(NSAMS-1)
         DO 44 I=1,NSAMS
         X2=X2U-DELXS*(I-1)
         Z2=F2-X2*X2/(4.*F2)
         ESUB(I)=(0.,0.)
         DO 100 JJ=1,NAP
         X3=SA3(JJ)
         Z3=Z0-X3*X3/(4.*F3)
         IF(X2U.NE.0.)GO TO 87
         CALL BLOCK(X2,X3,Z0,Z2,Z3,F2,X51,X52,IBLOCK)
         IF(IBLOCK.EQ.1)IBLCPA=IBLCPA+1
         IF(IBLOCK.EQ.1)GO TO 100
87       RL23=SQRT((X2-X3)**2+(Z2-Z3)**2)
         P=(Z2-Z3)/RL23
         PTR=P*P
         IF(SN.LT.0.8)PTR=P
C        EPH=ATAN2(AIMAG(ESI(JJ)),REAL(ESI(JJ)))
C        ESI(JJ)=A3*CEXP(J*EPH)
C        WRITE(5,9181)JJ,A3,EPH
9181     FORMAT(1X,*JJ,A3,EPH=*,2X,I4,2X,2F12.5)
         ECON=CONJG(ESI(JJ))*CEXP(-J*B*RL23)*PTR/(B*RL23)
C        WRITE(6,4499)X3,Z3,X2,Z2,ECON
4499     FORMAT(1X,4F12.5,2X,*ECON=*,2E10.3)
         ESUB(I)=ESUB(I)+ECON
100      CONTINUE
44       CONTINUE
```

294

```
          DO 7474 I=1,NSAMS                                        001360
          X2=X2U-DELXS*(I-1)                                       001370
          ESUBM=CABS(ESUB(I))                                      001380
          WRITE(6,5272)I,X2,ESUBM                                  001390
5272      FORMAT(1X,*I =*,I4,2X,*X2=*,F12.5,2X,*ESUBM=*,E12.5)     001400
7474      CONTINUE                                                 001410
          X1UM1=X1U-.001                                           001420
          X1UP1=X1U+.001                                           001430
          ISKIP=0                                                  001440
          ICT=0                                                    001450
          DELXP=(X1U-X1L)/(NSAMP-1)                                001460
          DXCENT=(X1U+X1L)/2.                                      001470
          DO 40 I=1,NMDSM1                                         001480
          IP1=I+1                                                  001490
          XA=T(I)                                                  001500
          XB=T(IP1)                                                001510
          ZA=XA*XA/(4.*F1)-F1                                      001520
          ZB=XB*XB/(4.*F1)-F1                                      001530
          IF(ISKIP.EQ.1)GO TO 912                                  001540
99        ICT=ICT+1                                                001550
          EL4(ICT)=(0.,0.)                                         001560
          X1=DELXP*(ICT-1)+X1L                                     001570
          IF(X1.GT.X1UM1.AND.X1.LT.X1UP1)X1=X1UM1                  001580
912       IF(X1.LE.XB)ZBP=ZB+ZBPP(I)                              001590
          IF(X1.LE.XC)ZAP=ZA+ZAPP(I)                              001600
          IF(X1.GT.XB)ISKIP=1                                      001610
          IF(X1.GT.XB)GO TO 40                                     001620
          ISKIP=0                                                  001630
          XAP=XA                                                   001640
          XBP=XB                                                   001650
          XBA=XB-XA                                                001660
          XBAP=XBP-XAP                                             001670
          ZBA=ZB-ZA                                                001680
          ZBAP=ZBP-ZAP                                             001690
          RMO=XBA/ZBA                                              001700
          RMN=XBAP/ZBAP                                            001710
          DELZ1=(X1-XBP)/RMN-(X1-XB)/RMO+ZBP-ZB                    001720
          Z1=X1*X1/(4.*F1)-F1+DELZ1                                001730
          ZDIF=Z1U-Z1                                              001740
          X4L(ICT)=X1                                              001750
          DO 101 JJ=1,NSAMS                                        001760
          X2=X2U-DELXS*(JJ-1)                                      001770
          Z2=F2-X2*X2/(4.*F2)                                      001780
          RL12=SQRT((X1-X2)**2+(Z1-Z2)**2)                         001790
          EPRI=ESUB(JJ)*CEXP(-J*B*(RL12+ZDIF))/(B*RL12)            001800
          EL4(ICT)=EL4(ICT)+EPRI                                   001810
C         WRITE(6,8877)X2,Z2,X1,Z1,EL4(ICT),ESUB(JJ)              001820
8877      FORMAT(1X,*X2,Z2,X1,Z1=*,4F12.5,2X,*EL4(ICT)=*,2E12.5,2X  001830
         2,*ESUB(JJ)=*,2E12.5)                                     001840
101       CONTINUE                                                 001850
          GO TO 99                                                 001860
40        CONTINUE                                                 001870
          FAC=1.0                                                  001880
          RNSBGN=NSBGN                                             001890
          RNSAMS=NSAMS                                             001900
          IF(IT.GT.1)FAC=RNSBGN/RNSAMS                             001910
C         WRITE(5,6767)IT,NSBGN,FAC                               001920
6767      FORMAT(1X,*IT =*,I5,2X,*NSBGN=*,I5,2X,*FAC=*,F12.5)      001930
          WRITE(6,71)F1,F2,F3                                      001940
71        FORMAT(1X,*F1=*,F12.3,2X,*F2=*,F12.3,2X,*F3=*,F12.5)     001950
          WRITE(6,72)X1L,X1U,X2L,X2U,X3L,X3U                       001960
72        FORMAT(1X,*X1L=*,F12.3,2X,*X1U=*,F12.3,2X,*X2L=*,F12.3,2X, 001970
         2*X2U=*,F12.3,2X,*X3L=*,F12.3,2X,*X3U=*,F12.3)            001980
```

295

```
      WRITE(6,73)TD,SN,NSAMP,FAC,NSAMS                                    001990
73    FORMAT(1X,*TD=*,F10.4,2X,*SN=*,F12.4,2X,*NSAMP=*,I7,2X,*FAC=*,      002000
     2F12.4,2X,*NSAMS=*,I7)                                               002010
      WRITE(6,700)NAP,NCON                                                002020
700   FORMAT(1X,*NAP=*,I5,2X,*NCON=*,I5)                                  002030
      WRITE(6,8354)X3RANG,X3AVE                                           002040
8354  FORMAT(1X,*X3RANG=*,F12.5,2X,*X3AVE=*,F12.5)                        002050
      DO 333 I=1,NMDS                                                     002060
      WRITE(6,222)I,T(I)                                                  002070
222   FORMAT(1X,*T(*,I3,*)=*,F15.5)                                       002080
333   CONTINUE                                                           002090
      DO 151 I=1,NAP                                                      002100
      EMG=CABS(ESI(I))                                                    002110
      IF(EMG.EQ.0.)GO TO 3681                                            002120
      EPH=ATAN2(AIMAG(ESI(I)),REAL(ESI(I)))*180./PI                      002130
      WRITE(6,159)SA3(I),EMG,EPH                                          002140
159   FORMAT(1X,*SA3=*,F14.4,2X,*EMG=*,E15.5,2X,*EPH=*,F14.5)            002150
3681  IF(EMG.EQ.0.)WRITE(6,4927)SA3(I)                                   002160
4927  FORMAT(1X,*SA3=*,F14.4,2X,*EMG=0*)                                 002170
151   CONTINUE                                                           002180
      DO 109 I=1,NMDSM1                                                   002190
      WRITE(6,75)I,ZAPP(I),ZBPP(I)                                        002200
75    FORMAT(1X,*SECTION#*,I3,2X,*ZAPP(I)=*,F15.7,2X,*ZBPP(I)=*,F15.7)   002210
109   CONTINUE                                                           002220
      BIGEST=0.0                                                         002230
      DO 42 I=1,NSAMP                                                     002240
      EL4MAG(I)=CABS(EL4(I))*FAC                                          002250
      IF(EL4MAG(I).EQ.0.)GO TO 4200                                      002260
      ELPHAD(I)=ATAN2(AIMAG(EL4(I)),REAL(EL4(I)))*180./PI                002270
      WRITE(G,50)I,X4L(I),EL4MAG(I),ELPHAD(I)                            002280
50    FORMAT(1X,*I=*,I5,2X,*X4L=*,F15.5,2X,*EL4MAG=*,E15.5,2X,           002290
     2*ELPHAD=*,F14.5)                                                   002300
4200  IF(EL4MAG(I).EQ.0.)WRITE(6,5000)X4L(I)                            002310
5000  FORMAT(1X,*X4L=*,F15.5,2X,*EL4MAG=0*)                             002320
      IF(EL4MAG(I).GT.BIGEST)BIGEST=EL4MAG(I)                           002330
42    CONTINUE                                                           002340
      WRITE(6,74)IBLCPA                                                   002350
74    FORMAT(1X,*IBLCPA=*,I5)                                            002360
      IF(IT.EQ.1)NSBGN=NSAMS                                            002370
C     WRITE(5,3131)                                                     002380
3131  FORMAT(1X,*WANT TO CALL APERTURE PLOTTING ROUTINE? T.OR.F*)       002390
      READ(5,*)WPLAPR                                                    002400
      IF(WPLAPR)9787,9788                                               002410
9787  CALL PLOTE(X1L,X1U,X4L,EL4MAG,BIGEST,ELPHAD,NSAMP,0)             002420
C***THIS PART COMPUTES THE FAR-FIELD PATTERN                            002430
C9788 WRITE(5,4121)                                                    002440
4121  FORMAT(1X,*PATTERN RANGE...TMIN=,TMAX=*)                         002450
9788  READ(5,*)TMIN,TMAX                                                002460
C     WRITE(5,4836)                                                     002470
4836  FORMAT(1X,*NUMBER OF POINTS=*)                                    002480
      READ(5,*)NPNTS                                                     002490
      BICE=0.0                                                          002500
      DINC=(TMAX-TMIN)/(NPNTS-1)                                        002510
      DO 59 K=1,NPNTS                                                    002520
      THETAD(K)=TMIN+DINC*(K-1)                                         002530
      THETAR=THETAD(K)*PI/180.                                          002540
      STH=SIN(THETAR)                                                   002550
      SUME=(0.,0.)                                                      002560
      DO 49 I=1,NSAMP                                                    002570
      EFARF=EL4(I)*CEXP(J*B*(X4L(I)-DXCENT)*STH)                       002580
      SUME=SUME+EFARF                                                   002590
49    CONTINUE                                                           002600
      EFF(K)=SUME                                                       002610
```

```
         IF(CABS(EFF(K)).GT.BIGE)BIGE=CABS(EFF(K))                      002620
59       CONTINUE                                                       002630
         DO 5898 K=1,NPNTS                                              002640
         EFFMAG=CABS(EFF(K))                                            002650
         EPHD=ATAN2(AIMAG(EFF(K)),REAL(EFF(K)))*180./PI                 002660
         WRITE(6,5117)THETAD(K),EFFMAG,EPHD                             002670
5117     FORMAT(1X,*THETAD=*,F12.4,2X,*EFFMAG=*,E17.7,2X,*EPHD=*,F12.4) 002680
5898     CONTINUE                                                       002690
         DO 111 K=1,NPNTS                                               002700
         ENORM(K)=20.*ALOG10(CABS(EFF(K))/BIGE)                         002710
         EPHD=ATAN2(AIMAG(EFF(K)),REAL(EFF(K)))*180./PI                 002720
         WRITE(6,223)THETAD(K),ENORM(K),EPHD                            002730
223      FORMAT(1X,*THETAD=*,F14.5,2X,*ENORM=*,F15.5,2X,*EPHD=*,F10.3)  002740
111      CONTINUE                                                       002750
C        WRITE(5,37)                                                    002760
37       FORMAT(1X,*WANT TO CALL PATTERN PLOTTING SUBROUTINE? T.OR.F*)  002770
         READ(5,*)WPLFF                                                 002780
         IF(WPLFF)31,32                                                 002790
31       CALL PLOTFF(ENORM,THETAD,TMIN,TMAX,NPNTS)                      002800
32       CALL APEREF(NSAMP,EL4,TR,X4L,AEF)                              002810
C        WRITE(5,25)AEF                                                 002820
         WRITE(6,25)AEF                                                 002830
25       FORMAT(1X,*APERTURE ILLUMINATION EFFICENCY=*,F15.5)            002840
321      CONTINUE                                                       002850
         CALL SECOND(ACPU2)                                             002860
         ACPU21=ACPU2-ACPU1                                             002870
         WRITE(6,52)ACPU21                                              002880
52       FORMAT(1X,*CPU FOR THIS RUN=*,F14.3)                           002890
         CALL EXIT                                                      002900
         END                                                            002910
         SUBROUTINE BLOCK(X2,X3,Z0,Z2,Z3,F2,X51,X52,IBLOCK)            002920
C***THIS SUBROUTINE DETERMINES IF THERE IS BLOCKAGE BY THE ARRAY        002930
         IBLOCK=0                                                       002940
         FNUM=X2*(X2-X3)+2.*F2*(Z2-Z3)                                  002950
         FDEN=SQRT((X2-X3)**2+(Z2-Z3)**2)                              002960
         F=FNUM/FDEN                                                    002970
         X2S=X2*X2                                                      002980
         FS=F*F                                                         002990
         A1=Z0-Z2                                                       003000
         A2=X2S-2.*F2*A1                                                003010
         A=FS-X2S                                                       003020
         B=2.*X2*(A2-FS)                                                003030
         C=FS*(A1*A1+X2S)-A2*A2                                         003040
         DIS=B*B-4.*A*C                                                 003050
C        IF(DIS.LT.O.)WRITE(5,1)                                        003060
1        FORMAT(1X,*ROOTS ARE COMPLEX*)                                 003070
         X51=(-B+SQRT(DIS))/(2.*A)                                      003080
         X52=(-B-SQRT(DIS))/(2.*A)                                      003090
         IF(X51.LT.O.AND.X52.LT.O.)IBLOCK=1                            003100
         RETURN                                                         003110
         END                                                            003120
         SUBROUTINE PLOTFF(EMAG,THETAD,TMIN,TMAX,NPNTS)                 003130
C***THIS SUBROUTINE PLOTS THE FAR-F.ELD PATTERN OF THE TWO             003140
C***REFLECTOR ARRAY CLUSTER SYSTEM.                                     003150
         DIMENSION EMAG(1),THETAD(1)                                    003160
         LOGICAL PLOT,HARDC,WPLOTA                                      003170
C        WRITE(5,22)                                                    003180
22       FORMAT(1X,*WANT TO PLOT? T.OR.F*)                              003190
         READ(5,*)PLOT                                                  003200
         IF(PLOT)7,88                                                   003210
7        CALL TEKTRN(960)                                               003220
99       CALL BGNPL(1)                                                  003230
         CALL BASALF("STANDARD")                                        003240
```

```
         CALL MIXALF("L/CGREEK")                                    003250
         CALL PAGE(10.89,11.0)                                      003260
         CALL GRACE(0.0)                                            003270
         CALL TITLE(17HFAR-FIELD PATTERN,17,11H(Q) DEGREES,11.      003280
      224HRELATIVE AMPLITUDE IN DB,24,5.,5.)                        003290
         CALL XTICKS(2)                                             003300
         CALL YTICKS(2)                                             003310
         CALL GRAF(TMIN,"SCALE",TMAX,-120,20,0)                     003320
         CALL GRID(1,1)                                             003330
         CALL MARKER(10)                                            003340
         CALL CURVE(THETAD,EMAG,NPNTS,0)                            003350
         CALL ENDPL(1)                                              003360
C88      WRITE(5,23)                                                003370
23       FORMAT(1X,*WANT HARD COPY? T.OR.F*)                        003380
88       READ(5,*)HARDC                                             003390
         IF(HARDC)12,77                                             003400
12       CALL FR80(3)                                               003410
         GO TO 99                                                   003420
C77      WRITE(5,24)                                                003430
24       FORMAT(1X,*WANT TO PLOT AGAIN? T.OR.F*)                    003440
77       READ(5,*)WPLOTA                                            003450
         IF(WPLOTA)7,42                                             003460
42       RETURN                                                     003470
         END                                                        003480
         SUBROUTINE APEREF(N,E,TR,X,EFF)                            003490
C***THIS SUBROUTINE CALCULATES THE APERTURE ILLUMINATION EFFICIENCY 003500
         COMPLEX E(1),SUMC,J,F(600)                                 003510
         DIMENSION X(1)                                             003520
         B=2.*3.14159265                                            003530
         J=(0.,1.)                                                  003540
         SUMR=0.0                                                   003550
         SUMC=(0.,0.)                                               003560
         DO 1 I=1,N                                                 003570
         F(I)=E(I)*CEXP(J*B*X(I)*SIN(TR))                           003580
         SUMC=SUMC+E(I)*CEXP(J*B*X(I)*SIN(TR))                      003590
         SUMR=SUMR+CABS(E(I))**2                                    003600
C        WRITE(6,74)I,F(I),SUMC,SUMR                                003610
74       FORMAT(1X,*I,F(I),SUMC,SUMR=*,I5,2X,5F17.7)                003620
1        CONTINUE                                                   003630
         EFF=CABS(SUMC)**2/(N*SUMR)                                 003640
         RETURN                                                     003650
         END                                                        003660
         SUBROUTINE PLOTE(X1L,X1U,S3,EMAG,EMAX,EPHAD,NPNTS,NDIF)    003670
         DIMENSION S3(1),EMAG(1),EPHAD(1)                           003680
         LOGICAL PLOT,HARDC,WPLOTA                                  003690
         XMX=ABS(X1L)                                               003700
         DO 1 I=1,NPNTS                                             003710
         WRITE(6,71)I,S3(I),EMAG(I),EPHAD(I)                        003720
71       FORMAT(1X,*I,S3,EMAG,EPHAD=*,I4,2X,F12.4,2X,E12.4,2X,F12.4) 003730
1        CONTINUE                                                   003740
C        WRITE(5,22)                                                003750
22       FORMAT(1X,*WANT TO PLOT? T.OR.F*)                          003760
         READ(5,*)PLOT                                              003770
         IF(PLOT)7,88                                               003780
7        CALL TEKTRN(960)                                           003790
99       CALL BGNPL(1)                                              003800
         CALL PAGE(10.897,14.103)                                   003810
         CALL GRACE(0.0)                                            003820
         CALL PHYSOR(2.5,1.0)                                       003830
         IF(NDIF.EQ.0)GO TO 61                                      003840
         CALL TITLE(16HPHASE DIFFERENCE,16,17HLOCATION ON ARRAY,17, 003850
      215HPHASE (DEGREES),15,4.,3.)                                 003860
         GO TO 64                                                   003870
```

```
61      CALL TITLE(10HPHASE OF E,10,20HLOCATION ON APERTURE,20,          003880
       215HPHASE (DEGREES),15,4.,3.)                                     0C3890
64      CALL XTICKS(4)                                                   003900
        CALL YTICKS(2)                                                   003910
        CALL GRAF(X1L,"SCALE",X1U,-180.,90.,180.)                       003920
        CALL GRID(1,1)                                                   003930
        CALL MARKER(10)                                                  003940
        CALL SCLPIC(0.5)                                                 003950
        CALL CURVE(S3,EPHAD,NPNTS,0)                                     003960
        CALL ENDGR(1)                                                    003970
        CALL BGNPL(2)                                                    003980
        CALL GRACE(0.0)                                                  003990
        CALL OREL(0.,4.)                                                 004000
        IF(NDIF.EQ.0)GO TO 62                                           004010
        CALL TITLE(20HAMPLITUDE DIFFERENCE,20,17HLOCATION ON ARRAY,17,   004020
       29HAMPLITUDE,9,4.,3.)                                             004030
        GO TO 65                                                        004040
62      CALL TITLE(14HMAGNITUDE OF E,14,20HLOCATION ON APERTURE,20,      004050
       211HMAGNITUDE E,11,4.,3.)                                         004060
65      CALL XTICKS(4)                                                   004070
        CALL YTICKS(2)                                                   004080
        IF(NDIF.EQ.0)GO TO 66                                           004090
        EMAXCS=-EMAX                                                    004100
        CALL GRAF(-X3U,"SCALE",XMX,EMAXCS,"SCALE",EMAX)                 004110
        GO TO 67                                                        004120
66      CALL GRAF(X1L,"SCALE",X1U,0.,"SCALE",EMAX)                     004130
67      CALL GRID(1,1)                                                   004140
        CALL MARKER(10)                                                  004150
        CALL SCLPIC(0.5)                                                 004160
        CALL CURVE(S3,EMAG,NPNTS,0)                                      004170
        CALL ENDPL(2)                                                    004180
C88     WRITE(5,23)                                                     004190
23      FORMAT(1X,*WANT HARD COPY? T.OR.F*)                            004200
88      READ(5,*)HARDC                                                  004210
        IF(HARDC)12,77                                                  004220
12      CALL FR80(3)                                                    004230
        GO TO 99                                                        004240
C77     WRITE(5,24)                                                     004250
24      FORMAT(1X,*WANT TO PLOT AGAIN? T.OR.F*)                        004260
77      READ(5,*)WPLOTA                                                 004270
        IF(WPLOTA)7,42                                                  004280
42      RETURN                                                          004290
        END                                                             004300
```

C.6   Program GRATE 2

```
      PROGRAM GRATE2(OUTPUT,TAPE 6=OUTPUT,FR80)
      DIMENSION THM(41),VDB(41)
      DIMENSION VP(15,15),XP(15,15),ZP(15,15)
C     COMPUTATION OF GRATING LOBES DUE TO SEGMENTED PARABOLIC REFLECTOR
      PI=3.1415927
      RD=50950.
      F1=83432.
C     MAX RADIUS RD AND FOCAL LENGTH F1 IN RADIANS AT RF
      VA=0.
      DX=RD/12.
      DO 1 I=1,15
      AI=I
      DO 2 J=1,15
      AJ=J
      X=DX*(.5+AI)
      Y=DX*(.5+AJ)
      RP=SQRT(X**2+Y**2)
      TP=TAN(Y/X)
      CALL ARC(RP,F1,AL0)
      RP1=2.*RP-AL0
      CALL ARC(RP1,F1,AL1)
      SARC=(RP-RP1)/(AL0-AL1)
      RP2=SARC*(RP-AL1)+RP1
      CALL ARC(RP2,F1,AL2)
      SARC=(RP1-RP2)/(AL1-AL2)
      RP2=SARC*(RP-AL2)+RP2
      XP(I,J)=RP2*COS(TP)
      ZP(I,J)=RP2**2/(4.*F1)
      IF(RD-RP2)3,3,4
    4 VP(I,J)=.316+.684*COS((PI*RP2)/(2.*RD))
C     VP GIVES COS ON A 10 DB PEDESRAL ILLUMINATION
      VA=VA+VP(I,J)
      GO TO 2
    3 VP(I,J)=0.
    2 CONTINUE
    1 CONTINUE
      TH=.001
C     TH IS FAR-FIELD ANGLE IN RADIANS
      THM(1)=1000.*TH
      VDB(1)=0.
      DO 5 K=2,41
      TH=TH+.00001
      VR=0.
      VI=0.
      DO 6 I=1,15
      DO7 J=1,15
      VER=COS(ZP(I,J)*(TH**2)/2.)
      VEI=SIN(ZP(I,J)*(TH**2)/2.)
      VEC=COS(XP(I,J)*TH)*VP(I,J)
C     SMALL ANGLE APPROX USED FOR SIN(TH) AND COS(TH)
      VER=VER*VEC
      VEI=VEI*VEC
      VR=VR+VER
      VI=VI+VEI
    7 CONTINUE
    6 CONTINUE
      V=SQRT(VR**2+VI**2)/VA
      VDB(K)=20.*ALOG10(V)
      IF(VDB(K).LT.-40.)VDB(K)=-40.
C     VDB IS LOBE AMPLITUDE IN DB RELATIVE TO
C     LOBE GIVEN BY A PLANAR ARRAY
      THM(K)=TH*1000.
C     THM IS FAR-FIELD ANGLE IN MILLIRADIANS.
```

```
      WRITE(6,8)THM(K),VDB(K)
    8 FORMAT(2F9.4)
    5 CONTINUE
      CALL FRBO(3)
      CALL BGNPL(1)
      CALL LINFLT(THM,VDB,41)
      CALL ENDPL(1)
      CALL DONEPL
      STOP
      END
      SUBROUTINE ARC(XMAX,F1,AL)
C     COMPUTES ARC LENGTH OF A PARABOLA FROM X=0. TOXMAX
C     F1=FOCAL LENGTH
C     PARABOLA EQUATION IS Z=X**2/(4.*F1)
      R=SQRT(XMAX**2+(2.*F1)**2)
      A=XMAX+R/2.
      B=(2.*(F1**2))*(ALOG((XMAX+R)/(2.*F1)))
      AL=(.5/F1)*(A+B)
      RETURN
      END                                        000860
```

APPENDIX D

Executive Summary

1. INTRODUCTION

This report covers the work done on contract No. F30602-79-C-0017, "Adaptive Techniques for Large Space Apertures". The contract covered the period 6 Nov. 1978 – 5 Nov. 1979. The three major tasks on the program were Task 1, Concept Development/Assessment; Task 2, Performance Analysis, Selected Approach; and Task 3, Specific Mission Designs. Much of the work done on Task 1, particularly in the structural concepts tradeoff, had been done by us on an earlier contract sponsored by SAMSO, No. F04701-77-C-0180, "On-Orbit Assembly Concept Study". Our preferred structural approach for large space-deployable antennas is a deployable box truss.

Two missions which utilize large space apertures were considered on the program. These were the space-based radar mission and the space-based milli-meter-wave radiometer mission. The greater part of the effort was spent on the radar mission. The intent of the program was to investigate reflector-based alternates to the space-fed phased array system that is the current baseline for the space-based radar program.

The adaptive techniques of interest were those that might be required to compensate for surface irregularities in the large, space-deployable reflectors that would be required for these missions. This and other system requirements were considered in selecting an antenna system for each mission.

Work done on the program is presented in detail in the Final Technical Report (Report No. MCR-79-644, dated 5 Nov. 1979). It is summarized briefly below.

2. THE TECHNICAL PROBLEM

Techniques for the deployment in space of very large structures, currently being developed, allow the consideration of a number of space missions utilizing very large aperture antennas. Two surviellance missions of particular interest to the Air Force are the Space-Based Radar (SBR) and the Milli-meter Wave Radiometer (MWR). Both of these missions were considered on the program. The principal technical problems associated with these applications are:

- The development of an appropriate structural concept capable of efficient packaging for launch, reliable deployment in space, and the achievement of adequate precision for use as an antenna.

- Accurate and stable attitude and figure control of these large flexible bodies to maintain the required pointing accuracy as well as the RF performance of the antenna with acceptable damping periods following any maneuver.

- An RF antenna system design that will give the desired flexibility, field of view (FOV), resistance to ECM, and beam agility to perform the desired mission.

304

3. PROGRAM APPROACH

A number of antenna concepts were traded off against the requirements of the two missions and a concept was selected for each mission. The current program baseline concept for the SBR is a space-fed lens-array using a very large number of active transceiver module, to form the array. The principal weakness of this design is the high cost risk associated with the modules. Our selected approach gives a marked reduction in the required number of modules while still providing the flexibility to do the radar mission. Our approach is shown in Figure 1. It uses a large primary reflector 70 meters in diameter to achieve the necessary gain. A smaller field reflector and a phased array feed are used to provide the agility, FOV, and ECCM capability to do the radar mission.

A brief look was also given to a reflectarray as another possible alternate to the baseline lens-array SBR system. This is sketched in Figure 2. Its main advantage over the baseline lens-array system is that a much shorter focal length can be used. This gives a lighter and stiffer structure.

The concept selected for the MWR mission is a reflective Schmidt telescope with diameter of 100 meters and a length of 300 meters. The reflecting surfaces are made up of metallized honeycomb panels. A linear array of feeds is used. This concept was selected for its wide FOV and relative simplicity. This system is shown in Figure 3.

Once these concepts were selected, a more detailed design effort was carried out. RF performance was analyzed by computation. The structure was sized, weights were estimated and a packaging design for a shuttle launch was made. This included a sizing of the propulsion required to place the vehicle in its operational orbit. A first-cut design was also made for the attitude control and figure control systems.

4. STUDY RESULTS

The selected design for the SBR uses a 70 meter primary reflector with an f/D of 1. The smaller field reflector is 28 meters in diameter and the planar phased array feed is also 28 meters in diameter. The total number of active modules is reduced by a factor of 4.3 from that used in the lens-array concept. The orbit altitude was selected as 5000 n.mi. The FOV for agile beam scanning is 20° x 11°, which is not sufficient for full-earth coverage. An attitude control concept was selected which uses gravity-gradient stabilization and rotation about the gravity-gradient axis to provide full-earth coverage using a combination of electronic and mechanical steering. The system was packaged for launch in a single shuttle, including the propulsion stage required to reach the operational orbit. Deployment is fully automatic and is done in the shuttle orbit under the control of the orbiter crew. It is then boosted to its operational orbit using a low-thrust liquid stage.

A similar design was made for a synchronous-orbit version of the SBR. It uses a primary reflector 300m. in diameter. It requires three shuttle flights to reach synchronous orbit using electric propulsion for orbit

Figure 1
RADAR ANTENNA

FIELD REFLECTOR

PHASED ARRAY

ASTROMASTS

GUYLINE STABILIZERS

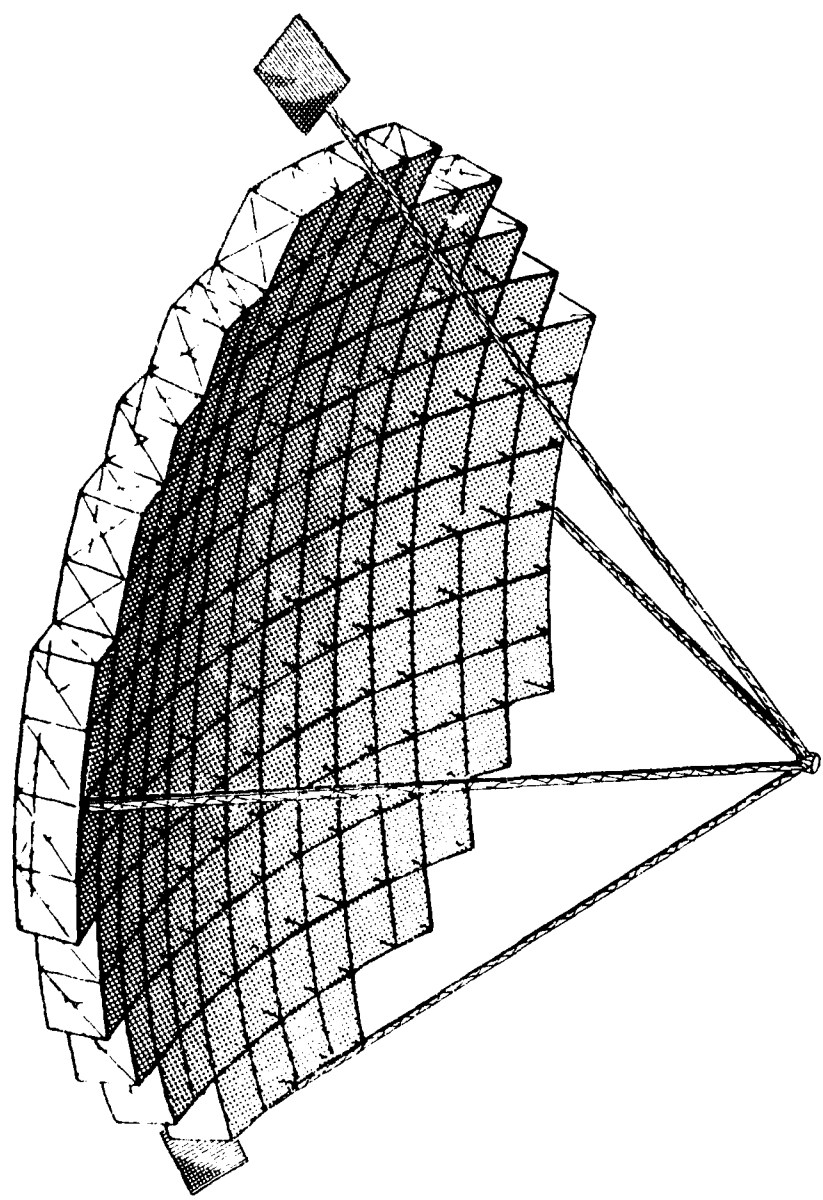SOLAR PANELS

FEED

MAIN REFLECTOR
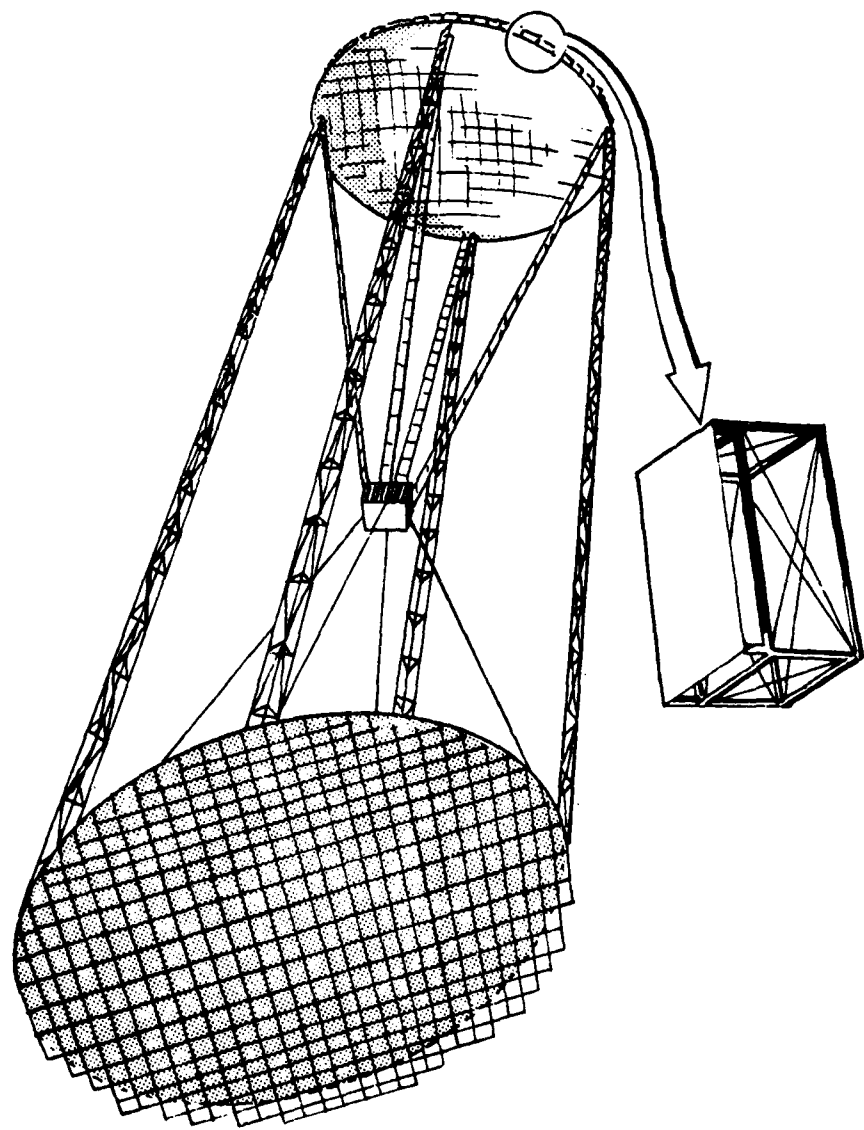
306
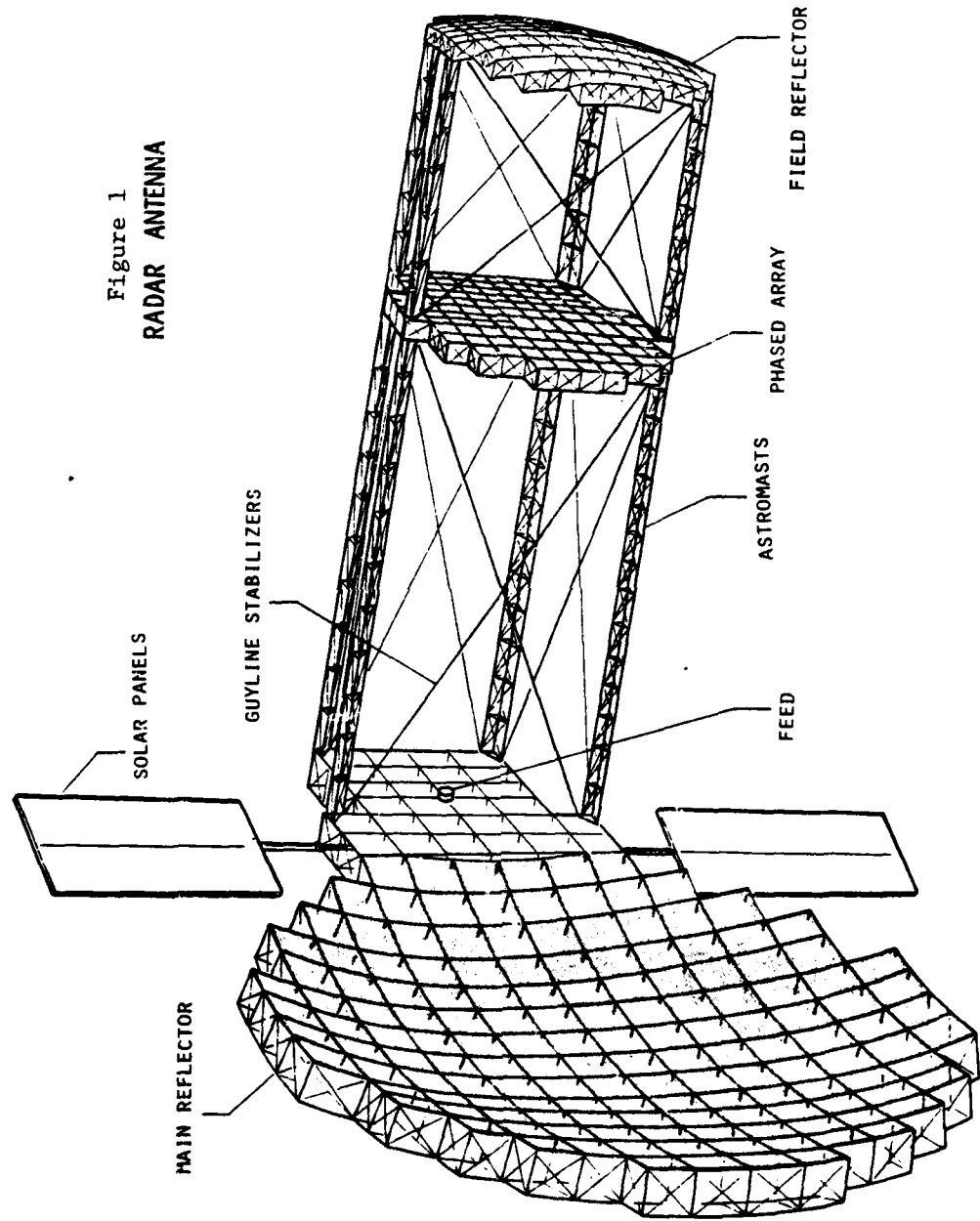
Figure 2. REFLECTARRAY RADAR

Figure 3   Reflective Schmidt Antenna For Millimeter-Wave Radiometry

transfer. Deployment and assembly is done in the shuttle orbit. The antenna system is designed for a smaller scan range than the 5000 mile orbit vehicle. This allows the field reflects and phased array feed to be smaller relative to the main reflector. They are 30 m. in diameter or only 1/10 that at the primary reflector. The spacecraft configuration is shown in Figure 4.

The reflectarray was sized at 91 m. with an f/D of 0.5 for the 500 n. mi. orbit. It uses passive (phase shift only) reflectarray modules. It can be packaged in a single shuttle vehicle.

A 400 n.mi. orbit was selected for the MWR mission. This was selected as the minimum altitude giving an acceptable level of atmospheric drag. It is gravity-gradient stabilized and nadir-pointing, operating in a pushbroom mode. Operating frequency was selected at the 95 GHz atmospheric window. The FOV is quite wide, 10,000 beamwidths. The pushbroom swath width on the ground is 125 n.mi. Sensitivity is sufficient to detect a military tank in most weather conditions except heavy rain. The resolution based on the individual beamwidths is 74 ft. but a data processing technique based on using monopulse sum and difference patterns can be used to improve this by a factor of 10 or more.
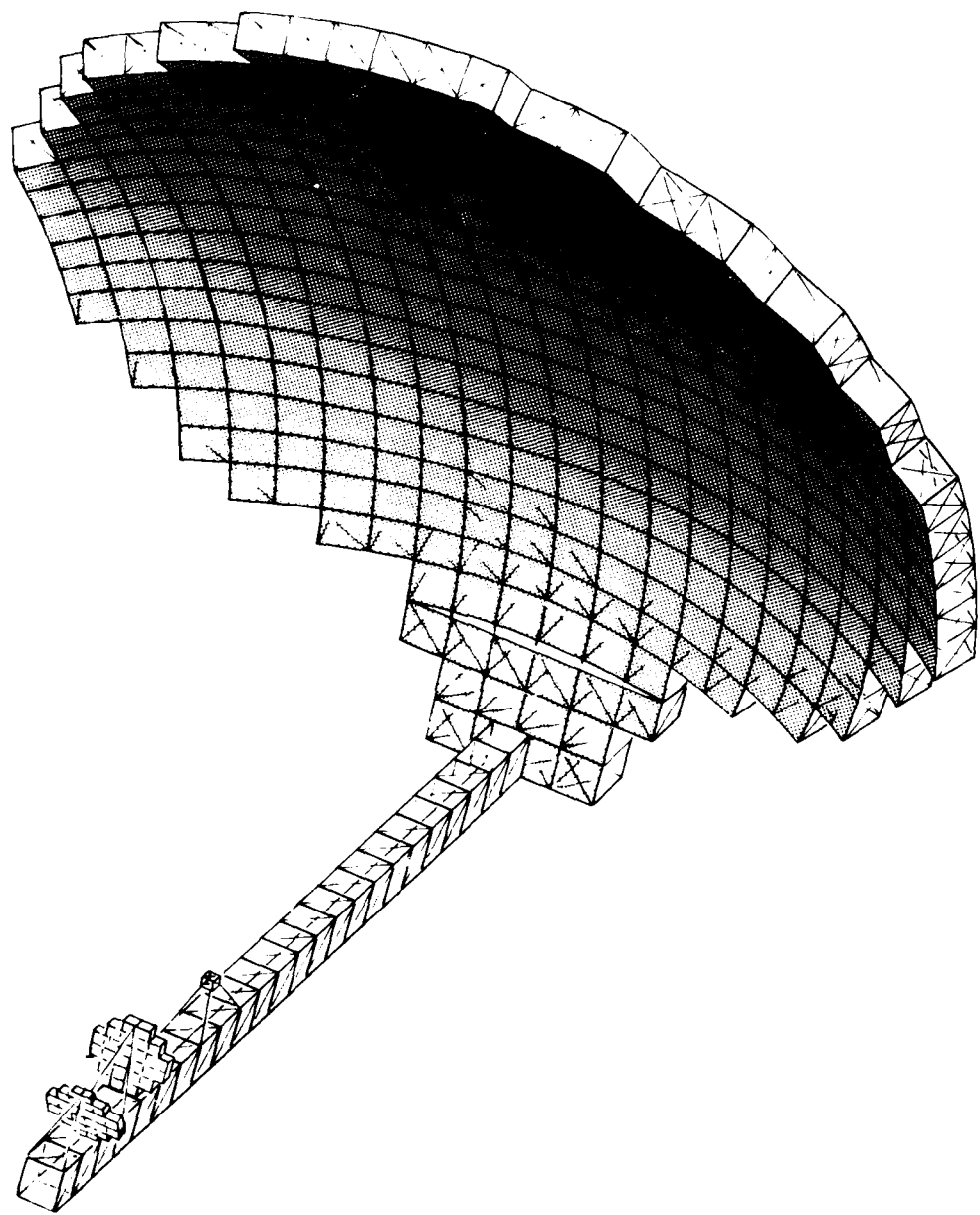
Figure 4   RADAR ANTENNA, SYNCHRONOUS ORBIT

310

MISSION
of
Rome Air Development Center

RADC plans and executes research, development, test and selected acquisition programs in support of Command, Control Communications and Intelligence (C^3I) activities. Technical and engineering support within areas of technical competence is provided to ESD Program Offices (POs) and other ESD elements. The principal technical mission areas are communications, electromagnetic guidance and control, surveillance of ground and aerospace objects, intelligence data collection and handling, information system technology, ionospheric propagation, solid state sciences, microwave physics and electronic reliability, maintainability and compatibility.